10

EXTERNAL TRANSMITTAL AUTHORIZED

ORNL
Central Files Number
57-8-10

OAK RIDGE SCHOOL OF REACTOR TECHNOLOGY

REACTOR DESIGN AND FEASIBILITY STUDY

SUPERHEATING WATER-BOILER

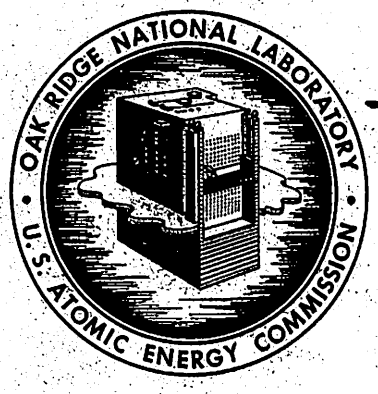

OAK RIDGE NATIONAL LABORATORY
operated by
UNION CARBIDE CORPORATION
for the
U.S. ATOMIC ENERGY COMMISSION

DISCLAIMER

OAK RIDGE SCHOOL OF REACTOR TECHNOLOGY

CF 57-8-10
Copy 72

Reactor Design and Feasibility Study

"SUPERHEATING WATER-BOILER"

Prepared by:

F. Marbury, Group Leader
J. W. Alden
R. E. Bedford
J. A. Bilenas
W. C. Coppersmith
J. DeVincentis
K. Hiroshige
O. H. Klepper

August 1957

Distribution:

1. A. M. Weinberg
2. J. A. Swartout
3. R. A. Charpie
4. W. H. Jordan
5. Lewis Nelson
6. D. C. Hamilton
7. C. O. Smith
8. J. H. Marable
9. P. G. Lafyatis
10. Herbert Pomerance
11. W. A. Lloyd
12. W. Zobel
13. E. D. Arnold
14. J. W. Ullman
15. A. T. Gresky
16. C. S. Walker
17. E. P. Blizard
18. L. B. Holland
19. W. R. Gall
20. A. P. Fraas
21. J. A. Lane
22. P. R. Kasten
23. A. F. Rupp
24. E. S. Bettis
25. C. E. Winters
26. R. B. Briggs
27. A. L. Boch
28. W. T. Furgerson
29. R. V. Meghreblian
30. L. R. Dresner
31. F. Marbury
32. J. W. Alden
33. R. E. Bedford
34. J. A. Bilenas
35. W. C. Coppersmith
36. J. DeVincentis
37. K. Hiroshige
38. O. H. Klepper
39. A. J. Taylor
40. J. E. Cunningham
41. J. L. English
42. E. L. Compere
43. R. C. Robertson
44. F. H. Neill
45. M. I. Lundin
46-47. Martin Skinner, Patent Office
48-49. REED Library
50-51. Central Research Library
52-61. Laboratory Records
62-67. ORSORT Files
68-82. TISE
83. P. P. Eddy
Maritime Reactor Branch
Division Reactor Development
AEC
Washington 25, D. C.
84. Document Reference Section

PREFACE

In September, 1956, a group of men experienced in various scientific and engineering fields embarked on the twelve months of study which culminated in this report. For nine of those months, formal classroom and student laboratory work occupied their time. At the end of that period, these eight students were presented with a problem in reactor design. They studied it for ten weeks, the final period of the school term.

This is a summary report of their effort. It must be realized that, in so short a time, a study of this scope can not be guaranteed complete or free of error. This "thesis" is not offered as a polished engineering report, but rather as a record of the work done by the group under the leadership of the group leader. It is issued for use by those persons competent to assess the uncertainties inherent in the results obtained in terms of the preciseness of the technical data and analytical methods employed in the study. In the opinion of the students and faculty of ORSORT, the problem has served the pedagogical purpose for which it was intended.

The faculty joins the authors in an expression of appreciation for the generous assistance which various members of the Oak Ridge National Laboratory gave. In particular, the guidance of the group consultant, W. R. Gall, is gratefully acknowledged.

Lewis Nelson

for

The Faculty of ORSORT

ACKNOWLEDGEMENTS

The group wishes to express its appreciation to its adviser, Wm. R. Gall, and M. I. Lundin for making this study possible, and to R. N. Lyon for his initial encouragement. We are no less indebted to Lewis Nelson and the faculty of the Oak Ridge School of Reactor Technology for putting us in shape for the work.

Thanks go also to A. J. Taylor, J. E. Cunningham, J. L. English, E. L. Compere, R. C. Robertson, A. L. Boch, F. H. Neill, P. R. Kasten and others for their time and trouble in helping us with our problems in their several fields. Michael Treshow of the Argonne National Laboratory and J. T. Holm of the Webb Institute of Naval Architecture gave not only advice but also that precious feeling that we might be useful.

Mrs. M. B. Hoy and Miss B. M. Helton are to be commended for much typing in a short time.

It has been a pleasure for all of us to work here for a while.

TABLE OF CONTENTS

TABLE OF CONTENTS

contd.

TABLE OF CONTENTS

contd.

TABLE OF CONTENTS

contd.

LIST OF ILLUSTRATIONS

ILLUSTRATIONS
contd.

PRELIMINARY DESIGN OF A SUPERHEATING WATER-BOILER

1. INTRODUCTION

1.1 Foreword

The subject of this ten weeks' effort is a boiling water reactor with integral nuclear superheater, which produces steam at 1200 psia, 950°F. A quick look at the problem last Spring indicated that such a reactor could be designed using stainless steel, UO_2 and ordinary water for materials and staying generally within the limits of existing reactor technology. The object was to design the best such reactor, consistent with the above and with the principle that the development effort entailed in building such a reactor be minimized.

The results of the study are presented herewith, the outline of a sound, but by no means optimum, reactor. Its design output is 129,445 pounds of steam per hour at the stated conditions, which corresponds to 17,500 shaft horsepower in a naval steam plant and to 47.25 Mw of heat. The design is believed to be conservative in that it appears able to carry its design load easily.

We have thought of this superheating water-boiler as a ship propulsion reactor, and its capacity, arrangement, shielding and control system are appropriate to that application.

In carrying out such a preliminary design, we had to limit what we undertook in order to keep the amount of work within bounds. We have

endeavored to establish three things about this reactor; feasibility, size and weight. We therefore attacked every problem necessary to the reactor's successful operation which had not already been solved by others and carried the design through far enough to assure successful operation. We likewise attacked every problem whose solution would significantly affect the weight or size of the reactor plant, notably biological shielding and mechanical design.

We did not consider such problems as water treatment and the mechanical design of control rod drives, which have been well solved elsewhere. In general, those matters pertaining to boiling reactors which we have not investigated are well treated in reference 34. Since this reactor is thermodynamically equivalent to a conventional oil fired boiler, we have not investigated its associated steam plant, except as to secondary shielding, which we have applied to an existing naval steam plant. The design is probably complete enough to serve as the basis of a rough cost estimate, though we have not made one.

1.2 General Description

This reactor has a core in the shape of the usual right circular cylinder (see Figure 1-1 and 1-2), divided radially into three regions; a central superheater, an annular boiler and a surrounding reflector. Moderators are beryllium oxide in the superheater and water in the boiler and reflector. Superheater fuel elements consist of three concentric tubes of type 347 stainless steel containing UO_2 particles in a stainless steel matrix (Figure 1-3). The boiler elements are of conventional plate type, also of UO_2 and stainless steel, type 347 (Figure 1-4).

UNCLASSIFIED
ORNL-LR-DWG. 28536

No.	ITEM	DESCRIPTION
1	CONTROL ROD DRIVES	PRESSURIZED MOTOR & COLUMN
2	STEAM SCRUBBERS	
3	HEAD THERMAL SHIELD	
4	REACTOR VESSEL HEAD	74" INSIDE DIA.
5	BOLTED CLOSURE	38-4" STUDS ON 92" B.C.
6	"O" RING SEALS	STAINLESS
7	CONTROL ROD DRIVE SHAFTS	
8	SUPERHEATER ALIGNMENT SEAL	
9	BOILER CONTROL RODS	BOX SHAPED - 8 REQRD.
10	SUPHTR. CONTROL RODS	CROSS SHAPED - 5 REQRD
11	COOLANT CIRCULATING LOOPS	3 LOOPS PER REACTOR
12	PUMP ISOLATING VALVES	HYDRAULICALLY OPERATED
13	STEAM GUIDE SHROUD	
14	HOLD DOWN PLATE	
15	HOLD DOWN RODS	
16	THERMAL SHIELD	
17	BOILING ELEMENTS	116 REQRD.
18	SUPHTR. HOUSING & INSULATION	INSULATION- CORRUGATED STAINLESS STEEL
19	SUPERHEATING ELEMENTS	32 REQRD.
20	SUPHTR. GUIDE TUBES	
21	REACTOR VESSEL	74" INSIDE DIA.
22	SUPHTR. SOLID MODERATOR	BeO
23	SUPHTR. STEAM OUTLET	DOUBLE WALL INSULATED
24	STEAM OUTLET PLENUM	DOUBLE WALL INSULATED
25	BLR. SUPPORT STRUCTURE	
26	SUPHTR. SUPPORT PLATE	
27	CONT. ROD GUIDE TUBE	GUIDES EXPELLED FUEL ELEMENT
28	CIRCULATING PUMP	CANNED ROTOR - DOUBLE SUCTION - 11,000 GPM @ 30' HEAD
29	PRESSURE RELIEF LINE	
30	FEEDWATER INLET	3 REQRD.
31	PREHEAT STEAM LINE	3 REQRD.

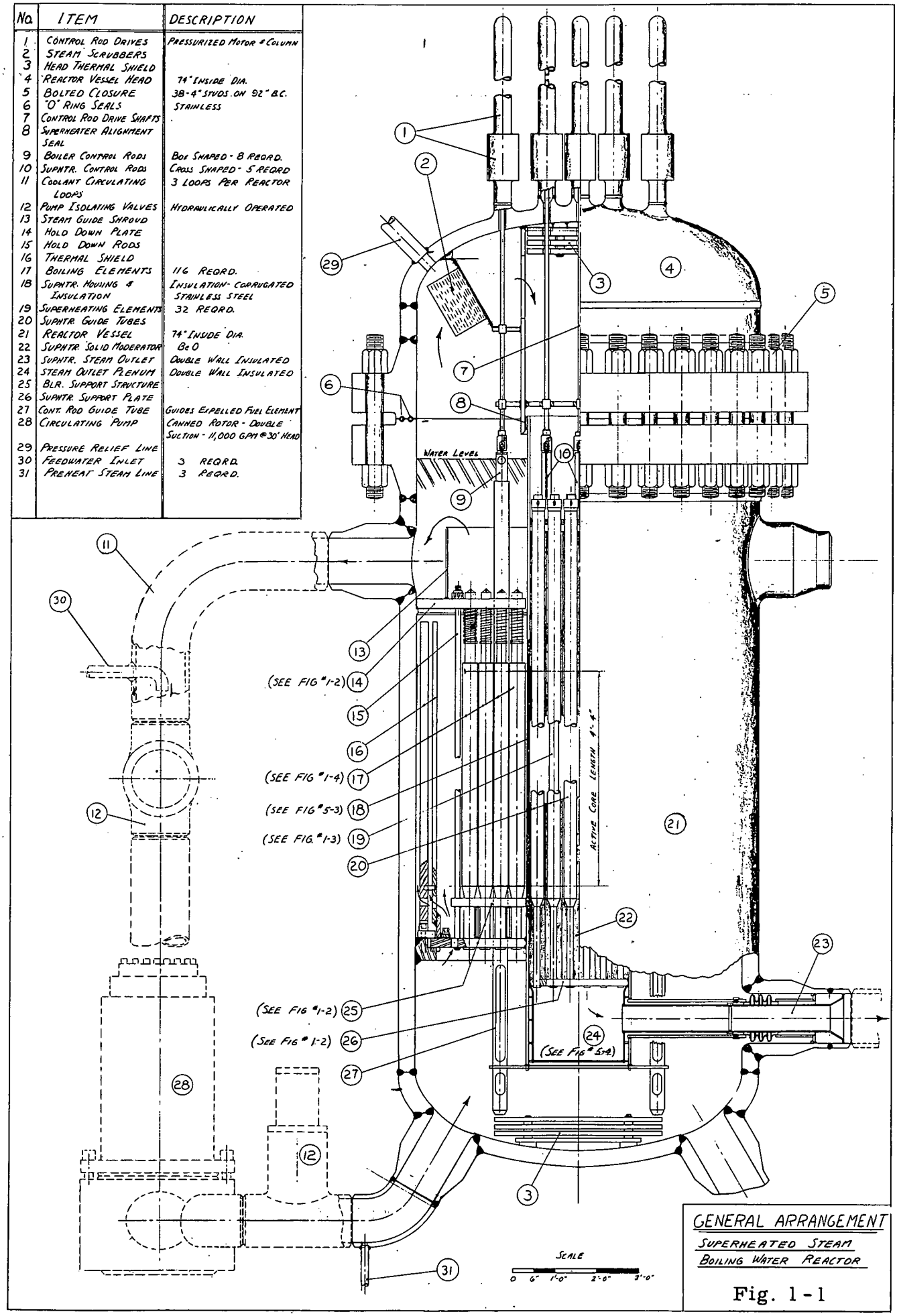

GENERAL ARRANGEMENT
SUPERHEATED STEAM
BOILING WATER REACTOR

Fig. 1-1

UNCLASSIFIED
ORNL-LR-DWG. 28537

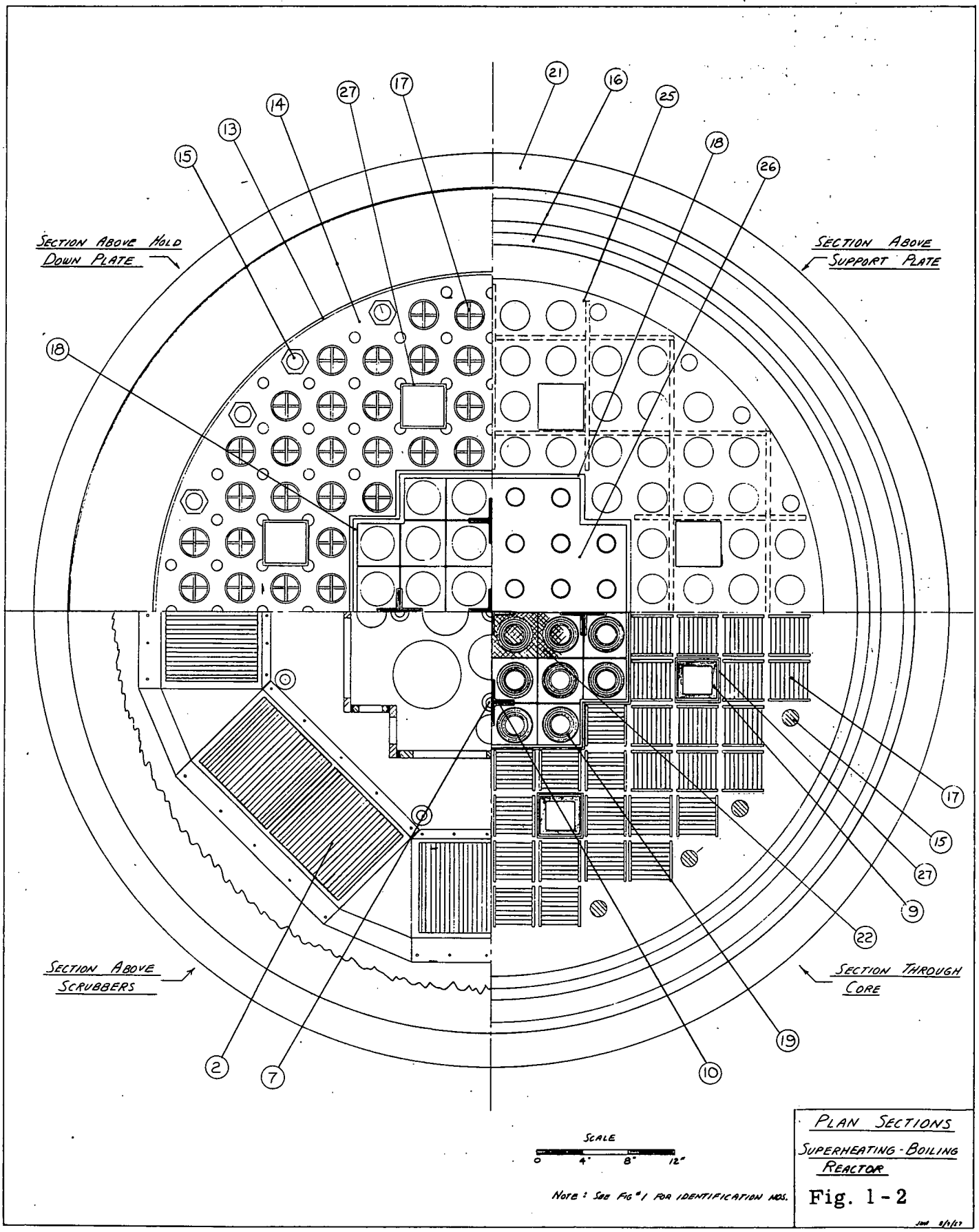

PLAN SECTIONS
SUPERHEATING-BOILING REACTOR
Fig. 1-2

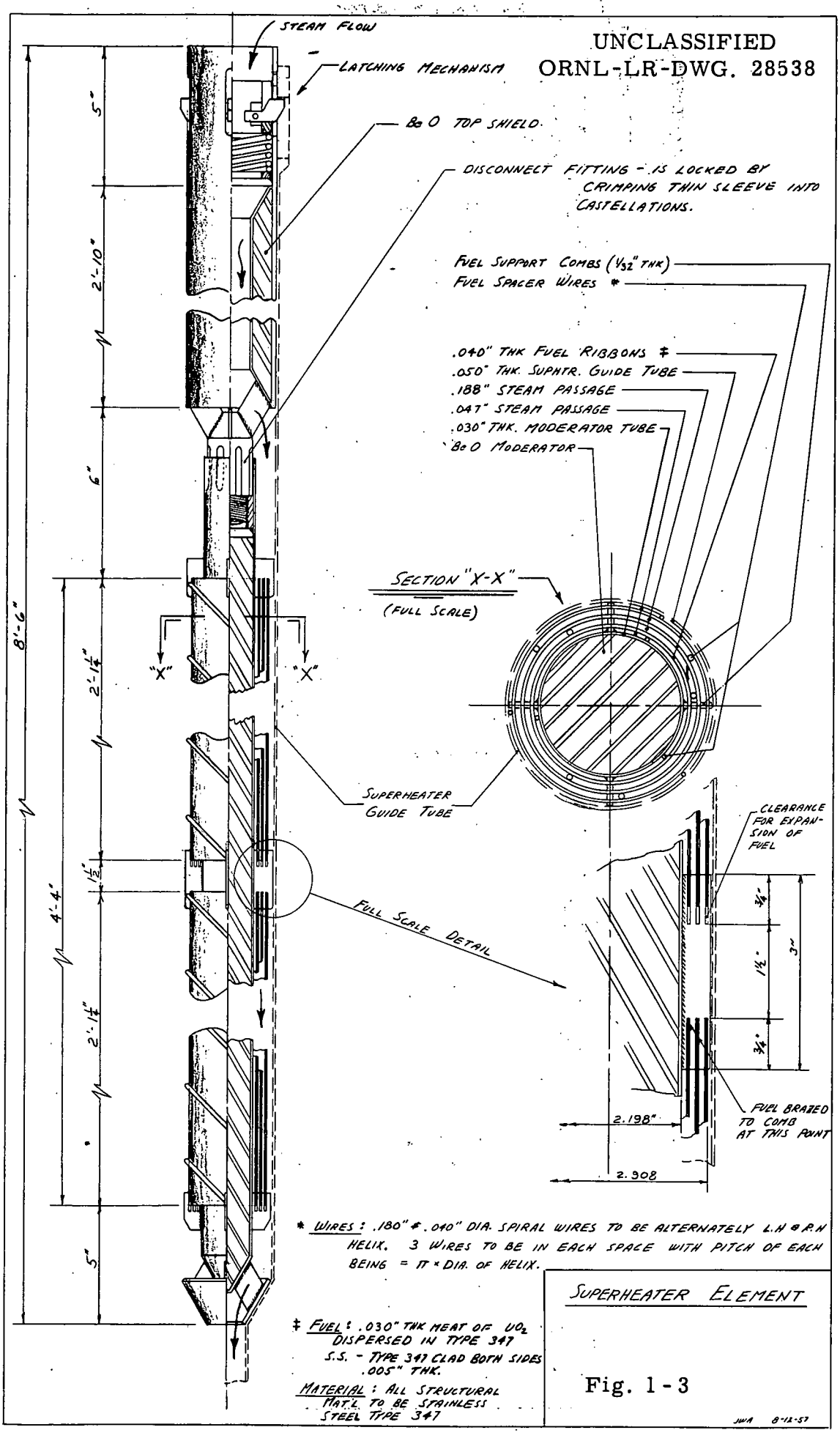

* WIRES : .180" # .040" DIA. SPIRAL WIRES TO BE ALTERNATELY L.H & R.H HELIX. 3 WIRES TO BE IN EACH SPACE WITH PITCH OF EACH BEING = π × DIA. OF HELIX.

‡ FUEL : .030" THK MEAT OF UO_2 DISPERSED IN TYPE 347 S.S. - TYPE 347 CLAD BOTH SIDES .005" THK.

MATERIAL : ALL STRUCTURAL MAT'L TO BE STAINLESS STEEL TYPE 347

SUPERHEATER ELEMENT

Fig. 1-3

JWA 8-12-57

UNCLASSIFIED
ORNL-LR-DWG. 28539

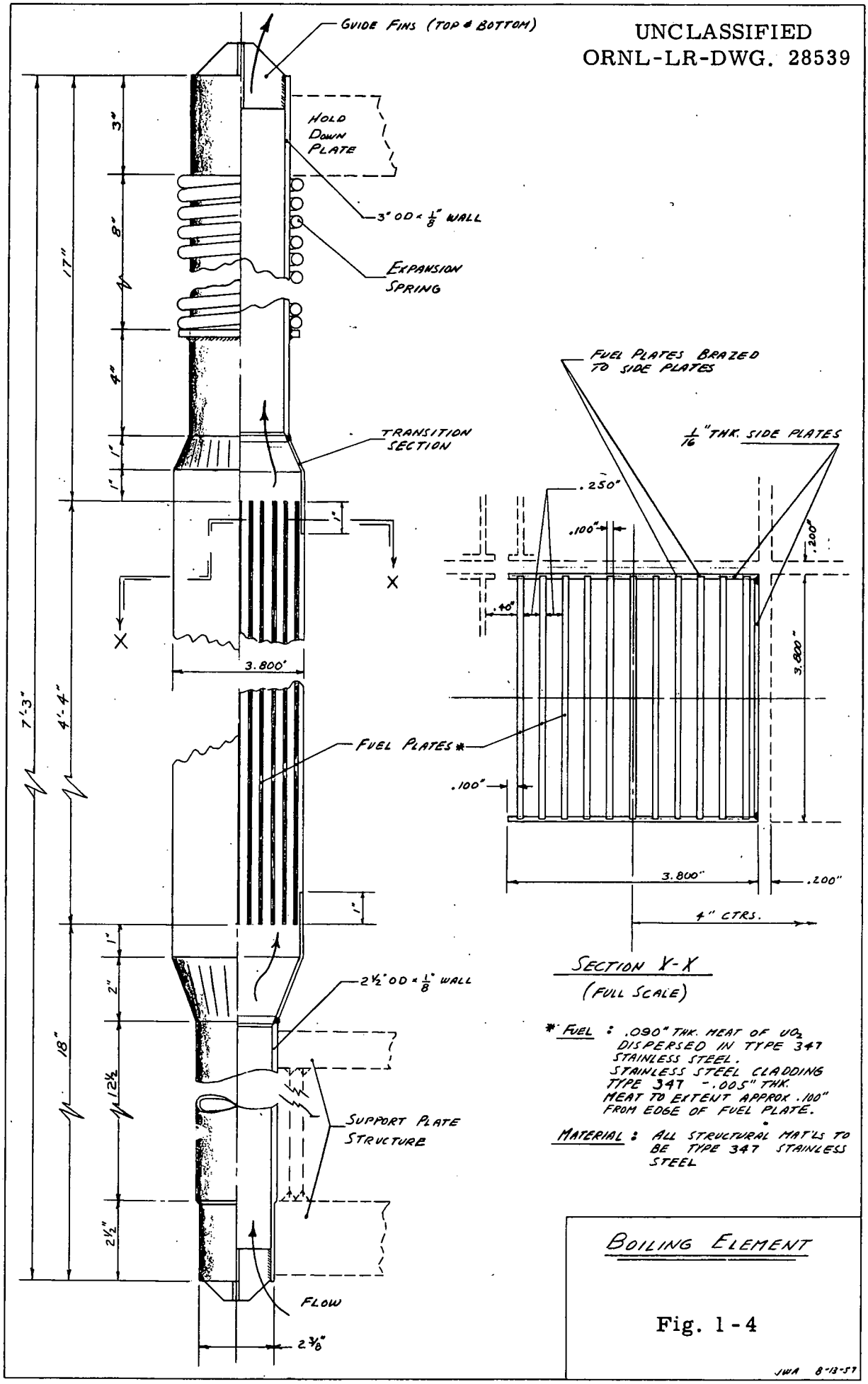

SECTION Y-X
(FULL SCALE)

* FUEL : .090" THK. MEAT OF UO_2 DISPERSED IN TYPE 347 STAINLESS STEEL. STAINLESS STEEL CLADDING TYPE 347 -.005" THK. MEAT TO EXTENT APPROX .100" FROM EDGE OF FUEL PLATE.

MATERIAL : ALL STRUCTURAL MAT'LS TO BE TYPE 347 STAINLESS STEEL

BOILING ELEMENT

Fig. 1-4

JWA 8-13-57

The entire core is laid out on a 4 in. by 4 in. square lattice, there being 32 elements in the superheater and 116 in the boiler, 148 in all. Steam generated in the boiler passes to the steam dome above, through steam dryers, thence through the superheater in a single downward pass and out through the bottom of the pressure vessel. Boiler water is circulated upward through the core by three canned motor pumps on external loops. Of the total power, 23% is developed in the superheater and 77% in the boiler.

1.3 Weights

The value of any reactor plant for ship propulsion, assuming it works and is safe, depends largely on its weight. Below is a summary of the weights of this superheating water-boiler and of the shielding chargeable to it in a marine plant.

Item	Weight, lbs.	Specific Weight, lbs/shp
Reactor, wet	279,600	8
Circulating pumps, valves and piping wet	70,000	2
Primary shield, wet	1,334,000	38
Secondary Shielding	60,900	2
Total	1,744,500	50

In a typical destroyer, the weight of the items which this reactor replaces amounts to 32 lbs/shp, in a WW II destroyer escort to 74 lbs/shp.

For contrast, the weight of shielding alone on one 22,000 shp pressurized water merchant ship propulsion plant design is 91 lbs/shp.

Evidently the reactor designed herein is light enough for most marine service. As is pointed out elsewhere, it can no doubt be made lighter by more careful and time consuming design.

1.4 Design Procedure

Design of a superheating water-boiler involves problems peculiar to the type; so that a brief description of the design procedure used may be of interest. First, consider the choice of reactor configuration.

Preliminary heat transfer calculations soon showed that little superheat can be obtained from combination boiling and superheating elements, fuel tubes with water outside and steam inside. Boiler and superheater had to be segregated from each other, and a thermal insulation barrier placed between them. The question was how to orient them with respect to each other.

The two alternatives found worth considering were 1) central superheater with surrounding boiler, and 2) central boiler with surrounding superheater, the core in both cases being in the shape of an upright circular cylinder.

Following is a brief discussion of the reasons for choosing the former.

With the central boiler configuration, one discovers the following undesirable conditions:

1. There is a strong radial variation of flux and heat generation across the superheater, giving rise to hot channels in the superheater where fuel element temperatures are limiting.

2. Critical loading of the superheater tends to be greater than the critical loading of the boiler, while the superheater power is only about one quarter that of the boiler.(5) As a result, it becomes difficult or impossible to maintain the boiler-superheater power balance during burnup, and the reactor's outlet steam conditions will change with time.

3. The superheater must be thermally insulated from the boiler water on two sides and on the bottom, introducing a quantity of unwanted material into the core.

4. Refueling of the superheater is hard to arrange. The top of the superheater must be watertight, because water leaving the boiler must pass over the superheater to get to the thermal shield and reflector.

5. Superheater inlet pipes pass through the horizontal leg of the boiler's water circulatin normal to the flow and impede boiler circulation.

All of the above difficulties are relieved by going to the central superheater. This design has a heat generation rate which is relatively flat across the superheater, resulting in radially uniform steam and fuel element temperatures. The critical mass is distributed 17% in the superheater, 83% in the boiler, as compared with the power distribution of 23% in the superheater, 77% in the boiler. Thus the power ratio is easily maintained. Thermal insulation is required only on the outer

boundary of the small central superheater, leaving the top accessible for refueling.

Ginsburgh, et al [1] chose the central boiler in spite of the above objections on the ground that it required only one quarter the critical mass of the central superheater. The difference was accentuated in their case, because they used zirconium boiling elements. Due to the fundamental complexity of designing a superheating water-boiler, both their investigation and ours were essentially one-shot propositions, producing one reactor each and little in the way of parameter studies. We believe that the evidence available is not sufficient to support any general statements as to the size of critical masses in superheating water-boilers or the economic importance of such size.

The design of this reactor was unusually intricate in that the boiler and superheater regions not only had to go critical jointly but also had to generate power in the proportions required by the outlet steam conditions. Additional restrictions were safe heat removal from the superheater and stable operation of the boiler. We had to satisfy these four major requirements by our choices of reactor configuration, region size, fuel element design, materials and uranium enrichment. Changing any one of the latter design parameters affects the reactor with respect to more than one of the four basic requirements; so it is not possible to satisfy all four requirements at once by a straightforward design procedure.

Briefly stated, the design procedure was:

1) Choose reactor configuration.

2) Choose superheater fuel element configuration and superheater reactor size from heat removal considerations.

3) Bearing in mind heat removal, stability and power balance requirements, choose a boiling element configuration and guess a boiling region size.

4) Satisfy criticality and power requirements by varying uranium enrichments in boiler and superheater separately.

Some of these steps were carried out concurrently, but the above was the basic pattern.

While carrying out step 4, one of course hopes that criticality and power balance can be satisfied by the reactor materials and geometry he has chosen. We were fortunate in that our first reactor design came through step 4 unscathed, with reasonable uranium enrichments and only slight radial flux variation across the superheater, where uniform heat generation is valuable. (See Figure 4-8.)

We thus obtained one reactor which satisfied all our requirements but had no time to tackle the design of another and possibly better one. As the work progressed, we saw ways in which the reactor might be improved on the next try at a design. It would be profitable to lower uranium enrichment in the boiler if a size increase could be avoided. This might be accomplished by going to pin type zirconium fuel elements containing bulk UO_2. Weight and space or cost, including that required

for shielding, might be saved either by going to natural circulation in the boiler, which eliminates external loops and canned-motor pumps, though it increases pressure vessel size, or by employing more strongly forced circulation, which reduces pressure vessel size and primary shield weight. We are not presently able to recommend the one course over the other.

2. FUEL ELEMENT MATERIALS

2.1 Boiler

Saturation temperature for 1220 psia steam is 569°F, and, consequently, both Zircaloy-2 and stainless steel were considered as cladding and matrix material.

A one-speed, one-region, critical mass calculation was made for stainless steel fuel elements assuming a 2:1 water to metal ratio, 2100 ft^2 heat transfer area, 93% enriched UO_2 fissionable materials in a stainless steel matrix; a similar calculation was made for Zircaloy fuel elements assuming fully enriched uranium in a zirconium-uranium alloy. The stainless steel core required a critical mass about three times that of the Zircaloy core. However, assuming a Zircaloy fabrication cost a conservative five times greater than for stainless steel, (Ref. 2), a price of $17/gram for fully enriched U-235, an investment charge of 4% per year, fuel life of one year, and equal fuel processing costs, then, the stainless steel fuel costs were only about one-fourth the Zircaloy fuel costs.

While fuel costs were estimated by crude methods, it was concluded that stainless steel would be more economical. It was, therefore, selected for the boiler fuel elements.

Ref. 3 showed that 304L low carbon stainless steel was suitable for cladding in pure water at temperatures up to 800° - 1000°F. Type 347 stainless steel has similar corrosion resistance to water, but it is stabilized against carbide precipitation at the grain boundaries; consequently, it was specified for boiler fuel element cladding and matrix.

10,000 hours of full power operation result in the destruction of 1.5% of the uranium atoms, while 0.1% of all atoms in the fuel meat are destroyed. Radiation damage and dimensional changes should be minor at these low burnup rates, and possibly it might be more economical not to change boiler fuel elements each time the superheater is refueled.

Powdered stainless steel containing 35% by volume of powdered 7.2% enriched UO_2 was chosen for the 0.090" thick matrix because of the substantial development background this material has from its use in the Army Package Power Reactor, APPR-1. The weight percent of UO_2 in the fuel meat is 40%, or about 14% more than in the APPR elements, however, it is considered fabricable with present technology. (Ref. 2.)

2.2 Superheater

Among fuel element materials suitable for service at 1216°F surface temperature in superheated steam, only stainless steel was thought to be sufficiently developed from the fabrication standpoint to merit consideration for this feasibility study.

Limited tests in Ref. 4 showed low corrosion rates for 347 stainless steel in supercritical water in this temperature range, this steel also has shown good resistance to intergranular carbide precipitation, and it was consequently adopted for cladding and matrix.

Early in this study, nuclear considerations indicated a highly enriched superheater fuel element, and again a powdered stainless steel matrix containing dispersed UO_2 appeared to require least amount of development.

Cladding thickness is .005", fuel matrix is .030" thick, resulting in a 16% weight fraction of 93% enriched UO_2 in the matrix, sufficient for 10,000 hours of operation at full power.

Burnup will result in the destruction of 26% of uranium atoms, and 0.8% destruction of all the atoms in the fuel meat. No data were found defining the burnup limitations of UO_2 - powdered stainless steel fuel matrices operating near the design temperature of 1216°F.

Extrapolation of limited data given in reference 5, indicated that 26% burnup might be optimistic, but the information was considered inconclusive because results were limited to conditions outside the region of interest. If tests were to show that 26% burnup is unobtainable, the endurance of the plant would, of course, have to be reduced accordingly.

3. HEAT TRANSFER

3.1 Superheater Region

3.1.1 Choice of the Fuel Elements

A removal of the heat generated in the superheater is a difficult problem due to the poor heat transfer properties of the superheated steam. Hence, three types of fuel elements were investigated.

3.1.1.a Element Boiling the Water and Superheating the Steam

A tubular element was considered with water boiling on the outside of the tube and superheated steam flowing down through the inside of the tube.

This type of element was rejected because of two main reasons.

First, the thermodynamic power cycle requirements demand that 23% of the total heat is transferred to the dry steam and the rest of it to the boiling water. This was impossible to accomplish with the above elements without insulating each element on the boiling side. The calculation indicated that most of the heat flowed from the tube wall to the boiling water due to a much lower thermal resistance at the boiling surface of the tube. Enough heat could not be transferred to the steam side to raise steam conditions to the desired level of superheat.

Secondly, this type of element would have a very high temperature gradient across its wall due to boiling on one side and superheated steam on the other.

3.1.1.b Small Diameter Tubes

As a result of the difficulties encountered with the above fuel elements, it was decided to design a three region reactor with a separate

superheater in the center of the core, the boiler surrounding the superheater, and the downcomer acting as a reflector on the periphery of the core.

Small diameter tubes were considered as fuel elements in the superheater region. The smaller the tubes the better heat transfer. It was calculated that about 1580 tubes 1/8" I.D. and 5'-10" long would be needed. This arrangement was rejected because of structural reasons and high pressure drops.

The situation could be improved by the multipass arrangement of the superheater elements. However, this would present several structural problems, not reduce the high pressure drops, and in addition would introduce pressure gradients from one pass to another.

3.1.1.c Concentric Rings with Helical Wires

The heat transfer rate is improved by a small equivalent hydraulic diameter, or in other words, by a small flow area and a large heat transfer surface per element. Therefore, a concentric ring element was tried and chosen as a final superheater fuel element. (Fig. 1-3.)

To improve the heat transfer, it was necessary to decrease the flow area even more than shown on the drawing. A further narrowing of the steam gaps was impractical. Therefore, it was decided to distort the straight axial steam flow by forcing the steam to flow around the tubes in a helical path provided by the wires wrapped inside the gaps and welded to the fuel tubes. (See description in 5.3.3.)

The pitch of the helix was chosen to be equal to πD. A smaller pitch would increase the steam velocity and thus improve the heat transfer even more. However, structurally this would not be sound, since the wire would be too loose between the spot welds.

From the geometry of the element it may be shown that the axial flow area A_a is reduced to a helical flow area A_h:

$$3.(1) \qquad A_h = \frac{A_a}{\sqrt{1 + \left(\frac{\pi D}{l}\right)^2}}$$

where l is the ptich of the helix and D diameter of the tube. For $l = \pi D$, $A_h = 0.707\ A_a$.

The calculations show that 32 elements 4'-4" long are needed. They are arranged in a square lattice on 4" centers.

Practically all the heat generated in the fuel tubes is picked up by the steam flowing down the steam gaps. There is some heat generated in the moderator due to neutron scattering collisions and gamma attenuation. However, there are partial steam passages provided close to the moderator. Hence, the heat generated in BeO is removed by the steam flowing next to the moderator. Heat leakage from the superheater is negligible (see 5.3.3).

This type of fuel element has four steam gaps that are not equivalent to each other from the heat transfer point of view. Two of these gaps are bounded by the fuel tubes on both sides, while the outermost and the innermost gaps are bounded by a fuel tube on one side and moderator on another. The heat flux at the moderator surface is much lower than that

at the fuel tube. Hence, there exists a problem of the unequal steam temperatures in different stam gaps.

The radial steam temperature variation was reduced by two means. First, the width of the steam passages facing the moderator was narrowed; and secondly, a discontinuity in the fuel tubes was provided along the path of the steam. Flow obstructions were introduced at the discontinuities to stimulate the radial mixing of the steam. This mixer was located in the middle of the steam path to assure about equal steam temperatures immediately below the midpoint of the element where the wall surface temperatures are expected to be maximum.

3.1.2 Maximum Temperature in the Superheater

The temperatures in the superheater are expected to be much higher than in the boiler. The maximum fuel temperature in the superheater is a limiting factor in the design of the reactor. Its magnitude must be known relatively accurately, as it is decisive in the feasibility of the reactor.

The maximum expected temperature may be obtained from the neutron track length and the geometric configuration of the superheater elements.

In addition, there are contingent effects that may or may not exist. Inclusion of all these contingencies determines the maximum possible temperature.

3.1.2.a The Maximum Expected Temperature

Temperatures in the superheater depend on the internal heat generation rate. The average heat generation rate per unit volume is,

3.(2) $$\bar{\bar{\bar{g}}} = \frac{Qsh}{Vsh} = \frac{37.4 \times 10^6 \text{ Btu/hr}}{.726 \text{ ft}^3} = 51.5 \times 10^6 \text{ Btu/hr. ft}^3$$

The volumetric heat generation rate is proportional to the neutron track length, which in turn is a function of the core radius and its height $\phi(r, z) = \psi(r)\, \xi(z)$.

First, the hottest channel was picked in the superheater at the center of the superheater where the generation rate is maximum. $\bar{\bar{\bar{g}}}(r = 0)$ here is related to the average $\bar{\bar{\bar{g}}}$ by the radial flux factor

3.(3) $$\frac{\bar{\bar{\bar{q}}}(r=0)}{\bar{\bar{\bar{g}}}} = \frac{\Sigma_{f,1}\, \psi_1(0) + \Sigma_{f,2}\, \psi_2(0)}{\Sigma_{f,1}\, \bar{\psi}_1 + \Sigma_{f,2}\, \bar{\psi}_2} = 1.05.$$

This was evaluated by using nuclear constants known from the flux plot obtained by a two-group, three-region machine calculation. The constants in the superheater are:

$\Sigma_{f,1}$	$= 0.00203 \text{ cm}^{-1}$	fast fission cross section
$\Sigma_{f,2}$	$= 0.0215 \text{ cm}^{-1}$	thermal fission cross section
$\frac{\psi_1(0)}{\bar{\psi}_1}$	$= \frac{1}{0.905} = 1.107$	ratio of radial fast flux in the center of the superheater to average fast flux
$\frac{\psi_2(0)}{\bar{\psi}_2}$	$= \frac{0.108}{0.107} = 1.01$	ratio of radial thermal flux in the center of the superheater to average thermal flux
$\frac{\bar{\psi}_1}{\psi_2}$	$= \frac{0.905}{0.107} = 8.46$	ratio of average fast radial flux to average thermal flux.

Next, the axial variation of the heat generation rate was investigated. A cosinu-soidal variation of the neutron track length was assumed in the axial direction (this would not be true near the boiling region, but in the center of the superheater the assumption is valid). Also no neutron reflection was assumed at the ends (this is a conservative assumption tending to increase the ratio of the maximum axial flux to the average flux).

The maximum axial flux in a cosinu-soidal variation is at the midpoint of the steam flow down the hot channel. However, the maximum fuel element surface temperature is below the midpoint. A direct solution to locate the maximum surface temperature is very cumbersome in an unsymmetrical configuration. However, a graphical solution located the maximum surface temperature at $Z/L = 0.74$. See Appendix A, Fig. A(2).

$$3.(4) \qquad \frac{\xi\,(z/L = .74)}{\bar{\xi}} = \frac{\sin(.74\pi)}{2/\pi} = \frac{.730}{.636} = 1.15$$

Having obtained the radial flux factor = 1.05 and the axial flux factor = 1.15, the maximum superheater temperature could be calculated using a set of equations derived in the Appendix A.

$$A(24) \qquad q_4'' = \frac{(t_{s4} - t_{s1}) - q'''\left[\frac{R_3^2 \ln R_3/R_2}{2k_m} + (R_3^2 - R_2^2)\left(\frac{1}{2h_1R_1} + \frac{\ln R_2/R_1}{2k_c} - \frac{1}{4k_m}\right)\right]}{\frac{R_4}{k_c}\ln\frac{R_1R_3}{R_2R_4} - R_4\left(\frac{\ln R_3/R_2}{k_m} + \frac{1}{h_1R_1} + \frac{1}{h_4R_4}\right)}$$

$$= 86{,}415 \ \frac{BTU}{hr\text{-}ft^2}$$

The above equation was evaluated at the hottest spot in the superheater or at the inner-most fuel ring of the center channel at Z/L = 0.74. The constants used in equation A(24) are listed below and also in Appendix A.1:

$\ddot{q}''' = \bar{\ddot{q}}''' \times 1.05 \times 1.15 = 62 \times 10^6$ Btu/hr-ft^3

$t_{s4} \simeq t_{s1} = 895$ obtained from equation A(35)

$h_1 = 375$ Btu/hr-ft^2-$^\circ$F, read from the graph A(1)

$h_4 = 470$ Btu/hr-ft^2-$^\circ$F, read from the graph A(1)

From equation A(23):

$$\ddot{q}_1'' = \ddot{q}_4'' \frac{R_4}{R_1} - \ddot{q}''' \frac{(R_3^2 - R_2^2)}{2R_1} = 68.275 \frac{Btu}{hr\text{-}ft^2}$$

From equation A(19):

$$t_1 = t_{s1} - \frac{\ddot{q}_1''}{h_1} = 895 + 182 = 1077^\circ F$$

From equation A(21):

$$t_2 = t_{s1} - \frac{\ddot{q}_1''}{h_1} - \frac{\ddot{q}_1'' R_1}{K_c} \ln \frac{R_2}{R_1} = 1077 + 2 = 1079^\circ F$$

From equation A(22):

$$t_3 = t_{s4} + \frac{\ddot{q}_4''}{h_4} - \frac{\ddot{q}_4'' R_4}{K_c} \ln \frac{R_3}{R_4} = 895 + 184 + 3 = 1082^\circ F$$

From equation A(20):

$$t_4 = t_{s4} + \frac{\ddot{q}_4''}{h_4} = 895 + 184 = 1079^\circ F$$

Maximum temperature located radially by equation A(25)

$$R_{max} = \sqrt{\frac{\frac{2K_m}{q'''}(t_3 - t_2) + \frac{1}{2}(R_3^2 - R_2^2)}{\ln \frac{R_3}{R_2}}} = .09728 \text{ ft.} = 1.167 \text{ in.}$$

Maximum temperature obtained from equation A(26)

$$t_{max} = t_2 + \frac{q'''}{4K_m}(R_2^2 - R_{max}^2) + \left[(t_3 - t_2) + \frac{q'''}{4K_m}(R_3^2 - R_2^2)\right] \frac{\ln \frac{R_{max}}{R_2}}{\ln \frac{R_3}{R_2}} = 1089^\circ F$$

3.1.2.b Maximum Possible Temperature

The expected temperatures may be altered by several contingent effects discussed in the Appendix A.5. The maximum possible temperature was calculated by using total hot channel factors of Appendix A.5:

t_s =		= 567°F, inlet steam temperature
$(\Delta t_s)_A = F_s(\Delta t_s)_4$	= 1.61 x 328	= 528°F, steam temperature rise
$(\Delta t_h)_A = F_h(\Delta t_h)_4$	= 1.21 x 182	= 220°F, film temperature drop
Δt_{sc_1}		= 28°F, scale temperature drop
$(\Delta t_f)_A = F_f(\Delta t_f)_4$	= 1.44 x 12	= 17°F, fuel tube temperature drop

The maximum possible temperature = 1360°F.

3.1.2.c Design Temperature

1360°F, the maximum possible temperature, would occur if all the adverse effects considered in Appendix A.5 existed simultaneously. This is very unlikely to take place. A reasonable maximum temperature was estimated assuming only the effect of a large distortion of axial neutron

track length due to a sudden withdrawal of the central control rod.

The maximum reasonable temperature was calculated by using the hot channel factors for the effects of the control rods.

t_s = = 567, inlet steam temperature

$(\Delta t_s)_A = F_s(\Delta t_s)_4 = 1.27 \times 328 = 416$, steam temperature rise

$(\Delta t_h)_A = F_h(\Delta t_h)_4 = 1.27 \times 182 = 231$, film temperature drop

$(\Delta t_f)_A = F_f(\Delta t_f)_4 = 1.27 \times 12 = 15$, fuel tube temperature drop

The maximum reasonable temperature = 1229°F (This was used as a design limitation)

3.1.2.d Summary of Hot Channel Temperature Distribution

The maximum temperature is expected in the inner-most fuel tube of the center channel at $^{Z}/_{L} = 0.74$.

Radial Location	Expected Radial Temp. Distribution	Approximate Maximum Reasonable Radial Temp. Distribution	Approximate Maximum Possible Radial Temp. Distribution
Narrow steam gap	$t_{s1} = 895°F$	$t_{s1} = 983°F$	$t_{s1} = 1095°F$
Surface of the Inner Scale	t_{sc1} =	t_{sc1} =	$t_{sc1} = 1315$
$R_1 = 0.09550$ ft	$t_1 = 1077$	$t_1 = 1214$	$t_1 = 1343$
$R_2 = 0.09592$	$t_2 = 1079$	$t_2 = 1217$	$t_2 = 1346$
$R_{max} = 0.09728$	$t_{max} = 1089$	$t_{max} = 1229$	$t_{max} = 1360$
$R_3 = 0.9842$	$t_3 = 1082$	$t_3 = 1220$	$t_3 = 1350$
$R_4 = 0.09883$	$t_4 = 1079$	$t_4 = 1216$	$t_4 = 1346$
Surface of the Outer Scale	t_{sc4} =	t_{sc4} =	$t_{sc4} = 1310$
Main Steam Gap	$t_{s4} = 895$	$t_{s4} = 983$	$t_{s4} = 1095$

3.1.3 Pressure Drop through the Fuel Elements

The total pressure drop consists of the friction drop, end losses, and the loss at the mixer.

(a) The friction drop is calculated for the full width steam gaps Ref.(9)

3.(5) $$\Delta p = f \cdot \frac{L}{De} \cdot \frac{\rho U^2}{2g} = 5.61 \text{ psi}$$

f = 0.02 friction factor for drawn tubing at R_e = 82,300

$L = 4.33\sqrt{1 + \left(\frac{\pi D}{1}\right)^2} = 4.33\sqrt{1 + 1} = 6.13$ ft, length of steam path

D_e = 0.01566 ft. equivalent hydraulic diameter

ρ = 1.9 #/ft.^{3} average specific weight of steam at 1200 psi and

$$t_s = 758^\circ F$$

$$U = \frac{G}{\rho \times 3600} = \frac{405{,}000}{1.9 \times 3600} = 59.2 \text{ fps, average steam velocity}$$

(b) End Losses

$$\text{Inlet loss} = 0.5\left(\frac{\rho U^2}{2g}\right) = 0.358 \text{ psi}$$

$$\text{Outlet loss} = 1\left(\frac{\rho U^2}{2g}\right) = 0.716 \text{ psi}$$

$$\text{Total end losses} = 1.074 \text{ psi}$$

(c) Pressure loss at the mixer. At the mixer there is a discontinuity of fuel tubing. Hence, there are inlet and outlet losses as computed above, and in addition a pressure loss due to an obstruction provided by the mixer. These losses were added up

$$\Delta p \simeq 1.074 + 0.242 = 1.316 \text{ psi}$$

The total superheater loss is a sum of the pressure losses computed in parts a, b, and c.

Total $\Delta p = 5.61 + 1.074 + 1.316 =$ 8 psi .

3.1.4 Thermal Stresses in the Fuel Elements

The maximum thermal stresses are expected near the center of the fuel meat and at the surface of cladding in the hot channel. The thermal stresses could be approximated by the equations given in Ref. (6), page 709.

At the center of the fuel meat

$$3(6)\quad \sigma = -\left(\frac{\alpha E}{2k_m(1-\nu)}\right) q''' \left(\frac{R_3-R_2}{2}\right)^2 \left[\frac{2(R_4-R_3)}{(R_3-R_2)} + \frac{2(R_3-R_2)}{3(R_4-R_1)}\right] = -2{,}700 \text{ psi}$$

At the surface of the cladding

$$3(8)\quad \sigma = \left(\frac{\alpha E}{2k_c(1-\nu)}\right) q''' \left(\frac{R_3-R_2}{2}\right)^2 \left[1 + \frac{2(R_4-R_3)}{(R_3-R_2)} - \frac{2(R_3-R_2)}{3(R_4-R_1)}\right] = 1{,}960 \text{ psi}$$

where $\frac{\alpha E}{2k_m(1-\nu)} = \frac{10.7\times10^{-6}\times20\times10^{6}}{2 \times 9.2 \times .7} = 16.6 \ \frac{\#\text{-hr-ft}}{\text{Btu-in}^2}$ in the fuel meat

$$\frac{\alpha E}{2k_c(1-\nu)} = \frac{10.7\times10^{-6}\times20\times10^{6}}{2\times 12.8 \times .7} = 12 \ \frac{\#\text{-hr-ft}}{\text{Btu-in}^2}$$ in the cladding

$$q''' = \frac{Q_{SH}}{V_{SH}} \times 1.05 \times 1.15 \times 1.44 = 51.5 \times 10^6 \times 1.05 \times 1.15 \times 1.44$$

$$= 89.5 \times 10^6 \text{ Btu/hr-ft}^3$$

The elements are not likely to fail by thermal stresses, because the computed stresses are considerably below 3500 psi, the creep strength required to produce 1% creep in 10,000 hr. for 347 stainless steel at the maximum possible temperature of 1360°F.

3.2 Boiler Region

3.2.1 Choice of the Fuel Element

The temperatures in the boiler are relatively low due to a better heat transfer rate and a lower coolant temperature. The choice of the MTR-type fuel elements was dictated by structural and nuclear considerations.

3.2.2 The Burnout Heat Flux

The limiting factor in the boiler is not a maximum temperature, but the burnout flux or a heat flux at which the nucleate boiling ceases and the partial film boiling starts. It was necessary to check the actual heat flux and see that it remained below the burnout flux.

$$3(9) \quad \bar{q}'' = \frac{Q_{Blr}}{S_{Blr}} = \frac{123.9 \times 10^6 \text{ Btu/hr}}{3200 \text{ ft}^2} = 38{,}700 \frac{\text{Btu}}{\text{hr-ft}^2}$$

The radial flux factor in the boiler is

$$3(10) \quad \frac{q'''(R=32.4 \text{ cm})}{\bar{q}'''} = \frac{\Sigma_{f21}\Psi_{21}(32.4) + \Sigma_{f22}(32.4)}{\Sigma_{f21}\bar{\Psi}_{21} + \Sigma_{f22}\bar{\Psi}_{22}} = 1.53$$

Nuclear constants used in the evaluation of the radial flux factor were obtained from the two-group, three-region criticality calculations. The constants in the boiler are

$\Sigma_{f21} = 0.00272 \text{ cm}^{-1}$, fast fission cross section

$\Sigma_{f22} = 0.0335 \text{ cm}^{-1}$, thermal fission cross section

$\frac{\Psi_{21}(32.4)}{\bar{\Psi}_{21}} = \frac{0.8058}{0.4539} = 1.78$ ratio of radial fast flux at R = 32.4 cm to the average fast flux in the boiler

$\frac{\Psi_{22}(32.4)}{\bar{\Psi}_{22}} = \frac{0.1132}{0.0796} = 1.42$ ratio of radial thermal flux at R = 32.4 cm to the average thermal flux in the boiler

$$\frac{\bar{\Phi}_{21}}{\bar{\Phi}_{22}} = \frac{0.4539}{0.0796} = 5.7$$ ratio of average fast flux to the average thermal flux in the boiler

The axial component of the neutron track length is not cosinusoidal in the boiler. The axial flux ratio in a cosinusoidal distribution would be $\pi/2 = 1.57$. However, this was increased to 2 due to a flux distortion in the boiler region.

The maximum heat flux is expected to be below the midpoint of the boiler channels facing the boundary of the superheater region

$$3(11) \quad q''_{max} = \bar{q}'' \times 1.53 \times 2 \times 1.44 = 171{,}000 \text{ Btu/hr-ft}^2$$

A conservative value of the burnout flux is about 500,000 Btu/hr-ft^2, which is considerably above the maximum expected heat flux.

3.2.3 Maximum Temperature in the Boiler

3.2.3.a The Maximum Expected Temperature

The maximum temperature in the boiler was determined by the equation A(41) in the Appendix A.2

$$A(41) \quad t_{max} = t_{sat} + q'' \left(\frac{1}{h} + \frac{x_2 - x_1}{k_c} + \frac{x_1}{2k_m}\right) = 569 + 10 + 24 = 607^{\circ}\text{F}$$

where $t_{sat} = 569^{\circ}$F, saturation temperature at 1220 psi

$q'' = 118{,}500$ Btu/hr-ft^2, max. expected heat flux

$x_1 = 0.045" = 0.00375$ ft, half the thickness of fuel meat

$x_2 - x_1 = 0.005" = 0.000416$ ft, thickness of the cladding

From Ref. 18), page 52

$$3(12) \quad t_2 - t_{sat} = \frac{60 \left(\frac{q''}{10^6}\right)^{.25}}{1^{P/129{,}000}} = 10^{\circ}\text{F}$$ temperature drop through the film

t_2 = surface temperature

P = 1220 psi x 144 = 176,600 #/ft^2 saturation pressure

From equation A(36)

a(36) $$h = \frac{q''}{t_2 - t_{sat}} = \frac{11,850}{10} = 118,500 \frac{Btu}{hr\text{-}ft^2\text{-}^\circ F}$$

3.2.3.b The Maximum Possible Temperature

Expected maximum temperature in the boiler was increased by the hot channel factors. These factors are smaller in the boiler than in the superheater. However, the same factors were used to be safe.

t_{sat}	$= 569^\circ$
$(\Delta t_h)_A = F_h (\Delta t_h)_\Psi = 1.21 \times 10$	$= 12$
$\Delta t_{sc} = \frac{118,500 \times 0.005}{1 \times 12}$	$= 50$
$(\Delta t_f)_A = F_f (\Delta t_f)_\Psi = 1.44 \times 28$	$= 40$
The maximum possible temperature	$= 671^\circ F$

3.2.3.c Summary of Hot Channel Temperature Distribution

	Expected Temp. Distribution	Approx. Max. Possible Temperature Distribution
Boiling water	$t_{sat} = 569^\circ F$	$t_{sat} = 569^\circ F$
Surface of the scale	$t_{sc} =$	$t_{sc} = 581$
Surface of the cladding	$t_2 = 579$	$t_2 = 631$
Surface of the fuel meat	$t_1 = 583$	$t_1 = 637$
Center of the fuel meat	$t_{max} = 607$	$t_{max} = 671$

3.2.4 Pressure Drop through the Boiler

3.2.4.a Design Basis

Stability and control considerations required that the average void fraction in the boiling region be limited to 10%. Data for uniform heat generation (Ref. 10) indicate an exit void fraction of 20% corresponding to an average core void fraction of 10%. These calculations did not include the effect of nonuniform heat generation because of the limited scope of this feasibility study.

R, the recirculation ratio, assmuming an exit steam to water slip ratio of unity, was given by the equation

3(12) $$R = \frac{(1 - \alpha_o)\rho_\ell}{\alpha_o \rho_2}$$

resulting in a total coolant flow rate of 7.9×10^6 #/hr.

Average coolant speed in the nonboiling region at the fuel channels was 6 ft/sec while the speed in the external piping was 31 ft/sec.

Primary coolant water is circulated through three separate loops, any two of which are capable of handling full power coolant flow, while one loop will provide standby power. Any loop can be fully isolated in case of pump failure.

3.2.4.b Friction and Turbulence Pressure Drop

Friction pressure drop in the external loop and in the nonboiling region of the reactor was computed by the Darcy equation:

3(5) $$\Delta P = \frac{fLU^2}{D_e 2g}$$

Only fragmentary data are available on the extent of the boiling region, which is a function of the geometrical configuration of the core, flux

distribution, and inlet subcooling. For the purpose of computing the pressure drop in the reactor core, the nonboiling and coiling core height fractions of 0.4 and 0.6 of the EBWR (Ref. 34) were assumed. The friction factor for the boiling region two-phase flow was obtained from Reference (12).

Losses due to contraction, expansion, entrances, elbows, valves, etc., were computed by conventional methods.

3.2.4.c Static Pressure Drop

This pressure drop provided a driving force for the coolant since the average fluid density in the riser passages is smaller than the density in the downcomers. It was computed by taking the average void fraction in the core, α_o, as 10%, the void fraction between the top of the core and the top of the shroud, $\bar{\alpha}_{sh}$, as 20%. The following equation,

3(13) $$\Delta P = (H_c \bar{\alpha}_o + H_{sh} \bar{\alpha}_{sh})(\rho_\ell - \rho_v)$$

indicated a pressure differential of 0.3 psi.

3.2.4.d Acceleration Pressure Drop

The acceleration pressure drop due to the change in density of the coolant and, hence, in the speed of the fluid was given by the following equation:

3(14) $$\Delta P = \frac{\rho_1 U_1 (U_2 - U_1)}{2g}$$

when subscripts 1 and 2 refer to before and after expansion respectively. This loss amounted to only 0.04 psi.

3.2.4.c Results

Total head loss in the recirculating loop amounted to 30 ft. requiring 125 Hp pumps operating at 80% efficiency.

Water leaves the reactor near the saturation temperature. Consequently, the circulation pumps were located as low in the system as possible to provide sufficient net suction head. Applying the Thoma cavitation criterion (Ref. 13), it was estimated that a 11,000 GPM, 900 RPM double suction "mixed flow" pump could operate satisfactorily at a net suction head of 8.5 ft.

3.2.5 Thermal Stresses

The maximum thermal stresses are expected at the center of the fuel meat and at the surface of cladding of the hot channels. The stresses could be approximated by the equation given in Ref. (6), page 709.

At the center of the fuel meat

$$3(15) \quad \sigma = -\left(\frac{\alpha E}{2k_m(1-\gamma)}\right) q''' X_1^2 \left[\frac{X_2-X_1}{X_1} + \frac{2X_1}{3X_2}\right] = -9{,}150 \text{ psi}$$

At the surface of the cladding

$$3(16) \quad \sigma = \left(\frac{\alpha E}{2k_c(1-\gamma)}\right) q''' X_1^2 \left[1 + \frac{X_2-X_1}{X_1} - \frac{2X_1}{3X_2}\right] = 4{,}710 \text{ psi}$$

where $q''' = \frac{Q_{Blr}}{V_{Blr}} \times 1.53 \times 2 \times 1.44 = \frac{123.9 \times 10^6 \text{ Btu/hr}}{12 \text{ ft}^3} \times 1.53 \times 2 \times 1.44$

$$= 45.5 \times 10^6 \frac{\text{Btu}}{\text{hr-ft}^3}$$

$$\frac{\alpha E}{2k_m(1-\gamma)} = \frac{10.7 \times 10^{-6} \times 24.3 \times 10^6}{2 \times 12.8 \times .7} = 20.2 \frac{\#\text{-hr-ft}}{\text{Btu - in}^2} \text{ in the fuel meat}$$

$$\frac{\alpha E}{2k_c(1-\gamma)} = \frac{10.7 \times 10^{-6} \times 24.3 \times 10^6}{2 \times 9.2 \times .7} = 14.5 \frac{\#\text{-hr-ft}^3}{\text{Btu - in}^2} \text{ in the cladding}$$

The elements are not likely to fail by thermal stresses, because the computed stresses are considerably below 14,870 psi, the allowable stress for 347 stainless steel at the maximum possible temperature of 671°F.

3.3 Heat Removal After Shutdown of the Reactor

3.3.1 Design Basis

Decay heat removal after shutdown presents no difficulty if the main circulating pumps are operating, however, it was thought desirable to show that the reactor could be shutdown safely without excessive element temperatures should the circulating pumps have to be secured.

It was assumed that the reactor was shutdown by a scram after continuous full power operation, that the main circulating pumps were stopped simultaneously, while sufficient feedwater was being added to the system to maintain normal water level in the reactor. Six percent of full power steam flow, or 7750 lb/hr, at normal operating pressure and temperature, was taken as the operating condition after shutdown.

The situation at lower heat generation rates, lower pressures and temperatures was left to be analyzed by a more complete study.

3.3.2 Superheater

Heat flow across a unit of superheater heat transfer area can be expressed as $q'' = h\Delta t_h$ where h the heat transfer coefficient was taken as

A.(42) $$h = .023 \frac{k_s}{D_e} (R_e)^{.8} (P_r)^{.4}$$

Under the assumed condition, flow speed would be the only variable in this equation during shutdown, so that the heat flow can be rewritten as

3(17) $$q'' = \lambda U^{.8} \Delta t_h$$

where λ is a constant. Differentiating q" with respect to flow speed and solving for Δt_h, one obtains

3(18) $$\Delta t_h = \frac{U^{.2}}{.8\lambda} \frac{d(q'')}{dU}$$

Assuming the spatial distribution of heat generation in the reactor to be independent of power level, $\frac{d(q")}{dU}$ will be constant for fixed steam temperature and pressure.

The film temperature drop will, therefore, be proportional to $U^{.2}$ and consequently superheater fuel element temperature will decrease with decreasing power. It is therefore concluded that decay heat can be safely removed from the superheater under this particular condition.

3.3.3 Boiler

One circulating loop was considered closed while the pump impellers in the remaining two loops were stationary, with a flow resistance of one velocity head.

The driving head produced by the lower density of the boiling mixture in the core and the normal liquid density in the external downcomers was computed in the same manner as described in Section 3.2.4. A successive number of exit void fractions were assumed, to determine the correct fraction which produced equal driving head and pressure drop in the loop. Average coolant flow speed in the nonboiling region of the core was 0.65 ft/sec, and flow speed in the external coolant piping was 3.4 ft/sec, with a total loop pressure drop of 0.11 psi.

Total flow through the core under these conditions was 880,000 lb/hr, recirculation ratio was 112/1, and core exit steam quality was 0.8%.

According the reference (13) exit steam qualities of 2-3% are adequate for heat transfer, and, therefore, the coolant recirculation in this system is 2-4 times greater than needed for safe heat removal.

3.4 Conclusions

The heat transfer analysis indicated that reactor temperatures, pressure drops and thermal stresses could be maintained at safe levels. However, a more thorough refinement of the design could result in a lighter and probably more reliable system.

Superheater proved to be the most critical region in the reactor. The following are the areas that would need a future study and development:

(a) Helical wires in the superheater elements and

(b) Limiting design temperatures in the superheater.

(a) The helical wires present several problems and possibilities:

1. Thermal stresses would exceed the yield strength of the wires, if expansion loops were not provided.

2. Manufacturing the wires as integral part of the tube cladding would eliminate the thermal stresses and increase the rigidity of the assembly.

3. Varying the pitch of the helix could adjust the heat transfer rate in such a way that the need of half width steam gaps is eliminated.

(b) The temperature limitations in the superheater could be relieved by several design features.

1. The allowable temperatures could be raised appreciably by using nickel or molybdenum base alloys, or pure UO_2.

2. Eliminating the central control rod or preventing it from a rapid withdrawal could result in a smaller distortion of the axial neutron track length.

3. Varying the fuel loading would decrease the ratio of maximum to average neutron track length and thus reduce the maximum operating temperatures.

4. Increasing the cross-sectional area of the steam passages in the central fuel elements would decrease the operating temperatures in the center of the superheater.

4. NUCLEAR DESIGN

4.1 Introduction

Nuclear requirments for the system are dictated by heat transfer criteria as discussed in Chapter 3. These criteria along with materials, Chapter 2, and mechanical design considerations, Chapter 5, fixed the size and geometry of the system. Thus, the nuclear problem consisted of proving the feasibility of a stable, critical system that would operate at the desired ratio of superheater to boiler power density.

Other parameters that were fixed relative to the nuclear calculations are as follows:

For stability in the boiler, the water to metal ratio was fixed at 2:1 with an operating void fraction in the water at 10% (see Fig. 7-1). In the superheater 75% of the volume is moderator which was imposed by the size and heterogeneity of the region. In order to facilitate the study, the parameter chosen to vary was fuel enrichment, in a matrix that contained 35 volume % UO_2.

The procedure consisted of a migration area hand calculation (section 4.2), which enabled one to choose a range of values that would make the most efficient use of computer time. From the ORACLE results a clean critical loading was chosen (Fig. 4-5). This was found to be 19.5% and 5% enrichment in the superheater and boiler, respectively. A calculation of the burnout of fuel in the 10,000 hour lifetime of the system and of the additional amount of fuel necessary to override peak Xe^{135} buildup resulted in an initial loading of 32% and 7% in the —

superheater and boiler, respectively. Inasmuch as a 32% enrichment is not economically practical, a fully enriched superheater was calculated to have a 13 volume % UO_2 in the meat.

ORACLE cases are shown in Table 4-4, and the flux plot is shown in Fig. 4-8.

4.2 Preliminary Calculations

A preliminary determination of the critical loading was carried out by hand calculation to provide a "starting point" for the subsequent machine calculations. For this purpose a migration area model was chosen because of the computational difficulties of a two-group treatment of a three-region reactor. A one-region homogeneous model was considered too crude to give useful results. The equations which were used are derived in Appendix B 1.

The critical equation (Appendix B 1) yields an infinite number of combinations of superheater and boiler loadings that are critical, as shown in Figure 4-1. However, there is only one loading that will give the proper heat generation in each region. The power requirement is:

$$\frac{P_1}{P_2} = \frac{\int_0^{R_1} \Sigma_f^{(1)} \phi_1(r,z)dV}{\int_{R_1}^{R_2} \Sigma_f^{(2)} \phi_2(r,z)dV} = \text{a constant set by the steam flow rate and conditions}$$

ORNL-LR-Dwg.-28540
UNCLASSIFIED

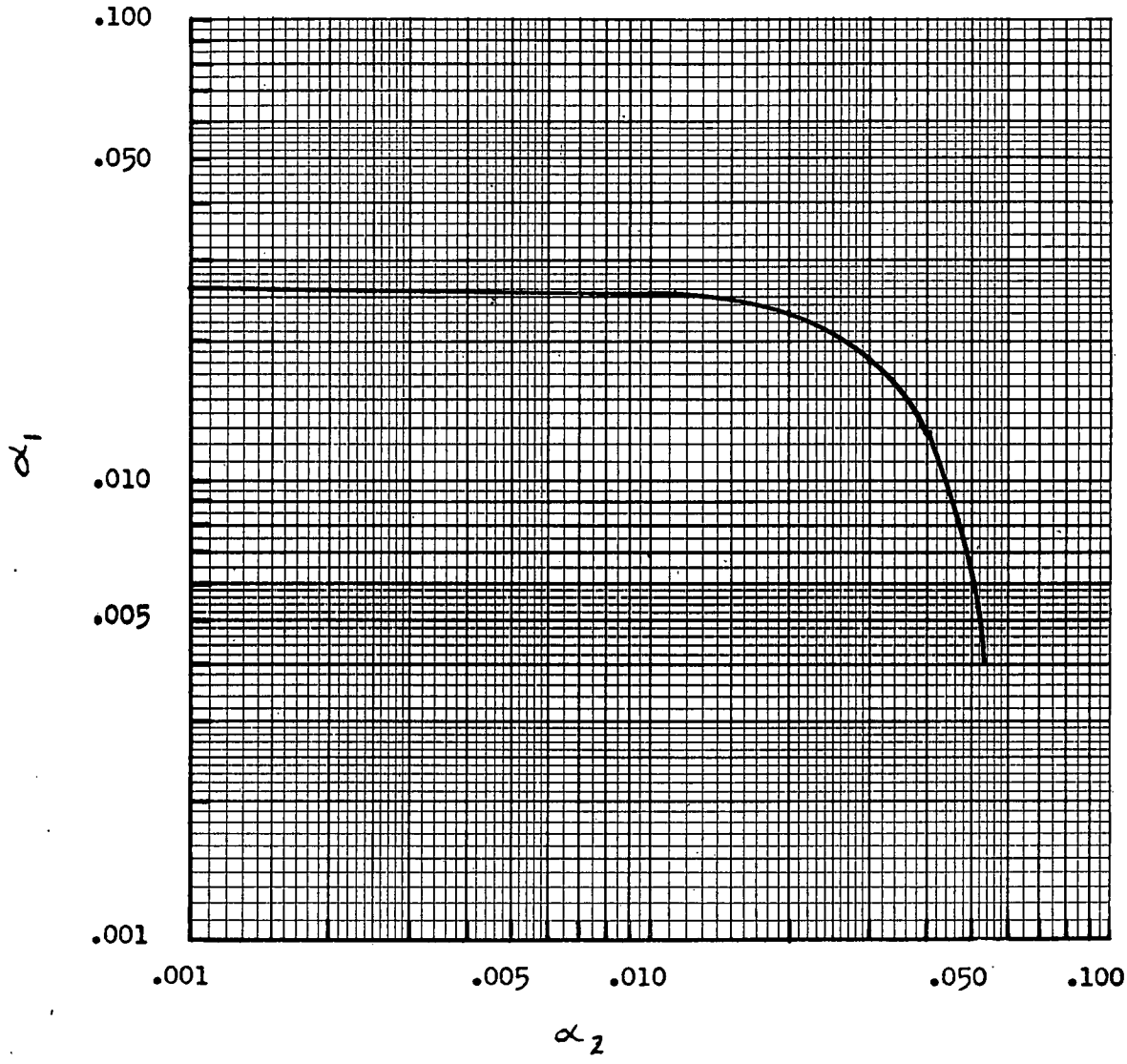

α_1 vs α_2 for critical system

$$\alpha_1^2 = \frac{k_\infty - 1}{M^2} - \left(\frac{\pi}{2h}\right)^2 \quad \text{for superheater}$$

$$\alpha_2^2 = \frac{k_\infty - 1}{M^2} - \left(\frac{\pi}{2h}\right)^2 \quad \text{for boiler}$$

FIGURE 4-1

or in terms of average power densities,

$$\frac{P_1}{P_2} = \frac{\int_0^{R_1} \Sigma_f^{(1)} \phi_1(r,z)dV}{\int_{R_1}^{R_2} \Sigma_f^{(2)} \phi_2(r,z)dV} \left(\frac{V_2}{V_1}\right) = 1.11$$

The radii of the superheater and boiler and the height of the reactor were principally fixed by heat transfer considerations; therefore, the migration area calculation was basically a problem of making a given reactor size critical. In order to facilitate the calculations, several approximations were made: (1) It was assumed that the product ϵP_{RE} was unity; (2) the regions were considered to be homogeneous, that is, disadvantage factor equal to one; (3) the reflector was assumed to be of infinite thickness; (4) "streaming" losses in the superheater steam channels were neglected; (5) steam volumes were assumed to be completely void of nuclei.

The water to metal volume ratio in the boiler was set by stability requirements as estimated from water moderated reactor data, and it was thought, at first, that the reactor might operate on slightly enriched uranium in the form of UO_2 in a stainless steel matrix. For these reasons the nuclear calculations were made by varying fuel enrichment while holding all volume fractions constant. Calculations were further simplified since the quantities τ, D, and M^2 show small variation with fuel enrichment and may be considered

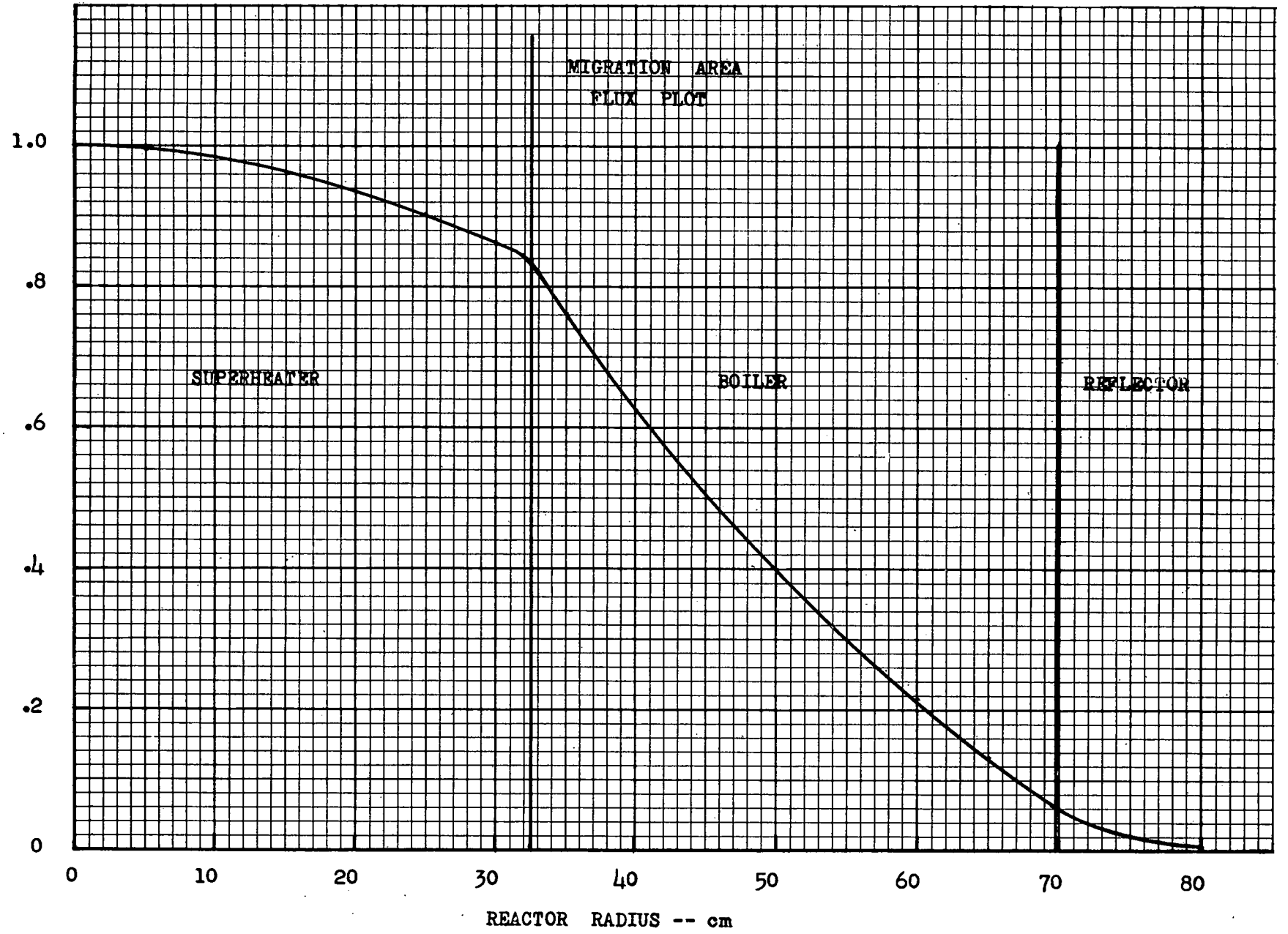

FIGURE 4-2

ORNL-LR-Dwg.-28541
UNCLASSIFIED

as constants. The effects of changes in volume fractions are presented in Section 4-3.

Constants used in the hand calculations are listed in Fig. 4-3. At operating temperatures (569°F in boiler and ~750°F in superheater), and in a clean condition, the uranium required for criticality and the proper power density ratio is: in the superheater, 61.6 Kg at 18.5% enrichment; in the boiler, 1181 Kg at 6.25% enrichment. The flux distribution for this loading is shown in Figure 4-2.

4.3 ORACLE Calculations

The "Three-group - Three-region Reactor Code for ORACLE" (Ref. 15) was used. This code may be applied as a two-group three region code. Two groups were used in this study.

Figure 4-4 is a list of the cases that were computed. Thirty cases were run in which the enrichment in the superheater and boiler was the variable. For these cases the boiler meat thickness was .090" with 35 volume % UO_2. Fig. 4-5 is a plot of the results. Each case consisted of a change in the superheater or boiler enrichment. The power density ratio for each case was calculated by utilizing the relative fast and thermal average fluxes as given in the ORACLE output. This was done as follows:

MIGRATION AREA CONSTANTS

CONSTANT	SUPERHEATER	BOILER
Radius, R	32.4 cm	69.7 cm
Age, τ	157.8 cm^2	81.4 cm^2
Diffusion Length, L	4.6 cm	1.72 cm
Migration Area, M^2	179.0 cm^2	84.4 cm^2
Diffusion Coef., D	.846 cm	.272 cm
Vol. fraction mod.	.7506	.600
Vol. fraction void	.1384	.060
Vol. fraction clad	.0654	.100
Vol. fraction meat	.0456	.240
Vol. UO_2/Vol. meat	.35	.35
Disadvantage factor	1.00	1.00

FIGURE 4-3

Fig. 4-4a

ORACLE CASES

Radii and Volume Fractions Given in Fig. 4-3

Reflector Thickness 4"

Case	Enrichment %		k	p_1 / p_2	Total Fissions/TH Fissions	
	Superheater	Boiler			Superheater	Boiler
0	13	2	.6461037			
1	13	4	.8263682			
2	13	6	1.0414380			
3	13	8	1.2357220			
4	15	2	.6876603	4.760	1.6757	1.3524
5	15	4	.8462532	1.105	1.6679	1.4304
6	15	6	1.0519562	.528	1.6717	1.5215
7	15	8	1.2431769	.358	1.6825	1.5960
8	15	10	1.4569646	.285	1.6493	1.6781
9	15	12	1.5852836			
10	15	14	1.7403425			
11	17	.714	.6917533			
12	17	2	.7359706	5.75	1.748	1.353
13	17	4	.8728754	1.40	1.740	1.434
14	17	6	1.0658349	.645	1.740	1.515
15	17	8	1.2526882	.417	1.751	1.595
16	20	.714	.7576738			
17	20	2	.7974139	7.01	1.822	1.359
18	20	4	.9121898	1.845	1.815	1.439
19	20	6	1.0868035	.822	1.813	1.503
20	20	8	1.2666165	.510	1.821	1.600
21	25	2	.9031449			
22	25	4	.9913404	2.75	1.964	1.445
23	25	6	1.1329934	1.19	1.964	1.533
24	25	8	1.2964440	.708	1.968	1.602
25	30	4	1.0741350	3.73	2.105	1.447
26	30	6	1.1885514	1.67	2.100	1.523
27	30	8	1.3326079	.958	2.104	1.606
28	50	2	1.3708506			
29	50	4	1.4164081			
30	50	6	1.4760849			
31	19.5	5	1.0078647	1.062		

Fig. 4-4b

Case	Enrichment % Superheater	Boiler	$\frac{V_{H_2O}}{V_{metal}}$ Blr	% Void in Blr Mod.	Reflector Thickness	Blr Radius	Disadvantage Superheater	Factor Boiler	k
32	15	8	4.15	10	4"	69.7 cm	1.00	1.00	.8186014
33	15	12	4.15	10	4"	69.7	1.00	1.00	.9536112
34	15	16	4.15	10	4"	69.7	1.00	1.00	1.1310123
35	10	8	4.15	10	4"	69.7	1.00	1.00	.8192218
36	10	12	4.15	10	4"	69.7	1.00	1.00	.9186270
37	10	16	4.15	10	4"	69.7	1.00	1.00	1.0833773
38	19.5	5	2	6	4"	69.7	1.00	1.00	1.0078647
39	19.5	5	2	14	4"	69.7	1.00	1.00	1.0071509
40	19.5	5	2	10	6"	69.7	1.00	1.00	1.0088048
41	93[1]	5	2	10	4"	69.7	1.00	1.00	1.0102994
42	93[2]	5	2	10	4"	69.7	1.55	1.13	1.0571420
43	93[3]	5.65	2	10	4"	69.7	1.55	1.13	1.0557646
44	93[4]	5	2	10	4"	69.7	1.00	1.00	1.0681810
45	19.5	5	2	10	7"	69.7	1.00	1.00	1.0090894
46	19.5	5	2	10	8"	69.7	1.00	1.00	1.0092675
47	19.5	5	2	10	9"	69.7	1.00	1.00	1.0093204
48	19.5	5	2	10	4"	67.7	1.00	1.00	1.0002944
49	19.5	5	2	10	4"	65.7	1.00	1.00	.9936918
50	19.5	5	2	10	8"	67.7	1.00	1.00	1.0025890
51	19.5	5	2	10	8"	65.7	1.00	1.00	.9962038
52	19.5	5	2	20	4"	69.7	1.00	1.00	1.0238412

All other volume fractions and radii are given in Fig. 4-3

$$\frac{P_1}{P_2} = \frac{(\Sigma_f^{SH} \bar{\phi}_{SH})_{fast} + (\Sigma_f^{SH} \bar{\phi}_{SH})_{thermal}}{(\Sigma_f^{B} \bar{\phi}_{B})_{fast} + (\Sigma_f^{B} \bar{\phi}_{B})_{thermal}}$$

The cases with the same superheater enrichment compose one set of parallel curves while those of the same boiler enrichment compose the other. Fig. 4-6 is an interpolation plot of k vs. superheater enrichment with a constant power density ratio of 1.11, the points being taken from Fig. 4-5. Fig. 4-7 is similar for the boiler. Thus, at k = 1 and $\frac{P_1}{P_2}$ = 1.11 the clean critical enrichments were chosen. A case was then computed for these chosen clean critical enrichments of 19.5% and 5% in superheater and boiler (See Fig. 4-8).

Four cases were computed in which the reflector thickness was the variable (See Section 4.7 and Fig. 4-10). Six cases were run varying the boiler and superheater enrichments with .030" meat at the same UO_2 volume % (See Fig. 4-11 and Section 4.8).

In the above 45 cases the void fraction in the boiler water was constant at 10%; however, two cases were run with 6% and 14% void fractions in order to display a safe boiling condition in which reactivity decreases with an increase in voids. Unfortunately, the results were inconsistent with known water moderated reactors. This inconsistency is more probably due to a necessity for greater accuracy in computation of the input group constants.

The remainder of the cases are also listed in Table 4-4.

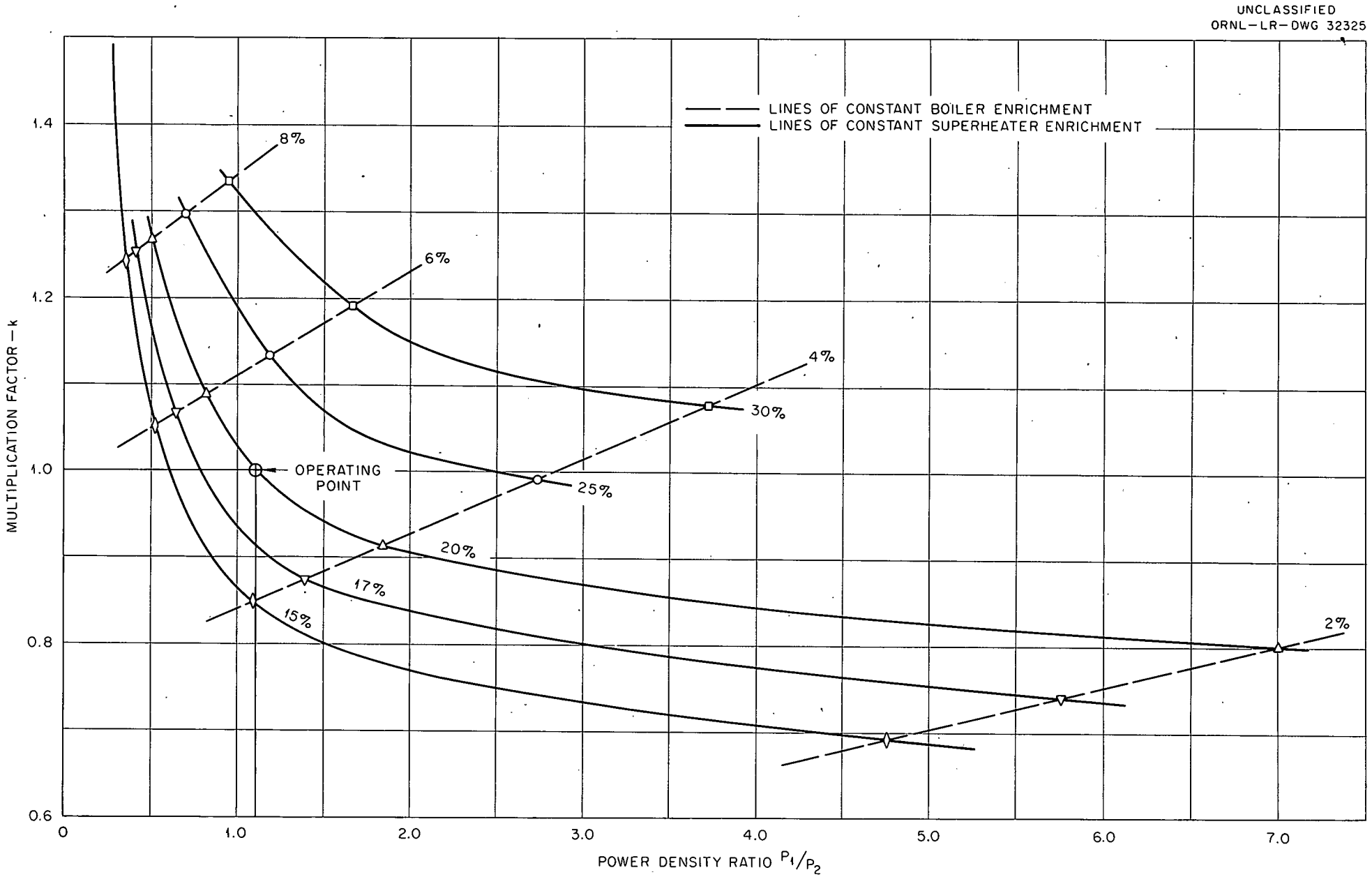
UNCLASSIFIED
ORNL-LR-DWG 32325
LINES OF CONSTANT BOILER ENRICHMENT
LINES OF CONSTANT SUPERHEATER ENRICHMENT
8%
6%
4%
2%
30%
25%
20%
17%
15%
OPERATING POINT
MULTIPLICATION FACTOR — k
POWER DENSITY RATIO P_1/P_2
1.4
1.2
1.0
0.8
0.6
0
1.0
2.0
3.0
4.0
5.0
6.0
7.0

Fig. 4-5

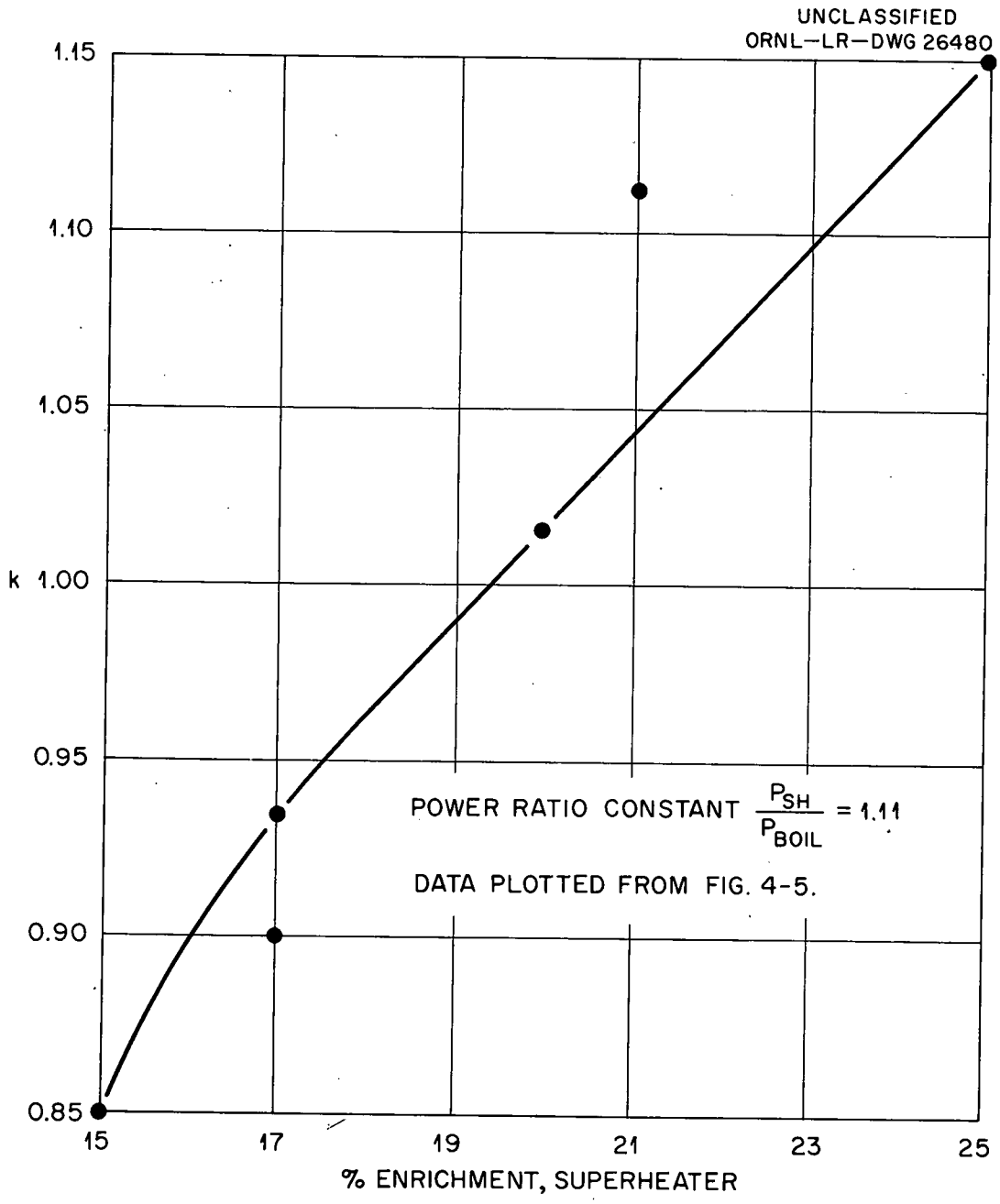

Fig. 4-6. k vs Superheater Enrichment.

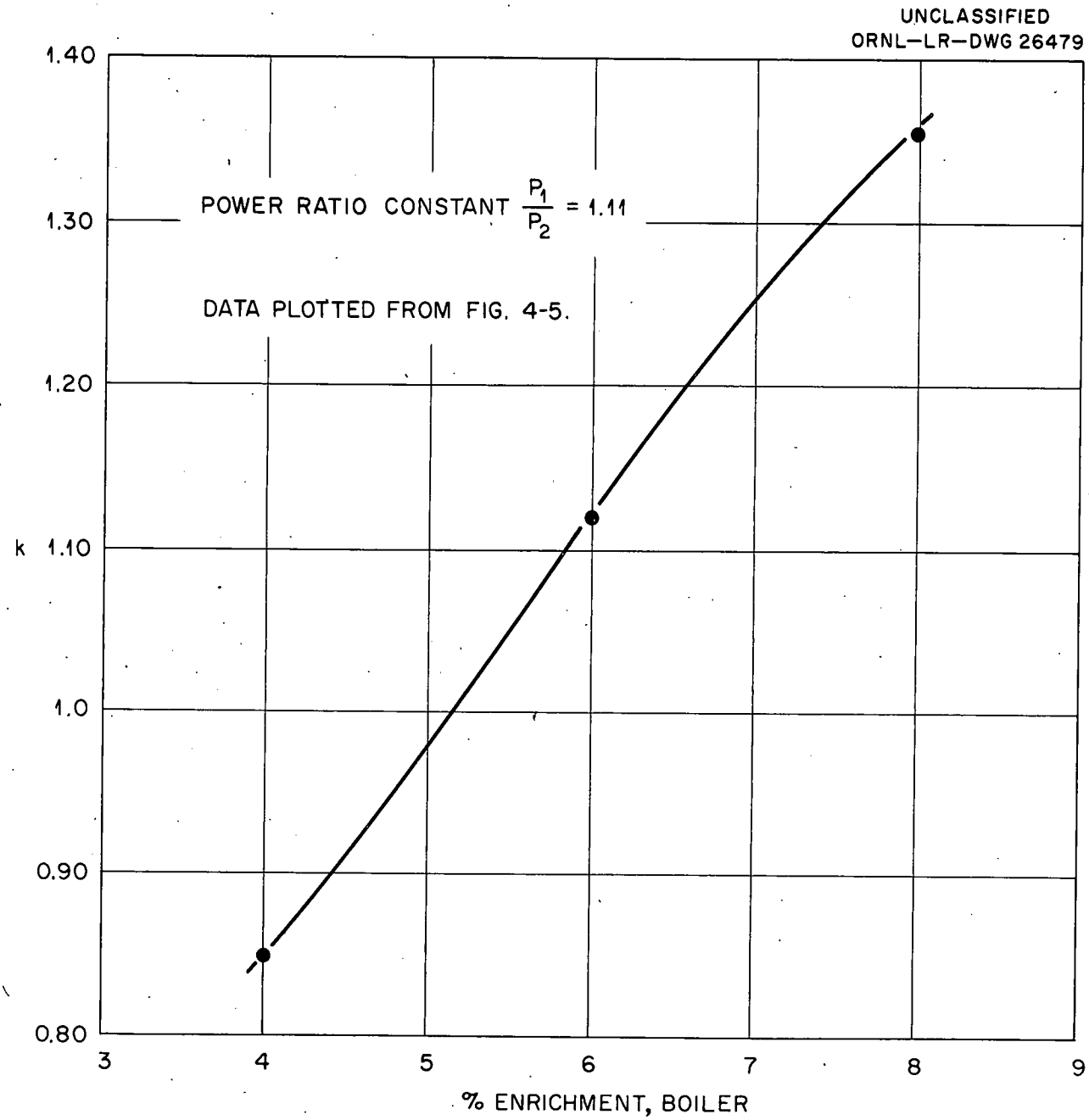

Fig. 4-7. k vs Boiler Enrichment.

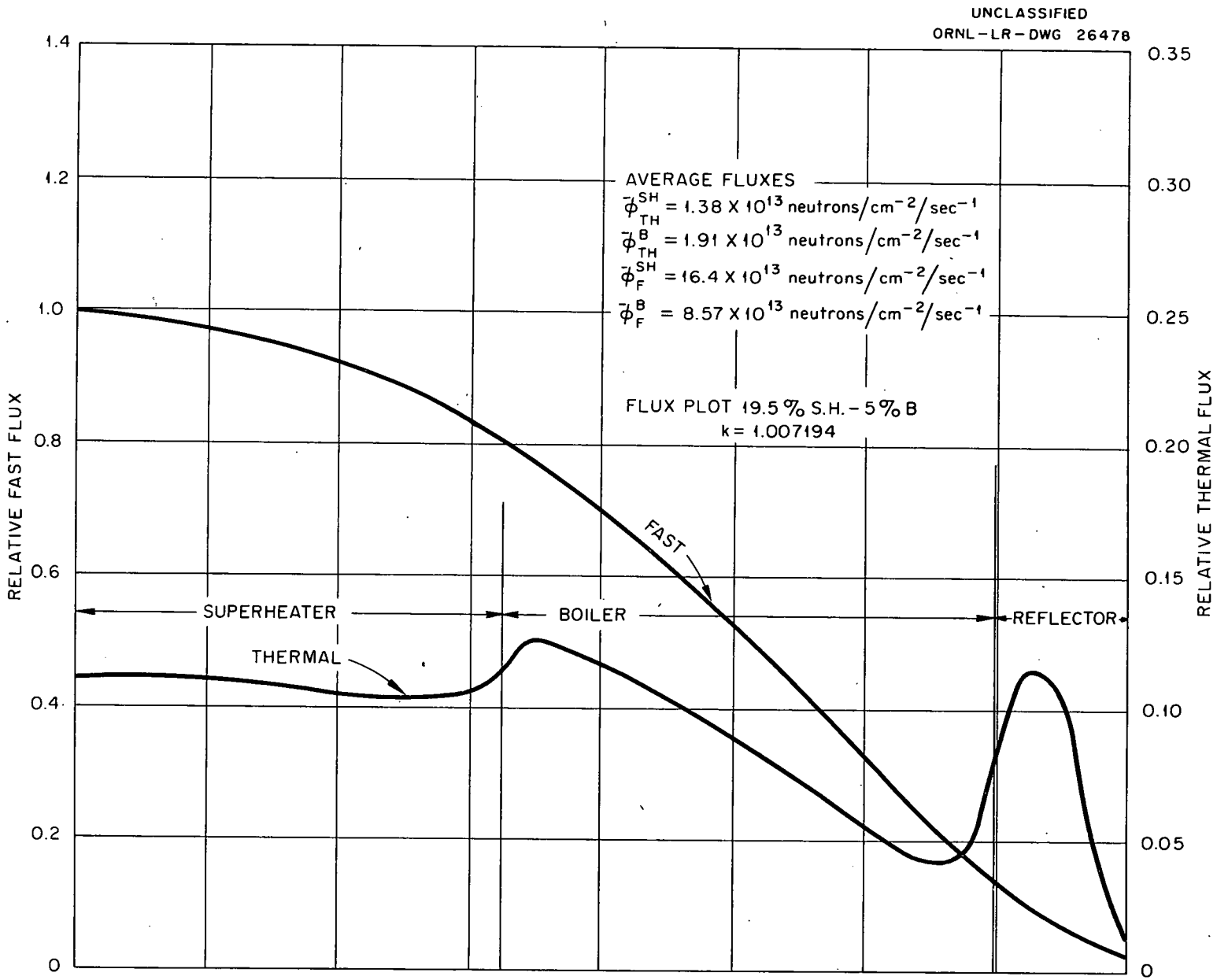

Fig. 4-8. ORACLE Results.

The thermal cutoff was chosen at the energy associated with the average velocity of neutrons with a Maxewell-Boltzmann distribution for the average temperatures in the respective regions. These temperatures and energies are:

Superheater - 705°K, .0770 ev.

Boiler - 569°K, .0620 ev.

Reflector - 569°K, .0620 ev.

The high energy, upper cutoff was chosen at the average energy of fission neutrons, 2 Mev.

Appendix B3 shows the method of calculating the 2G- 3R code group constants.

4.4 Heterogeneity

Due to the large absorption cross-section of uranium the thermal neutron flux is appreciably depressed in the fuel region, particularly in the superheater. To account for this depression the disadvantage factor $f = \bar{\phi}_{mod} / \bar{\phi}_{fuel}$, was calculated by one group diffusion theory assuming that the slowing down density, q, was constant throughout the moderator region and negligibly small in the fuel region. The necessary equations for this calculation are developed in Appendix B2.

The values of f for the superheater are shown in Figure 4-9. Only one value of f for the boiler was determined; it was found to be 1.13 for a fuel enrichment of 5% when $V_{UO_2} / V_{meat} = .35$.

As indicated in Section 4.2 no heterogeneity corrections were made in the hand calculations; however, several cases in the machine calculations were corrected by multiplying the fuel cross-sections by the reciprocal of f (14). The results of these cases are given in Figure 4-4b.

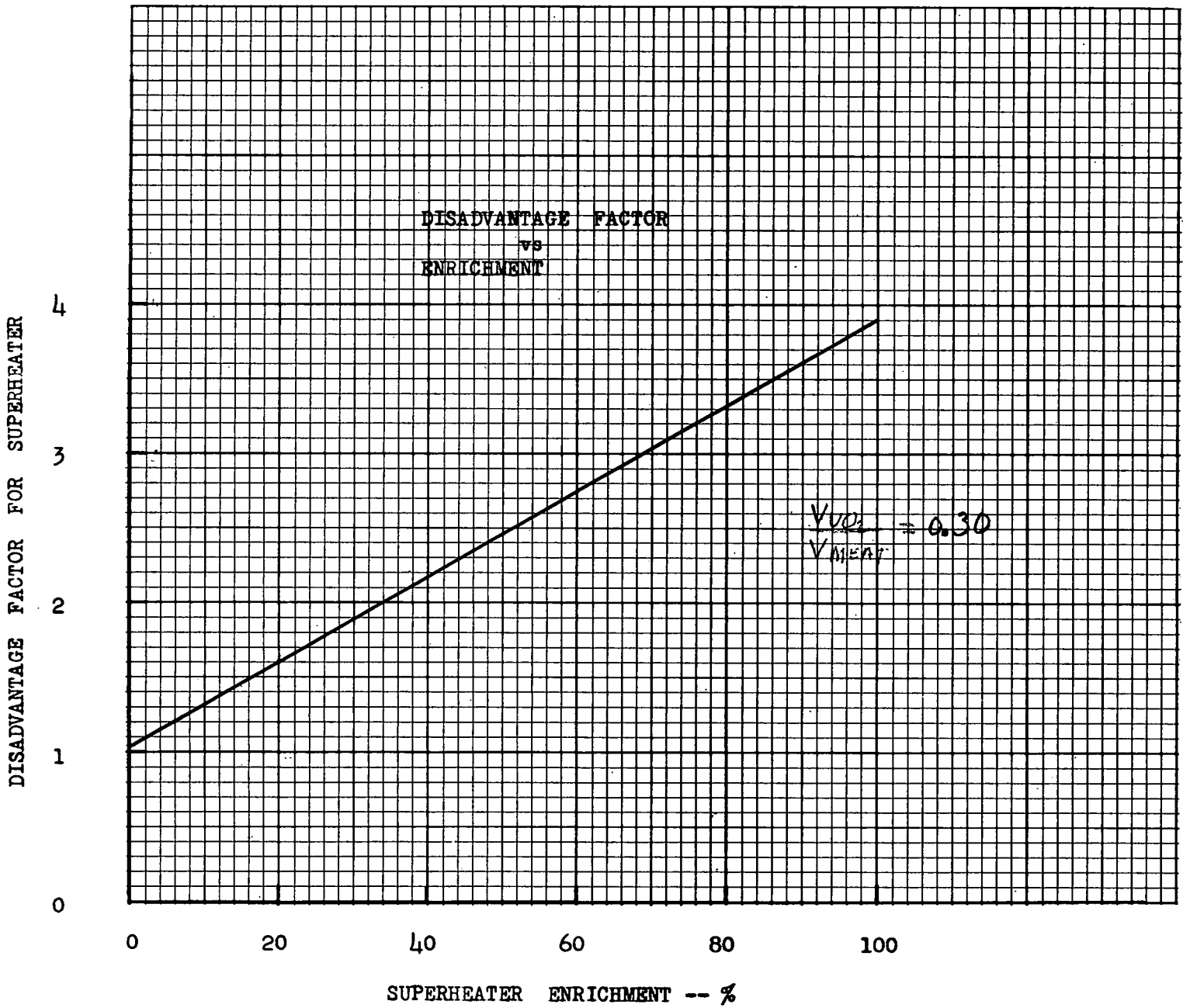

ORNL-LR-Dwg.-28542
UNCLASSIFIED

In all other cases, however, no correction for heterogeneity was made in the machine calculations. To our knowledge, there is no general agreement as to how to handle heterogeneity in the 3-group 3-region ORACLE code. The disadvantage factor calculation served mainly to demonstrate that the factor was reasonably low.

4.5 Maximum Xe-135 Override *

To determine the excess quantity of U-235 needed to override Xe-135, when it is at its maximum concentration after shutdown, the following assumptions were made:

1. There is no direct yield of Xe-135. Actually, the total number of iodine atoms produced per fission is .059, while that for Xe-135 is 0.062.

2. All Xe-135 rise after shutdown comes from simple decay of I-135 which neglects any isomeric holdup.

3. The lifetime of the I-135 parent, Te, is ignored.

4. Average fluxes for the superheater and boiler will apply.

After the reactor has been operating for some time the steady state equation is:

$$\bar{\Phi} N^{25} \sigma_f^{25} y = \bar{\Phi} N_o^x \sigma_c^x + N_o^x \lambda_x \qquad (1)$$

$\bar{\Phi}$ = average thermal neutron flux

y = Xe-135 atoms produced per fission

N_o^x = steady state atomic density of Xe-135

σ_c^x = microscopic capture cross section of Xe-135

λ_x = Xe-135 decay constant

N^{25} = atomic density of U-235

σ_f^{25} = microscopic fission cross section U-235

*See Ref. 16

Assuming no neutron capture in I-135 before it decays, its steady state equation is:

$$\bar{\Phi} N^{25} \sigma_f^{25}{}_y = N_o^I \lambda_I \qquad (2)$$

After shutdown the rate of change of Xe-135 density is:

$$\frac{dN^x}{dt} = \lambda_I N_o^I e^{-\lambda_I t} - \lambda_x N^x \qquad (3)$$

The solution of equation (3) is:

$$N^x = N_o^x e^{-\lambda_x t} + \frac{\lambda_I}{\lambda_I - \lambda_x} N_o^I (e^{-\lambda_x t} - e^{-\lambda_I t}) \qquad (4)$$

The maximum Xe-135 buildup occurs after shutdown when $\frac{dN^x}{dt} = 0$. Solving this for the time yields:

$$t_{max} = \frac{1}{\lambda_I - \lambda_x} \ln \frac{\lambda_I}{\lambda_x + (\lambda_I - \lambda) F} \qquad (5)$$

$$F = \frac{\lambda_x}{\bar{\Phi} \sigma_c^x + \lambda_x}$$

In order to solve for the maximum Xe concentration (N_m^x) after shutdown, the average thermal flux must be determined.

$$\bar{\Phi} = \frac{P_{th} w}{\Sigma_f V} \qquad (6)$$

P_{th} = power developed by thermal fissions

w = 3×10^{10} fissions watt^{-1} sec^{-1}

V = volume of reactor region

$\bar{\Phi}$ must be computed separately for the boiler and superheater.

As the total power developed in each region is known, P_{th} may be computed as follows:

$$\frac{P_{th}}{P_F} = R$$

P_F = Power developed by group 1 fissions.

$$P_F + P_{th} = P_t$$

$$P_{th} = (P_t - P_{th})R$$

$$P_{th} = \frac{R\,P_t}{1 + R}$$

R for the superheater was determined as follows:

$$R_{SH} = \frac{P_{th}^{SH}}{P_F^{SH}} = \frac{\Phi_{th}^{SH}\,\Sigma_f^{th}(SH)}{\Phi_f^{SH}\,\Sigma_f^{F}(SH)}$$

$\frac{\Phi_{th}^{SH}}{\Phi_F^{SH}}$ is given in the ORACLE case of the clean critical condition for 19.5% and 5% enrichment in the superheater and boiler. Thus, R_{SH} and R_{Boiler} may be determined.

$$R_{SH} = 1.23$$

$$R_B = 1.94$$

The total power requirements are:

$$P_T^{SH} = 1.095 \times 10^7 \text{ watts}$$

$$P_T^{B} = 3.61 \times 10^7 \text{ watts}$$

Thus, the average thermal fluxes are:

$$\bar{\Phi}_{Th}^{SH} = 1.38 \times 10^{13} \text{ neutrons cm}^{-2} \text{ sec}^{-1}$$

$$\bar{\Phi}_{Th}^{B} = 1.91 \times 10^{13} \text{ neutrons cm}^{-2} \text{ sec}^{-1}$$

N_o^x may now be calculated for the superheater and boiler.

$$N_o^x(SH) = 4.37 \times 10^{14} \text{ atoms cm}^{-3}$$

$$N_o^x(B) = 2.63 \times 10^{14} \text{ atoms cm}^{-3}$$

From eq. (5)

$$t_{max}^{SH} = 7.9 \text{ hrs}$$

$$t_{max}^{B} = 7.35 \text{ hrs}$$

Assuming that the total fission yields of I-135 and Xe-135 are equal enables one to write N_o^I in terms of N_o^x. From eq. (1) and (2):

$$\frac{N_o^I}{N_o^x} = \frac{\lambda_x}{\lambda_I} \frac{1}{F} \qquad (7)$$

Thus, substituting t_m, N_o^x, N_o^I from eq. (7) into eq. (4):

$$N_m^x(SH) = 7.56 \times 10^{14} \text{ atoms cm}^{-3}$$

$$N_m^B(B) = 3.86 \times 10^{14} \text{ atoms cm}^{-3}$$

In order to determine the critical loading necessary to override Xe, $\frac{\Sigma_f^F}{\Sigma_a^T}$ for the clean system was equated to the same ratio with Xe present at maximum concentration.

$$A = \frac{\Sigma_f^F}{\Sigma_a^F + \Sigma_a^M + \Sigma_a^x} \qquad (8)$$

$\Sigma_f^F = N_{oR}^{25} \sigma_f^{25}$ = macroscopic fission cross section necessary to override maximum Xe-135

$A = \frac{\Sigma_{fc}^F}{\Sigma_{ac}^T}$ = ratio of clean system with 19.5% and 5% superheater and boiler enrichments.

$\Sigma_a^F = N_{oR}^{25} \sigma_a^{25} + N^{28} \sigma_a^{28}$ = macroscopic absorption cross section present when overriding maximum Xe-135

Σ_a^x = Xe absorption cross section

Σ_a^M = Absorption cross section of all other material.

N_{oR}^{25} = atomic density of U-235 necessary to override maximum Xe.

The volume of UO_2 is held constant at 35 volume % in the meat.

$$\therefore \quad N^{28} + N_{oR}^{25} = C$$

C is known for superheater and boiler, thus solving eq. (8) for N_{oR}^{25}:

$$N_{oR}^{25} = \frac{A(\Sigma_a^M + \Sigma_a^x + C\,\sigma_a^{28})}{\sigma_f^{25} - A(\sigma_a^{25} - \sigma_a^{28})}$$

N_{oR}^{25} (SH) = .836 x 10^{20} atoms cm^{-3}

N_{oR}^{25} (B) = 1.050 x 10^{20} atoms cm^{-3}

N_{clean}^{25}(SH) = .722 x 10^{20} atoms cm^{-3}

N_{clean}^{25} (B) = .971 x 10^{20}atoms cm^{-3}

$N_{oR}^{25} - N_{clean}^{25} = N_{excess}^{25}$

N_{excess}^{25} (SH) = .114 x 10^{20} atoms cm^{-3} = 1.98 Kg U-235

N_{excess}^{25} (B) = .079 x 10^{20} atoms cm^{-3} = 4.90 Kg U-235

N^{25}_{excess} = Excess amount of U-235 needed to override maximum Xe.

4.6 Reflector

The density of the water reflector with no voids at 565°F and 1200 psia is .720 gms cm^{-3}. Adjacent to the outer boiling elements is the 4 in. water reflector, followed by a 1 in. stainless steel thermal shield, 1 in. water gap, 2 in. stainless steel thermal shield, 1 in. water gap and the 3-3/4 in. carbon steel pressure vessel. (See Fig. 5-1)

Fig. 4-10 indicates 9 in. of water at the above density, with 19.5% and 5% superheater and boiler enrichments, to be equivalent to an infinite reflector. With the additional water gaps in this design, the effective reflector thickness will be greater than 4 in. A critical experiment could determine this effective thickness and thus justify reducing the boiler loading. A major consideration in choosing the optimum reflector would be determined by a comparison of the fuel savings with the increase in pressure vessel size.

4.7 Boiler Meat Thickness

In determining the optimum design, a parameter study would have to be made in order to choose the meat thickness that would result in a minimum fuel loading, yet still satisfy the thermal stress and rigidity requirements, stability requirements relative to the water to metal ratio, and maximum volume % of UO_2 in the meat.

Six cases were run using .030 in. meat thickness, three at 15%, and three at 10% superheater enrichment with 8%, 10%, and 12% boiler enrichments. In Fig. 4-11 the .030 in. meat requires a lower $\nu\Sigma_f$ for criticality than the .090 in. meat. $\Delta\nu\Sigma_f$ = .018.

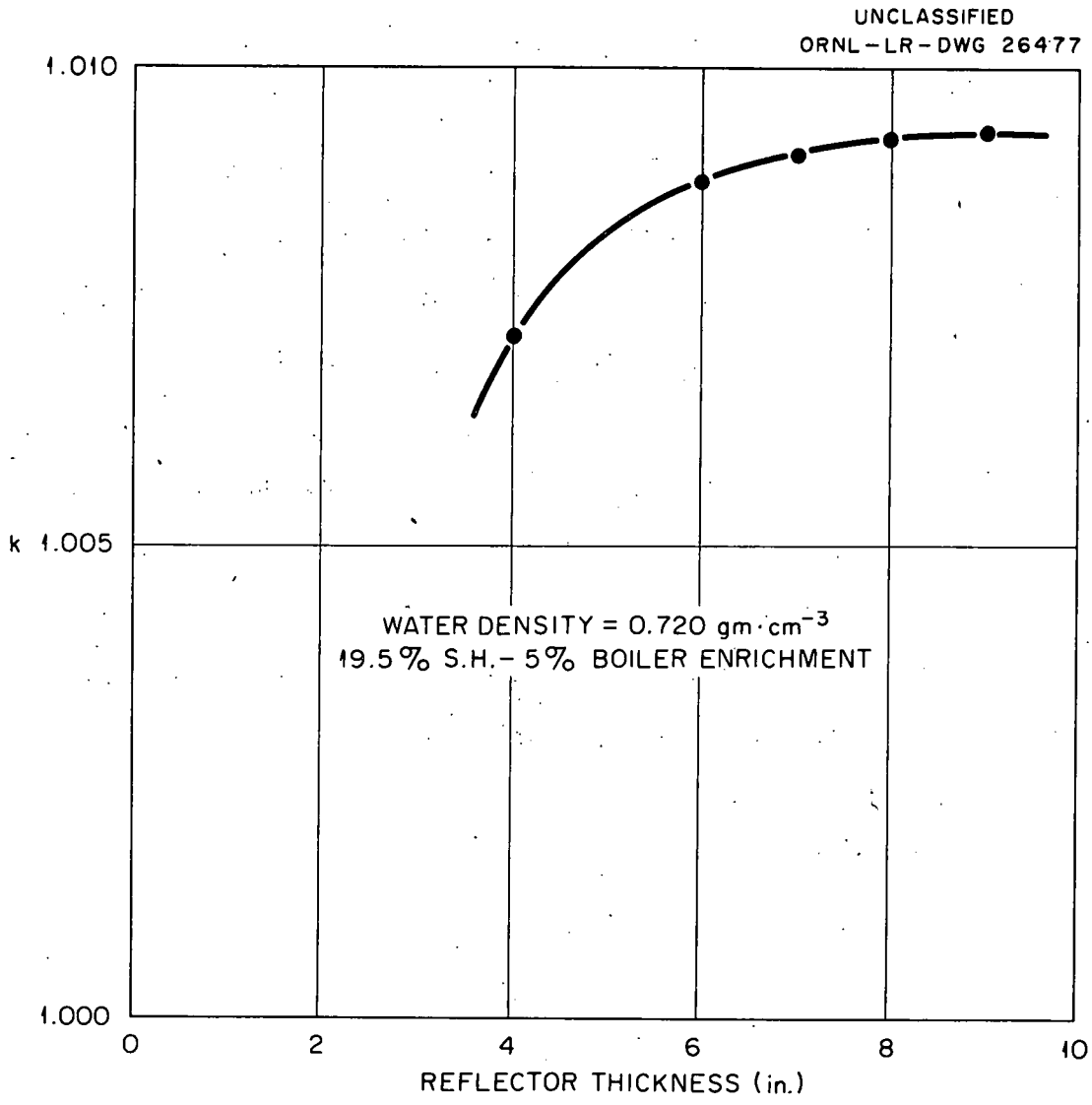

Fig. 4-10. ORACLE - Results k vs. Reflector Thickness.

To determine an accurate fuel savings, cases should be run at 5% and 3% in the superheater which would envelope the condition of k = 1 at $\frac{p_1}{p_2} = 1.11$.

Using the same procedure, and limiting the range of meat thicknesses by determining the limits imposed by rigidity and thermal stresses, one could choose the optimum meat thickness.

4.8 Conclusion

Meeting the heat transfer and power requirements is not a sufficient nuclear solution for this reactor, since these are myriad when previously fixed parameters are varied. Thus, to choose the best solution one is obviously confronted with a time-consuming, but desirable, parameter optimization study.

Subjects that must necessarily be investigated to complete this study are the control problem and the introduction of burnable poisons into the system, radial loading of varying enrichments for both the superheater and boiler, the effective $\delta K/(\text{void fraction})$ for the boiler, and essential critical experiments to determine more exactly the heterogeneity characteristics of the system.

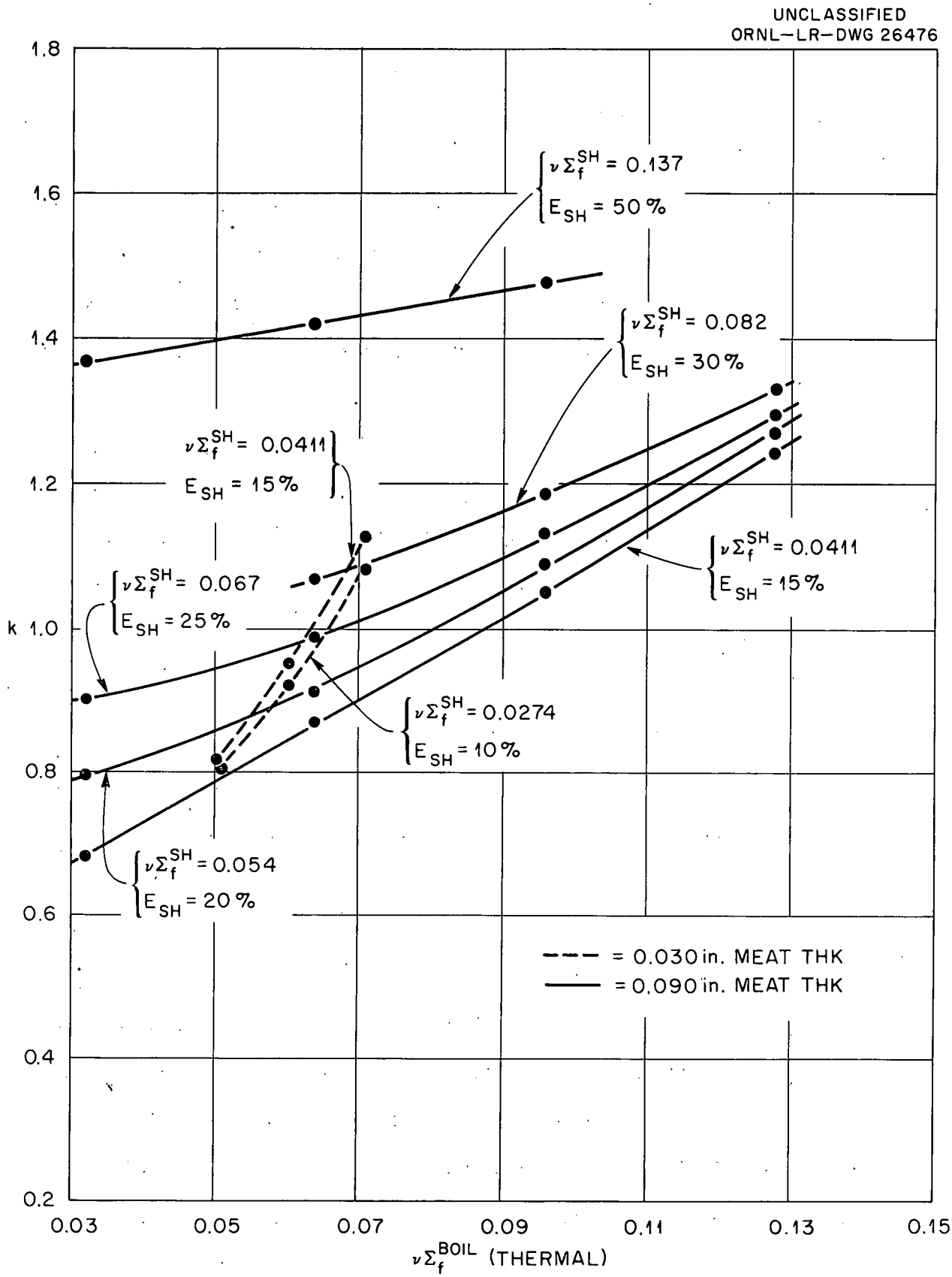

Fig. 4.11. ORACLE Results k vs $\nu\Sigma_f^{BOIL}$.

CHAPTER 5

5.1 Reactor Vessel Design

5.1.1 Vessel

The reactor vessel will be 74" ID x 81" OD (6'9") and approximately 19'-6" overall length. The diameter was determined by the size of superheater and boiler core as well as necessary reflector and thermal shield thicknesses. The vessel length has been held to a minimum because of possible marine application.

A bolted closure has been selected because of the large amount of experience with this type and because of its simplicity and reliability. 38 - 4" diameter studs will be required (See pressure calculations 5.1.2).

Two (2) concentric pressurized stainless steel "O" rings similar to those used on PWR provide the seal between head and vessel flanges. These are considered suitable to withstand the design pressure but if thought necessary an omega type seal could be provided for additional reliability but at a penalty in refueling time as shown in Figure 5-1.

The vessel materials are discussed in Section 5.1.2.

The steam flow within the vessel has been selected so that the vessel walls will not be in contact with superheated steam thus allowing the use of low alloy materials throughout.

The elliptical heads will be formed from plate in one section. Vessel and head flanges of the size indicated in Fig. C-4 will present no fabrication problem after the experience gained with PWR. The main vessel body will be made from 2 - 180° rolled segments and assembled with 2 axial welds. The shell and heads will be pierced and nozzles welded and machined as shown

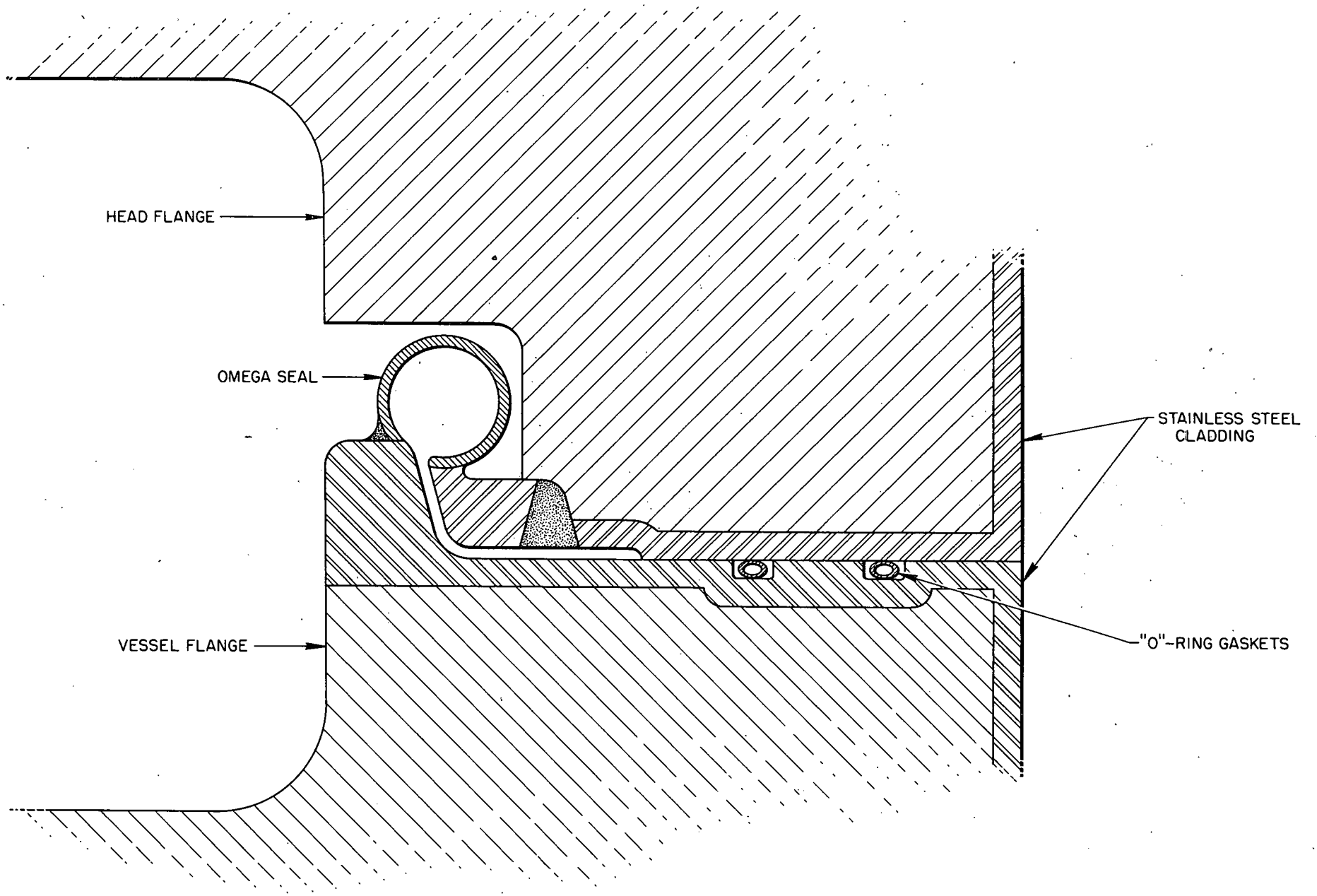
HEAD FLANGE
OMEGA SEAL
STAINLESS STEEL CLADDING
VESSEL FLANGE
"O"-RING GASKETS

Fig. 5-1

on Fig. 1-1. All welds are to be radiographed and the assembled vessel stress relieved and hydro tested to 1950 psi. The circulating loop and control rod drive housing butt welds will be made in the field and locally stress relieved and radiographed.

The vessel will cause no shipping difficulty and it has been assumed that shipment will be with reactor completely assembled, less fuel elements, control rods and control rod drives. The weight for shipment in this condition would be approximately 55 tons. (See Section 5.6)

The design of this vessel is relatively conventional in the nuclear field and should present no unusual fabrication problems.

5.1.2 Pressure Calculations

The pressure calculations were based on the Unfired Pressure Vessel Code (Section VIII) 1956. (Reference 31) The design pressure was selected as 1300 psi as follows:

Superheater outlet pressure	1200 psi
Superheater pressure drop	8
Steam scrubber pressure drop	5
Boiling element pressure drop	5
Water head	7
Normal operating pressure fluctuation (see Section 7.3.3)	60
	1285 psi

∴ Nominal design pressure = 1300 psi

A pressure relief system has been provided to insure that the pressure will never exceed this value.

The design temperature of the vessel (with the exception of the superheater steam outlet) was taken as 650°F. The saturated steam temperature corresponding to 1300 psi (1314 psia) is 574°F, thus leaving a margin of 76°F for gamma heating of the vessel wall. (The actual heating within the vessel wall is 15°F - see Section 6.3)

The vessel material will be carbon steel ASTM Specification A-212B with the exception of the outlet end of the superheater outlet nozzle which will be stainless steel ASTM Specification A-376, Type 347. The carbon steel portion of the vessel which is in contact with the water will be clad with 1/4" of Type 347 stainless steel. This cladding is integral with the vessel wall and is applied either by forging the cladding plate to the carbon steel or by welding and subsequent machining of the stainless on the carbon steel. Per (31) UCL-23(b) the pressure calculations are based on the total wall thickness, less the minimum cladding thickness, ie the carbon steel thickness only.

S = Maximum Allowable Stress of A-212B at 650°F = 17,500 psi per (31) Table UCS-23

E = Axial ligament efficiency for weld (radiographed and stress relieved) = 95% per (31) UW-12

Vessel Wall

(31) UG-27 $$t = \frac{PR}{SE - 0.6P}$$

$$t = \frac{1300 \times 37.25}{17{,}500 \times 0.95 - 0.6 \times 1300} = \underline{3.06"}$$

t = minimum wall thk.

P = design pressure (1300 psi)

R = inside radius acted on by pressure

S = maximum allowable stress

E = ligament efficiency

∴ Will use 3-1/4" A-212B + 1/4" Type 347 cladding

Ellipsoidal Heads (2:1 Ellipse)

(31) UG-32(d) $t = \frac{PD}{2\,SE - 0.2P}$ D = inside diameter

E = 100% since all openings in heads are fully reinforced (see nozzle calc.)

$$t = \frac{1300 \times 74.5}{2 \times 17{,}500 \times 1.00 - 0.2 \times 1300} = \underline{2.79"}$$

Will use 3-1/4" A-212B + 1/4" Type 347 clad (the additional thk. provides needed reinforcement for penetrations and matches the vessel wall thickness).

Nozzles

(Per (31) UG-37 and UG-40) See Appendices C-1.1, 1.2, 1.3.

Vessel Flanges

(Per (31) UG-47, 49, 50, and 51) See Appendices C-1.4.

5.1.3 Vessel Support

The vessel weight of approximately 140,000#-(15 x 140,000 = 2,100,000# during 15G shock loading) will be supported by a circumferential skirt located just below the circulating outlet nozzles. The lower end of the vessel is supported laterally, and at the same time allowed to expand, by a guide located on the lower head. (See Figure 5-2) The load of the vessel is transmitted through the 1" thick shield tank wall to the structural steel.

The support skirt could be scalloped if necessary, as shown, to reduce the bending rigidity of the shell if the temperature gradient through the skirt tends to generate excessive stresses. The skirt length should be as long as possible to reduce the temperature gradients in the skirt.

The method of support of the circulating piping, valves and pump is yet to be developed. This must be accomplished in such a manner as to not impose excessive stresses on the piping due to expansion or shock loading forces.

5.1.4 Support Plate Structure

The supporting structure for the boiler and superheater sections is shown on Figure 1-1. This structure is to be fabricated from Type 347 stainless steel throughout. The superheater support has been offset below the boiler support because of the temperature difference of these two structures and the subsequent difference in expansion. Due to differences of expansion between the stainless steel boiler support and the carbon steel vessel (both at approximately same temperature), we have shown the support structure resting on a support ring, but allowed to expand radially relative to the ring by means of four (4) guide lugs. Upward movement of the support structure due to shock loading or hydraulic forces from the hold down structure above are prevented by the annular ring around the edge of the support structure.

A single thickness plate is sufficient to support the superheater loading. However, any reasonable single thickness plate would experience excessive deflection in the boiler section during shock loading. Therefore, the boiler support has been designed with a double plate, grid type construction as shown in Figure 1-1 and 1-2. This construction will also serve to align the boiling elements after installation prior to lowering the hold down plate.

5.1.5 Hold Down Structure

The restraint of the boiling element against upward movement due to hydraulic and shock forces as well as alignment of the elements and control rods is accomplished by means of a hold down plate and hold down rod as shown in Figure 1-1 and 1-2. Openings are provided in the plate to allow steam formed in the thermal shield and outside of boiling elements to pass upwards. A shroud is welded to the plate to prevent steam from being drawn into the circulating pump suction. The outside diameter of the plate is accurately machined to a matching fit in the vessel to insure control rod alignment. To eliminate difficulty due to relative expansion between the hold down plate and reactor vessel the hold down plate will be fabricated from carbon steel A-212B nickel plated by the "Kanigen Process" (see Ref. 32). This process was extensively used for vessel internals of the EBWR.

Sixteen (16) hold down rods of approximately 2" diameter are required to carry the upward forces on the hold down plate. These rods are threaded into and seal welded to the lower flange of the support plate. To allow removal of the hold down plate, for refueling, these rods are provided at the top with a removable (locked type) fitting.

5.1.6 Superheater Housing Structure

This structure serves several purposes:

1. Contains solid BeO moderator
2. Insulates superheater and boiler regions from each other
3. Aligns the upper end of superheater elements and superheater control rods.
4. Contains seal to prevent wet steam from bypassing scrubbers.

The cross sectional geometry of this structure conforms to that of the superheater (square with corners removed) as shown in Figure 1-2 and extends for its full length. The structure will be 3/8" thick at its upper and lower ends and 1/8" thick in the core region for neutron economy and to provide a 1/4" space for corrugated insulation (see Figure 5-3) in the high temperature region.

The corrugated construction inhibits convection heat losses as well as stiffening the 1/8" sheet. (See Section 5.3.3 for heat loss from superheater to boiler). In addition the corrugations provide an expansion joint to insure contact between the superheater housing and the BeO. This is required due to the higher coefficiency of expansion of stainless over BeO.

The lower end of the housing extends below the boiler support plate where it is attached to the superheater support plate and forms the structure of the superheater outlet plenum.

A stainless steel seal is provided at the housing top. Because of the housing shape this seal must be especially made. The seal is located far enough above the water level to allow a 30° roll of the ship before immersing the seal. The fit between the seal and the internal structure at the head aligns the upper end of the superheater structure.

A cover plate over the solid moderator is welded to the superheater housing and aligns the superheater guide tubes and superheater control rod cruciforms. The cover plate prevents any solid moderator from getting into the steam system and allows the superheater guide tubes to expand upward through it. The clearance space between guide tubes and cover plate serve as vents to equalize the pressure inside and outside the superheater housing during load and steam pressure changes.

In the design of the superheater as shown, the saturated steam vapor will contact the BeO moderator due to venting the moderator container (superheater housing). BeO does not react with water at ordinary temperatures. Ref. #45 Pg. 39 states that beryllia forms a volatile compound at temperatures of 2280°F or greater. Therefore no difficulty is expected from the BeO - Water contact.

5.1.7 Auxiliary Piping

Preheat steam connections are located at the bottom of the circulating loops for gradual preheating of vessel prior to startup and for superheater cooling before a supply of saturated steam is available from boiling section of reactor. (See Section 7.5 on startup)

Feedwater is returned to the system in the circulating loop as shown on Fig. 1-1. The water is inserted at the center of the 11.5" L.D. suction line and with proper mixing should present no thermal shock problem due to the high recirculation ratio (61.3 to 1).

A pressure relief outlet is provided in the head. This seems advisable in case of an unforeseen pressure rise. The pressure relief valve would be set at 1300# (max. design pressure) and under normal operating conditions will not open. This line will vent to the main condensers or possibly to the ocean. Provision must be to provided to break this relief line when the head is removed.

5.1.8 Steam Separators

The steam separation or moisture removal from the saturated steam is obtained by conventional corrugated plate steam scrubbers located in the vessel head (see Figure 1-1, 1-2).

The steam velocity leaving the water surface is less than one (1) fps. Ref. 33, Pg. 9-9 suggests that for velocities less than 3 fps gravity separation at steam and water is possible for "large steam drum diameters". However, in the interest of reducing vessel length it was decided to use steam scrubbers and locate these approximately 2 ft. above the water level. This location will allow a 60° roll of the ship before priming will occur.

The steam velocity through the scrubbers will be 2.6 fps and using data and assuming same type scrubbers as given in Ref. 34, Pg. 72 (EBWR) the pressure drop was calculated to be approximately 5 psi.

Assuming a water purity to be maintained at 1.0 ppm (maximum) (per EBWR) and a moisture carry over through the scrubbers of 0.1% would give a saturated steam solids content of only 0.001 ppm.

5.1.9 Thermal Shielding

Two concentric thermal shields 1" and 2" thick are used, extending approx. 1 ft above and below the active core length. The 2 shields are attached together and installed as a unit (Total weight 13,000#). The shield is restrained against movement by attachment to the support plate. Openings are provided at the bottom of the shield to allow water circulation for cooling.

Addition thermal shielding is provided in the top and bottom heads to protect the vessel from end streaming from the superheater core region. These shields are cooled by water in the lower head and saturated steam in the upper.

All thermal shield material is to be stainless steel type 304L.

5.1.10 Thermal Insulation

The vessel, vessel flanges and circulating piping are to be thermally insulated by 4 inches of suitable insulation. This material should be able to resist packing down, withstand wetting and shock loading. Materials considered in the past for applications of this type have been foamglass or packed steel wool.

5.2 Circulation System

The piping for the 3 circulating loops has been kept at a minimum in order to reduce the space requirements of the system. All of the piping and valves are located inside the primary shield tank. The insulation on these parts will be surrounded by a steel water tight housing which will be welded into the shield tank at the ends. This will keep water out of the thermal insulation and allow expansion of the piping relative to the shield tank. No expansion loops should be necessary since all of the loop is at the same temperature.

The valves will be remotely operated gate valves. It was felt that valves should be used in order to isolate the pumps in case a pump failure or leak occured. (In case of isolating a pump, the feed water normally entering that loop would be diverted to the other loops.)

The pumps selected are of the canned rotor type of sufficient capacity to operate at full load on two pumps. A double suction, mixed flow impeller suitable for 11,000 gpm at 900 rpm and 30 ft. head is required. The mixed flow was selected to delivery larger capacities at low discharge heads. The double suction was selected to reduce the suction pressure drop and to eliminate the additional head room required for a bottom suction inlet below the pump. The pump was located as low as possible

discharging into the bottom of the vessel. This location will give as much suction head as possible (15 ft). Calculations made in Section 3.2.4 indicate a pressure drop of approximately 6 ft. in the loop and also that a pump of this type should have a net suction head of 8.5 ft. The 15 ft. suction head condition is therefore satisfactory.

The location of the suction nozzle in the vessel with respect to the water level is such that a permanent roll of 30° can be sustained without loss of pump suction.

5.3 Superheater Core

5.3.1 General Arrangement

The 32 superheater elements are arranged in a 4 inch square pattern. The square arrangement was selected so the superheater core would merge smoothly with the square boiling elements without giving large water gaps. The moderator will be in 4" square blocks (of as long a length as practical) drilled or slotted axially to receive the guide tubes and control rod cruciforms. (See Fig. 1-2) The lower end of the guide tube is reduced to 1 1/2" dia. to:

1) Provide a ledge to support the superheater elements
2) Reduce neutron streaming
3) Reduce the size of penetrations in support plate.

5.3.2 Superheater Elements (See Fig. 1-3)

Fabrication of flat fuel plates for the boiler and superheater would be essentially the same. (see 5.4.2) The flat fuel plate, 25-1/4 inches long would be rolled into a tubular shape of somewhat smaller diameter than desired, the seam then brazed, excess brazing material ground off flush,

UNCLASSIFIED
ORNL-LR-DWG 26482

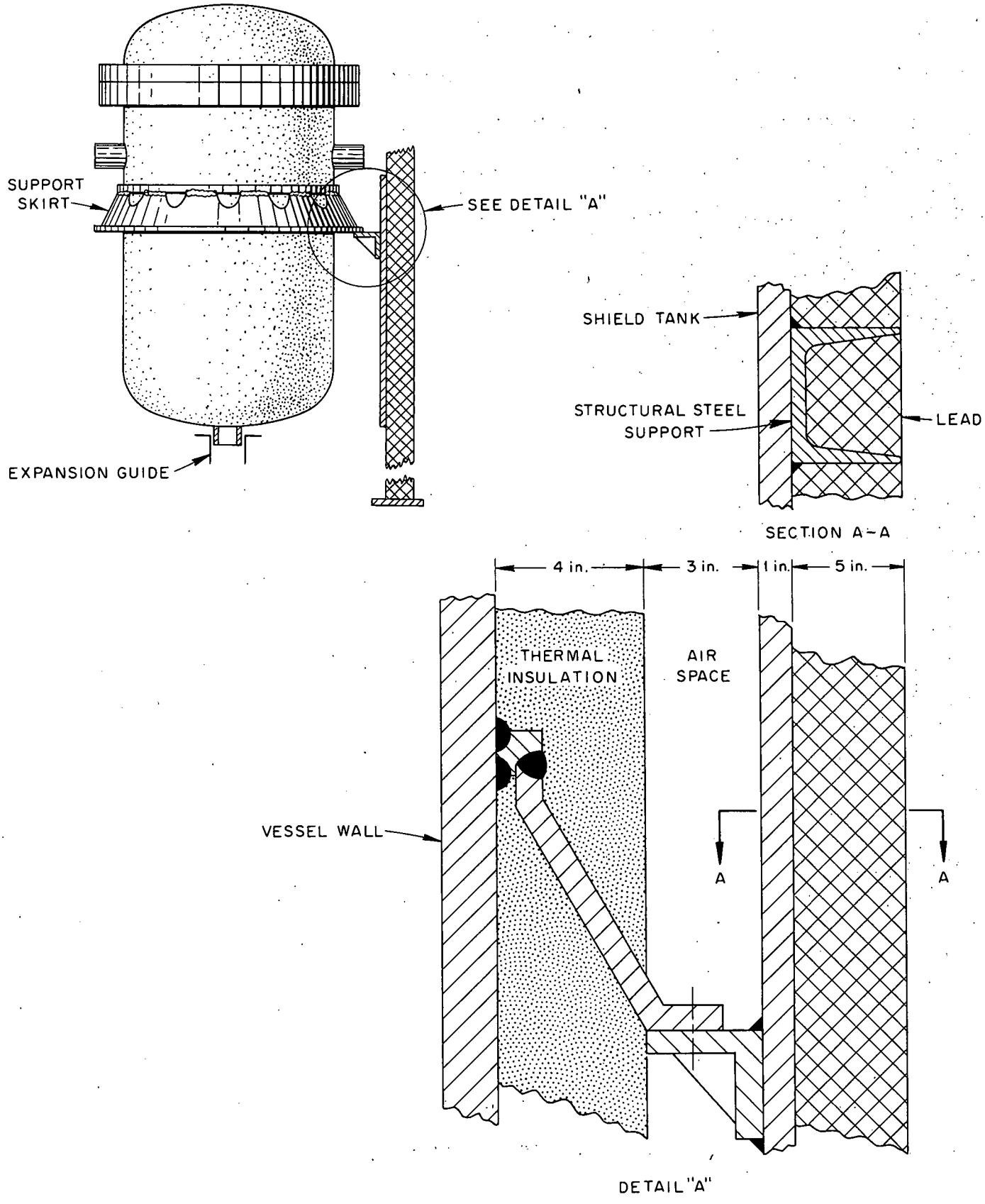

Fig. 5-2.

and the tube expanded in a drawing operation to the dimensions required. Minimum bending radius of the innermost fuel cylinder is about 1.1 inches which is acceptable. Ref. 43 (ORNL-1915).

The element is designed to be held down in place in the guide tube by the latching mechanism at its top. This mechanism will allow for expansion of the element relative to the guide tube and carry shock loads.

A shielding section approx. 3 ft. long is designed into the top of the element to eliminate direct neutron streaming.

The annular fuel tubes are physically spaced by means of small dia. wires helically wraped around each fuel tube. These wires are brazed to the fuel tubes where they cross the axial braze seam in the tube. The fuel tubes are fixed into the support combs by brazing at one end and guided by slots in the comb at the opposite end. The individual fuel tubes are thus free to expand relative to the center moderator tube and each other.

For reasons discussed in Section 3.1.1.c a temperature equalizing or mixing chamber has been provided at the mid point of the fuel tubes.

A "disconnect fitting" has been provided between the fuel element proper and the upper BeO top shielding end. This will allow the salvage of this top for re-use after element reprocessing.

5.3.3 Insulation From Boiler Region

The method of insulating the superheater from the boiler in the active core region was discussed in Section 5.1.6 (Suphtr. Housing Structure). The method of insulating the superheater outlet plenum and outlet steam line from the saturated temperature water is shown on Fig. 1-1 and 5-4 below. The method used is a double wall container with a "stagnant" steam layer between the walls. The outer wall is of sufficient thickness to resist

UNCLASSIFIED
ORNL–LR–DWG 26481

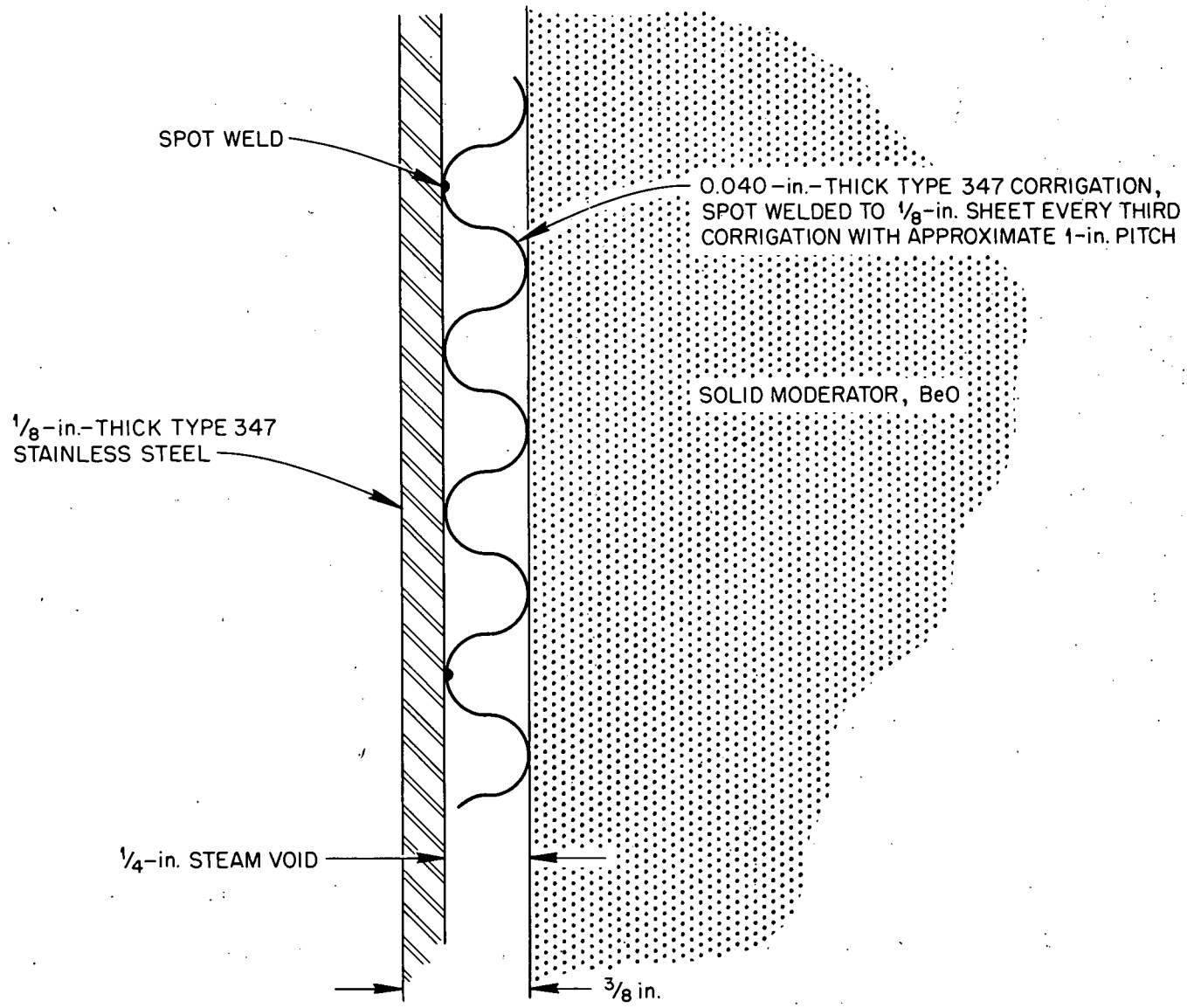

Fig. 5–3

the collapsing pressure of approximately 25 psi which exists at this point between superheater and boiler. The inner wall has small orfices in it to allow the pressure to equalize during load changes; this wall may be relatively thin and is provided with frequent fins to serve as convection inhibitors within the "stagnant steam" space.

A summary of the results from the heat loss calculations of the superheater housing and outlet plenum follows:

Superheater Housing Radiation Loss	62,500 BTU/hr
Superheater Housing Convection Loss	113,500
Superheater Plenum Radiation Loss	45,600
Superheater Plenum Convection Loss	59,300
Total =	280,900 BTU/hr

This is less than 1% of the total heat release in the superheater and does not represent a loss to the overall system since heat lost from the superheater is being absorbed by boiler water.

Calculations were made to determine the heat loss from the lower plenum if only a single wall had been used. This was 752,000 BTU/hr. or 7.2 times the heat loss with the proposed design. Because of the complicated construction of the double wall it might be better to accept the higher heat loss of the single wall construction if this wall could withstand the thermal stresses due to the 950° to 575°F temperature differential.

5.4 Boiler Core

5.4.1 General Arrangement

The 116 boiling elements are arranged on a 4" square pattern as were the superheater elements. 8 of the elements are attached to the lower end

of the boiler control rods and as the rods are inserted the elements are expelled into the control rod guide tubes below the core. The plate type fuel elements have been oriented so that the plates are normal to the net. neutron current as much as possible. (See Fig. 1-2)

5.4.2 Boiler Elements
(See Fig. 1-4)

The primary coolant flow for these elements is up through the lower tang and between the fuel plates. However in order to cool the outside surface of the end plates a small opening has been left between the end plates and the transition sections to allow coolant flow between the boiling elements. Any steam generated on the element exterior passes through holes in the hold down plate.

The tapered transition section will allow fuel elements to be lowered into place without danger of hanging up on adjacent elements.

An expansion spring is provided at the top to allow for thermal expansion of the element. This spring must be fairly stiff in order to resist the approx. 50 lb. hydraulic load on each element plus the possibility of a (15G x 115#) 1725# shock load without excessive deflection. If a max. deflection of 2 inches were allowed during shock loading (lower tang would still be engaged in support plate) a spring constant of 862# /inch would be required. If a helical spring of 3/8" dia wire (max. possible with clearance available) can not be designed to give this high a spring constant a helical spring of rectangular cross section can be used.

The guide fins at top and bottom tangs will allow the elements to be lowered easily into the support plate and simplify the problem of dropping the hold down plate into place after refueling.

The fuel element meat would be jacketed by a picture-frame technique which hermetically seals the fuel from the cooling water and also retains fission products, providing a cladding thickness of 0.005".

Eleven fuel plates would be brazed to grooved side plates of 347 stainless steel 0.060" thick, to form one fuel element.

It is intended to follow the APPR fuel element fabrication procedure and processing quite closely, and for further details on fabrication the reader is referred to Ref. 44 (ORNL-2225, "Specifications for Army Package Power Reactor (APPR-1) Fuel and Control Rod Components").

5.5 Control

5.5.1 Rods

The geometric arrangement of the control rods is best shown in Fig. 1-2. There are 5 rods in the superheater region; the center rod being intended for a regulating rod and the other 4 for shim and safety rods. There are 8 rods in the boiler region; 4 of these are intended for regulating rods and 4 for shim and safety rods. Thus there is a total of 5 regulating and 8 shim and safety rods.

The superheater rods have been roughly estimated on a volume of neutron absorbing material (hafnium) basis. Using a cross shaped rod with 1/8" thk. sections, a 3 1/2" x 3 1/2" cross running the full (4' - 4") length of the core is required. Control rod guide cruciforms fabricated from type 347 stainless steel will be required. Slots have been provided in the moderator for these cruciforms which are attached to the lower superheater support plate and guided by the superheater cover plate. These rods must be cooled by steam passing over them and between rod and cruciform. When fully withdrawn these rods appear as shown in Figure 1-1.

The boiler section control rods are of a box shape construction of hafnium backed by stainless steel for structural rigidity. The lower ends of these rods have a fuel element attached which makes the rod more effective by displacing fuel while inserting poison. The guide tube for these rods is approximately 13 ft. long extending above and below the core as shown in Fig. 1-1 and is fixed to the boiler support plate and is guided by the hold down plate and the bracket from the outlet plenum. This guide tube will be 4" square outside dimensions thus allowing the 3.8" square full element to pass through it. The control rod is cooled by water passing up through its center and is below the water level in the fully withdrawn position as shown in Fig. 1-1.

Dashpot mechanisms to decelerate the boiler control rods after scram are provided in the bottoms of the guide tubes using boiler water as the energy absorbing medium. The superheater decelerating device will have to be built into the driving mechanism.

5.5.2 Drives

As mentioned in the Introduction the actual details of the driving mechanism have not been analyzed. The drive would probably be of the canned rotor type of motor. The control rod shafts are withdrawn into guide tubes above the head. These tubes are designed to hold the reactor pressure and are approximately 5 ft. long to provide for full rod withdrawal. The motor and guide tube assembly is welded to the vessel head thus eliminating the need for a pressure seal around the drive shaft.

The drive shafts are prevented from deflecting during "scram" operation of the rods by guide bushings along their length. Latches are provided at the end of the drive shafts to disconnect from the control rod proper prior to head removal.

5.6 Reactor Weights

A breakdown of the estimated weights of the reactor vessel assembly follows:

Reactor Vessel (less head)	56,400 #
Vessel Head (plus control drive and intervals)	23,500 #
Vessel Intervals and Thermal Shield	21,300 #
Solid Moderator	4,100 #
Water (Cold at normal water level)	17,100 #
Superheater Elements (120 ea.)	3,800 #
Boiler Elements (115 ea.)	13,600 #
Total	139,800 #

5.7 Refueling Procedure

The following procedure would be followed for refueling with all of the operations being performed remotely;

1) Superheater flooded with water to provide cooling for elements and additional shielding. Calculations and experiments must be made to insure that $k < 1$ when the superheater is flooded with cold water.

The moderator will not be damaged by flooding with water (See Section 5.1.6) and when the reactor is started up the water will be vaporized through the vents in the superheater cover plate.

2) Upper shielding plug removed.

3) Control rods unlatched from drives (Rods fully inserted).

4) Flange closure nuts loosened by inserting induction heaters in axial hole drilled through studs.

5) Studs and head are removed from disconnecting the connection on the discharge side of the relief valve (See 5.1.7).

6) Temporary cooling discharge lines dropped into boiler and superheater regions to draw off water heated by fission product decay gammas. (Cooling water for boiler inserted through "preheat" steam connection and that for superheater through the main steam line.)

7) The hold down plate securing device is removed and the hold down plate lifted off the fuel elements and control rod guide tubes.

8) The elements may now be removed and placed in cooled coffins. (The boiler elements may simply be lifted out of the core but the superheater elements must be unlatched from their guide tubes.)

If the superheater section only is to be refueled the above procedure would be identical except for omitting step 7.

To provide additional shielding it would be possible to flood the entire reactor compartment since the thermal insulation is water resistant. Another method would be to construct a water tight top of the radiation shield. This could be flooded during refueling for additional shielding.

6. SHIELDING

6.1 Introduction

The purpose of this chapter was to design a thermal shield for the reactor and to estimate the shielding weight for the entire system. The weight of the shielding necessary for the protection of personnel and materials limits the application of any mobile reactor. Determining this weight involves the optimizing of such items as reactor size, machinery and compartment arrangements, and type of application. To conform to the purpose of this report and the time restrictions, it was decided to design: (1) A thermal shield that would adequately protect the reactor pressure vessel with little regard to optimizing the size, position, and materials of the shield; (2) a primary and secondary shield to allow a minimum access time to the reactor compartment at full power of 1 hour/week. The shielding weight of such a plant would put a limitation on its use and would require a complete study of its own. The shielding weight as reported in this short study is intended to serve as a rough index on the size of the ship the reactor could be used on. Once this has been decided, a complete shielding study could be made. If the arrangement of a particular ship were such that members of the crew must spend more than a few hours per day in compartments adjacent to the reactor and/or turbine spaces, more shielding would be required.

6.2 Heat Generation in the Pressure Vessel

6.2.1 Method

The method used for calculating the gamma heating was essentially that used in reference (35). A summary of this method and formulas used are presented in this report.

6.2.2 Sources

An operating reactor emits radiation in the form of neutrons, alpha and beta rays, and gamma rays. Because of the short mean free paths associated with alpha and betas it was assumed that their energy is released entirely within the core. Neutrons were separated into two groups, fast and thermal. Heating from neutrons is of two types, direct and indirect. The heating from the direct effect is negligible at the pressure vessel walls. Heating from the indirect effect, production of gamma rays by capture and inelastic scatter was accounted for.

Gamma heating depends upon the relative number and energy of (1) fission gammas, (2) capture gammas, (3) decay gammas from fission products, and (4) decay gammas from irradiated reactor materials.

As the prediction of a reactor gamma spectrum from basic physical data is marked with uncertainties, it was assumed that the Bulk Shielding Reactor spectrum (experimental) could be corrected to the SSBWR conditions.

6.2.3 The Gamma Flux (Primary)

The measured spectrum of the BSR as found in reference (36) was converted to four energy groups (1, 3, 5, and 7 Mev) for ease in calculations. These groups were normalized to agree with more reliable dose data and are shown in Figure 6-1.

The inside surface of the SSBWR pressure vessel is 9.0 inches from the equivalent core surface. The normalized gamma flux at this distance from the BSR (and at 50 Mw) is given below

Group (Mev)	Gamma Flux (Photons/cm^2-sec)
1	1.65×10^{14}
3	3.0×10^{13}

ORNL-LR-Dwg.-28543
UNCLASSIFIED

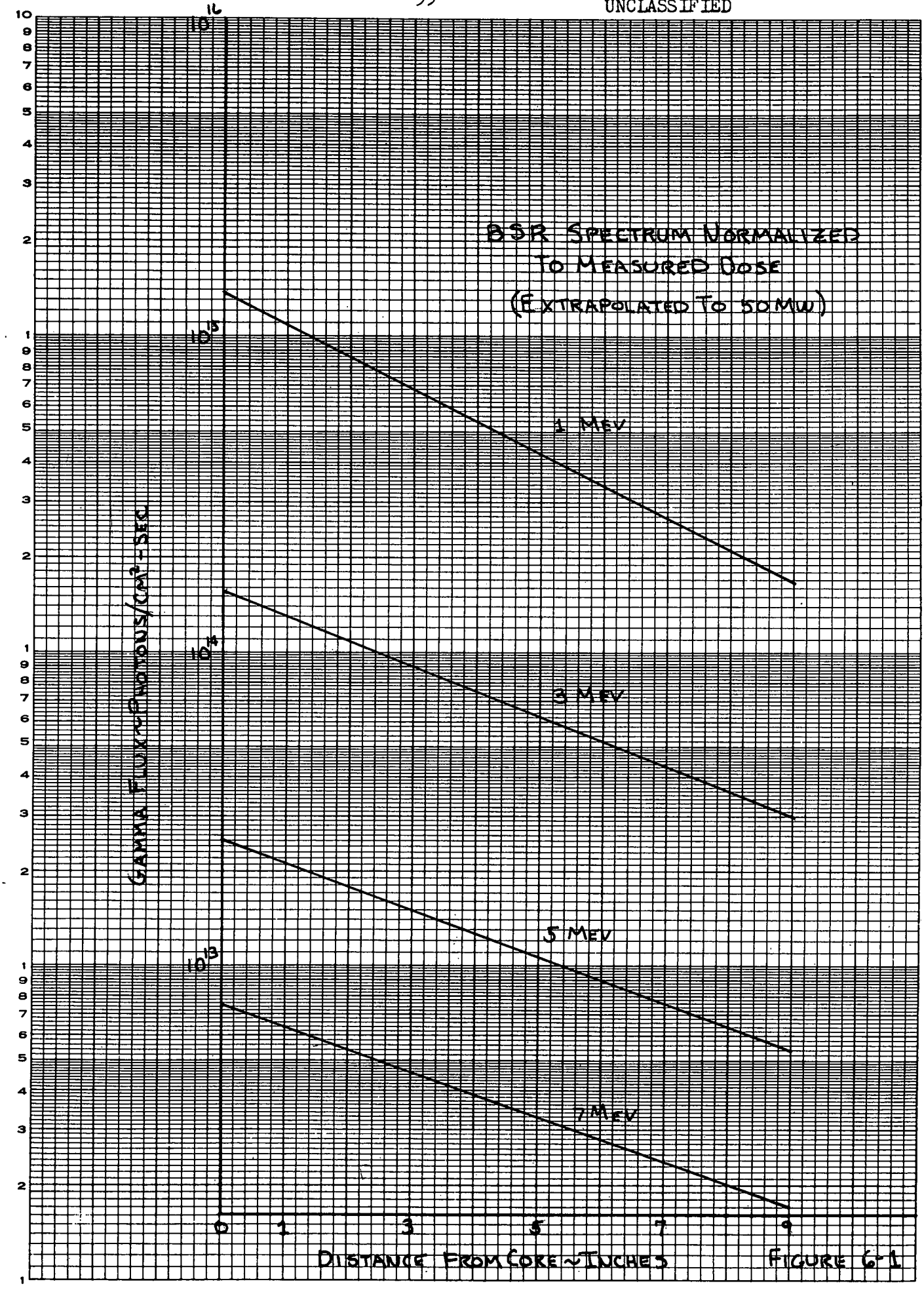

FIGURE 6.1

Group (Mev)	Gamma Flux (Photons/cm^2-sec)
5	5.35×10^{12}
7	1.70×10^{12}

The above spectrum is due to all gammas that arrive 9 in. from the core surface. Therefore to find the contribution from the core gammas only the water capture gammas (2.2 Mev) must be deducted.

The water capture gammas were determined from the expression

$$I = \frac{\phi_o C e^{-\mu t}}{2(A - \mu)} \left[1 - e^{-t(A-\mu)} \right]$$

ϕ_o is the incident thermal neutron flux (BSR)

C gamma ray contribution of the material involved and relates the absorption cross section, the fractions of gammas produced per absorption and the volume fraction of the material present.

A is the attenuating coefficient of the neutrons in the material.

μ is the linear absorption coefficient for gammas.

t is the slab thickness in cm.

$I = 2.64 \times 10^{12}$ Photons/cm^2-sec

The equivalent core spectrum is now:

Group	Gamma Flux
1	1.65×10^{14}
3	$3.0 \times 10^{13} - 0.26 \times 10^{13}$ $= 2.74 \times 10^{13}$
5	5.35×10^{12}
7	1.70×10^{12}

The SSBWR flux differs from that of the BSR for several reasons. (1) Attenuation from the reactor core is through hot rather than cold water. (2) The geometry and self absorption properties of the cores differ. (3) The gamma spectrum is different due to different core materials.

The method which was used for allowing for these differences is outlined below.

1. The BSR spectrum (core only) at 9 inches from the core surface was converted to a uniform volume source of an equivalent cylindrical core.

2. Synthetic volume sources were constructed for both BSR and SSBWR type cores. The ratio of these values which involve power density and spectrum corrections times the converted BSR volume source provided an equivalent SSBWR volume source normalized to measured gamma dose rates.

3. The gamma flux at the SSBWR pressure vessel was computed from the above volume source with due allowance for core size, self absorption attenuation through reflector and thermal shield, and buildup.

4. The equation and geometrical considerations for the transformation from a cylindrical volume source to an equivalent gamma flux are given in Figure 6-2.

The resulting primary gamma flux at the SSBWR pressure vessel is:

Group	I Photons/cm^2-sec
1	1.9×10^{12}
3	5.52×10^{11}
5	1.56×10^{11}
7	2.34×10^{11}

ORNL-LR-Dwg.-28544
UNCLASSIFIED

PRIMARY GAMMA GEOMETRY

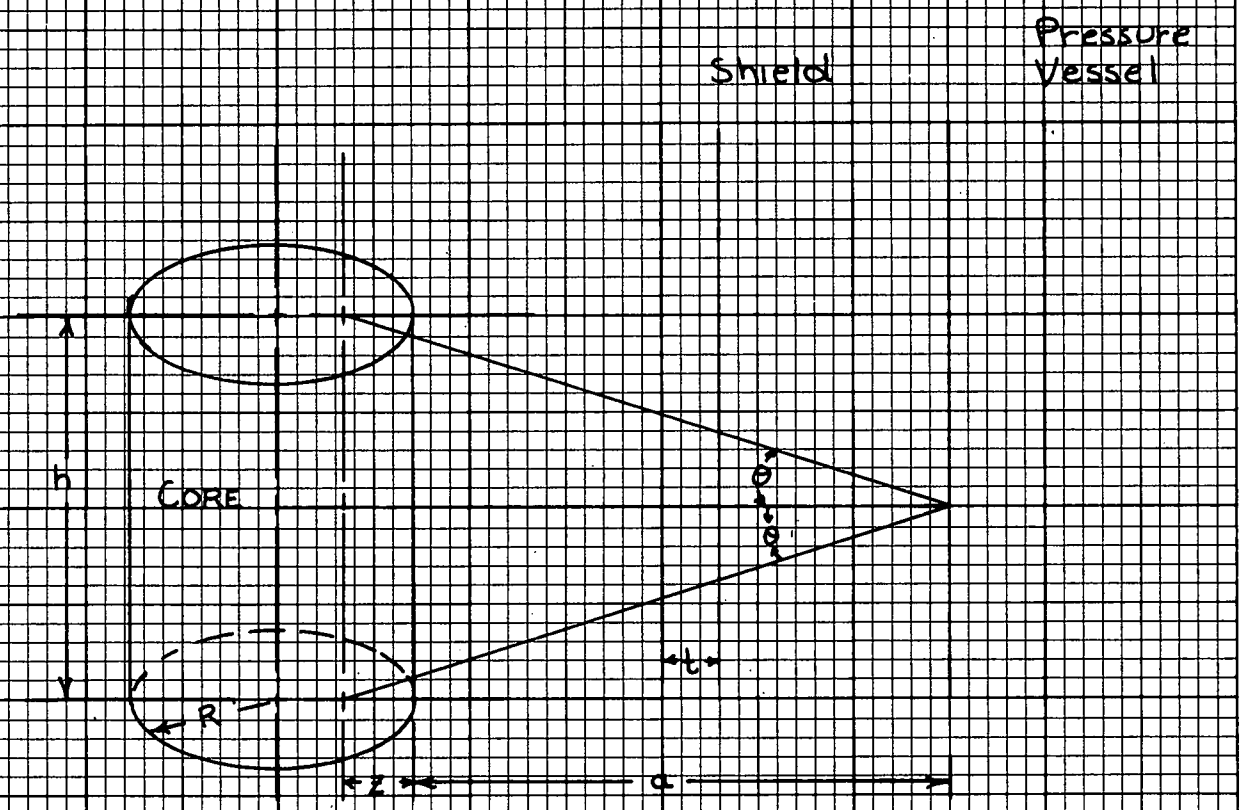

$$I(a) = \frac{B S_v R^2 F(\theta, b)}{2(a+z)} = \text{gamma flux} \sim \text{photons/cm}^2\text{-sec}$$

S_v is the core volume source ~ photons/cm³-sec

R is the core radius ~ cm.

$$F(\theta, b) = \int_0^{\theta} e^{-b \sec\theta'} \, d\theta'$$

$$b = \mu_w (a-t) + \mu_{ss} t + \mu_c z$$

a is the core to vessel distance ~ cm.

t is the thermal shield thickness ~ cm.

z is an effective distance due to self absorption

B is the build-up factor

FIGURE 6-2

6.2.4 The Secondary Gamma Flux

The secondary gamma flux at the pressure vessel includes gammas from the capture of thermal neutrons in the water, thermal shield and pressure vessel itself and gammas from the inelastic scattering of fast neutrons. Therefore thermal and fast flux distribution through the reflector and thermal shields had to be determined.

6.2.4.1 Thermal flux

The thermal flux at the outside surfaces of the thermal shields was estimated (from LID tank data (37) to be 1/3 of that for an all-water reflector. The effective thermal flux attenuation in the shield was assumed equal to e^{-Ax} where $A = \frac{1}{L}$, and $L = 0.652\ cm^{-1}$ is the diffusion length in stainless steel. Figures 6-3 and 6-4 show the details of the flux computation within the thermal shields.

6.2.4.2 Fast Flux

The attenuation of the fast flux by the thermal shield was based on the use of an effective removal cross section σr = 2 barns). Figure 6-5 shows a plot of the fast flux in the reflector and thermal shields.

6.2.4.3 Capture-gamma Production

The capture gamma rays leaving a slab of finite thickness are related to the incident flux by the expression

$$I = \frac{\phi_o C e^{-\mu t}}{2(A - \mu)}\left[1 - e^{-t(A-\mu)}\right]$$

(Symbols are defined in Section c.2.3)

In order to determine the contribution to heat generation in the pressure vessel the above gammas were attenuated through interposed material.

ORNL-LR-Dwg.-28545
UNCLASSIFIED

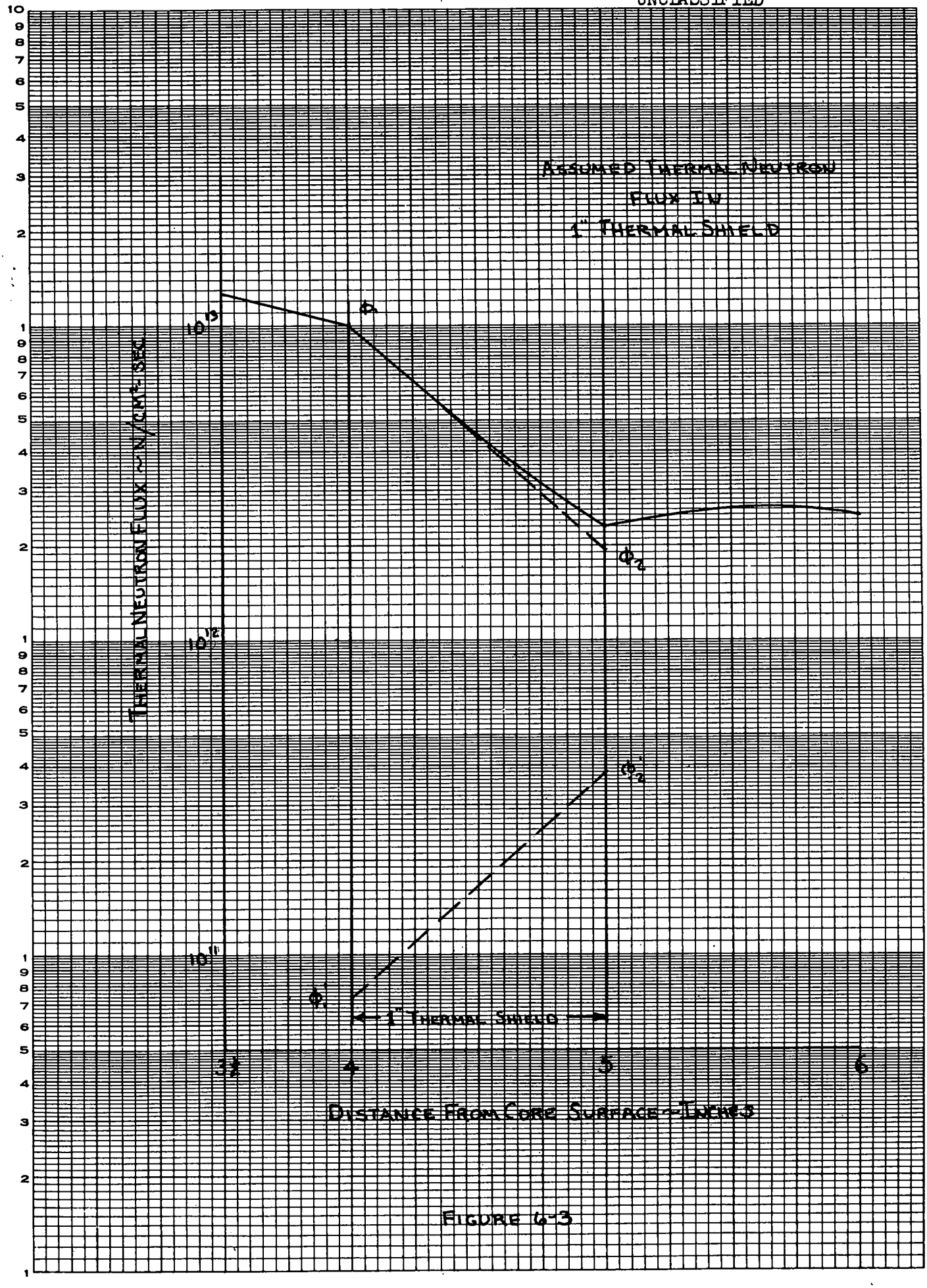

FIGURE 6-3

ORNL-LR-Dwg.-28546
UNCLASSIFIED

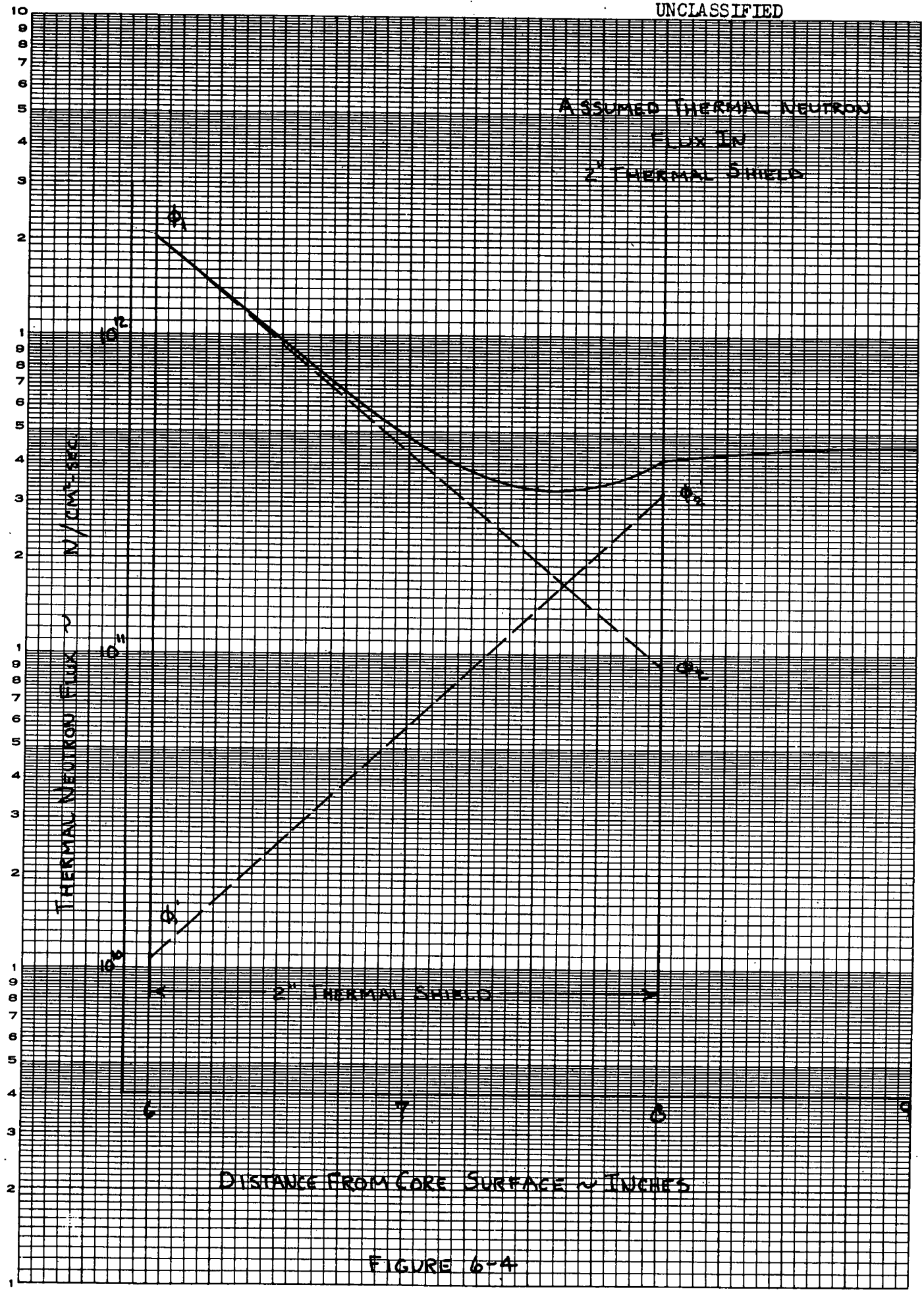

FIGURE 6-4

The attenuations through water were obtained from BSR data corrected for lower water density.

$$I/I_o = f(R)\ B\ e^{-\mu x}$$

$$I/I_o = f(R)\ B'\ e^{-\mu' x}$$

$$\therefore \quad I' = I \frac{B'}{B} \frac{e^{-\mu' x}}{e^{-\mu x}}$$

where I' results from attenuation through 570°F water

μ' is the linear absorption coefficient in hot water

$= 0.72\ \mu \sim 570^{\circ}F$

The attenuation due to stainless steel was computed using the conventional expression

$$I/I_o = f(R)\ Be^{-\mu t}$$

$$f(R) = \frac{R_o + a}{R_o + a + t}$$

R_o = effective radius of core

a = distance from core to attenuating slab

t = slab thickness

B = appropriate buildup factor

a. Capture gammas from the thermal shields

The thermal shield consists of a 1-inch thick stainless steel slab located 4 inches from the effective core surface and a 2-inch thick stainless steel slab located 6 inches from the effective core surface. The capture gammas generated were assumed to be the sum of those due to the exponentials shown in Figures 6-3 and 6-4, and can be computed using the following expression.

$$I = \frac{\phi_1\ Ce^{-\mu t}}{2(A-\mu)}\left[1 - e^{-t(A-\mu)}\right] + \frac{\phi_1'Ce^{-\mu t}}{2(A'-\mu)}\left[1 - e^{-t(A'-\mu)}\right]$$

ORNL-LR-Dwg.-28547
UNCLASSIFIED

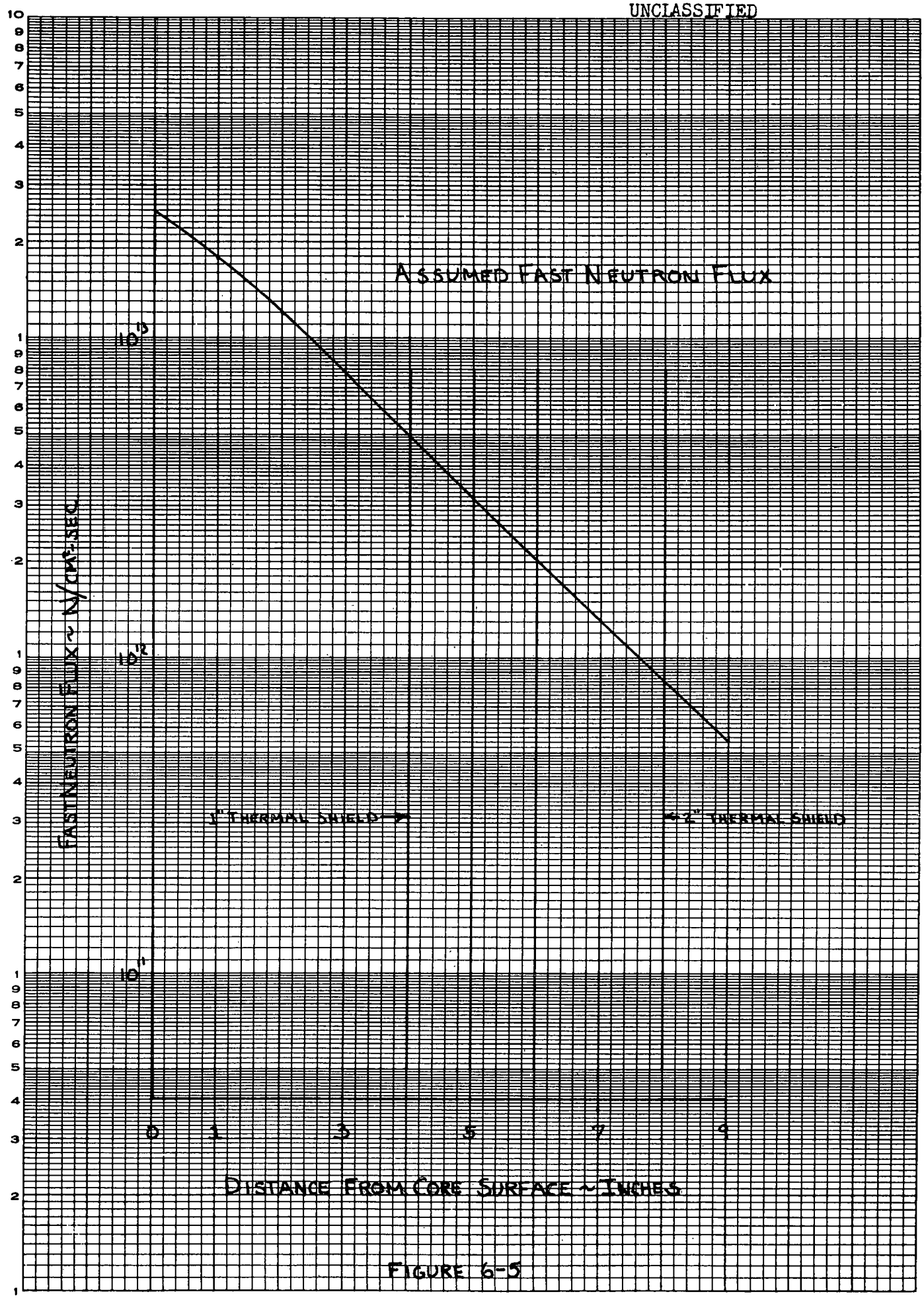

FIGURE 6-5

Using appropriate attenuation factors the capture gammas reaching the pressure vessel are:

Group	I (From 1 in. th. Shield)	I (from 2 in. Th. Shield)
1	1.1×10^{10} γ's/cm^2-sec	2.1×10 γ's/cm^2-sec
3	3.62×10^{10} "	3.94×10^{10} "
5	5.35×10^{10} "	5.90×10^{10} "
7	1.52×10^{11} "	1.92×10^{11} "

b. Capture gammas from the pressure vessel

The pressure vessel for the SSBWR consists of a 1/4-inch thick stainless steel cladding backed by 3-1/2-inches of pressure vessel steel.

The heating effect of gammas generated in the pressure vessel wall is a maximum inside the wall. An approximate and somewhat conservative approach is to consider an equivalent source of gammas incident on the inside surface of the pressure vessel.

The gamma production at any point in the thermal shield can be computed from the general expression (35)

$$I = \frac{\phi_o C}{2}\left[\frac{e^{-\mu x}}{A-\mu}\left[1 - e^{-x(A-\mu)}\right] + \frac{e^{\mu x}}{A+\mu}\left[e^{-x(A+\mu)} - e^{-t(A+\mu)}\right]\right]$$

The equivalent incident gammas are:

Group	I(photons/cm^2-sec)
1	2.35×10^9
3	1.045×10^{10}
5	1.52×10^{10}
7	3.61×10^{10}

c. Capture gammas from the water

The absorption of a thermal neutron by water (hydrogen) produces one gamma photon of about 2.2 Mev energy. The assumed flux pattern and slab thicknesses are shown in Figure 6-6.

The total gamma flux from water capture incident on the pressure vessel is:

Group	I (photons/cm^2-sec)
2.2	1.03×10^{11}

6.2.4.4 Inelastic-scatter-gamma Production

Gamma rays from the inelastic scattering of fast neutrons are produced in the thermal shields and pressure vessel. The resulting gamma flux at the inside of the pressure vessel can be estimated by the same methods used for the capture gammas. The resulting gamma fluxes are:

	Group	I (photons/cm^2-sec)
1-inch Thermal Shield	1	3.52×10^{10}
2-inch Thermal Shield	1	8.05×10^{10}
Pressure Vessel	1	1.88×10^{11}

6.2.4.5 Summary of Gamma Fluxes

It was assumed that the total radiation heating effect in the pressure vessel wall is due to the primary and secondary gammas generated by the operating reactor as estimated above. The following table summarizes the gamma flux incident on the pressure vessel wall:

Group (Energy)	1	3	5	7
Primary (Core) Gammas $\times 10^{-11}$	19.0	5.52	1.56	2.34
Secondary Gammas $\times 10^{-11}$				
Capture-1 in. Thermal Shield	0.11	0.36	0.53	1.52

ORNL-LR-Dwg.-28548
UNCLASSIFIED

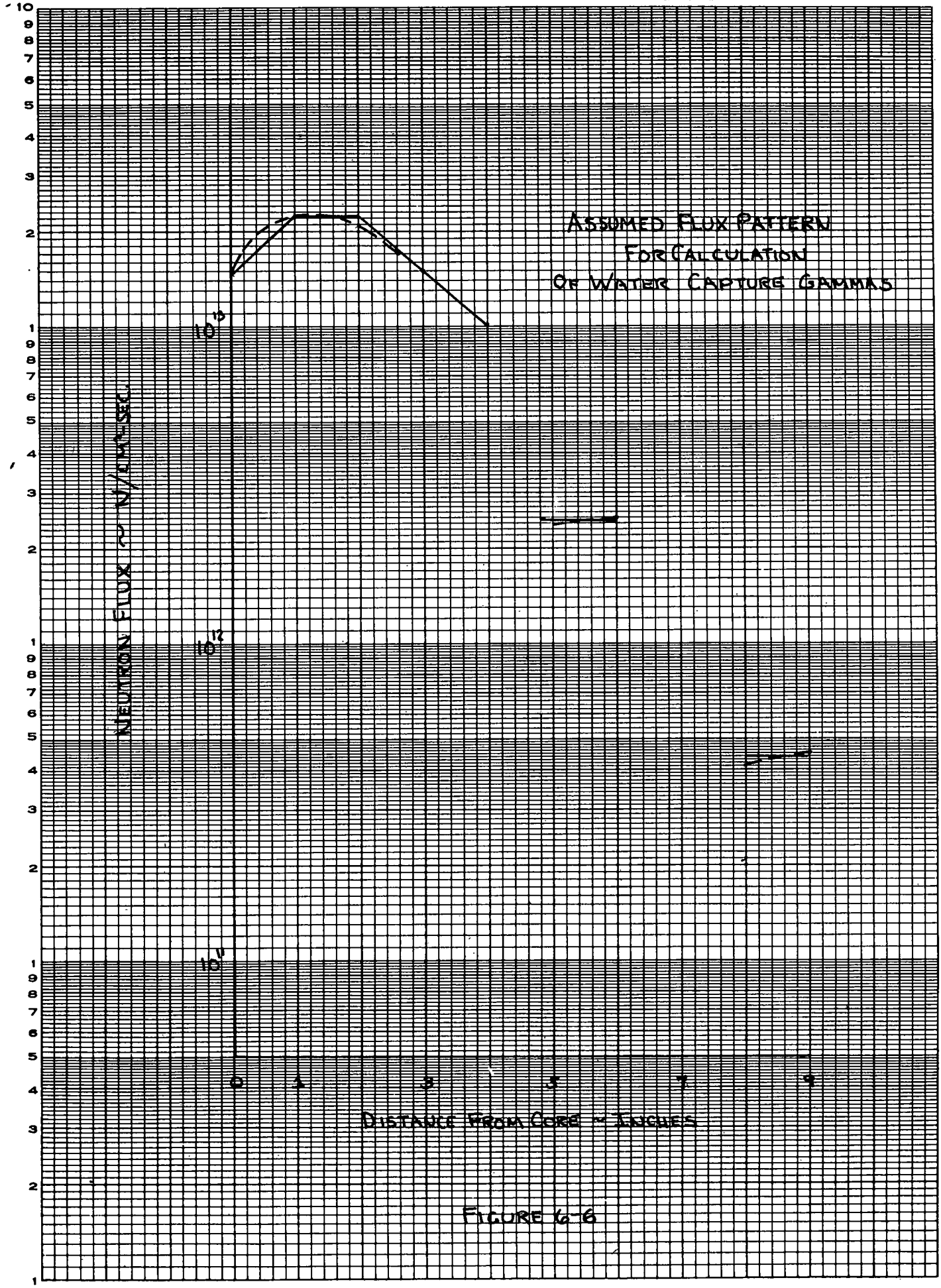

FIGURE 6-6

ORNL-LR-Dwg.-28549
UNCLASSIFIED

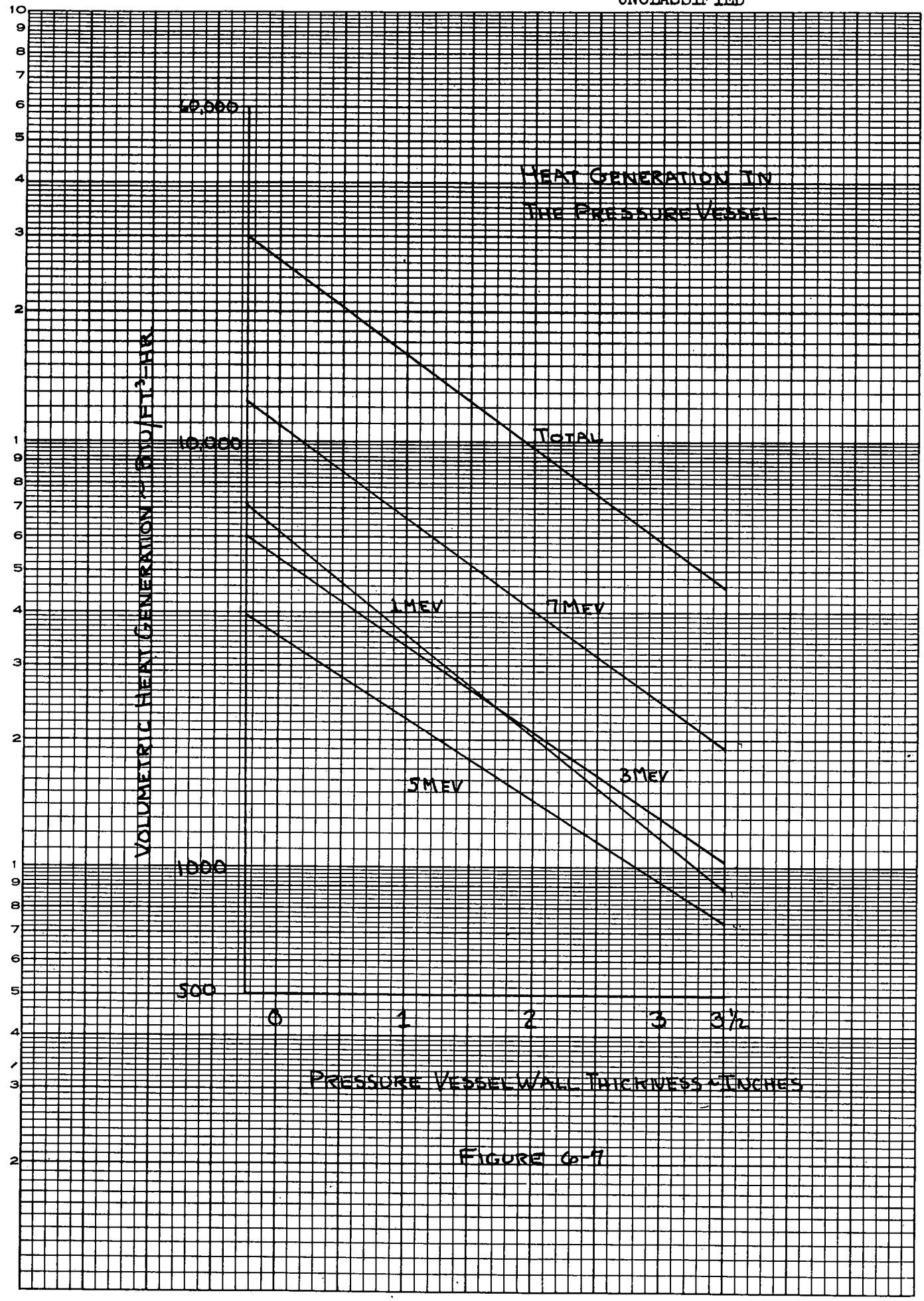

FIGURE 6.9

Secondary Gammas x 10^{-11} (cont.)				
Capture-2 in. Thermal Shield	0.21	0.39	0.59	1.92
Capture Pressure Vessel	0.02	0.11	0.15	0.36
Capture Water		1.03		
Group (Energy)	1	3	5	7
Capture Total x 10^{-11}	0.34	1.89	1.27	3.80
Inelastic Scattering 1-in. thk Shield	0.35			
Inelastic Scattering 2" thk Shield	0.80			
Inelastic Scattering Pressure Vessel	1.88			
Inelastic Scattering - Total x 10^{-11}	3.03			
Secondary Totals x 10^{-11}	3.37	1.89	1.27	3.80
Total Gammas x 10^{-11}	22.37	7.41	2.83	6.14

6.3 Pressure Vessel Temperatures

The SSBWR pressure vessel is essentially a 74-inch inside diameter cylinder welded of 3-1/2-inch SA 212-B steel plate, clad on the inside with 1/4" of Type 304 stainless steel. The entire vessel is enclosed in 4-inches of thermal insulation.

Because of the insulation it is assumed that there would be essentially no temperature drop across the pressure vessel if no gamma radiation were present. It is assumed that all the radiation generated heat in the wall is removed by the reactor coolant.

In general the temperatures (and resulting thermal stresses) which exist in the pressure vessel wall depend upon the incident gamma flux, the wall thickness, and the method of cooling (or insulating) the wall. For this analysis the wall thickness and method of cooling were fixed. The maximum temperature difference is thus a function of the incident radiation only.

The volumetric heat release at the inside surface of the pressure vessel was computed for each energy group by the expression:

$$Q_o = I \times E \times \mu_e \times 1.55 \times 10^{-8}$$

where I is the incident gamma flux in photons/cm^2-sec

E is the group energy in Mev

μ_e is the linear energy abs. coefficient

1.55×10^{-8} is the conversion factor for Mev/cm^3-sec to Btu/ft^3-hr

The volumetric heat release at points in the pressure shell was computed by

$$Q = Q_o e^{-\mu e x} f(R)$$

X is the distance inside the shell in cm^{-1}

$f(R)$ is the geometric factor $= \frac{R_o}{R_o + t}$

Figure 6-7 shows the volumetric heat generation in the SSBWR pressure vessel wall.

The temperature distribution in the pressure vessel was shown to be:

$$T = \frac{Q_o}{KA^2} (1 - e^{-Ax} - xAe^{-At})$$

In order to approximate the operating temperature it was necessary to estimate the heat flow and resistance to heat flow. The quantity of heat flowing across the inner surface was found by the expression

$$H = \frac{Q_o}{A} (1 - e^{-At})$$

$$H = 4150 \text{ Btu/ft}^2\text{-hr}$$

The temperature drop across the coolant film was found from the expression

$$H = h_f \Delta T$$

The film coefficient was estimated from the expression (6)

$$h_f \cong 170\ (1 + T \times 10^{-2} - T^2 \times 10^{-5})\ \frac{V^{0.8}}{D_e^{0.2}}$$

where T is the bulk water temperature

V is the average coolant velocity

D_e is the equivalent hydraulic dia.

$\therefore\ h_f = 480$

and $\Delta t = \frac{4150}{480} = 8.6^{\circ}F$

If a scale condition on the inside of the pressure vessel is assumed then a temperature drop across the scale can be estimated by the expression

$$H \cong \frac{K_s}{t_s}\ \Delta T$$

where K_s is the thermal conductivity of the scale ≈ 1

t_s is the scale thickness $\approx$ 0.01 inches

$$\Delta T = \frac{4150}{1} \times \frac{.01}{12} = 3.5^{\circ}F$$

For the temperature distribution in the 1/4" cladding

$Q_o = 29375$ Btu/ft^3-hr

$A = 6.0$ ft^{-1}

$K = 11.7$ (at 577°F)

$$\Delta T_o = \frac{Q_o}{KA^2}\ (1 - e^{-Ax - xA\Theta - At})$$

$\Delta T_{1/4"} = 6.2^{\circ}F$

For the temperature distribution in the pressure vessel proper

$Q_o = 26{,}500$ Btu/ft^3-hr

$$A = 6\ ft^{-1}$$

$$K = 25.6 \text{ (at } 587^{\circ}F)$$

$$\Delta T_{1''} = 8.8^{\circ}F$$

$$\Delta T_{2''} = 13.2^{\circ}F$$

$$\Delta T_{3-1/2''} = 15.0^{\circ}F$$

The temperature profile in the pressure vessel wall is shown in Figure 6-8.

6.4 Pressure Vessel Stresses

The total stress in the pressure vessel wall is assumed to be the algebraic sum of the pressure stress and the thermal stress. For both the pressure stress and thermal stress, the tangential stress at the inside is the greatest of the three components. The maximum thermal stress occurs at the reactor mid-plane, therefore the maximum total stress in the reactor vessel is the sum of the pressure and thermal tangential stresses at the reactor mid-plane.

6.4.1 The Tangential Pressure Stress

The reactor vessel is essentially a cylinder 74" -inch inside diameter with a 3.75-inch thick wall. Because of the 1/4-inch stainless steel wall the effective inside diameter is 74.5-inches and the wall thickness is 3.5-inches.

The maximum tangential pressure stress was computed from the following expression:

$$S_{TP} = p\left[\frac{a^2}{b^2 - a^2}\right]\left[\frac{b^2}{a^2} + 1\right]$$

S_{TP} is the tangential pressure stress

p is the design pressure 1300 psi

ORNL-LR-Dwg.-28550
UNCLASSIFIED

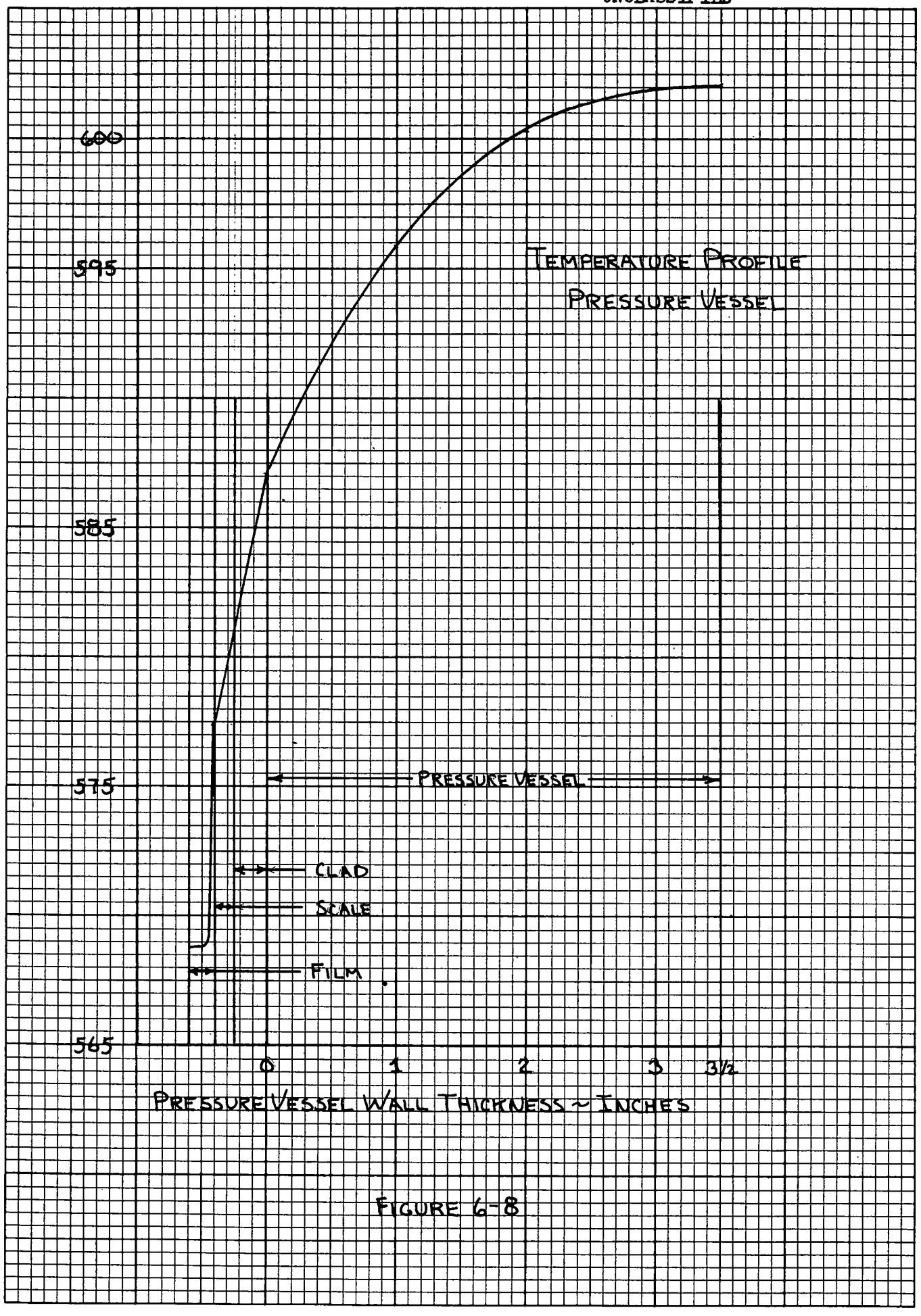

FIGURE 6-8

a is the inside radius 37.25 inches

b is the outside radius 40.75 inches

$\therefore$ S_{TP} = 14,600 psi

6.4.2 Tangential Thermal Stress

The tangential thermal stress was computed from the following expression (35)

$$STT = \left(\frac{\alpha E}{1-\nu}\right)\left(\frac{Q_o}{KA^2}\right)\left(\frac{2}{b^2 - a^2}\right)\left[a\left\{c - \frac{1}{A} + e^{-Ac}\left(\frac{1}{A} - \frac{A_c^2}{2}\right)\right\} + \left\{\frac{C^2}{2} - \frac{1}{A^2} + e^{-Ac}\left(\frac{A_c + 1}{A^2} - \frac{A_c 3}{3}\right)\right\}\right]$$

where α is the linear coefficient of expansion of the vessel steel

7.20×10^{-6} at 591°F

E is Youngs Modulus, 25.8×10^6 psi at 591°F

ν is Poisson's ratio = 0.3

C is the wall thickness = 0.292 ft

a and b are the inner and outer radius in feet. 3.1 ft and 3.4 ft

STT = 2720 psi

6.4.3 Summary of Pressure Vessel Stresses

The maximum total stress is then the sum of these two tangential stresses and is equal to 17,320 psi which is conservatively under the maximum allowable stress of 1.5 S_A (26,250 psi) as suggested in Code Case # 1234.

6.5 Heat Generation In the Thermal Shields

The calculation of the heat generation in the thermal shield cannot be simplified as was done for the pressure vessel. The total energy absorption depends upon the incident energy from the inside, the incident energy from

the outside, and the gammas generated within the thermal shield. The total absorption distribution across the thermal shield will be required to compute the total heat generated.

6.5.1 The Gamma Flux

The primary and secondary gamma flux incident on and generated in the thermal shield were computed by the same techniques used for the pressure vessel wall. The resulting volumetric heat generation rates in the thermal shield are plotted in Figures 6.9 and 6-10.

6.6 Thermal Shield Temperatures

The thermal shield temperature profile can be computed from the expression

$$T = \frac{Q_o}{KA^2} \left[1 - e^{-Ax} - \frac{x}{c}\left(1 - e^{-Ac}\right)\right]$$

where T is the temperature above the surface temperature

The point of maximum temperature in the thermal shield was found from the expression

$$X'(max) = -\frac{1}{A} \ln \frac{1 - e^{-Ac}}{Ac}$$

X' (for 1 in. thermal shield) = 0.486 inches = 0.0406 ft

X' (for 2 in. thermal shield) = 0.916 in. = 0.0765 ft

The heat transferred through the thermal shield was obtained from the expressions

$$Hi = \int_0^{x'} Q(x)dx = \frac{Q_o}{A}\left(1 - e^{-x'A}\right)$$

$$H_o = \int_{x'}^{c} Q(x)dx = \frac{Q_o}{A}\left(e^{-x'A} - e^{-cA}\right)$$

ORNL-LR-Dwg.-28551
UNCLASSIFIED

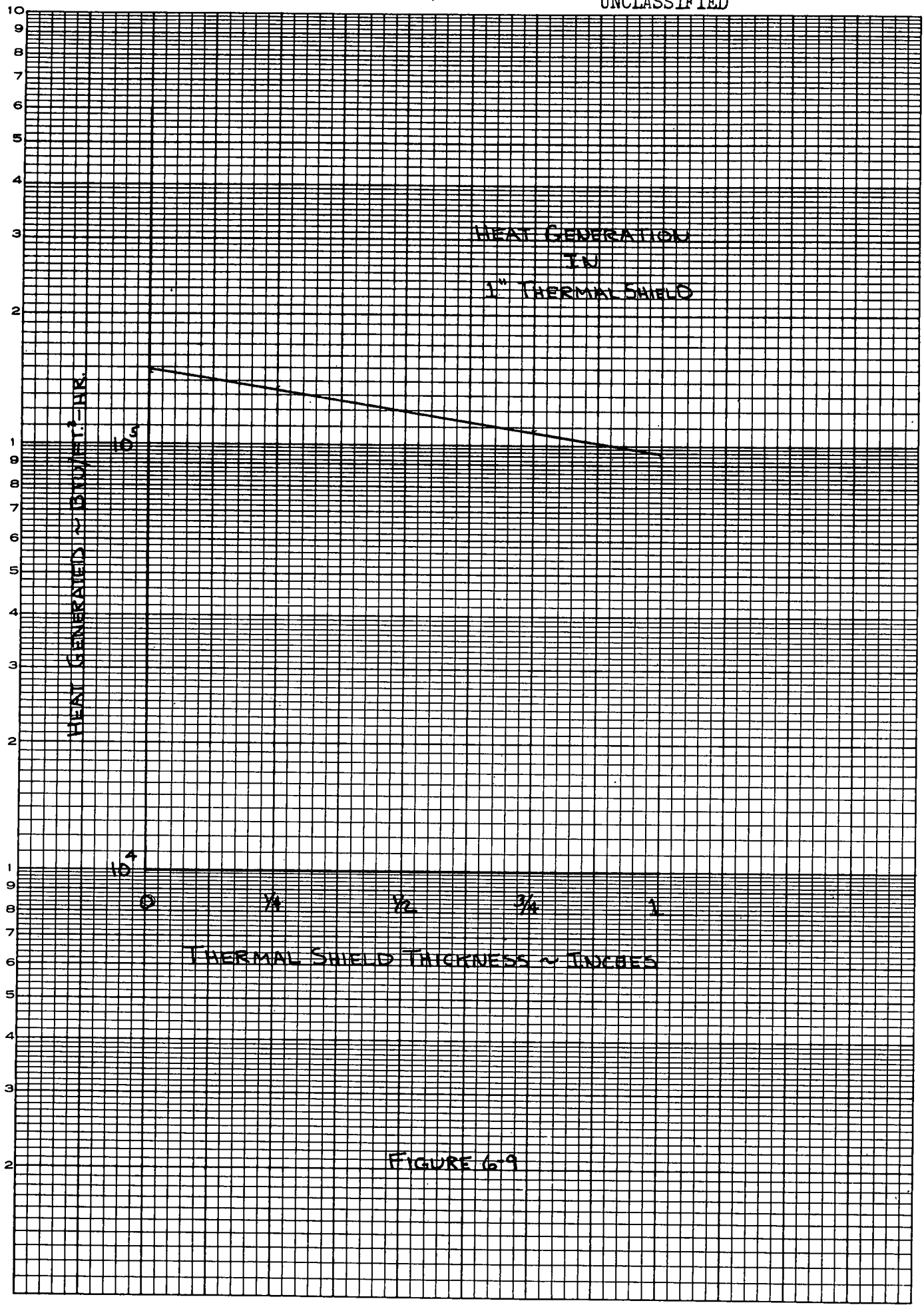

FIGURE 6-9

ORNL-LR-Dwg.-28552
UNCLASSIFIED

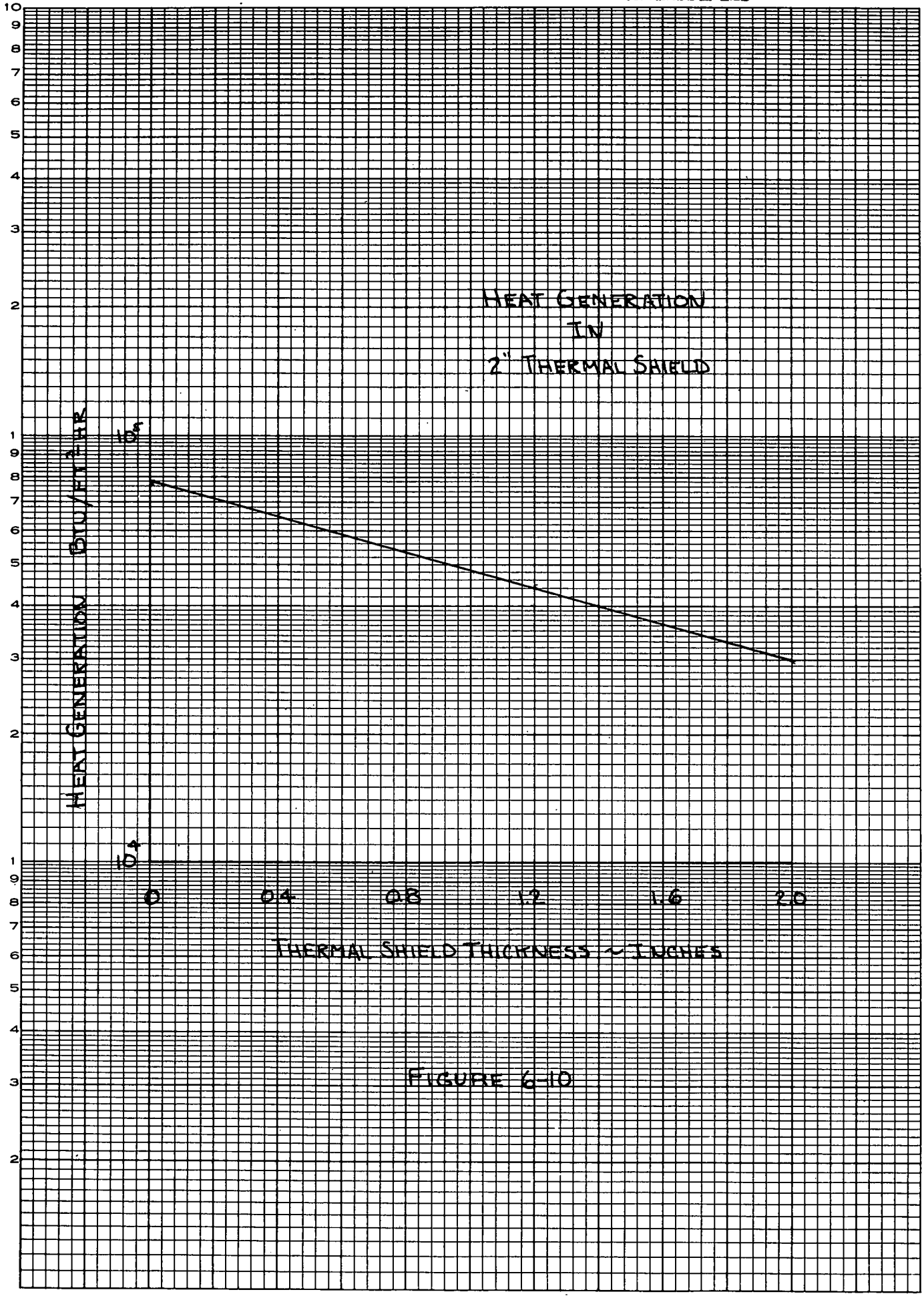

FIGURE 6-10

The temperature profile in the thermal shields is shown in Figures 6-11 and 6-12.

The coolant velocity between the thermal shields, computed to be 0.7 ft/sec, results in a 10% average void fraction in the thermal shield coolant.

6.7 Thermal Shield Stresses

It was assumed that a negligible pressure difference between the sides of the thermal shield exists. The maximum stress in the thermal shield is simply the tangential component of the thermal stress at either surface. This stress can be computed using the expression in Section 6.4.2. The stresses are:

STT (for 1" Thermal shield) = 2180 psi

STT (for 2" Thermal shield) = 3310 psi

6.8 The Primary Shield

6.8.1 Sources

The primary shield as shown in Figures 6-13, 14 and 15 is designed to allow a 1 hour/week acess to the operating reactor compartment. Reactor primary and secondary gammas as summarized in Section 6.2.4.5 were further attenuated to the outside of the shield tank. Gammas produced in the primary shield were calculated using the methods employed in the thermal shielding calculation and these were referred to the outside of the shield tank. The thermal neutron flux distribution through the primary shield was estimated using removal cross sections (37) and is shown with the estimated uncollided neutron flux on Figure 6-16.

6.8.2 Geometry

The reactors were arranged so that full advantage of their self attenuating properties could be employed. A high degree of operational flexibility

ORNL-LR-Dwg.-28553
UNCLASSIFIED

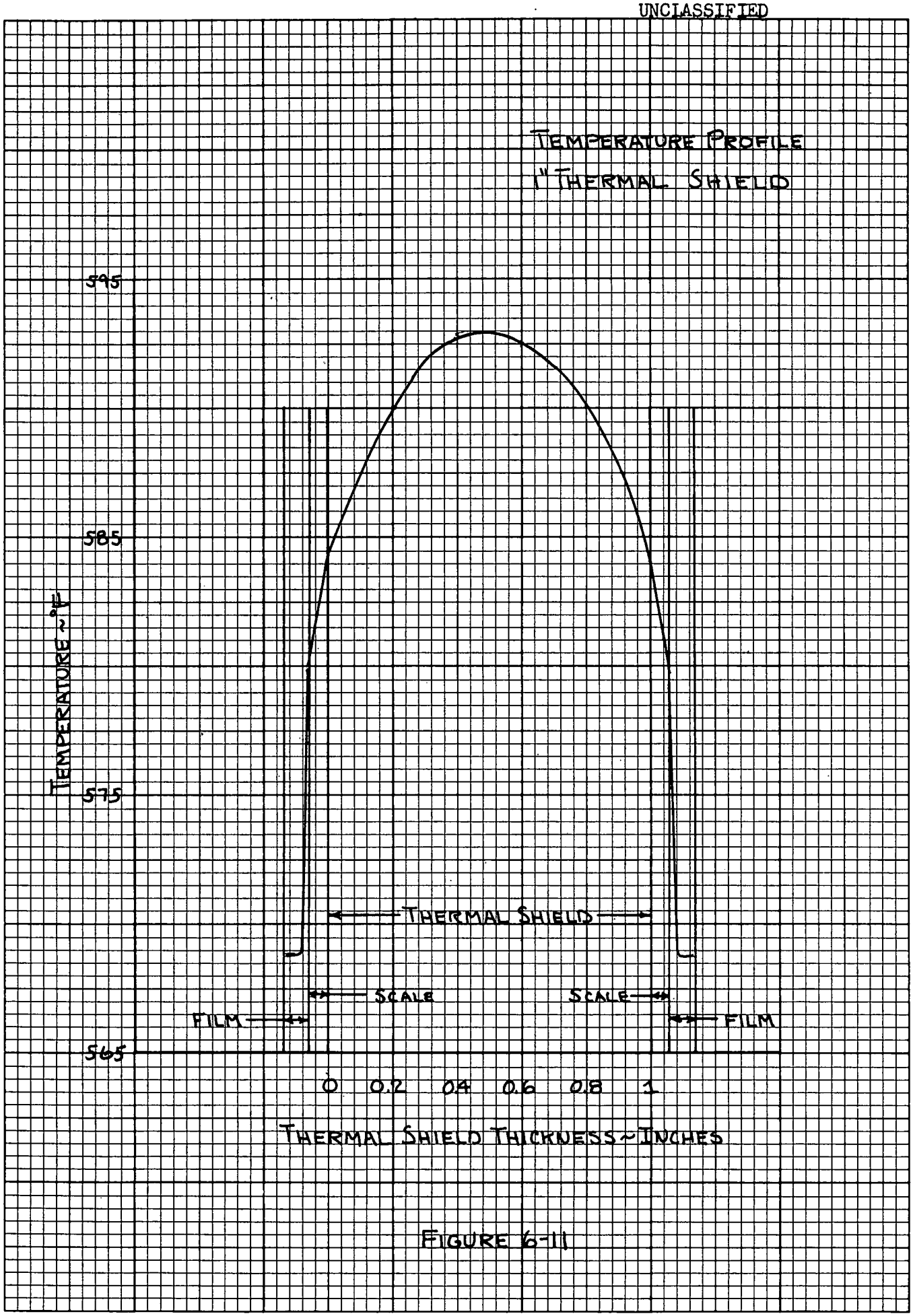

FIGURE 6-11

ORNL-LR-Dwg.-28554
UNCLASSIFIED

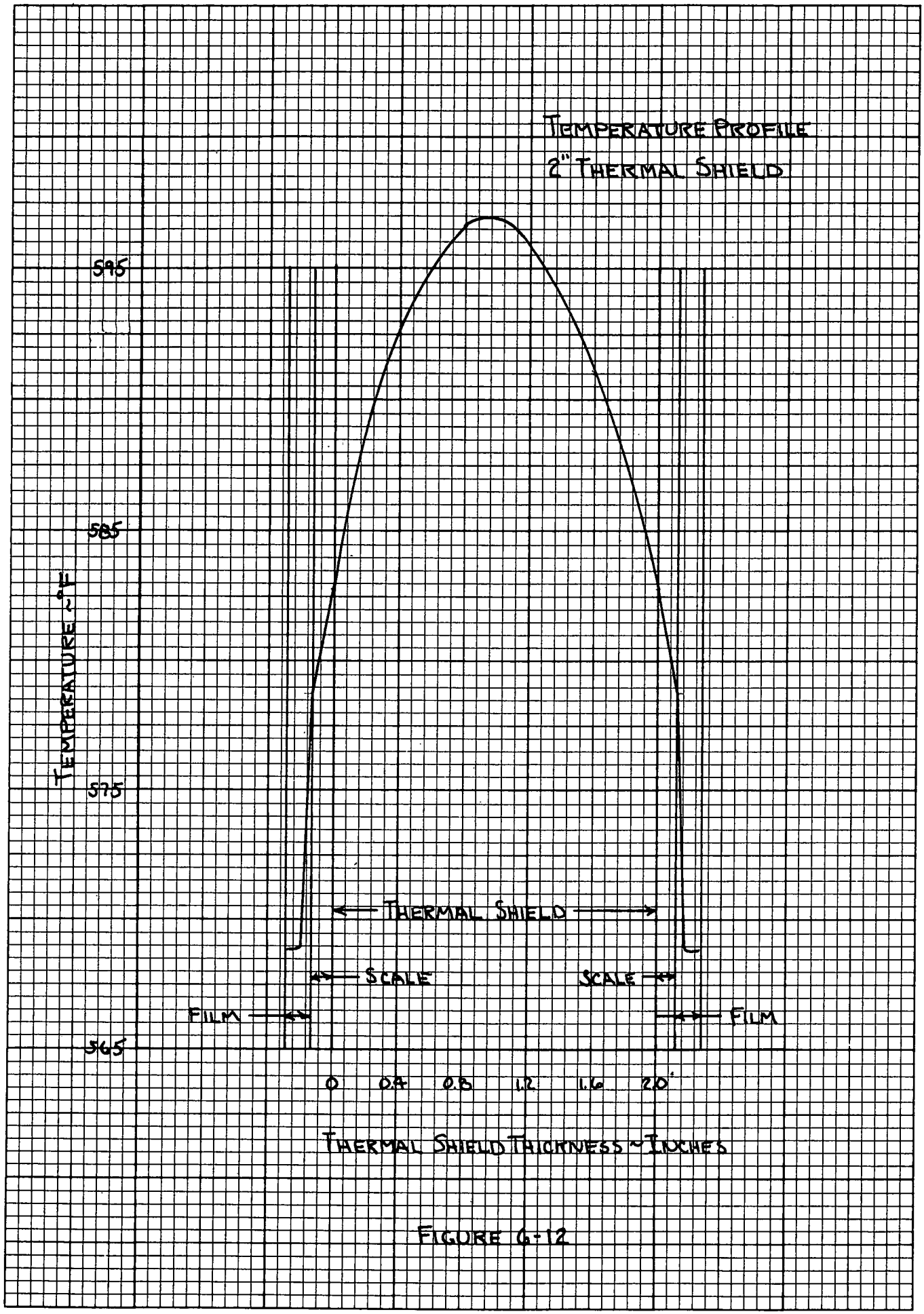

FIGURE 6-12

is insured by using 2 reactors as opposed to one larger reactor. For shielding weight optimization however, one reactor would be better. The highly active recirculation lines are contained by the shield tank as shown in Figure 6-13. Streaming from the superheater has been minimized by fuel element design as shown in Figure 1-3.

6.8.3 Doses

Doses at the outside of the shield tank at the reactor midplane and with the reactor operating at full power are shown in the following table.

	Dose (mr/hr)				
Source Group	1	3	5	7	Total
Primary Core Gammas	0	1.2	7.7	15.4	24.3
Secondary Core Gammas	0	14.2	10.6	17.5	42.3
Water Capture Gammas	-	27.0	-	-	27.0
Fast Neutrons	-	-	-	-	25.0
Thermal Neutrons	-	-	-	-	11.9
Total					130.5

6.8.4 Shield Tank Materials and Weights

The shield tank at its maximum thickness is 42" thick. The inner wall is made up of a 1-inch thick steel plate, and a 5 in. slab of lead canned with 1/4-steel sheet. The outer wall is similarly constructed. Water makes up the remaining 29-1/2-inches of attenuating material. The 10-inches of lead was necessary to attenuate all core gammas and the 5-inches of lead was necessarily placed at the outer wall to attenuate

ORNL-LR-Dwg.-28555
UNCLASSIFIED

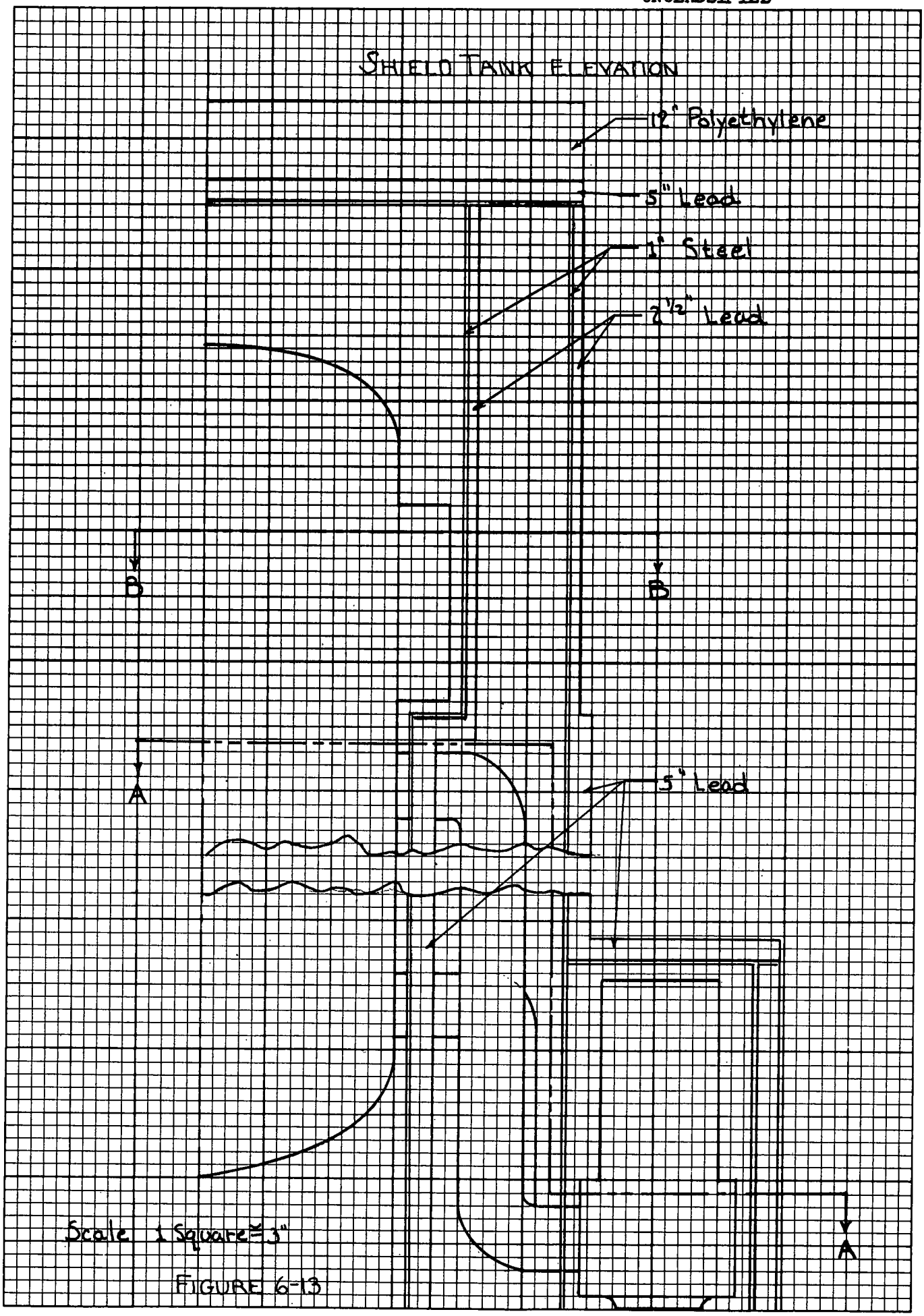

FIGURE 6-13

ORNL-LR-Dwg.-28556
UNCLASSIFIED

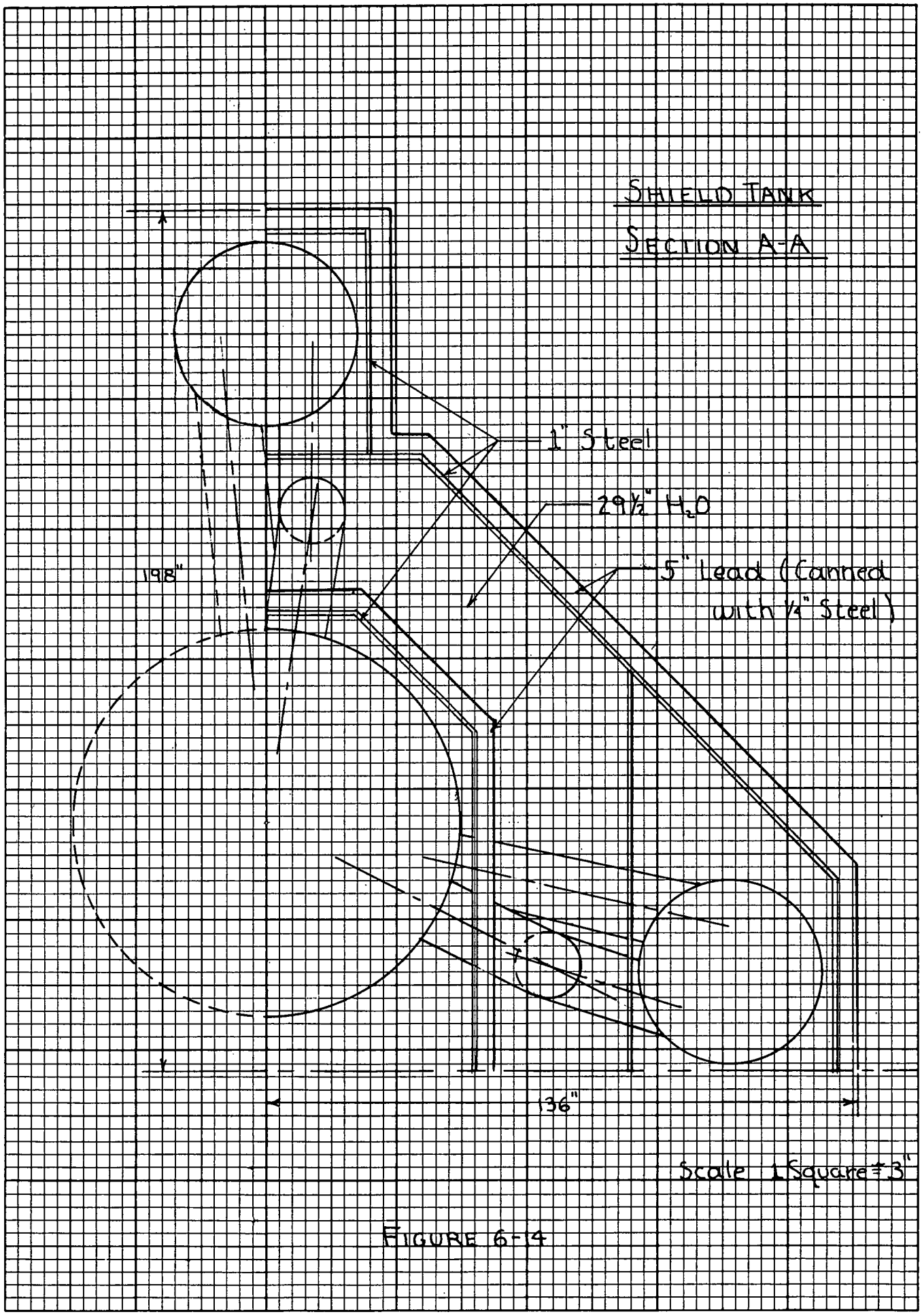

FIGURE 6-14

ORNL-LR-Dwg.-28557
UNCLASSIFIED

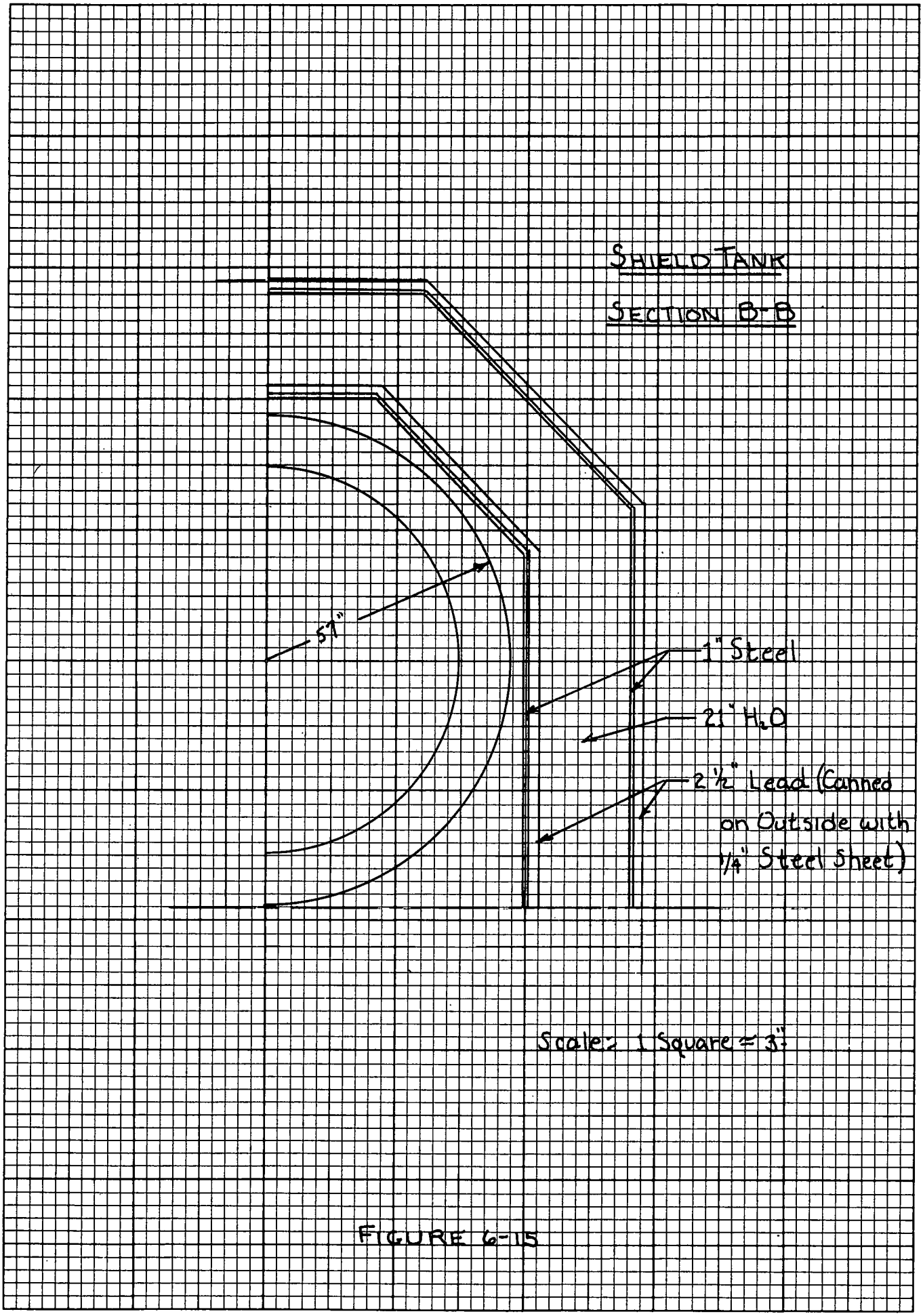

FIGURE 6-15

ORNL-LR-Dwg.-28558
UNCLASSIFIED

FIGURE 6-16

water capture gammas. The weight of the primary shield was 595 tons per plant, (38.1 lbs per shaft horse power).

6.9 The Secondary Shield

6.9.1 Results

An investigation was made to determine how much extra weight for biological shielding must be applied to a conventional steam power plant when radioactive steam from this reactor is used in lieu of boiler steam. The conventional plant selected was a naval steam propulsion plant of 35,000 shaft horsepower, requiring two of these reactors at their design ratings. A block diagram of the plant, a simple one, is shown in Figure 6-17.

Experience with the EBWR (34) has shown that the only activity of consequence in a heterogeneous boiling reactor's steam is that of N_{16}, formed from the O_{16} of the water, which emits a gamma ray of 6.1 or 7.1 Mev. This is also the principal source in pressurized water plants, but steam, being much less dense than water, is a weaker source. Experience with the EBWR (34) shows carryover to be a negligible source.

Our calculations showed, as we had expected, that the only components in the plant requiring shielding in addition to their normal structure were the hotwell, where the condensate collects, and the piping and pump which carry the condensate to the deaerating feedwater heater. In addition, the reactor will require a demineralizer, which must be shielded. The high pressure end of the turbine may require light shielding, depending on how long one wishes to remain near it during operation. All steam pipes and other steam-filled components, on the other hand, gave doses of from

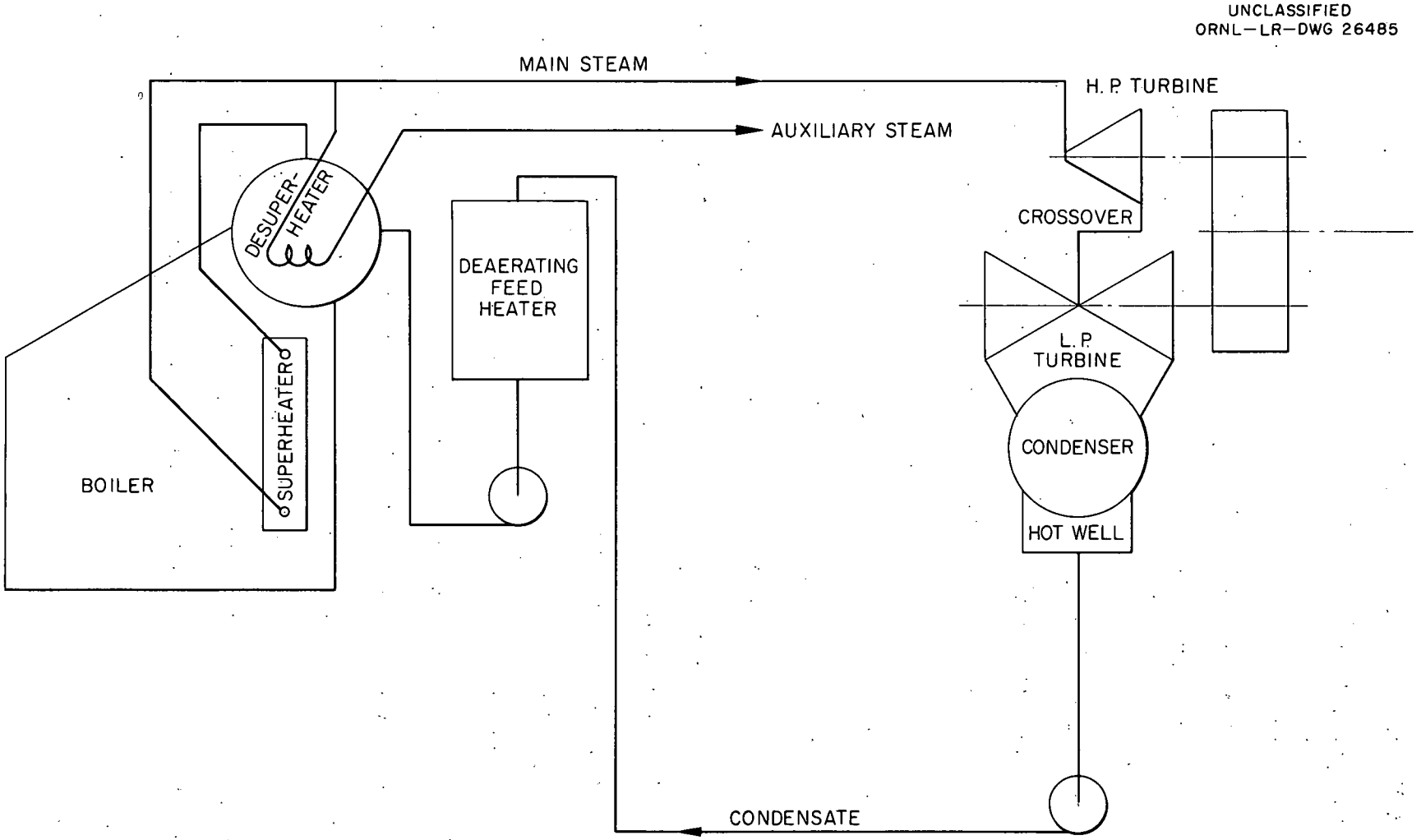

Fig. 6—17. Block Diagram of Typical Naval Steam Plant.

40 to 160 mr/hr at a distance of two feet, which we considered not to require shielding.

Results of our full power calculations are summarized in Figure 6-18, below:

FIGURE 6-18

Component	Approx. time in component, sec	Specific activity gammas/cm^3-sec	Unshielded Dose mr/hr
Core	120		
Main Steam Line	0	3.58×10^4	160
H. P. Turbine	0	1.80×10^4	236
Crossover	0	3.8×10^3	122
Turbine Exhaust	0	1.8×10^2	40
Condenser	0	2.2×10^2	64
Hotwell	0.5	1.4×10^6	55,000
Condensate Line	1.4	1.2×10^6	1,720
Deaerating Feed Heater	110	6.9×10^3	58

In the plant investigated, the secondary shielding required is 1.5 inches of lead on the condensate line and 5.3 inches of lead on the hotwell. The total weight of this, including also a 5' x 7' x 10' lead box 1 inch thick for watch standers, is 60,900 pounds for one 35,000 shaft horsepower plant, or 1.74 lbs/shp.

6.9.2 Methods of Calculation

This calculation followed closely the methods set forth in reference (37) for coolant activation and decay. Steady state formulas were used throughout. Sizes and geometries of the sources were scaled from machinery arrangements of the 35,000 shp naval plant, and shell thicknesses of the components were estimated according to the Code for Power Piping (42), a procedure

which probably yielded shells thinner than they are.

Detailed drawings of the components were not available. However, the approximations made are believed to be justified for the purpose of this calculation, which is to estimate weight. The secondary shielding is only 3.9% of the total weight of reactor and shielding; so errors in its weight would scarcely affect the total.

7. STABILITY AND CONTROL

7.1 Scope of Study

To establish the feasibility of the proposed reactor, it was decided that the following must be proved:

1. The reactor is inherently stable.

2. A control system can be designed such that (a) the reactor power follows the load demand, (b) steam pressure is controlled, (c) output steam temperature is controlled.

3. Safety devices can be designed to handle effects of failures and maloperations.

4. A practical start-up procedure can be developed.

The major effort in this study was devoted to (1) and a lesser effort to (2). Only token efforts were devoted to (3) and (4).

7.2 Analysis for Inherent Stability

A stability analysis for boiling water reactors in general is presented in Appendix D.1. In this analysis the relationships between the physical constants and operating conditions of the system for which the system will oscillate were determined. Applying these results to the boiling region of the proposed reactor, the curve in Figure 7-1 results. For this curve all the physical constants and operating conditions except $\frac{\partial K}{\partial \bar{f}_v}$ and $\bar{f}_{v_o}$ were assumed held constant. The values used are those in Table D.1 in Appendix D for the 1200 psi. operating pressure. The proposed reactor is expected to operate with $f_{v_o} = 1$. The curve shows that a $-\frac{\partial K}{\partial f_v}$ $\approx$ .1 to .2 will be acceptable with an adequate margin of stability. $\bar{f}_{v_o}$ is the steady state average vapor fraction. $\frac{\partial K}{\partial \bar{f}_v}$ is the fractional

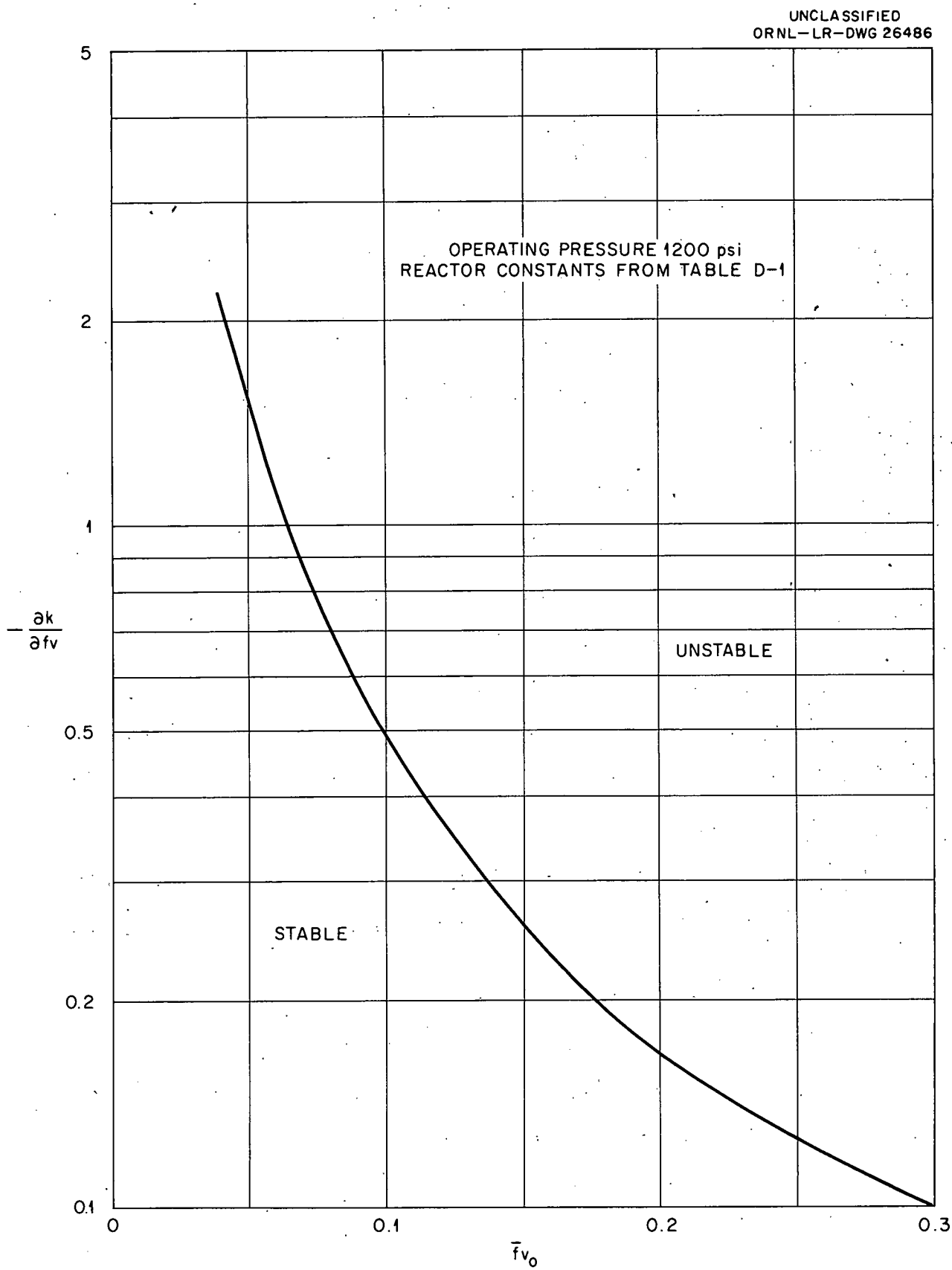

Fig. 7—1. Curve Showing Region of Stability for $-\frac{\partial k}{\partial fv}$ and $\bar{f}v_o$

reactivity change per fractional vapor fraction change.

7.3 Control System Design

7.3.1 Design Philosophy

The control system for the proposed reactor must maintain constant steam pressure and temperature over the range of expected operating power. This necessitated the inclusion of two external control loops. The reasons for this are as follows:

1. A change in operating power will always result in a change in the boiler region pressure unless a change is made in the system, i.e. a change in control rod setting, coolant flow rate, or amount of subcooling. This can be seen from Figure 7-2. If no changes are made except the reactor power, the average coolant density must remain the same for steady state operation. This requires that the operating pressure (corresponding to saturation temperature) must change.

2. Assuming that changes will be made to maintain constant pressure, the amount of superheat will not, in general, be constant. This is because the ratio between the power densities in the boiler region and superheater region depends on the flux shape, and the flux shape will change with control rod settings.

7.3.2 Description and Operation of Control System

The control system proposed is shown in Figure 7-3. It can be seen that two external loops exist; one to control the pressure and the other to control output steam temperature. The operation of the control system is as follows:

When a pressure error exists, the pressure control loop attempts to drive this error to zero by moving both boiler and superheater control rods

together to establish a different steady state reactor power. If this process results in a change in the power density ratio, the output steam temperature will change and a temperature error will develop. If the steam temperature is too high, the rod in the superheater will move in and the rod in the boiler will move out. Ideally, this would occur with no effective change in reactivity. In general, however, this will not happen and there will be some coupling back into the pressure control loop and the cycle will be repeated. By designing the control loops properly, it is expected that this hunting can be reduced to a few cycles before a new steady state is attained.

The pressure and temperature control loops are also the means whereby the reactor power follows small changes in load demand. If there is an increase in load demand, the pressure will drop and the pressure control loop will raise the reactor power until a new steady state condition is established.

For large changes in load demand when it is desired to have the reactor power follow as fast as possible, another loop is provided. This loop is designed to anticipate large changes in load and changes the reactor power faster than if the system had to wait for a pressure change before acting.

7.3.3 Synthesis of Control System

The complete system can be assumed to be properly designed if both loops are stable independent of each other, if the coupled system is stable, and if the response of the system to load demand is sufficiently fast.

A simplified design study for the pressure control loop and the temperature control loop is carried out in Appendix D.2. The required

Constant Power Removal Lines with Fractional Void, Average Coolant Density, and Operating Temperature as Parameters

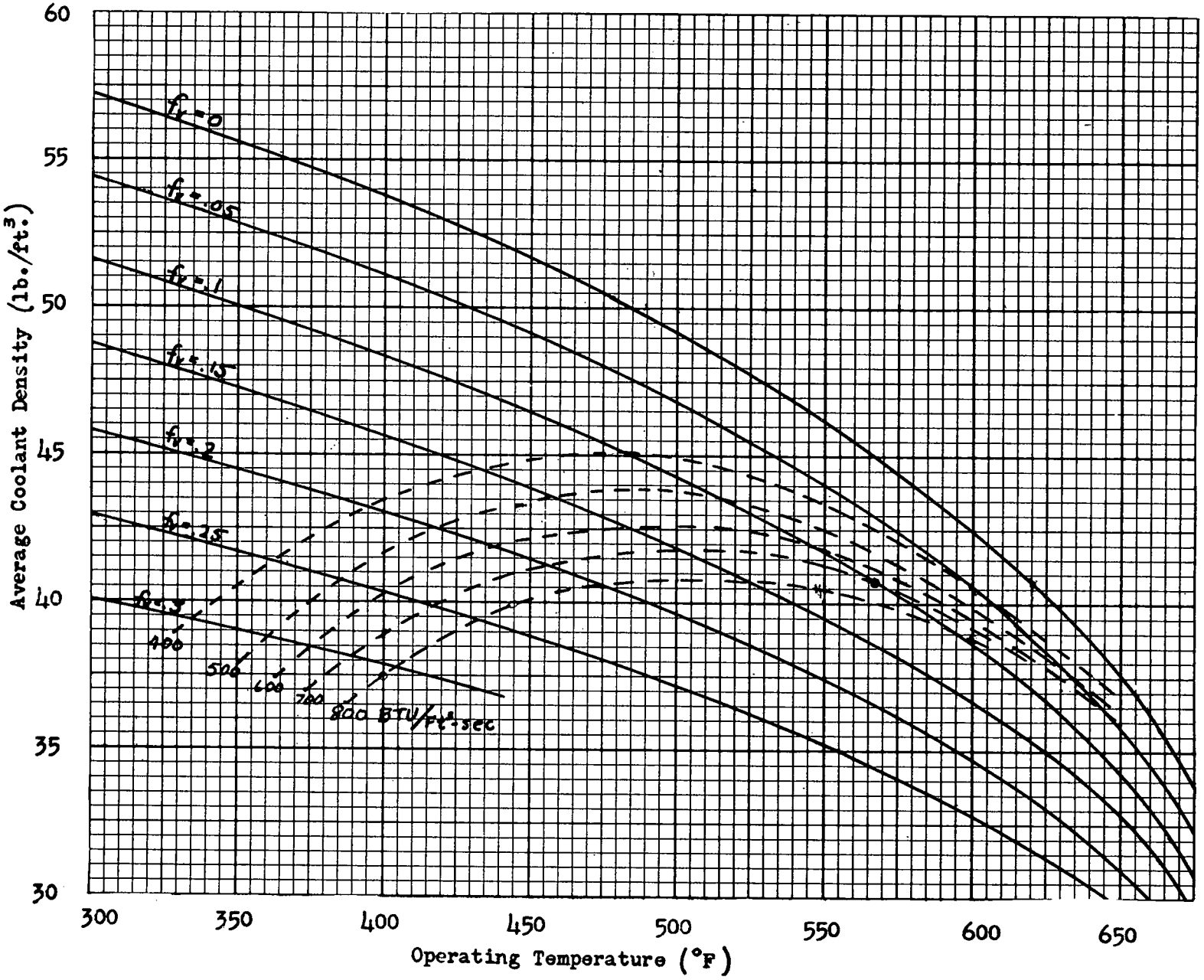

ORNL-LR-Dwg.-28559
UNCLASSIFIED

UNCLASSIFIED
ORNL-LR-DWG 26487

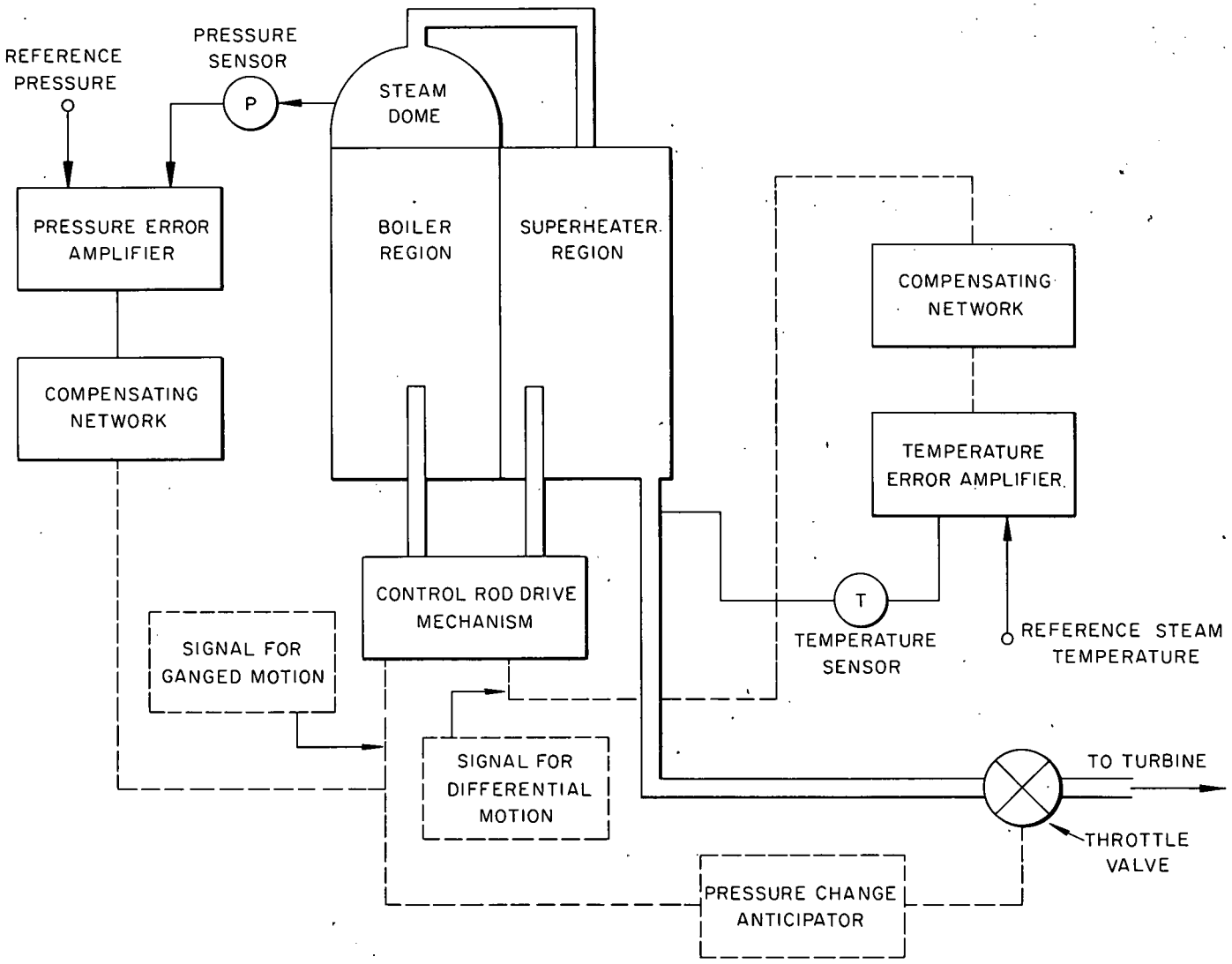

Fig. 7-3. Block Diagram of Control System.

form of the control equations for the two loops and the control system parameters were established.

The control equations with the system parameters for normal operating conditions are:

Boiler region control rod

$$\frac{dk^b}{dt} = -.000114\left[\Delta p + 1.25\,\frac{dp}{dt}\right] + .00002ld\left[\Delta Tg + .14\,\frac{dTg}{dt}\right]$$

The pressure p is in psi and the temperature Tg in ^{o}F. d represents the fractional amount the boiler rod will move with respect to the superheater rod when there is a temperature error.

Superheater control rod

$$\frac{dk^s}{dt} = -.000114\left[\Delta p + 1.25\,\frac{dp}{dt}\right] - .000021\left[\Delta Tg + .14\,\frac{dTg}{dt}\right]$$

In transfer function notation (Ref. 20) the equations are:

Boiler region control rod

$$\delta k^b = \frac{-.00114\,[1 + 1.25s]}{s}\,\Delta p + \frac{.00002ld\,[1 + .14s]}{s}\,\Delta Tg$$

Superheater region control rod

$$\delta k^b = \frac{-.00114\,[1 + 1.25s]}{s}\,\Delta p - \frac{.000021\,[1 + .14s]}{s}\,\Delta Tg$$

It can be seen that the low frequency components of the pressure and temperature error signals will call for rates of motion of control rods. For steady state, therefore, the error signals will be driven to zero. The derivitive terms were required to stabilize the systems for the higher frequency components. No problems are anticipated in the implementing of these control equations since they do not represent any radical departure from conventional electro-mechanical system designs.

The simplified design study assumed an ideal drive mechanism. In effect, this meant drive mechanisms that introduce negligible phase lags, $<5^{\circ}$ at $\omega \approx 20$ rads/sec. If actual drive mechanisms introduce more phase lag than this, it will be necessary to add additional lead in the control equations. (Increase the derivative term)

The effect of finite δk insertion and removal rates were also studied. For a maximum δk insertion and removal rates of .001 δk/sec, the pressure error signal must be limited to <30 psi. and the temperature error to $<75^{\circ}$F. Greater errors than this may exist physically, but the electrical error signals must be limited to the above values to prevent nonlinear oscillations. It is expected that the maximum physical pressure error can be held to 60 psi.

A possible method for the analysis of the coupling between the pressure control and temperature control loops is indicated in Appendix D.2.

No design study was attempted on the anticipation circuit to handle large load changes. The transient response to large changes in load demand was, therefore, not determined. An analogue computer would have been required for this study since the effects of non-linearities in the system must be taken into account.

7.4 Safety Considerations

Much of the safety measures developed for existing boiling water reactors are applicable to the proposed reactor.

Possibly the worst set of circumstances conceived of for boiling reactors is for the throttle valve to be closed, recirculation pump to be stopped, the control systems to be inoperative, and the reactor to be

at some power. The system behavior under these circumstances can be seen by examining Figure 7-2. The operating point for the reactor is operating temperature = 567°F, and fractional void f_v = .1. When the throttle valve is closed, the pressure will build up and the saturation temperature will rise. The operating point will move to the right. This will continue until a point at which f_v = 0 is reached. Any further increase in temperature will result in a reactor shutdown. If there were no control rod motion, this occurs when the temperature = 640°F or a pressure of 1800psi.

To prevent this excessive build-up in pressure, a pressure relief valve will be provided. Reactor shutdown can then result from expulsion of water. Coincident with the opening of the relief valve however, the safety rods will be inserted. This will be required since reactor shutdown must not lag the vapor flow stoppage to prevent superheater fuel element burnout.

Other circumstances that will demand a reactor shutdown are:

1. Boiler water level too high or too low.
2. Power failure
3. Excessively low period during start-up
4. Excessive reactor power.

The circumstances under which reactor shutdown is demanded are meant to be those over which the operator has lost control or never had control. A few examples of circumstances over which he normally has control are:

1. Development of resonance instability since it is necessary only to reduce the operating power to get out of trouble.

2. Malfunction of control system since the rods can be operated manually to maintain the pressure and steam temperature at the desired values.

In effect emergency reactor shutdowns will be avoided whenever possible.

The normal reactor shutdown is expected to proceed as follows: A bypass valve will be opened at some point beyond the superheater outlet, and the steam will be dumped to a condenser. The reactor power will be decreased while maintaining operating pressure and temperature by programing the bypass valve opening.

The effects of numerous possible mechanical failures have not been covered.

7.5 Start-up Problems

Start-up procedures developed for existing boiling water reactors are applicable to the proposed reactor except for one major problem. It is necessary for the proposed reactor to have a vapor flow during start-up to prevent superheater fuel element burnout.

A possible method for accomplishing this is to have small auxiliary boiler and pass the steam from it through the water in the boiler region of the reactor. This will serve two purposes:

1. It will raise the water temperature. This is desired since the higher the water temperature, the more inherently stable the system.

2. It will provide the required vapor flow through the superheater section.

8. CONCLUSIONS

8.1 General Discussion of the Design

The superheating water-boiler is best classified as a species of boiling water reactor. It shares with other water-boilers the advantages of low radioactivity in the external loop and ability to operate on a direct cycle, without heat exchangers and other auxiliaries; and the disadvantage of low power density.

Adding a superheater to a heterogeneous water-boiler has not in this case incurred a penalty of larger size. The superheater average power density of this reactor is 1.11 times that of the boiler. Superheated steam, on the other hand, benefits the steam plant by increasing its thermodynamic efficiency, reducing erosion of the turbine blades and, very important in marine applications, reducing the weight and size of the steam machinery.

For naval purposes, the biggest disadvantage of having a superheater is that failure of a superheater fuel element would send fission products to the turbine and condenser, possibly making the main machinery room untenable at a critical time. The same failure in the boiler would have less serious consequences, because the process of evaporation keeps most solids in the core. On the EBWR, decontamination factors of 10^{-3} to 10^{-4} were measured for solids in the core water (34).

This possibility of contaminating the machinery seems to be the inescapable price of having a superheater. How heavy a price it is depends on how reliable the superheater fuel elements are. It should be emphasized that no one knows how reliable such elements are or how reliable they can be made. (See also Chapter 2.)

8.2 Reliability of the Design Calculations

Standard methods of calculation were used wherever possible in this design. The heat transfer and fluid flow claculations in particular were intended to be conservative. Although critical mass calculations are inaccurate, our investigation covered so wide a range of nuclear characteristics that we are confident that the reactor with k = 1.000 and the correct boiler-superheater power balance lies within the range investigated. For the accuracy of the shielding calculation, it can be said that the shield we obtained is about what one would expect by comparison with those used on pressurized water naval propulsion plants.

8.3 The Weak Link

As pointed out in 2, fuel plates of the type we propose for the superheater have never been tested at the temperatures and burnups required by this reactor. It appears that Type 347 stainless will stand the temperatures, all less than 1250°F, to which these elements will be subjected, but the possibility exists that UO_2 - stainless steel elements as presently made will not stand reasonably high burnups at such temperatures.

The superheater fuel element is the only major untried item in this reactor, and tests will be required to settle the question as to whether or not it is suitable for this service. Should stainless steel - UO_2 plates prove unsuitable for 1200 - 1400°F service, this reactor would remain unfeasible until an adequate fuel form is developed and tested. It seems to us reasonable to suppose that fuel elements capable of operating up to 1400°F in a steam atmosphere will be developed.

8.4 The Strong Point

A possible significant contribution to the general knowledge of

boiling reactors is the resonance instability investigation, Chapter 7. Ever since the BORAX experiments, boiling reactors have been known to be subject to a phenomenon known as resonance instability, which occurs when their power is increased beyond a certain point. A mathematical model of a boiling reactor has been constructed which shows resonance instability at about the same operating conditions under which it has been observed in the EBWR, for example. Needless to say, this superheating water-boiler is designed to operate in the stable region.

A.1 Radial Temperature Distribution in the Superheater Elements

(Unsymmetrical Temperature Distribution in a Cylindrical Geometry)

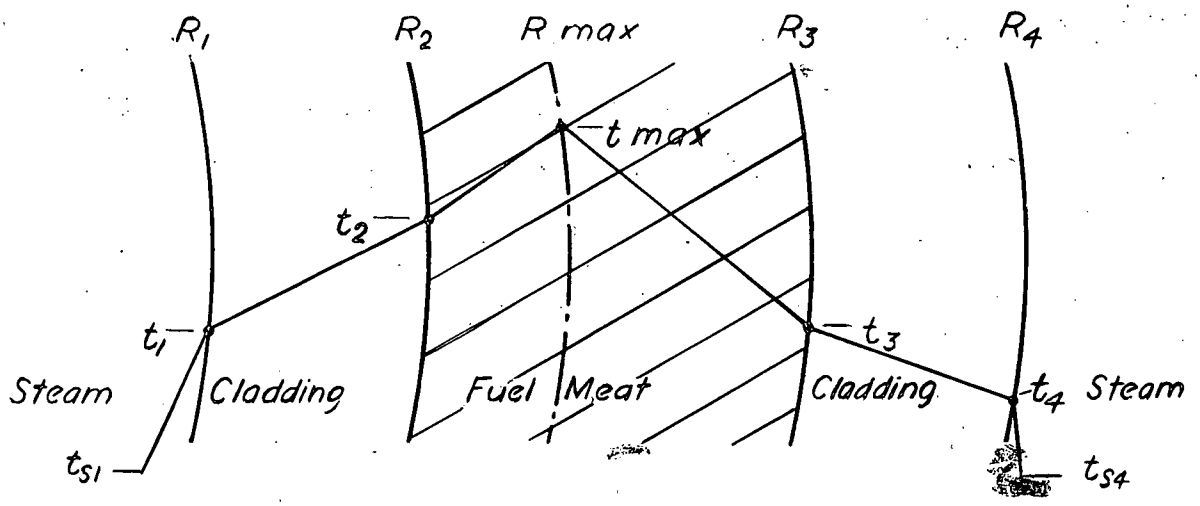

The temperature distribution in the fuel meat and cladding was described by three differential equations

A. (1) $\frac{q'''}{k_m} = -\nabla^2 t$ for $R_2 < r < R_3$

A. (2) $q'' = -k_c \frac{dt}{dr}$ for $R_1 < r < R_2$

A. (3) $q'' = -k_c \frac{dt}{dr}$ for $R_3 < r < R_4$

The heat flux was expressed as a function of radius and substituted in the above differential equations

A. (5) $q''(r) = q''_1 \frac{R_1}{r}$ for $R_1 < r < R_2$

A. (6) $q''(r) = q''_4 \frac{R_4}{r}$ for $R_3 < r < R_4$

Integrating the three differential equations, three general solutions were obtained

A. (7) $t = -\frac{q'''}{4k_m} r^2 + c_1 \ln r + c_2$ for $R_2 < r < R_3$

A. (8) $t = -\frac{q''_1 R_1}{k_c} \ln r + c_3$ for $R_1 < r < R_2$

A. (9) $t = -\frac{q''_4 R_4}{k_c} \ln r + c_4$ for $R_3 < r < R_4$

The integration constants were evaluated by the following boundary conditions:

A. (10) $t\,(R_2) = t_2$

A. (11) $t\,(R_3) = t_3$

A. (12) $t\,(R_1) = t_1$

A. (13) $t\,(R_4) = t_4$

The particular solutions in terms of t_1, t_2, t_3, t_4

A. (14) $t = t_2 + \frac{q'''}{4k_m}\left(R_2^2 - r^2\right) + \left[(t_3 - t_2) + \frac{q'''}{4k_m}\left(R_3^2 - R_2^2\right)\right] \frac{\ln r/R_2}{\ln R_3/R_2}$

for $R_2 < r < R_3$

A. (15) $t = t_1 - \frac{q''_1 R_1}{k_c} \ln \frac{r}{R_1}$ for $R_1 < r < R_2$

A. (16) $t = t_4 - \frac{q''_4 R_4}{k_c} \ln \frac{r}{R_4}$ for $R_3 < r < R_4$

Neither of the four boundary temperatures were known, but they could be obtained by using the solutions A(15) and A(16) in conjunction with the

following two relationships at the boundary layers:

A. (17) $q_1'' = h_1 (t_{s1} - t_1)$

A. (18) $q_4'' = h_4 (t_4 - t_{s4})$

A simultaneous solution of the equations A(15, 16, 17, and 18) resulted in the explicit expressions for the four boundary temperatures

A. (19) $t_1 = t_{s1} - \frac{q_1''}{h_1}$

A. (20) $t_4 = t_{s4} + \frac{q_4''}{h_4}$

A. (21) $t_2 = t_{s1} - \frac{q_1''}{h_1} - \frac{q_1'' R_1}{k_c} \ln \frac{R_2}{R_1}$

A. (22) $t_3 = t_{s4} + \frac{q_4''}{h_4} - \frac{q_4'' R_4}{k_c} \ln \frac{R_3}{R_4}$

It remains to find q_1'' and q_4''. The former was obtained in terms of the latter by writing a heat balance equation and solving for q_1''

$$q''' \pi (R_3^2 - R_2^2) = q_4'' 2\pi R_4 - q_1'' 2\pi R_1$$

A. (23) $q_1'' = q_4'' \frac{R_4}{R_1} - q''' \frac{(R_3^2 - R_2^2)}{2R_1}$

The heat flux q_4'' was found by differentiating equation A(14), evaluating at $r = R_2$, and substituting expression A(23) for q_1''. The Fourier's equation

$$q_2'' = - k_m \left.\frac{dt}{dr}\right|_{r = R_2}$$

Differentiating equation A(14)

$$q_1'' = - \frac{R_2}{R_1} k_m \left[- \frac{q''' r}{2k_m} + \frac{1}{r} \frac{(t_3 - t_2) + \frac{q'''}{k_m}(R_3^2 - R_2^2)}{\ln R_3/R_2} \right] \Bigg|_{r = R_2}$$

This was solved by substituting equation A(23) for q''_1, equations A(21 and 22) for t_2 and t_3 respectively

$$A.\ (24)\quad q''_4 = \frac{(t_{s4}-t_{s1}) - q'''\left[\frac{R_3^2 \ln R_3/R_2}{2k_m} + (R_3^2-R_2^2)\left(\frac{1}{2h_1R_1} + \frac{\ln R_2/R_1}{2k_c} - \frac{1}{4k_m}\right)\right]}{\frac{R_4}{k_c}\ln\frac{R_1 \cdot R_3}{R_2 \cdot R_4} - R_4\left(\frac{\ln R_3/R_2}{k_m} + \frac{1}{h_1R_1} + \frac{1}{h_4R_4}\right)}$$

To locate the maximum temperature, equation A(14) was differentiated, equating $\frac{dt}{dr} = 0$. Solving for R_{max}

$$A.\ (25)\quad R_{max} = \sqrt{\frac{\frac{2km}{q''}(t_3-t_2) + \frac{1}{2}(R_3^2-R_2^2)}{\ln R_3/R_2}}$$

Substitution of equation A(25) for r in equation A(14) resulted in the determination of the maximum temperature

$$A.\ (26)\quad t_{max} = t_2 + \frac{q'''}{4k_m}(R_2^2-R_{max}^2) + \left[(t_3-t_2) + \frac{q'''}{4k_m}(R_3^2-R_2^2)\right]\frac{\ln \frac{R_{max}}{R_2}}{\ln \frac{R_3}{R_2}}$$

The constants used in the superheater are listed below:

R_1 = 1.146" = .09550 ft, inside radius of the smallest fuel tube

R_2 = 1.151" = .09592 ft, radius of inner interface

R_3 = 1.181" = .09842 ft, radius of outer interface

R_4 = 1.186" = .09883 ft, outside radius of the smallest fuel tube

k_c = 12.8 Btu/hr-ft-°F thermal conductivity of the cladding

k_m = 9.2 Btu/hr-ft-°F thermal conductivity of the fuel meat

A.2 Temperature Distribution in the Boiler Elements

(Symmetrical Temperature Distribution in a Slab Geometry)

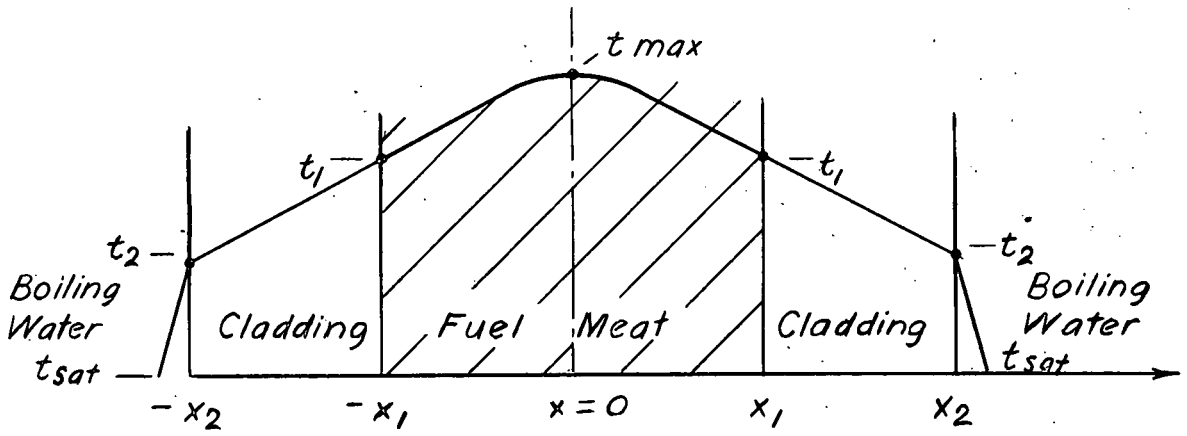

The saturation temperature of the boiling water and heat transfer rates are the same on both sides of the plate. Therefore, the temperature distribution is symmetrical, and only two differential equations are needed to describe the temperature behavior in the fuel meat and cladding.

A. (27) $\frac{q'''}{k_m} = -\nabla^2 t$ for $-x_1 < x < x_1$

A. (28) $q''' = -k_c \frac{dt}{dx}$ for $-x_2 < x < -x_1$ and $x_1 < x < x_2$

Integrating these differential equations, two general solutions were obtained

A. (29) $t = -\frac{q'''}{2k_m} x^2 + c_1 x + c_2$

A. (30) $t = -\frac{q''}{k_c} x + c_3$

Integration constants were evaluated by the following boundary conditions:

A. (31) $\left.\frac{dt}{dx}\right|_{x=0} = 0$ (symmetry condition)

A. (32) $t(x_1) = t_1$

A. (33) $t(x_2) = t_2$

Then the particular solutions in terms of t_1 and t_2 were obtained

A. (34) $t = t_1 + \frac{q'''}{2k_m}(x_1^2 - x^2)$ for $-x_1 < x < x_1$

A. (35) $t = t_2 + \frac{q''}{k_c}(x_2 - x)$ for $-x_2 < x < -x_1$

Neither t_1 nor t_2 was known, but they were found using equation A(35) in conjunction with the boundary layer relationship

A. (36) $q'' = h(t_2 - t_{sat})$

A. (37) $t_2 = t_{sat} + \frac{q''}{h}$

A. (38) $t_1 = t_{sat} + \frac{q''}{h} + \frac{q''}{k_c}(x_2 - x_1)$

q'' was found from the heat balance equation

$q'''(x_1 + x_1) = 2q''$

A. (39) $q''' = \frac{q''}{x_1}$

The maximum temperature was determined by evaluating equation A(34) at x = 0

A. (40) $t_{max} = t_1 + \frac{q'''}{2k_m} x_1^2$

Or in terms of t_{sat} and q'' this was rewritten as follows:

A. (41) $t_{max} = t_{sat} + q''\left(\frac{1}{h} + \frac{x_2 - x_1}{k_c} + \frac{x_1}{2k_m}\right)$

The constants used in the boiler are listed below

x_1 = .045" = .00375 ft, half thickness of the fuel meat

x_2 = .050" = .00417 ft, half thickness of the fuel plates

k_c = 12.8 Btu/hr-ft-°F, thermal conductivity of the cladding

k_m = 9.2 Btu/hr-ft-°F, thermal conductivity of the fuel meat

A.3 Heat Transfer Coefficients and Flow Distribution in the Superheater Elements

The local heat transfer coefficient is given in Ref. (9, page 219)

A. (42) $$h = .023 \frac{k_s}{De} (Re)^{.8} (Pr)^{.4}$$

The heat transfer coefficient varies axially along the path of the steam. Also it is different for the full-size and half-size steam gaps.

To calculate h in the main and narrow gaps, it is necessary to determine the flow distribution of steam. This was done by imposing a condition of equal pressure drops

A. (43) $$\left(\frac{L\phi}{2g}\right) f_m \frac{U_m^2}{De_m} = \left(\frac{L\phi}{2g}\right) f_n \frac{U_n^2}{De_n}$$

where $\frac{De_m}{De_n} \simeq 2$ ratio of equivalent diameter

$$\frac{f_m}{f_n} = \left(\frac{Re_n}{Re_m}\right)^{.2} = \left(\frac{U_n}{U_m}\right)^{.2} \left(\frac{De_n}{De_m}\right)^{.2}$$ ratio of friction factors

Equation A. (43) could be rearranged

A. (44) $$\frac{U_m}{U_n} = \left(\frac{De_m}{De_n}\right)^{2/3} = (2)^{2/3} = 1.5875$$ Condition of equal pressure drops

A. (45) $$W = aW + (1-a)W$$

A. (46) $$G_m = \frac{aW}{A_m} = \rho U_m$$

A. (47) $$G_n = \frac{(1-a)W}{A_n} \rho U_n$$

mass balance equation

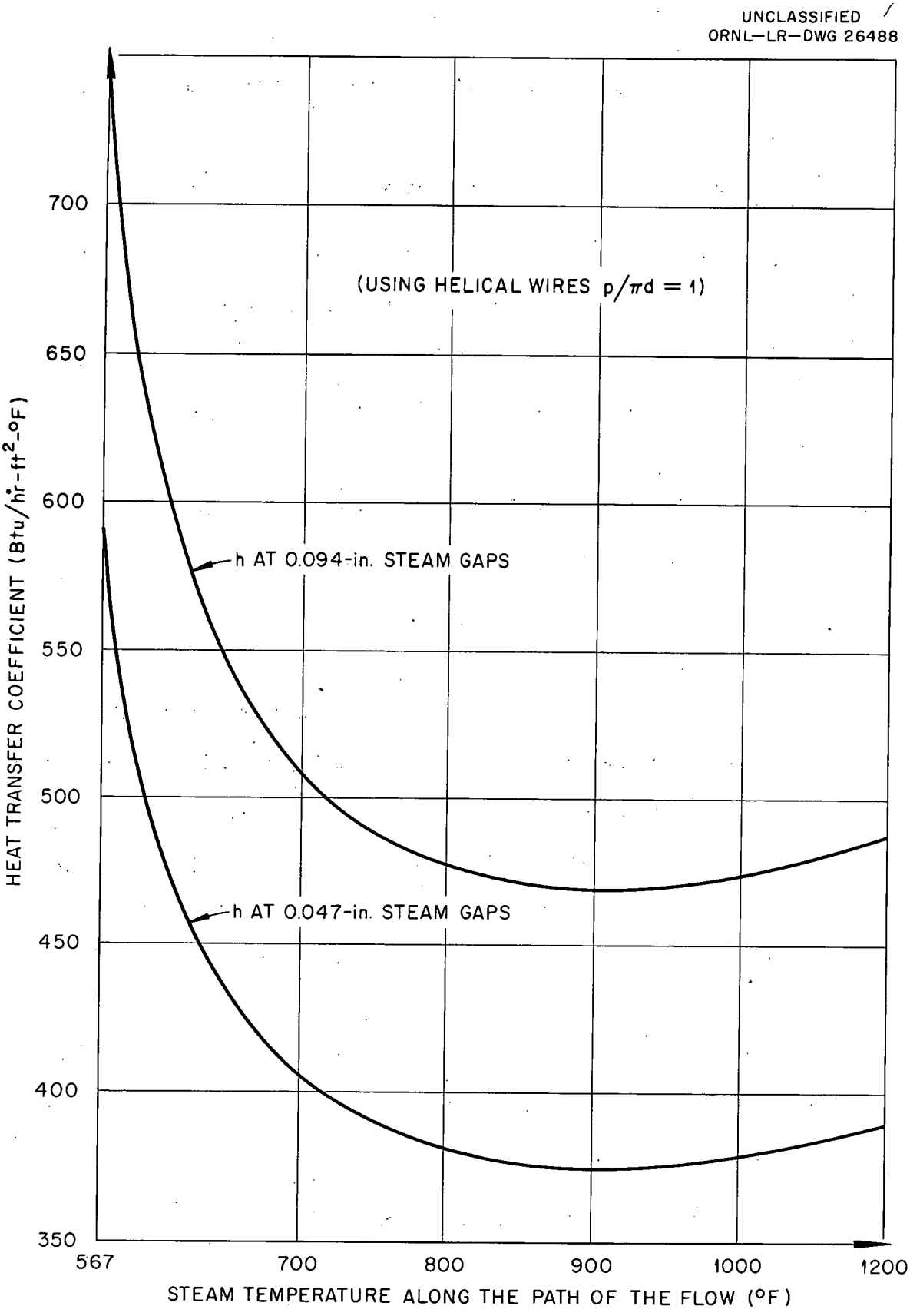

Fig. A.—1. Superheater Heat Transfer Coefficients.

Equations A. (44, 45, 46, 47) were solved simultaneously using the following constants

$W = \frac{129{,}000 \text{ lb/hr}}{32 \text{ elements}} = 4030 \text{ lb/hr-element}$

Dem = .01566 ft equivalent diameter of the main gaps

Den = .00783 ft equivalent diameter of the narrow gaps

A_m = .00756 ft^2 flow area of two main gaps

A_n = .00385 ft^2 flow area of two narrow gaps

The results are

a = .758, fraction of steam flowing through the main gaps

$G_m = \frac{.758 \times 4030}{.00756} = 405{,}000 \text{ lb/hr-ft}^2$

$G_n = \frac{.242 \times 4030}{.00383} = 255{,}000 \text{ lb/hr-ft}^2$

Using these results together with the properties required by equation A(42), an axial variation of the heat transfer coefficients was obtained and presented in a graphical form in Fig. A(1).

3.4 Axial Temperature Distribution in the Hot Channel of the Superheater

To determine the maximum surface temperature in the hot channel, it was necessary to know the axial variation of the steam and surface temperatures.

Choosing the origin of the coordinate system at the top of the hottest superheater element, it could be shown Ref. (6, page 670) that for a sinusoidal flux distribution

A. (48) $t_s(z) = t_s(o) + \frac{Q(.5)}{\pi W c_p}\left(1 - \cos\frac{\pi z}{L}\right)$

Or in terms of steam enthalpies

A. (49) $H(\bar{z}) = H(o) + \frac{\Delta H}{2}\left(1 - \cos\frac{\pi \bar{z}}{L}\right)$

Where $\bar{z}$ is a distance from the top of the hot channel

$H(\bar{z})$ variable enthalpy of steam at point $\bar{z}$

$H(0) = 1183.4$ Btu/lb enthalpy of steam at $\bar{z} = 0$

$H(L) = 1470$ Btu/lb enthalpy of steam at 1200 psi 950°F

$\Delta H = 1.05\left[H(L) - H(0)\right] = 1.05(1470 - 1183.4) = 300$ Btu/lb

Equation A(49) in terms of steam temperature in the hot channel was plotted in Fig. A(2).

To find surface temperature, q''_4 must be known. This was obtained from equation A(24). Then from equation A.(20) the surface temperature was calculated and also plotted in Fig. A.(2).

From Fig. A.(2) the maximum surface temperature $t_4 = 1079°F$ was located at $\bar{z}/L = 74$. It is expected that the maximum temperature will occur at this point.

A.5 Hot Channel Factors for the Superheater

Temperature distribution in the core is affected by several contingent factors that must be considered in the determination of the maximum possible surface temperature. The application of hot channel factors to the temperature rise of the steam and to the temperature drop through the film and fuel tube is a convenient method of treatment. Ref. 7.

A. (50) $F_s = \frac{\text{steam temperature rise in the affected channel}}{\text{steam temperature rise in unaffected channel}} = \frac{(\Delta t_s)A}{(\Delta t_s)U}$

A. (51) $F_h = \frac{\text{film temperature drop in affected channel}}{\text{film temperature drop in unaffected channel}} = \frac{(\Delta t_h)A}{(\Delta t_h)U}$

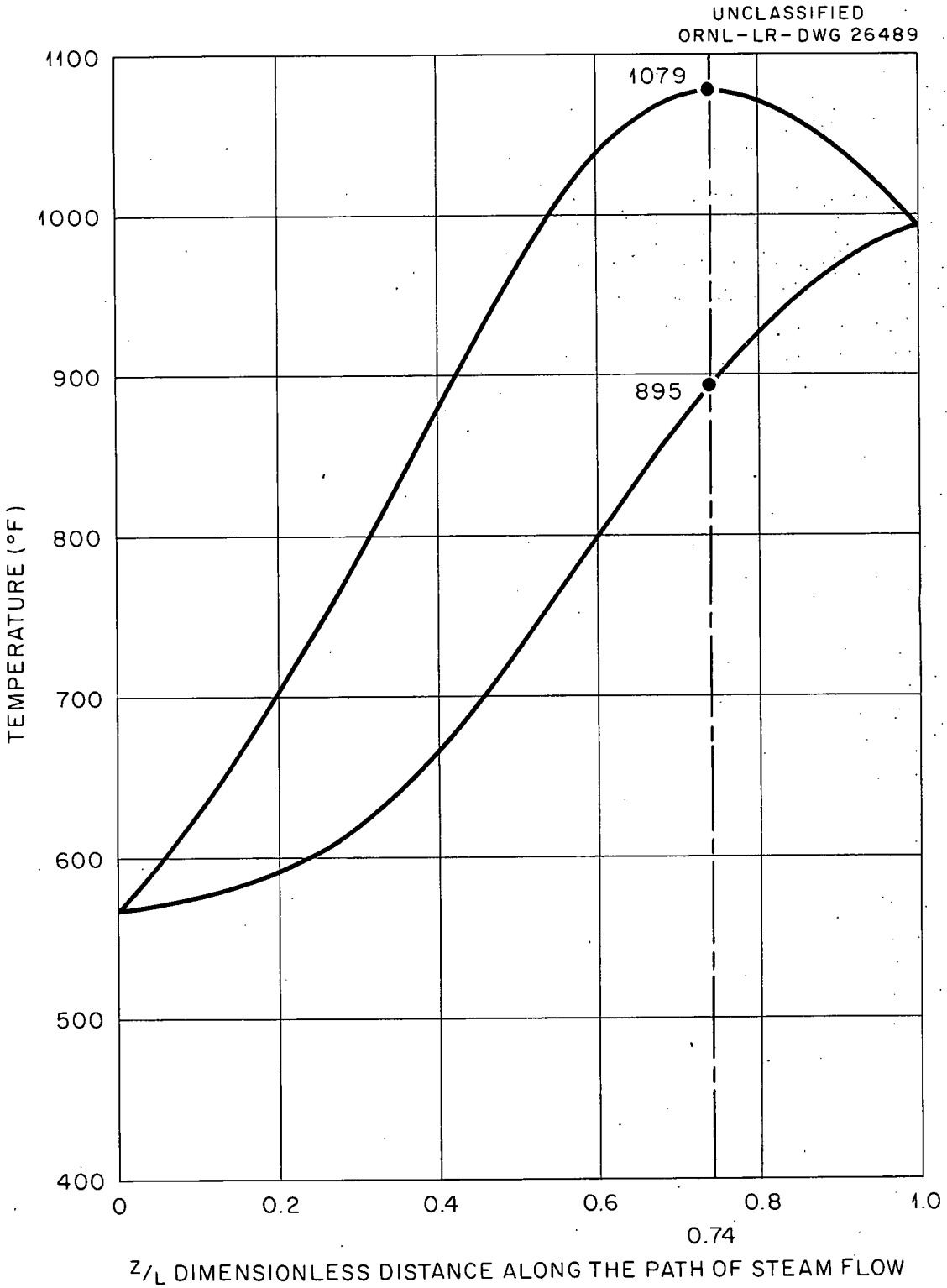

Fig. A(2). Axial Temperature Distribution in the Hot Channel of the Superheater.

A. (52) $F_f = \frac{\text{fuel tube temperature drop in affected channel}}{\text{fuel tube temperature drop in unaffected channel}} = \frac{(\Delta t_f)A}{(\Delta t_f)U}$

Several possible effects were investigated in the hot channel.

(a) Effect of plenum chambers. 5% decrease in flow rate was assumed due to the flow irregularities at the plenum chambers.

Then $\frac{W_A}{W_U} = \frac{U_A}{U_U} = 1 - .05 = .95$

$$F_s = \frac{(\Delta t_s)A}{(\Delta t_s)U} \quad \frac{W_U}{W_A} \quad \frac{1}{.95} = 1.05$$

$$F_h = \frac{(\Delta t_h)A}{(\Delta t_h)U} = \frac{h_U}{h_A} = \left(\frac{U_U}{U_A}\right)^{.8} \left(\frac{1}{.95}\right)^{.8} = 1.04$$

(b) Effect of plate spacing. Two mil decrease was allowed in the .047" steam gap.

Then $\frac{(De)A}{(De)U} = \frac{A_A}{AU} = \frac{.045}{.047} = .9575$

$$\frac{U_A}{U_U} = \left[\frac{(De)_A}{(De)_U}\right]^{2/3} = (.9575)^{2/3} = .9715$$

$$F_s = \frac{(\Delta t_s)_A}{(\Delta t_s)_U} = \left(\frac{U_U}{U_A}\right) \cdot \left(\frac{A_U}{A_A}\right) = \frac{1}{.9715 \times .9575} = 1.075$$

$$F_h = \frac{(\Delta t_h)_A}{(\Delta t_h)_U} = \left(\frac{U_U}{U_A}\right)^{.8} \cdot \left[\frac{(De)A}{(De)U}\right]^{.2} = \left(\frac{1}{.9715}\right)^{.8} (.9575)^{.2} = 1.015$$

(c) Effect of tolerance on Uranium content in the fuel plates. 1% increase in uranium content was assumed

Then $\frac{q'''_A}{q'''_U} = 1.01$

$$F_s = F_h = F_f = \frac{q'''_A}{q'''_U} = 1.01$$

(d) Effect of irregular distribution of uranium in the fuel plates. 4% increase in the localized uranium loading was assumed. Only 2% was used for F_s, because irregularities tend to be localized

$$F_s = \frac{q'''_A}{q'''_U} = 1.02$$

$$F_h = F_f = \frac{q'''_A}{q'''_U} = 1.04$$

(e) Effect of tolerance in the meat thickness. One mil increase in the thickness of .030" meat was allowed

$$F_s = F_h = F_f = \frac{q'''_A}{q'''_U} = \frac{.031}{.030} = 1.03$$

(f) Effect of inability to predict the neutron flux distribution. It was assumed

$$F_x = F_h = F_f = 1.05$$

(g) Effect of tolerance in the clad thickness. It was assumed

$$F_s = F_h = 1.01$$

(h) Effect of the control rods. A large distortion in axial flux was assumed.

Then $$\frac{q'''_A}{q'''_U} = \frac{2}{\pi/2} = \frac{2}{1.57} = 1.27$$

$$F_s = F_h = F_f = 1.27$$

(k) Effect of scale. Five mil scale was allowed to grow. This reduces .047" steam gap considerably.

Then: $\frac{(De)_A}{(De)_U} = \frac{A_A}{A_U} = \frac{.037}{.047} = .7875$

$$\frac{U_A}{U_U} = \frac{(De)_U}{(De)_A} = 1.27$$

$$F_h = \frac{(\Delta t_h)_A}{(\Delta t_h)_U} = \left(\frac{U_U}{U_A}\right)^{.8}\left[\frac{(De)_A}{(De)_U}\right]^{.2} = \left(\frac{1}{1.27}\right)^{.8}(.7875)^{.2} = .788$$

$$\Delta t_{sc1} \simeq \frac{q_1'' \frac{.005}{12}}{k_{sc}} = \frac{68{,}275 \times \frac{.005}{12}}{1} = 28^{\circ}F$$

$$\Delta t_{sc4} \simeq \frac{q_4'' \frac{.005}{12}}{k_{sc}} = \frac{86{,}415 \times \frac{.005}{12}}{1} = 36^{\circ}F$$

SUMMARY OF ALL EFFECTS

	EFFECTS	F_s	F_h	F_f	t_{sc}
a	Plenum chambers	1.05	1.04		
b	Plate spacing	1.075	1.015		
c	Uranium content	1.01	1.01	1.01	
d	Uranium distribution	1.02	1.04	1.04	
e	Meat thickness	1.03	1.03	1.03	
f	Neutron track length	1.05	1.05	1.05	
g	Clad thickness	1.01	1.01		
h	Control rods	1.27	1.27	1.27	
k	Scale		.788		$28^{\circ}F$
	Total effect	1.61	1.21	1.44	$28^{\circ}F$

A.6 List of Symbols

A	cross sectional or flow area	ft^2
A_a	cross sectional area for axial flow	ft^2
A_b	cross sectional area for helical flow	ft^2
a	fraction of steam flowing through the main steam gaps in the superheater elements	dimensionless
C	integration constant	
c_p	specific heat at constant pressure	Btu/lb-^oF
D	diameter	ft
D_e	equivalent diameter	ft
E	Young's modulus of elasticity	psi
e	base of the natural logarithm	
F_s	steam temperature rise factor	dimensionless
F_h	film temperature drop factor	dimensionless
F_f	fuel tube temperature drop factor	dimensionless
f	Darcy friction factor	dimensionless
G	flux of the mass (or weight) flow	lb/hr-ft^2
g	gravitational constant	= 32.2 ft/sec^2
$H(Z)$	variable steam enthalpy at point Z	Btu/lb
$H(0)$	steam enthalpy at Z = 0	Btu/lb
$H(L)$	steam enthalpy at 1200 psi and 950^oF	Btu/lb
H_c	active core height in the boiler	ft
H_{sh}	height of shroud above core	ft
h	heat transfer coefficient	Btu/hr-ft^2-^oF
k	thermal conductivity	Btu/hr-ft-^oF

L	length of the fuel elements	ft
l	pitch	ft
P	Pressure	lb/ft^2
ΔP	Pressure drop	lb/ft^2
Δp	pressure drop	psi
Pr	Prandtl number = $\frac{C_p \mu}{k}$	dimensionless
Q	heat generation rate	Btu/hr
q''	heat flux	$Btu/hr\text{-}ft^2$
q'''	volumetric heat generation rate	$Btu/hr\text{-}ft^3$
$q'''(r=o)$	volumetric heat generation rate at the center of the superheater	$Btu/hr\text{-}ft^3$
R	recirculation ratio in boiler = $\frac{\text{weight of water recirculated}}{\text{steam flow}}$ constant radius	
r	radial coordinate	ft
R_e	Reynolds number = $\frac{GD_e}{\mu}$	dimensionless
S	heat transfer surface	ft^2
t	temperature	^oF
Δt_s	steam temperature rise	^oF
Δt_h	film temperature drop	^oF
Δt_{sc}	scale temperature drop	^oF
Δt_f	fuel tube temperature drop	^oF
U	speed	fps
V	volume	ft^3
W	Mass (or weight) flow rate	lb/hr
x	horizontal coordinate (distance from the center of the boiler fuel plate)	ft

Z/L	dimensionless distance from the top of the superheater,	dimensionless
Z	axial coordinate (distance from the top of the superheater)	ft
α	thermal coefficient of linear expansion,	$\frac{in.}{in.-^oF}$
	steam void fraction in the boiler	dimensionless
μ	viscosity	lb/hr-ft
ν	Poisson's ratio	dimensionless
ρ	specific weight (or weight density)	lb/ft^3
Σ_f	macroscopic fission cross-section	cm^{-1}
σ	thermal stress	psi
$\phi(r,z)$	neutron track length	$neuts-cm/cm^3-sec$
$\Psi(r)$	radial component of ϕ	$neuts-cm/cm^3-sec$
$\Psi(o)$	radial component of ϕ at the center of superheater	$neuts-cm/cm^3-sec$
$\Psi(32.4)$	radial component of ϕ at the interface between superheater and boiler	$neuts-cm/cm^3-sec$
$\zeta(Z)$	axial component of ϕ	$neuts-cm/cm^3-sec$
∇^2	Laplacian operator	

Subscripts

A	conditions affected by some contingent factors
U	nominal or standard conditions unaffected by any factors
c	cladding
l	liquid phase in the boiler
m	fuel meat, or
	main steam gaps in the superheater fuel elements

n	narrow steam gaps in the superheater fuel element
o	exit
v	vapor phase in the boiler
max	maximum or location of max temperature
S.H.	superheater
Blr	boiler
1	surface of the inner cladding in the superheater, or interface between cladding and fuel meat in the boiler
2	interface between inner cladding and fuel meat in the superheater, or surface of the cladding in the boiler
3	interface between outer cladding and fuel meat in the superheater
4	surface of the outer cladding in the superheater
11	superheater region, fast energy group
12	superheater region, thermal energy group
21	boiler region, fast energy group
22	boiler region, thermal energy group

Superscripts

-	bar on the top of a symbol designates the average value

APPENDIX B1

DERIVATION OF MIGRATION AREA MODEL EQUATIONS

The critical equation for the following geometry is derived below:

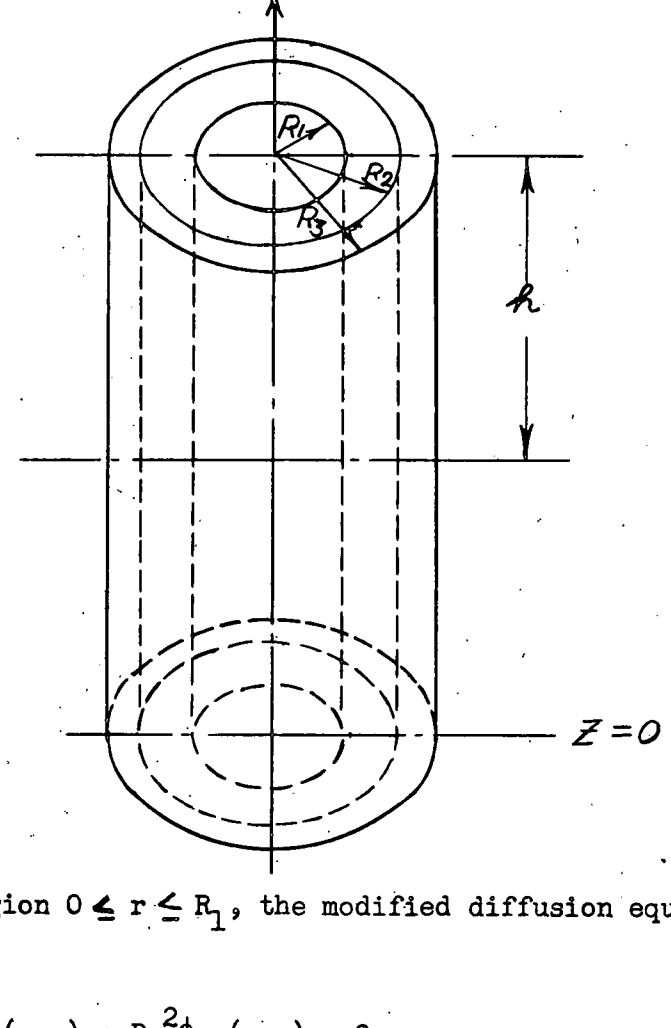

In the region $0 \leq r \leq R_1$, the modified diffusion equation is applicable:

$$(1)\quad \nabla^2\phi_1(r,z) + B_1^2\phi_1(r,z) = 0$$

$$\text{where } B_1^2 = \frac{k_\infty^{(1)} - 1}{M_1^2} \quad \text{and} \quad M_1^2 = L_1^2 + \tau_1$$

The applicable equation in the region $R_1 \leq r \leq R_2$ is:

$$(2)\quad \nabla^2\phi_2(r,z) + B_2^2\phi_2(r,z) = 0$$

where: $B_2^2 = \dfrac{k_\infty^{(2)} - 1}{M_2^2}$ and $M_2^2 = L_2^2 + \tau_2$

For the region $R_2 \leq r \leq R_3$ the applicable equation is:

(3) $\nabla^2 \phi_3(r,Z) - \dfrac{1}{L_3^2} \phi_3(r,z) = 0$

where $L_3^2 = \dfrac{D_3}{\Sigma_{a3}}$

In cylindrical geometry, assuming ϕ varies only with r and z

$$\nabla^2 \phi = \left(\frac{\partial^2}{\partial r^2} \frac{1}{r} \frac{\partial}{\partial r} + \frac{\partial^2}{\partial z^2}\right) \phi$$

Then equation (1) becomes

(1a) $$\left[\frac{\partial^2}{\partial r^2} + \frac{1}{r}\frac{\partial}{\partial r}\right]\phi_1(r,Z) + \frac{\partial^2}{\partial z^2} \phi_1(r,Z) + B_1^2 \phi_1(r,Z) = 0$$

Equation (2) becomes

(2a) $$\left[\frac{\partial^2}{\partial r^2} + \frac{1}{r}\frac{\partial}{\partial r}\right] \phi_2(r,Z) + \frac{\partial^2}{\partial z^2} \phi_2(r,Z) + B_2^2 \phi_2(r,Z) = 0$$

Equation (3) becomes

(3a) $$\left[\frac{\partial^2}{\partial r^2} + \frac{1}{r}\frac{\partial}{\partial r}\right] \phi_3(r,Z) + \frac{\partial^2}{\partial Z^2} \phi_3(r,Z) - \frac{1}{L_3^2} \phi_3(r,Z) = 0$$

Assume a solution for each equation of the form

$$\phi_i(r,Z) = \Psi_i(r) \mathcal{P}_i(Z) \qquad i = 1,2,3$$

and define

$$B_{1,2}^2 \equiv \alpha_{1,2}^2 + \beta_{1,2}^2 \; ; \quad \frac{1}{L_3^2} \equiv -\mu^2 + \lambda^2$$

Applying the usual separation of variables procedure on (1a)

(1r) $$\frac{\partial^2 \Psi_1(r)}{\partial r^2} + \frac{1}{r}\frac{\partial \Psi_1(r)}{\partial r} + \alpha_1^2 \Psi_1(r) = 0$$

$$(1z)\quad \frac{\partial^2 \mathcal{S}_1(z)}{\partial z^2} + \beta_1^2 \mathcal{S}_1(z) = 0$$

A general solution of (1r) is

$$(4)\quad \Psi_1(r) = A_1 J_o(\alpha_1 r) + C_1 Y_o(\alpha_1 r) \qquad \text{provided } \alpha_1 \text{ is real,}$$

and a solution of (1z) is

$$(5)\quad \mathcal{S}_1(z) = H_1 \sin\beta_1 z + F_1 \cos \beta_1 z$$

By a similar treatment

$$(6)\quad \Psi_2(r) = A_2 J_o(\alpha_2 r) + C_2 Y_o(\alpha_2 r)$$

and

$$(7)\quad \mathcal{S}_2(z) = H_2 \sin \beta_2 z + F_2 \cos \beta_2 z$$

$$(8)\quad \Psi_3(r) = A_3 I_o(\lambda r) + C_3 K_o(\lambda r)$$

and

$$(9)\quad \mathcal{S}_3(z) = H_3 \sin \mu z + F_3 \cos \mu z$$

A_i, C_i, H_i and F_i are arbitrary constants to be determined from the following boundary conditions.

(a) $0 \leq \phi(r,z) < \infty$

(b) $\phi_3(R_3,z) = 0$

(c) $\phi_{1,2,3}(r,h) = 0$

(d) $\phi_1(R,z) = \phi_2(R,z)$

(e) $\phi_2(R_2,z) = \phi_3(R_2,z)$

(f) $\hat{n} \cdot \underline{J_1}(R,z) = \hat{n} \cdot \underline{J_2}(R,z)$

(g) $\hat{n} \cdot \underline{J_2}(R_2,z) = \hat{n} \cdot \underline{J_3}(R_2,z)$

(h) $\int_{\text{reactor}} \frac{1}{w} \Sigma_f(r)\, \phi(r,z)\, dV = \text{Power}$

$\zeta_i(z)$ is symmetric about the z-axis and reaches a maximum value at $z = 0$; therefore

$$\frac{d\zeta_i(Z)}{dZ}\Big|_o = H_i\beta_i \cos \beta_i Z - F_i\beta_i \sin \beta_i Z = 0$$

hence $H_i \beta_i \cos 0 = 0$

$\therefore \quad H_i = 0$

hence $\zeta_i = F_i \cos \beta_i Z$

From condition (a), it is evident that $C_1 = 0$ since $Y_o(0) = -\infty$

From condition (c), $\cos \beta_i z = 0$

$$\beta_1 = \mu = \left(\frac{\pi}{2h}\right)$$

From condition (d)

$$(10) \quad A_1 J_o (\alpha_1 R_1) F_1 = \left[A_2 J_o (\alpha_2 R_1) + C_2 Y_o (\alpha_a R_1)\right] F_2$$

and from (f)

$$(11) \quad D_1 \alpha_1 A_1 F_1 J_1 (\alpha_1 R_1) = \alpha_2 D_2 F_2 \left[A_2 J_1 (\alpha_2 R_1) + C_2 Y_1 (\alpha_2 R_1)\right]$$

Dividing (10) by (11) and solving for C_2

$$(12) \quad C_2 = \frac{A_2\left[\frac{\alpha_2 D_2}{\alpha_1 D_1} \frac{J_o (\alpha_1 R_1)}{J_1(\alpha_1 R_1)} J_1 (\alpha_2 R_1) - J_o(\alpha_2 R_1)\right]}{Y_o (\alpha_2 R_1) - \frac{\alpha_2 D_2}{\alpha_1 D_1} \frac{J_o(\alpha_1 R_1)}{J_1(\alpha_1 R_1)} Y_1(\alpha_2 R_1)}$$

from condition (b)

$$(13) \quad A_3 = -C_3 \frac{K_o (\lambda R_3)}{I_o(\lambda R_3)}$$

Applying conditions (e) and (g)

$$(14) \quad \frac{A_2 J_o(\alpha_2 R_2) + C_2 Y_o(\alpha_2 R_2)}{\alpha_2 D_2\left[A_2 J_1(\alpha_2 R_2) + C_2 Y_1(\alpha_2 R_2)\right]} = \frac{\frac{K_o(\lambda R_3)}{I_o(\lambda R_3)} I_o(\lambda R_2) + K_o(\lambda R_2)}{\lambda D_3\left[-\frac{K_o(\lambda R_3)}{I_o(\lambda R_3)} I_1(\lambda R_2) + K_1(\lambda R_2)\right]} =$$

$$= \frac{K_o(\lambda R_2)}{\lambda D_3 K_1(\lambda R_2)} \quad \text{for an infinite reflector}$$

Define $X \equiv \dfrac{K_o(\lambda R_2)}{\lambda D_3 K_1(\lambda R_2)}$

Combining (12) and (14) and simplifying, the critical condition is:

$$(15)\quad Q = \frac{Y_o(\alpha_2 R_1)\, P - 1}{\left[Y_1(\alpha_2 R_1)\, P - J_1(\alpha_2 R_1)\right]}$$

where: $$Q = \frac{\alpha_2 D_2}{\alpha_1 D_1} \frac{J_o(\alpha_1 R_1)}{J_1(\alpha_1 R_1)}$$

and $$P = \frac{J_o(\alpha_2 R_2) + X_2 D_2 J_1(\alpha_2 R_2)}{Y_o(\alpha_2 R_2) + X_2 D_2 Y_1(\alpha_2 R_2)}$$

The flux distribution is given by :

$$\phi_1(r, z) = G\, J_o(a_1 r) \cos\left(\frac{\pi}{2h}\right) z$$

$$\phi_2(r,z) = \frac{G J_1(\alpha_1 R_1)\left[Y_o(\alpha_2 R_1) - \frac{\alpha_2 D_2}{\alpha_1 D_1} \frac{J_o(\alpha_1 R_1)}{J_1(\alpha_1 R_1)} Y_1(\alpha_2 R_1)\right]}{\frac{2D_2}{\pi R_1 \alpha_1 D_1}} \left\{ J_o(\alpha_2 r) \right.$$

$$\left. + \left[\frac{\frac{\alpha_2 D_2}{\alpha_1 D_1} \frac{J_o(\alpha_1 R_1)}{J_1(\alpha_1 R_1)} J_1(\alpha_2 R_1) - J_o(\alpha_2 R_1)}{Y_o(\alpha_2 R_1) - \frac{\alpha_2 D_2}{\alpha_1 D_1} \frac{J_o(\alpha_1 R_1)}{J_1(\alpha_1 R_1)} Y_1(\alpha_2 R_1)}\right] Y_o(\alpha_2 r) \right\} \cos\left(\frac{\pi}{2h}\right) z$$

$\phi_3(r, z) = C_3 K_o(\lambda r) \cos\left(\frac{\pi}{2h}\right) z$ for infinite reflector

where:

$$C_3 = \frac{G J_1(\alpha_1 R_1)\left[Y_o(\alpha_2 R_1) - \frac{\alpha_2 D_2}{\alpha_1 D_1} \frac{J_o(\alpha_1 R_1)}{J_1(\alpha_1 R_1)} Y_1(\alpha_2 R_1)\right]}{\frac{2D_2}{\pi R_1 \alpha_1 D_1} K_o(\lambda R_2)} \left\{ J_o(\alpha_2 R_2) + \right.$$

$$+\left\{\left[\frac{\frac{\alpha_2 D_2}{\alpha_1 D_1}\frac{J_o(\alpha_1 R_1)}{J_1(\alpha_1 R_1)}J_1(\alpha_2 R_1) - J_o(\alpha_2 R_1)}{Y_o(\alpha_2 R_1) - \frac{\alpha_2 D_2}{\alpha_1 D_1}\frac{J_o(\alpha_1 R_1)}{J_1(\alpha_1 R_1)}Y_1(\alpha_2 R_2)}\right] Y_o(\alpha_2 R_2)\right\}$$

$G = A_1 F_1$ = arbitrary constant set by power level.

APPENDIX B2: Disadvantage Factor

A. Superheater

The square superheater unit cell was taken as infinitely long and for ease of calculation replaced by a cylindrical unit cell of equal cross-sectional area.

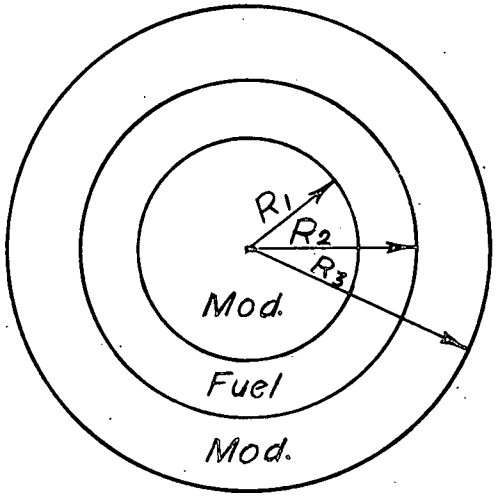

UNIT CELL

In the moderator regions the following equations are applicable:

$$D_M \nabla^2 \phi_1 - \Sigma_a^m \phi_1 + q = 0 \qquad (1)$$

$$D_M \nabla^2 \phi_3 - \Sigma_a^m \phi_3 + q = 0 \qquad (2)$$

where ϕ_1 = thermal flux in central "plug" of moderator

ϕ_3 = thermal flux in outer region of moderator

q = slowing down density at thermal energy, assumed to be constant in moderator regions and zero in fuel region.

The fuel region is assumed to be a homogeneous mixture of uranium and stainless steel in the shape of an infinite slab. The transmission of neutrons

through the slab either directly or after scattering is given by Reference 30 as

$$T = e^{-\Sigma_t^F a}\left[1 - \Sigma_t^F a\right] + (\Sigma_t^F a)^2 E_1(\Sigma_t a) + \frac{\frac{1}{2\Sigma_t^F a}\left[1 - 2E_3(\Sigma_t^F a)\right]^2 \frac{\Sigma_s^F}{\Sigma_t^F}}{1 - \frac{\Sigma_s^F}{\Sigma_t^F}\left\{1 - \frac{\left[1 - 2E_3(\Sigma_t^F a)\right]}{2\Sigma_t^F a}\right\}}$$

$$a = R_2 - R_1$$

The flux at the boundary of the slab is (Ref. 30):

$$\phi_F(0) = 2 + 2e^{-\Sigma_t^F a} - 2E_1(\Sigma_t^F a) + \frac{\frac{2\Sigma_s^F}{(\Sigma_t^F)^2 a}\left[1 - 2E_3(\Sigma_t^F a)\right]\left\{1 - \frac{\left[1 - 2E_3(\Sigma_t^F a)\right]}{2\Sigma_t^F a}\right\}}{1 - \frac{\Sigma_s^F}{\Sigma_t^F}\left\{1 - \frac{\left[1 - 2E_3(\Sigma_t^F a)\right]}{2\Sigma_t^F a}\right\}}$$

And the average flux in the fuel is (Ref. 30):

$$\bar{\phi}_F = \frac{\frac{2}{\Sigma_t^F a}\left[1 - 2E_3(\Sigma_t^F a)\right]}{1 - \frac{\Sigma_s^F}{\Sigma_t^F}\left\{1 - \frac{\left[1 - 2E_3(\Sigma_t^F a)\right]}{2\Sigma_t^F a}\right\}}$$

The ratio $\frac{\phi_F(R_1)}{\bar{\phi}_F}$ for the cylindrical cell is approximately equal to $\frac{\phi_F(0)}{\bar{\phi}_F}$ for the slab described by the above equations.

The boundary conditions to be applied to equations (1) and (2) are:

(a) ϕ_1 is finite at $r = 0$

(b) $\frac{\partial \phi_3}{\partial r} = 0 \qquad r = R_3$

$$(c) \quad J_1^{+}(R_1)\,\frac{R_1}{R_2}\,T = J_3^{+}(R_2)$$

$$(d) \quad J_1^{-}(R_1)\,\frac{R_1}{R_2} = T\,J_3^{-}(R_2)$$

Applying boundary conditions (a) and (b), the solutions of (1) and (2) are:

$$\phi_1 = C\,I_o(\gamma r) + \frac{q}{\Sigma_a^m}$$

$$\phi_3 = A\,I_o(\gamma r) + A\,\frac{I_1(\gamma R_3)}{K_1(\gamma R_3)}\,K_o(\gamma r) + \frac{q}{\Sigma_a^m} \quad \text{where } \gamma = \sqrt{\frac{\Sigma_a^m}{D^m}}$$

The arbitrary constants A and C are found from conditions (c) and (d) to be:

$$C = \frac{A\left[L_o(\gamma R_2) - 2\gamma D^m L_1(\gamma R_2)\right] + \frac{q}{\Sigma_a^m}\left(1 - T\,\frac{R_1}{R_2}\right)}{T\,\frac{R_1}{R_2}\left[I_o(\gamma R_1) - 2\gamma D^m I_1(\gamma R_1)\right]}$$

$$A = \frac{\frac{q}{\Sigma_a^m}\left\{T - \frac{R_1}{R_2} - \frac{\left(1 - T\frac{R_1}{R_2}\right)\left[I_o(\gamma R_1) + 2\gamma D^m I_1(\gamma R_1)\right]}{T\left[I_o(\gamma R_1) - 2\gamma D^m I_1(\gamma R_1)\right]}\right\}}{\left[L_o(\gamma R_2) - 2\gamma D^m L_1(\gamma R_2)\right]\left[I_o(\gamma R_1) + 2\gamma D^m I_1(\gamma R_1)\right] - T\left[L_o(\gamma R_2) + 2\gamma D^m L_1(\gamma R_2)\right]\left[I_o(\gamma R_1) - 2\gamma D^m I_1(\gamma R_1)\right]}$$

where:

$$L_o(\gamma r) = I_o(\gamma r) + \frac{I_1(\gamma R_3)}{K_1(\gamma R_3)}\,K_o(\gamma r)$$

$$L_1(\gamma r) = I_1(\gamma r) - \frac{I_1(\gamma R_3)}{K_1(\gamma R_3)}\,K_1(\gamma r)$$

The average flux in the moderator is:

$$\bar{\phi}_m = 2\pi \left[\frac{\int_0^{R_1} \phi_1(r) r dr + \int_{R_2}^{R_3} \phi_3(r) r dr}{\pi \left[R_1^2 + R_3^2 - R_2^2 \right]} \right]$$

$$= \frac{2\left[CR_1(\gamma R_1) - AR_2 I_1(\gamma R_2) + AR_2 \frac{I_1(\gamma R_3)}{K_1(\gamma R_3)} K_1(\gamma R_2) \right]}{\gamma \left[R_1^2 + R_3^2 - R_2^2 \right]}$$

$$\phi_m(R_1) = C\, I_o(\gamma R_1) + \frac{q}{\Sigma_a^m}$$

The disadvantage factor, ζ, is:

$$\zeta = \frac{\bar{\phi}_m}{\bar{\phi}_f}$$

$$= \frac{\bar{\phi}_m / \phi_m(R_1)}{\bar{\phi}_F / \phi_m(R_1)} \quad \text{but } \phi_m(R_1) = \phi_F(R_1)$$

$$\zeta \cong \frac{\bar{\phi}_m / \phi_m(R_1)}{\bar{\phi}_F / \phi_F(0)}$$

The calculated values of ζ are shown in Figure 4-9.

B. Boiler

The disadvantage for the boiler was taken as (Ref. 29).

$$\zeta = \frac{a\Sigma_a^F}{(b-a)\Sigma_a^m} \left\{ \frac{(b-a)\Sigma_a^m}{a\Sigma_a^F} \left[\left(\frac{1+T}{1-T} \right) 2a\Sigma_a^F \right] + \gamma(b-a) \coth \gamma(b-a) - 1 \right\}$$

$$T = e^{-2a\Sigma_a^F} \left[1 - 2a\Sigma_a^F \right] + (2a\Sigma_a^F)^2 E_1(2\Sigma_a^F a)$$

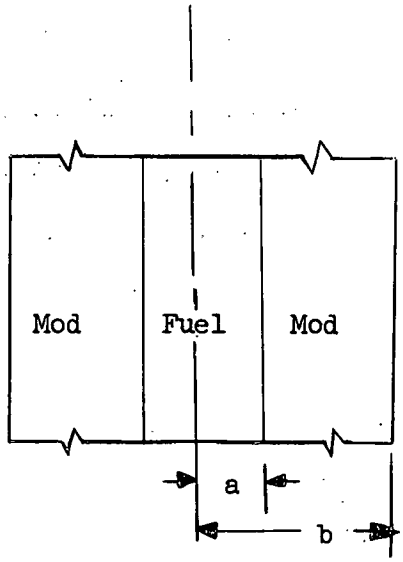

UNIT CELL

APPENDIX B3

Method of Obtaining Group Constants for 3G-3R Code for ORACLE

(The first notation is the memory position followed by the group constant symbol)

28C-g The input word was F0 000 01000, which means that it will be a 2G - 3R calculation with a computing time of about 2 minutes per case.

28E-Y Cylindrical geometry was used.

28F-R_1 Radius of superheater = 32.4 cm

29I-R_2 Thickness of boiler = 37.3 cm

293-R_3 Thickness of reflector = 4 in.

295-t_1 } Shell constants. The shell between the superheater and boiler is 1/8
2F3-30D-B } in. thick. It was neglected in view of the additional inaccuracy contributed by the inordinate amount of work necessary to determine the associated group constants. A rigorous treatment of anisotropic scattering of neutrons in thin shells is included in Ref. 18. This treatment yields the equations necessary to compute the shell constants.

29B-Σ_{all} Fast absorption cross section - superheater.

(See Fig. B-4)

$$\Sigma_{all} = \Sigma_{R1}(1 - P_{RE1})$$

If a fast point source in an infinite non-multiplying system is considered, it can be shown that: (See list of symbols pg 180).

$$\langle r^2 \rangle_{SD} = \int_{volume} r^2 \frac{P_{RE}\Sigma_R\phi_{Fd}{}^3r}{\int_{volume} P_{RE}\Sigma_R\phi_{Fd}{}^3r} = 6L^2 = 6\tau$$

where $L^2 = \frac{D}{\Sigma_R}$

$$P_{RE} = \exp - \int_{E_{TH}}^{E_o} \frac{\Sigma_a}{\xi \Sigma_t} \frac{dE}{E}$$

$$\therefore \quad \Sigma_{all} = \frac{D_{11}}{\tau_1} (1 - P_{RE1})$$

Method of computing τ (superheater)

$$\tau = \int_{E_{TH}}^{E_o(2Mev.)} \frac{D}{\xi \Sigma_t} \frac{dE}{E} \approx \sum_n \frac{\ln \frac{E_2}{E_1}}{3 \bar{\xi} \Sigma_t^2 (1-\bar{\bar{\mu}})}$$

n = number of energy intervals

E_1, E_2 = end points of interval

$$\bar{\xi} = \frac{\sum_i \Sigma_s^i \xi_i}{\sum_i \Sigma_s^i}$$

$$\bar{\bar{\mu}} = \frac{\sum_i \Sigma_s^i \bar{\mu}_i}{\sum_i \Sigma_s^i}$$

$$\Sigma_t = \sum_i \Sigma_t^i$$

Microscopic cross sections were averaged from BNL-325 over the energy range .077 ev to 2 Mev. This yields $\tau = 150.4$ cm^2. A first flight correction was made as follows:

$$\tau_{FC} = \frac{1}{3\Sigma_t^2(2Mev)} = 7.4 \text{ cm}^2$$

Thus $\tau_{11} = 158$ cm^2

Method of computing P_{RE} (superheater)

$$P_{RE} = \exp - \int_{E_{TH}}^{E_o} \frac{\Sigma_a}{\xi \Sigma_t} \frac{dE}{E} \qquad (1)$$

$\bar{\xi}$ = see above.

Assuming that $\bar{\xi}\,\Sigma_s$ is independent of energy in the resonance region:

$$P_{RE} \cong \exp \sum_i \left[\frac{1}{\bar{\xi}\,\Sigma_s} \int_{E_{TH}}^{E_o} \frac{\Sigma_a}{1+\frac{\Sigma_a}{\Sigma_s}} \frac{dE}{E} \right]_i$$

For absorption in stainless steel, values for the resonance integral of Fe, Cr and Ni were: (See Ref. 17)

Fe	2.1 barns
Ni	4 barns
Cr	1.9 barns

For the uranium resonance integrals, the effect of the dilution was considered. For both superheater and boiler regions, the system was homogenized in the calculation of Σ_s. The values of the effective capture integral

$$\int_{E_{TH}}^{E_o} \frac{\sigma_a^{28}}{1 + \frac{N^{U}\sigma_a^{28}}{\Sigma_s}} \frac{dE}{E}$$

were obtained from Ref. 17. The values of the effective capture integral for U-235 were approximated by assuming that the dilution will have the same effect as in the case of U-238.

29D-Σ_{a21} Thermal absorption cross section - superheater

Thermal energy = .077 ev

2A1-Σ_{x11} Transferal cross section from fast to thermal group - superheater.

$$\Sigma_{x11} = \Sigma_{a11} - \Sigma_{R1} = \Sigma_{a11} - \frac{D_{11}}{\tau_{11}}$$

(See Fig. B-4)

2A7-D_{11} Fast diffusion coefficient - superheater

$$D_{11} = \int_{E_{TH}}^{E_o} \frac{1}{\zeta \Sigma_t} \frac{dE}{E} \cong \sum_n^{\tau_1} \frac{\ln \frac{E_2}{E_1}}{\zeta \Sigma_t}$$

2A9-D_{21} Thermal diffusion coefficient - superheater

$$D_{21} = \frac{1}{3\Sigma_{tr}}$$

$$\Sigma_{tr} = \sum \Sigma_{tr}^i$$

Transport cross sections for stainless steel and U-235 were compiled from data in Ref. 18. The transport cross section for U-238 was extracted from data found in Ref. 19, and that for BeO from Ref. 26. In each case L^2 was measured thus:

$$\Sigma_{tr} = \frac{1}{3L^2\Sigma_a}$$

2AD-$\nu\Sigma_{f11}$ ν x Fast fission cross section - superheater

The microscopic fission cross section was averaged over the group 1 energy range, from BNL-325.

2AF-$\nu\Sigma_{f21}$ ν x Thermal fission cross section - superheater.

Thermal energy = .077 ev

2B7-Σ_{a12} Fast absorption cross section.

Computed similarly to Σ_{a11} except for the method of choosing τ. In this case τ was computed by the Flügge - Tittle method as described in Ref. 27.

$$\tau_{12} = 81.4 \text{ cm}^2$$

2B9-Σ_{a22} Thermal absorption cross section - boiler

Thermal energy = .062 ev

2BD-Σ_{x12} Transferal cross section from fast to thermal group - boiler.

Similar to Σ_{x11}.

2C3-D_{12} Fast diffusion coefficient - boiler.

Extrapolated from data in Ref. 18.

2C5-D_{22} Thermal diffusion coefficient - boiler.

Similar to D_{21}

2C9-$\nu\Sigma_{f12}$ ν x Fast fission cross section - boiler.

Similar to $\nu\Sigma_{f11}$.

2CB-$\nu\Sigma_{f22}$ ν x Thermal fission cross section - boiler.

Thermal energy = .062 ev

2D3-Σ_{a13} Fast absorption cross section - reflector.

Taken from Ref. 28.

2D7-Σ_{a23} Thermal absorption cross section - reflector.

Thermal energy = .062 ev

2D9-Σ_{x13} Transferal cross section from fast to thermal group - reflector.

Similar to Σ_{x11}.

2DF-D_{13} Fast diffusion coefficient - reflector.

Taken from data in Ref. 18.

2ED-B_1^2 Fast axial reactor buckling - boiler and superheater.

$$B_1^2 = \left[\frac{\pi}{2(h+2D)}\right]^2$$

h = 1/2 core height

2 D was added to the core half height to account for reflecting at the ends, inasmuch as the 2G-3R Code does not explicitly include end reflection.

2EF-B_2^2 Thermal axial buckling - boiler and superheater

Use same value as B_1^2

Following are the volume fractions used to determine the atomic densities:

APPENDIX FIG. B-1

Superheater	Boiler
$\frac{V_{BeO}}{V_{SH}} = .7506$	$\frac{V_{H_2O}}{V_B} = .60$
$\frac{V_{voids}}{V_{SH}} = .1384$	$\frac{V_{voids}}{V_B} = .06$
$\frac{V_{meat}}{V_{SH}} = .0456$	$\frac{V_{meat}}{V_B} = .24$
$\frac{V_{clad + wires}}{V_{SH}} = .0654$	$\frac{V_{clad + supports}}{V_B} = .10$

Atomic densities are as follows:

APPENDIX FIG. B-2

Superheater		Boiler	
Element	N x 10^{-24} atoms cm^{-3}	Element	N x 10^{-22} atoms cm^{-3}
$_{26}Fe^{56}$	.005730	$_{26}Fe^{56}$	.01545
$_{28}Ni^{58}$	.000625	$_{28}Ni^{58}$	.00168
$_{24}Cr^{52}$	.001567	$_{24}Cr^{52}$	.00422
$_{4}Be^{9}$	.05170	$_{1}H^{1**}$	.0289
$_{8}O^{16}$	.05231	$_{8}O^{16}$	.01767
U*	.000364	U	.00191

*35 volume % UO_2 in meat.

**10% voids in water

APPENDIX FIG. B-3

Table of Group Constants

19.5% S.H. 5% B

Σ_{a11}	.00425 cm^{-1}
Σ_{a21}	.0421 cm^{-1}
Σ_{x11}	.00482 cm^{-1}
D_{11}	1.43 cm
D_{21}	.846 cm
$\nu\Sigma_{f11}$	.00498 cm^{-1}
$\nu\Sigma_{f21}$	.0534 cm^{-1}
Σ_{a12}	.003635 cm^{-1}
Σ_{a22}	.0843 cm^{-1}
Σ_{x12}	.0143 cm^{-1}
D_{12}	1.47 cm
D_{22}	.272 cm
$\nu\Sigma_{f12}$	.0067 cm^{-1}
$\nu\Sigma_{f22}$	.0825 cm^{-1}
Σ_{a13}	0
Σ_{a23}	.0091
Σ_{x13}	.0329
D_{13}	2.1
D_{23}	.25
τ_{11}	157.8 cm^2
τ_{12}	81.4 cm^2

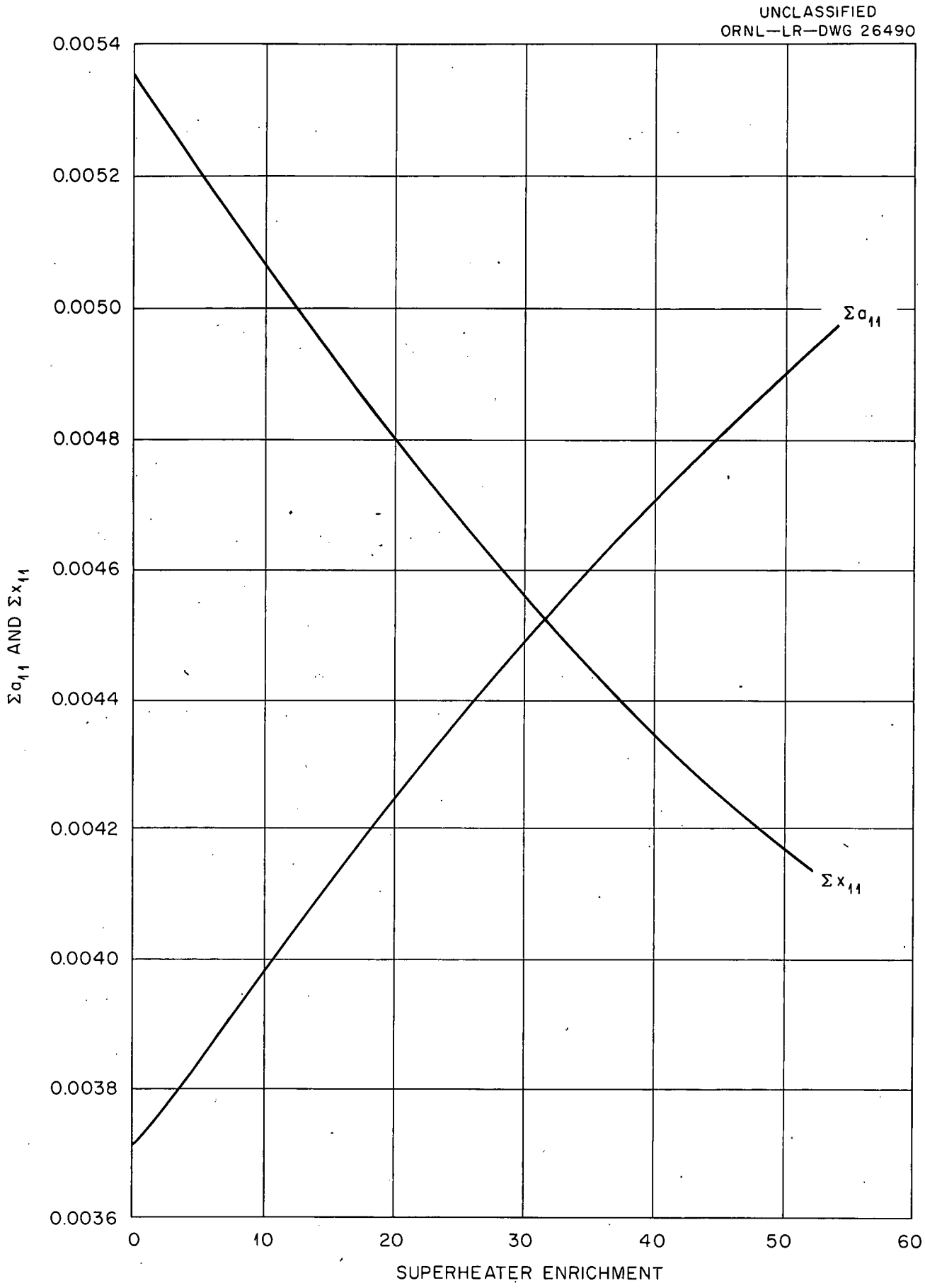

Fig. B-4. Superheater Group Constants Fast Group.

TABLE OF SYMBOLS USED IN CHAPTER 4 AND APPENDIX B

A, C, F, G, H	Arbitrary Constants
B^2	Buckling
D	Diffusion Coefficient
E_{SH}, E_B	Enrichment, %, superheater and boiler
E_{th}	Thermal cutoff energy
E_o	High energy cutoff (2 Mev)
f_v	Void fraction in boiler water
h	Half height of reactor, cm.
In(x)	Modified Bessel function of the first kind of order n
$\underline{J}$	Neutron current vector neutron/cm^2 sec
J^+, J^-	Neutron currents in opposite direction neutron/cm^2 sec
$J_n(x)$	Bessel function of order n of the first kind
$K_n(x)$	Modified Bessel function of the second kind of order n
k	Multiplication factor
k_∞	Multiplication factor with no leakage
L	Thermal diffusion length, cm; $\gamma = \frac{1}{L}$ in disadvantage factor calculation
M^2	Migration area, cm^2
m	Refers to moderator when used as subscript or superscript
N	Number density atoms/cm^3
P	Power
p	Average power density
P_{RE}	Resonance escape probability
q	Slowing down density at thermal energy

R	Radii of different regions
T	Neutron transmission
t	Time
V	Volume
w	Fission per watt • sec
$Y_n(x)$	Bessel function of the second kind of order n
α	Defined as $\sqrt{\frac{k_\infty - 1}{M^2} - \frac{\pi}{2h}}$
β	Axial buckling, $\frac{\pi}{2h}$
γ	Reciprocal of diffusion length in moderator
ϵ	Fast fission factor
λ_I, λ_x	Decay constants for I^{135} and Xe^{135} respectively
λ	Defined in migration area calculation as $\frac{1}{L_3^2} + \left(\frac{\pi}{2h}\right)^2$
$\bar{\mu}$	Average cosine of neutron scattering angle
μ	Defined in migration area calculation as $\frac{\pi}{2h}$
ν	Neutrons produced per fission
ξ	Average lethargy increment per collision
ρ	Density
Σ_a	Macroscopic absorption cross-section, cm^{-1}
Σ_f	Macroscopic fission cross-section, cm^{-1}
Σ_R	Removal cross-section, cm^{-1}
Σ_S	Elastic scattering cross-section, cm^{-1}
Σ_t	Macroscopic total cross-section, cm^{-1}
Σ_{tr}	Transport cross-section, cm^{-1}
Σ_x	Transferral cross-section, cm^{-1}

τ	Fermi age, cm^2
ϕ	Neutron flux, neutrons/cm^2·sec
$\bar{\phi}$	Average neutron flux, neutron/cm^2 sec
∇^2	Laplacian operator
S. S.	Denotes stainless steel, type 347

The subscripts used in the notation for the machine claculations refer to energy group and region in the reactor. For example, Σ_{aij} is the absorption cross-section for energy group i in region j of the reactor.

i = 1 refers to "fast" energy group

i = 2 refers to thermal energy group

j = 1 refers to superheater region

j = 2 refers to boiler region

j = 3 refers to reflector region

APPENDIX C

C-1 Nozzles

C-1.1 Circulating Inlet (10-3/4" ID x 1" wall See Figure C-1).

Reinforcement Required $A = dt_r$

$A = 10.75 \times 2.79 = 30 in^{-2}$

FIG. C-1

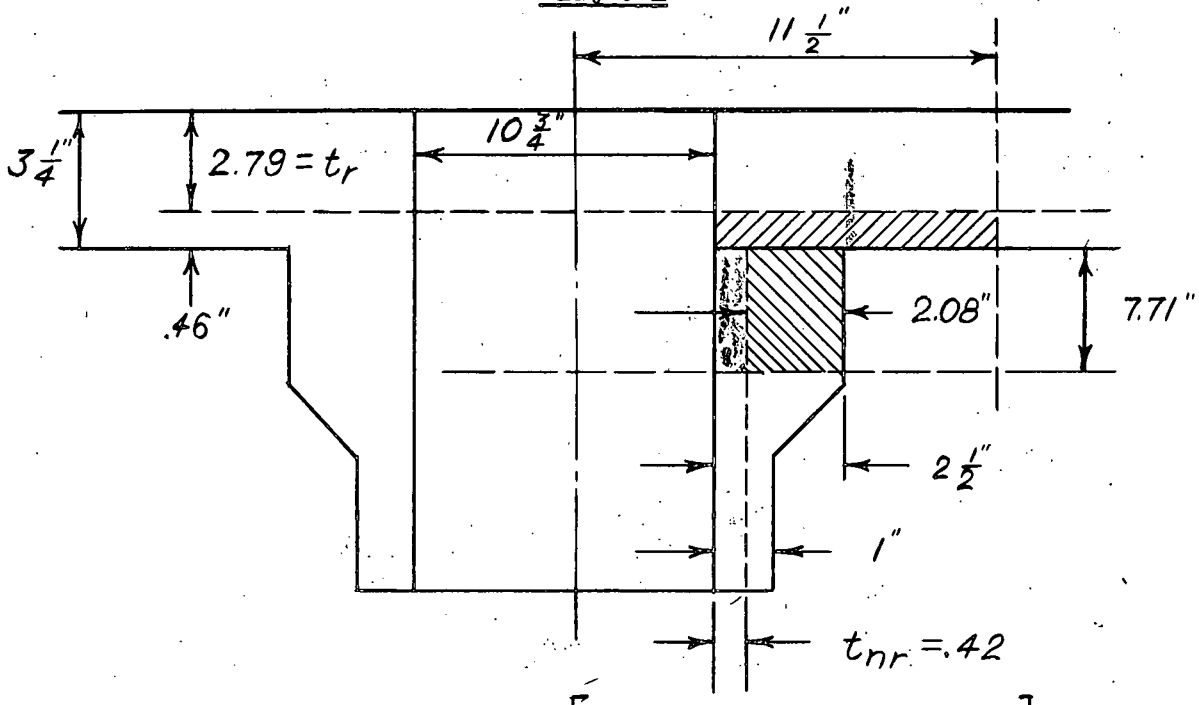

∴ Reinforcement available = $2\left[(5.75 \times .46) + (7.71 \times 2.08)\right]$

$= 37 \overline{in}^2$ ∴ Opening is fully reinforced

C-1.2 Circulating Outlet (11.5 ID x 1-1/4" wall - See Fig. C-2).

$$t_{nr} = \frac{PR}{SE - .6P} = \frac{1300 \times 5.75}{17{,}500 \times 1.00 - .6 \times 1300} = .450"$$

Refinforcement required $A = dt_r$

$A = 11.5 \times 3.06 = 35.2 \overline{in}^2$

FIG. C-2

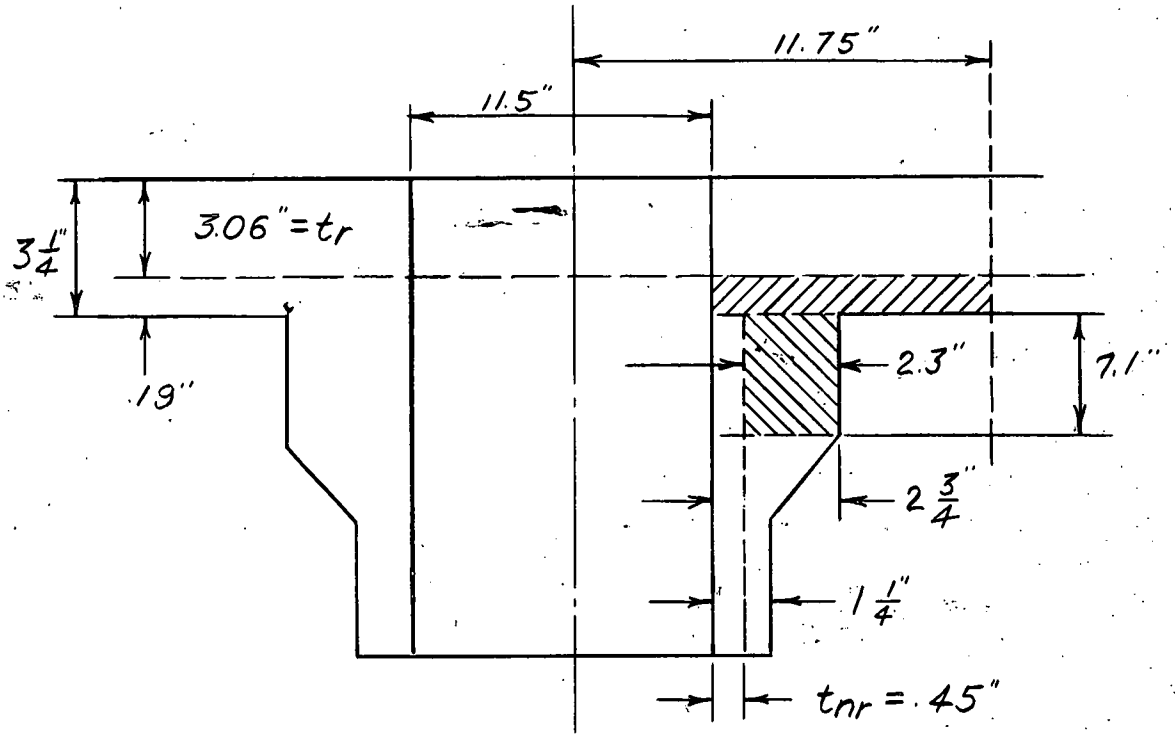

Reinforcement Available = $2\left[(6 \times .19) + (7.1 \times 2.3)\right] = 35.3\ \text{in}^2$

.°. opening is fully reinforced.

C-1.3 Superheater Outlet (9-1/2" ID See Fig. C-3)

FIG. C-3

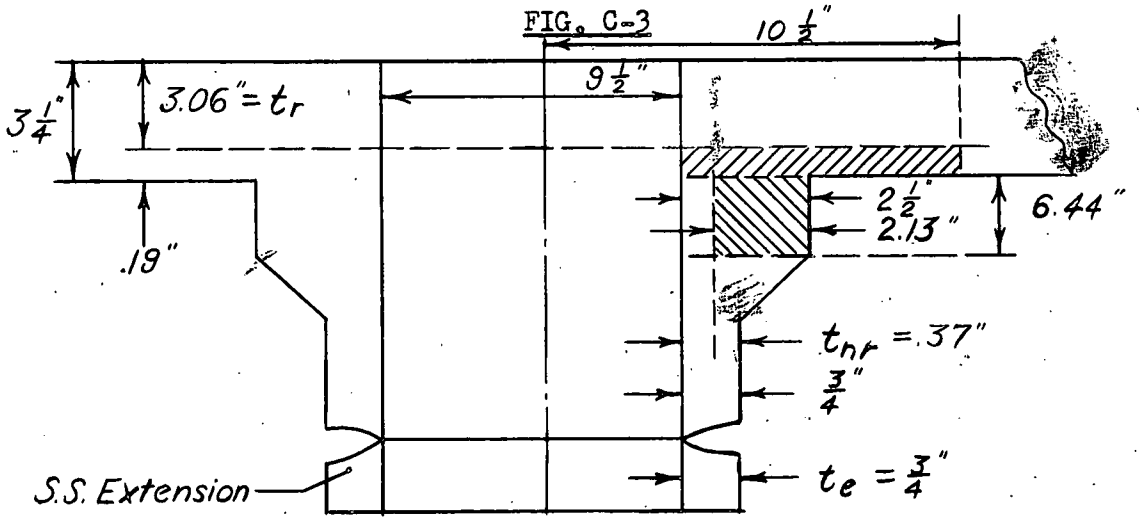

Extension thk $t_e = \frac{PR}{SE - .6P}$

S (Type 347 stainless steel at 950°F) = 13,850 psi

per (31) Table UHA-23

$\therefore\ t_e = \frac{1300 \times 4.75}{13{,}850 \times 1.00 - .6 \times 1300} = .48"$

Will use 3/4" thk due to additional piping loads.

$$t_{nr} = \frac{PR}{SE - .6P} = \frac{1300 \times 4.75}{17{,}500 - .6 \times 1300} = .37"$$

Reinforcement required $A = dt_r$

$A = 9.5 \times 3.06 = \underline{\underline{29}}\ in^2$

Reinforcement available = $2\left[(5.75 \times .19) + (6.44 \times 2.13)\right] = \underline{\underline{29.8}}\ in^2$

$\therefore$ Opening if fully reinforced

C-1.4 Vessel Flange

[Per (31)VA-47, 49, 50 and 51]

See Figure C-4

Bolt Load $W_{m_1} \cong .785\ G^2\ P$

$\cong .785\ \overline{84}^2 \times 1300 = \underline{7.2 \times 10^6\ lb}$

Maximum bolt load = W_{m1} + shock loading

A shock loading factor of 15 G's has been used in accordance with naval practice.

Estimated weight of head = 23,500 lb

$\therefore$ Maximum bolt load $W = 7.2 \times 10^6 + 15 \times 23{,}500$

$W = (7.2 + .35) \times 10^6 = \underline{7.55 \times 10^6\ lb}$.

Studs

Stud material will be SA-193 B-6 (13% chr.)

S (at 575°) = 17,210 psi per (31) UHA-23

Assuming 4" diameter studs with 8 pitch threads

$$\text{No. studs} = \frac{\text{Load}}{\text{S x root area}} = \frac{7.55 \times 10^6}{17{,}210 \times .785 \times 3.84^2}$$

No. studs = 38

FIGURE C-4

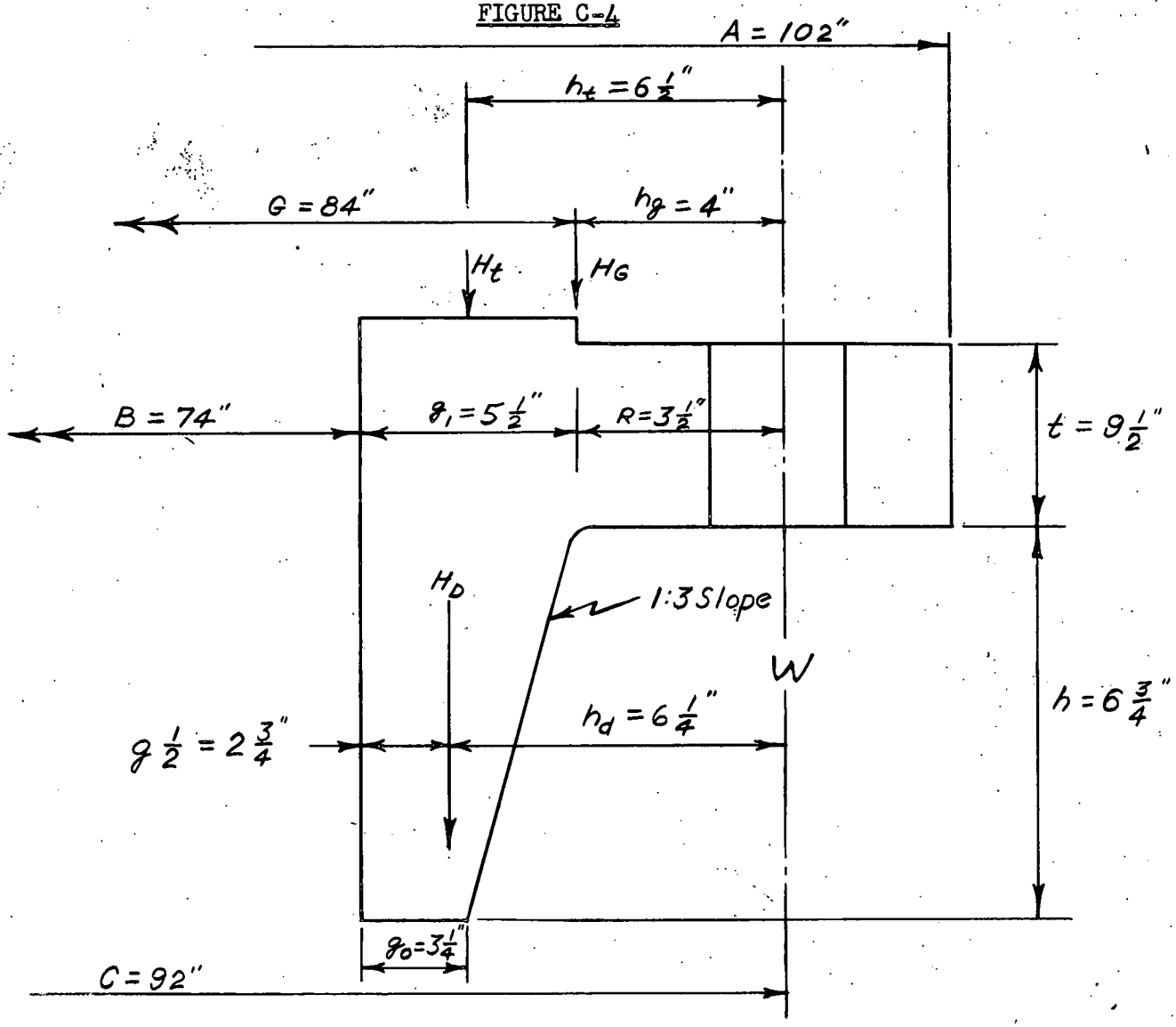

$h_d = R + .5\, g_1 = 3\text{-}1/2 + 2\text{-}3/4 = 6\text{-}1/4"$

$h_g = \frac{C - G}{2} = \frac{92 - 84}{2} = 4"$

$h_t = \frac{R + g1 + h_g}{2} = \frac{3\text{-}1/2 + 5\text{-}1/2 + 4}{2} = 6\text{-}1/2"$

$W = 7.55 \times 10^6$

$H = .785\, G^2P = .785 \times \overline{84}^2 \times 1300 = 7.2 \times 10^6$ lb.

$H_D = .785\, B^2P = .785 \times \overline{74}^2 \times 1300 = 5.58 \times 10^6$ lb.

$H_G = W - H = .35 \times 10^6$ lb

$H_t = H - H_D = 1.62 \times 10^6$ lb

Moments:

$M_D = H_D \times h_d = 5.58 \times 10^6 \times 6.25 = 34.9 \times 10^6$

$M_T = H_T \times h_t = 1.62 \times 10^6 \times 6.5 = 10.5 \times 10^6$

$M_G = H_G \times h_g = .35 \times 10^6 \times 4 = 1.4 \times 10^6$

$M_o = 46.8 \times 10^6$ in-lb

S_f = 17,500 psi (A-212B)

S_H = Longitudinal stress in hub

S_R = Radial stress in flange

S_T = Tangential stress in flange

$S_H < 1.5\, S_F$ $\qquad \frac{S_H + S_R}{2} < S_F$

$S_R < S_F$

$S_T < S_F$ $\qquad \frac{S_H + S_T}{2} < S_F$

$g_1/g_o = 1.69$ $\qquad \frac{h}{h_o} = \frac{h}{\sqrt{Bg_o}} = \frac{6.75}{\sqrt{74 \times 3.25}} = \frac{6.75}{15.5} = .435$

f(Fig. UA-51.6) = 1.03

$$L = \frac{te + 1}{T} + \frac{t^3}{d}$$

$t = 9.5"$

$$d = \frac{U}{V} h_o \overline{g_o}^2$$

UA-51.1

$$K = \frac{A}{B} = 1.39 \begin{cases} U = 6.8 \\ Y = 6.0 \\ Z = 3.2 \\ T = 1.8 \end{cases}$$

V(Fig. UA-51.3) = .29

$$d = \frac{6.8}{0.29} \times 15.5 \times \overline{3.25}^2 = 3820$$

$$e = \frac{F}{h_o}; \quad F \text{ (fig. UA 51.2)} = 0.85$$

$$e = \frac{0.85}{15.5} = 0.055$$

$$\therefore L = \frac{9.5 \times 0.055 + 1}{1.8} + \frac{\overline{9.5}^3}{3820} = 0.85 + 0.23$$

$L = 1.08$

$$S_H = \frac{fM_o}{L g^2 B} = \frac{1.03 \times 46.8 \times 10^6}{1.08 \times \overline{5.5}^2 \times 74} = \underline{20,000} \text{ psi}$$

Since $S_H < 1\text{-}1/2\ S_F$ (26,300 psi)

$$S_R = \frac{(4/3\ te + 1)M_o}{L t^2 B} = \frac{(4/3 \times 9.5 \times 0.055 + 1)\ 46.8 \times 10^6}{1.08 \times \overline{9.5}^2 \times 74}$$

$S_R = \underline{11,000}$ psi O.K., Since $S_R < S_F$

$$S_T = \frac{YM_o}{t^2 B} - Z\ S_R$$

$$S_T = \frac{6 \times 46.8 \times 10^6}{\overline{9.5}^2 \times 74} - 3.2 \times 11,000 = \underline{7,000} \text{ psi}$$

Since $S_T < S_F$

Also $\frac{S_H + S_R}{2} = \frac{20,000 + 11,000}{2} = 15,500 < S_F$

$\frac{S_H + S_T}{2} = \frac{20,000 + 7,000}{2} = 13,500 < S_F$

APPENDIX D1 Analysis of Resonance Instability in Boiling Water Reactors

D.1.1 Introduction

All boiling water reactors built and operated to date have experienced resonance or "chugging" instabilities at certain operating conditions. (Ref. 23) In order to get a basic understanding of this phenomena, a linearized analysis of the system was undertaken. It was felt that a linearized analysis was possible since the oscillations resulting from the instability appears to be sinusoidal prior to diverging into non-linear oscillations.

The steps taken in this analysis were the following:

1. Write simplified dynamic equations for the system.
2. Linearize these equations.
3. Non-dimensionalize the equations.
4. Use standard servomechanisms techniques to determine conditions for neutral stability.

Steps 2 and 3 were taken separately to help retain a physical feel for the equations. The step that is most susceptible to questioning is step 1. No evaluation was attempted on the assumptions underlying the simplified dynamic equations. The only justification for the equations is that the results of analysis seems to be consistent with emperical results. Or it appears that the basic features pertinent to the resonance instabilities in the particular type of system considered was included. The major distinguishing feature of this system is the closed steam dome on top of the reactor. This analysis is, therefore, applicable to boiling water power reactors.

The results of this analysis are presented in the form of two stability criteria and the applications of these criteria to a representative system.

D.1.2 Simplified Dynamic Equations

The equations along with a statement of their physical meaning and some of the underlying assumptions are as follows:

1. Core

$$\frac{dP}{dt} = \frac{K(1-\beta) - 1}{l} P + D\lambda C$$

$$\frac{dC}{dt} = \frac{\beta PK}{lD} - \lambda C$$

These are the standard kinetic equations for a reactor core which describes the total neutron balance and the delayed neutron balance when the delayed neutrons are lumped into one representative group. Only the lowest mode in the spatial distribution neutrons is considered.

2. Reactivity change

$$\delta K = \gamma \Delta_{mod}$$

The reactivity change is assumed to be premarily from a change in moderator density. The coolant is assumed to be the only moderator present.

3. Fuel element heat balance

$$c_F \rho_F V_F \frac{d T_F}{dt} = P - Q$$

The rate of change of heat in the fuel element is equal to the heat generation rate from fissions minus the heat transferral rate to the coolant.

4. Heat transferral rate to the coolant

$$Q = A_F h \left[T_F - T_S \right]$$

The heat transferral rate to the coolant from the fuel elements is proportional to the difference in temperature of the fuel element and the coolant. The coolant temperature is assumed to be at the saturation temperature determined by

the instantaneous steam dome pressure. The proportionality factor is assumed constant.

5. Heat removal rate from the core

$$2UA\ \bar{f}v\ \rho_g\ h_{fg} = Q(t - 1/2 \cdot z_1/U)$$

$$Q = P_o \text{ at } t \leq 0$$

The heat removal rate at the top of the core is equal to the steam mass flow rate at the top of the core times the latent heat of vaporization. This is true if the coolant enters the bottom of the core in the liquid phase only and is at saturation temperature as is assumed. The recirculation ratio must be large and/or the feedwater must be heated. At any time greater than t = 0, it is assumed that the heat removal rate at the top of the core lags the heat transferral rate to the coolant by the average time it takes for the bubbles formed along the height of the core to reach the top. The void fraction at the top of the core is assumed to be twice the average void fraction in the core which is true for a linear distribution of voids. It is also assumed that the flow velocity is constant and that there is no slip.

6. Heat balance in the steam dome

$$V_{S.D.}\ \frac{d\rho_g h_{gS.D.}}{dt} = 2UA\ \bar{f}v\ \rho_g\ h_{gc} - \rho_g\ h_{go}\ X$$

The rate of change of heat in the steam dome is equal to the rate at which heat leaves the top of the core and enters the steam dome minus the rate at which heat flows out through the throttle valve. All radiation and conduction losses are assumed negligible. The role of the water above the core is to transmit pressure only.

D.1.3 Linear Simplified Dynamic Equations

The equations were linearized by defining new variables which represent incremental changes from a steady state value. Products of incremental changes were dropped. The thermodynamic variables were expanded in a Taylor Series as a function of incremental saturation temperature change and only the linear term retained. This expansion as a function of one variable is possible because two phase equilibrium is assumed at all time and therefore one independent variable describes the thermodynamic state.

The linearized equations are the following:

1. Core

$$1 \frac{d^2F}{dt^2} + 1 \, (\lambda+\beta/1) \frac{dF}{dt} = \frac{d \, \delta K}{dt} + \lambda \, \delta K \quad \text{(Ref. 21)}$$

2. Reactivity change

$$\delta K = \gamma \left[\rho_{go} \delta \bar{f}v + \bar{f}v_o \mu \Delta T_s - (1-\bar{f}v_o) \, |\gamma| \Delta T_S - \delta \bar{f}_v \, \rho_{fo} \right]$$

3. Fuel element heat balance

$$\frac{C_F \rho_F V_F}{P_o} \frac{d\Delta T_F}{dt} = F - G$$

4. Heat transferral rate to the coolant

$$G = \frac{A_F h}{P_o} \left[\Delta T_F - \Delta T_S \right]$$

5. Heat removal rate from the core

$$\frac{2UA}{P_o} \left[\delta \bar{f}v \, \rho_{go} \, h_{fgo} + \bar{f}v_o \, \gamma \Delta T_S \right] = G \, (t - 1/2 \cdot z_1/U)$$

$$G = 0 \text{ at } t \leq 0$$

6. Heat balance in the steam dome

$$\frac{V_{SD} \, h_{fgo}}{P_o} \mu \frac{d\Delta T_S}{dt} = \frac{2UA \, h_{fgo} \, \rho_{go} \, \delta \bar{f}v}{P_o} - \frac{h_{fgo} \rho_{go}}{P_o} \Delta X$$

To arrive at this equation it is necessary to assume that the enthalpy of the steam entering, inside, and leaving the steam dome is the same.

The following relations between the constants of the system now exist:

$$P_o = A_F\, h \left[T_{Fo} - T_{So}\right]$$

$$= 2UA\, \rho_{go}\, h_{fgo}\, \bar{f}v_o$$

$$= X_o\, \rho_{go}\, h_{fgo}$$

These equations state that the steady state power is equal to the heat transferral rate from the fuel element to the coolant, the heat removal rate from the core, and the heat removal rate from the steam dome.

D.1.4 Non-dimensional Equations

In order to expedite a parameter study for the system, the variables were all non-dimensionalized. The constants for the system were grouped together into non-dimensional parameters. The parameters A_1 to A_5 are independent of operating condition while B_1 to B_9 depend only on operating condition and not on the extrinsic characteristics of the reactor.

The equations become the following:

1. Core

$$A_5^2 \frac{d^2F}{dY^2} + A_5\, B_8 \frac{dF}{dY} = A_5 \frac{dSK}{dY} + B_9 SK$$

2. Reactivity change

$$SK = -A_4 \left[B_5 A_2 Z + B_6 (1-A_2)\, R_S - A_2 B_3 B_7 R_S\right]$$

3. Fuel element heat balance

$$\frac{A_1 B_1}{2A_2} \frac{dR_F}{dY} = F - G$$

4. Heat transferral rate to coolant

$$G = R_F - R_S$$

5. Heat removal rate from core

$$Z + B_2 R_S = G(Y - 1/2)$$

$$G = 0 \text{ at } Y \leq 0$$

6. Steam dome heat balance

$$\frac{A_3 B_3}{2A_2} \frac{dR_S}{dY} = Z - I$$

The above set of six equations completely determines the dynamic characteristics of the system. I is an external input function for the system and if its time behavior is known, the time behavior of the remaining six variables can be determined. To analyze the system for inherent stability however, the external input function I is set equal to zero and only relationships between the remaining six coupled variables considered. Another possible external input function for the system, the control rod motion, was set equal to zero from the beginning of the analysis.

D.1.5 Derivation of Open Loop Transfer Function

A transfer function is defined as the ratio between the Laplace transforms of the output and input functions when the initial conditions can be taken as zero.

The Laplace transforms of the set of non-dimensional equations were derived with respect to the non-dimensional independent variable Y. All initial conditions were taken to be zero since the variables are defined in such a manner that this can be done.

The transformed equations are the following:

1. Core

$$A_5(A_5S + B_8)\, S\, f = (A_5S + B_9)\, \delta k$$

2. Reactivity change

$$\delta k = -A_4\left[B_5A_2z + B_6(1-A_2)r_S - A_2B_3B_7r\right]$$

3. Fuel element heat balance

$$\frac{A_1B_1}{2A_2}\, Sr_F = f - g$$

4. Heat transferral rate to coolant

$$g = r_F - r_S$$

5. Heat removal rate from core

$$z + B_2r_S = g\, e^{-S/2} = \frac{g}{\sum_{n=0}^{\infty} \frac{1}{n!}\left(\frac{S}{2}\right)^n}$$

$$\cong \frac{q}{1 + 1/2S + 1/8S^2}$$

This approximation was justified by determining that retaining another term in the series does not affect the result.

6. Steam dome heat balance

$$\frac{A_3\, B_3}{2A_2}\, Sr_S = z$$

Remembering that I has been set equal to zero.

For this set of coupled equations which describes a multi-loop system, the open loop analysis can be performed by opening the loop at a number of points. It was decided that the natural way to consider the system is as shown in Figure D-1. The core is in the forward loop with the input δk_{in} and the output f.

UNCLASSIFIED
ORNL-LR-DWG 26491

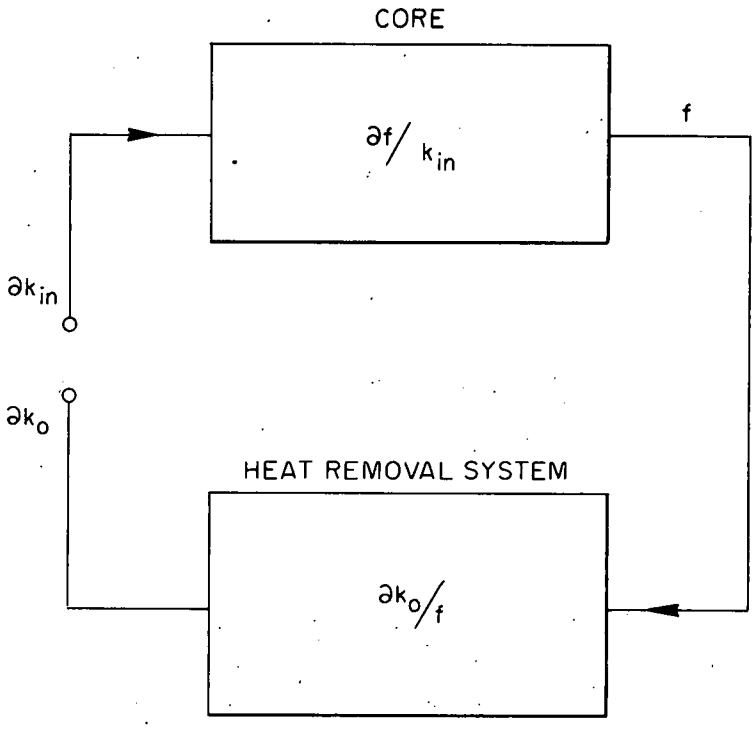

Fig. D-1. Block Diagram Showing Breakdown of System into Two Major Blocks.

In the feedback, the input is the output of the core, f, and the output is δk_o. In servo terminology $f/\delta k_{in}$ is the forward transfer function and $\delta k_o/f$ is the feedback transfer function.

The transfer function $f/\delta k_{in}$ can be obtained simply from the core equation.

$$f/\delta k_{in} = \frac{A_5 S + B_9}{A_5 S(A_5^5 + B_8)}$$

To get $\delta k_o/f$, the remaining equations can be written in the following manner:

$$\begin{bmatrix} 0 \\ f \\ 0 \\ 0 \\ 0 \end{bmatrix} = \begin{bmatrix} 1 & 0 & A_4B_6(1-A_2) - A_4A_2B_3B_7 & 0 & A_4B_5A_2 \\ 0 & \frac{A_1B_1}{2A_2}S & 0 & 1 & 0 \\ 0 & -1 & 1 & 1 & 0 \\ 0 & 0 & B_2(1+1/2S+1/8S^2) & -1 & (1+1/2S+1/8S^2) \\ 0 & 0 & \frac{A_3B_3}{2A_2}S & 0 & -1 \end{bmatrix} \begin{bmatrix} \delta k_o \\ r_F \\ r_S \\ g \\ z \end{bmatrix}$$

Solving for $\delta k_o/f$:

$$\frac{\delta k_o}{f} = \frac{-A_4\left[\frac{B_5A_3B_3}{2}S + B_6 - A_2(B_6 + B_3B_7)\right]}{B_2 + \left(\frac{A_1B_1}{2A_2} + \frac{B_2}{2} + \frac{A_3B_3}{2A_2} + \frac{A_1B_1B_2}{2A_2}\right)S}$$

$$+\left(\frac{A_1B_1}{2A_2}\left(\frac{B_2}{2} + \frac{A_3B_3}{2A_2}\right) + \frac{B_2}{8} + \frac{A_3B_3}{4A_2}\right)S^2$$

$$+\left(\frac{A_3B_3}{16A_2} + \frac{A_1B_1}{2A_2}\left(\frac{B_2}{8}\ \frac{A_3B_3}{4A_2}\right)\right)S^3$$

$$+ \frac{A_3B_3A_1B_1}{32A_2^2}S^4$$

D.1.6 Analysis for Stability

Standard servo techniques (Ref. 20) can now be applied to analyze the system for stability. In servo theory notation, the open loop transfer function is H(s)G(s).

For this system

$$-(\delta k_o/f)(f/\delta k_{in}) = H(s)G(s)$$

The minus sign appears because negative feedback is implied in H(s). The characteristic equation for the system is the numerator of 1+H(s)G(s). The problem of determining system stability is handled by a number of different methods. All these methods are basicly a means of determining whether any of the roots of the characteristic equation have a positive real part.

The methods commonly used are:

1. Routh's criterion
2. Nyquist's method
3. Root locus method
4. Bode plots

Methods 2, 3, and 4 normally use the open loop transfer function and yield a greater understanding of the system than 1. Method 4 is not as general as methods 2 and 3. Method 3 requires that the roots of both the numerator and denominator of the open loop transfer function be available. Since they are not readily available method 2 was applied in this analysis. Another advantage of the Nyquist method is that effects of certain non-linearities in the loop of the system analyzed can be determined.

For any fixed system (all constants known), the stability characteristics can be readily determined. For a parameter study, however, it is convenient to first simplify the open loop transfer function. This was done by first computing

the values of coefficients for a representative reactor and operating conditions. Terms were then dropped from the transfer function wherever possible.

Using the numbers in Table D-1 and comparing expected values of the terms in the transfer functions, the following simplification results: (A factor of 10 was assumed sufficient to permit the dropping of terms.)

$$\frac{\delta k_o}{f} = \frac{-A_4 \left[\frac{B_5 A_3 B_3}{2} S + B_6 - A_2 (B_6 + B_3 B_7)\right]}{B_2 + \left(\frac{A_1 B_1}{2A_2} + \frac{A_3 B_3}{2A_2}\right) S + \left(\frac{A_1 B_1 A_3 B_3}{4A_2^2} + \frac{A_3 B_3}{4A_2}\right) S^2 + \left(\frac{A_3 B_3}{16A_2} + \frac{A_1 B_1 A_3 B_3}{8A_2^2}\right) S^3 + \frac{A_1 B_1 A_3 B_3}{32A_2^2} S^4}$$

In applying the Nyquist method, $j\omega$ is substituted for s in H(s)G(s) for a range of ω from $-\infty$ to $+\infty$ and the resulting curve plotted in the complex plane. A vector is drawn from the $-1 + j0$ point to a point on this curve and the rotation of this vector as ω varies from $-\infty$ to $+\infty$ is observed. If the number of counter-clockwise revolutions of this vector is equal to the number of poles of H(s)G(s) with positive real parts, the system is stable.

Figure D-2 shows the Nyquist plot for the system considered for the operating pressure of 600 psi before any terms have been dropped. The amplitude is in units of A_4. The critical frequency can be seen to be $\omega \approx 3$ (The value of ω at which the curve crosses the negative real axis.) With this information, the open loop transfer function can be further simplified.

Putting in the value $S = 3j$, a number of terms can be dropped from the transfer functions, again using a factor of 10 to be sufficient. The transfer functions become:

$$f/\delta k_{in} \cong \frac{1}{B_8}$$

This implies that for the frequencies considered the core behaves like a system with a gain $\approx \frac{1}{\beta}$ for the output f and input δk_{in}.

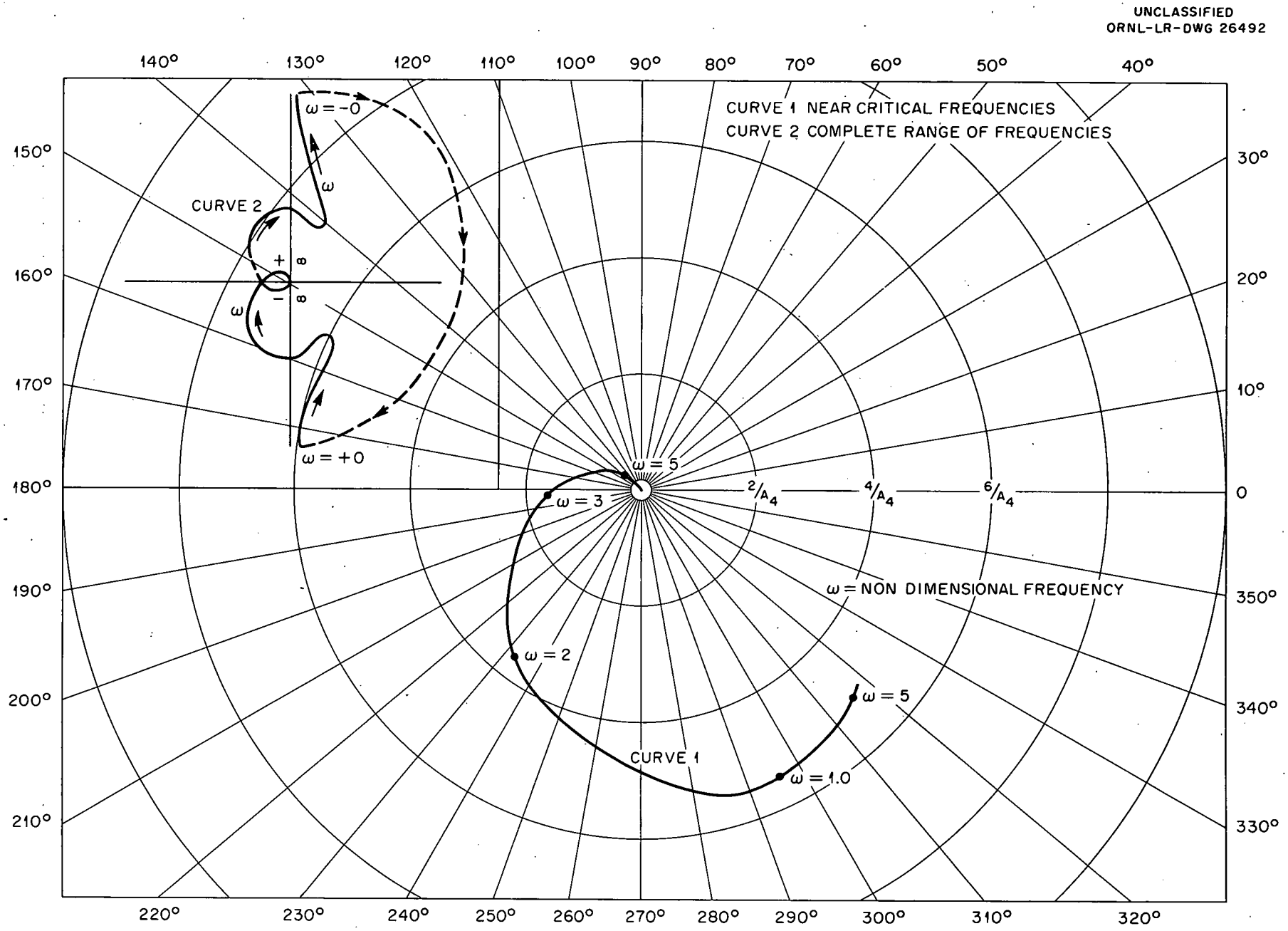

Fig. D-2. Nyquist Plot of Unsimplified Open Loop Transfer Function.

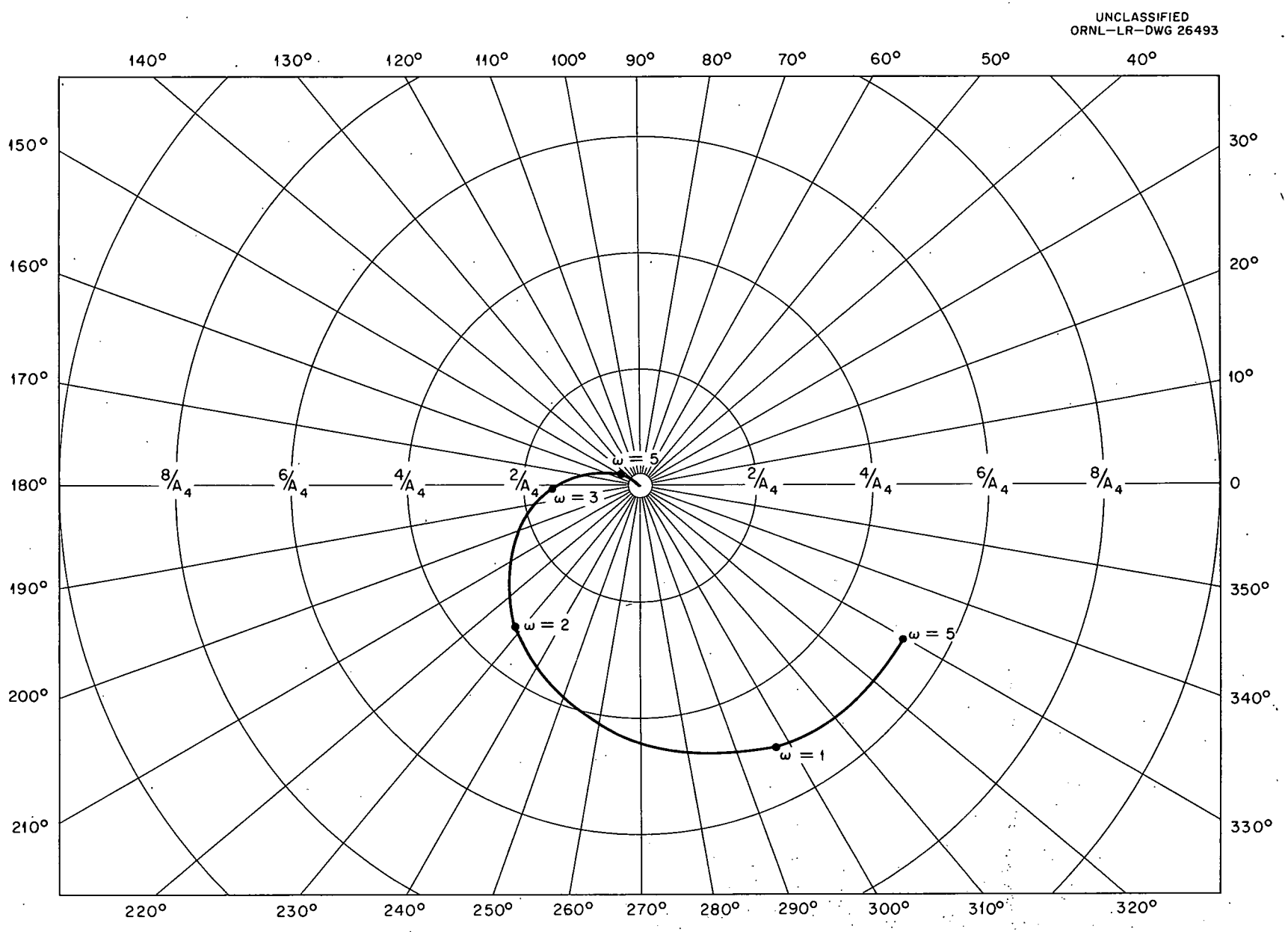

Fig. D—3. Nyguist Plot of Simplified Open Loop Transfer Function Near Critical Frequencies.

$$\frac{\delta k_o}{f} \cong \frac{-\frac{A_4B_5A_3B_3}{2}}{\frac{A_1B_1}{2A_2} + \frac{A_3B_3}{2A_2} + \frac{A_3B_3}{2A_2}\left(\frac{A_1B_1}{2A_2} + 1/2\right)S + \frac{A_3B_3}{2A_2}\left(\frac{A_1B_1}{4A_2} + 1/8\right)S^2 + \frac{A_3B_3A_1B_1}{32A_2^2}S^3}$$

or

$$H(s)G(s) = -\left(\frac{\delta k_o}{f}\right)\left(\frac{f}{\delta k_{in}}\right) = \frac{\frac{2A_4B_5A_2^2}{B_8A_1B_1}}{\frac{2A_2}{A_3B_3} + \frac{2A_2}{A_1B_1} + \left(1 + \frac{A_2}{A_1B_1}\right)S + \left(\frac{1}{2} + \frac{1}{4}\frac{A_2}{A_1B_1}\right)S^2 + \frac{1}{8}S^3}$$

A Nyquist plot of this function if shown in Figure D-3. It can be seen that near the critical frequency, this curve is similar to that in Figure D-2. This shows that the dropping of the terms was justified.

D.1.7 Criteria for Stability

Examining the shape of the curves on the Nyquist plots and the form of the simplified transfer function, two criteria for stability suggest themselves.

I. There must be no poles with positive real parts since if there are, there is no means to effect the necessary counterclockwise encirclements of the -1 + 0j point without introducing lead terms (terms in the numerator) by external means.

II. When the curve crosses the negative real axis, its amplitude must be less than one; otherwise there will be two net clockwise encirclements of the -1 + 0j point and the system will be unstable.

Mathematical expressions for these criteria can be derived from the simplified transfer function.

Criterion I can be derived by applying Routh's criterion to the denominator of the open loop transfer function. There will be no poles with positive real parts if

$$\frac{1}{2}\left(1 + \frac{1}{2}\frac{A_2}{A_1B_1}\right)\left(1 + \frac{A_2}{A_1B_1}\right) > \frac{1}{4}\left(\frac{A_2}{A_3B_3} + \frac{A_2}{A_1B_1}\right) \text{ or}$$

Criterion I

$$\frac{\frac{1}{2}\left(\frac{A_2}{A_3B_3} + \frac{A_2}{A_1B_1}\right)}{\left(1 + \frac{1}{2}\frac{A_2}{A_1B_1}\right)\left(1 + \frac{A_2}{A_1B_1}\right)} < 1 \qquad \text{for stability}$$

Criterion II can be derived by determining the amplitude of the transfer function when the frequency ω is such that the phase angle is exactly 180°. This occurs when the imaginary part goes to zero

$$\left(1 + \frac{A_2}{A_1B_1}\right)\omega - \frac{1}{8}\omega^3 = 0$$

or when

$$\omega^2 = 8\left(1 + \frac{A_2}{A_1B_1}\right)$$

The amplitude of the transfer function for this value of ω is

$$\left|H(j\omega_o)G(j\omega_o)\right|_{\omega_o = 8\left(1+\frac{A_2}{A_1B_1}\right)} = \frac{2A_4B_5A_2^2}{B_8A_1B_1\left|\frac{2A_2}{A_3B_3} + \frac{2A_2}{A_1B_1} - 4\left(1 + \frac{1}{2}\frac{A_2}{A_1B_1}\right)\left(1 + \frac{A_2}{A_1B_1}\right)\right|}$$

or

Criterion II

$$\frac{A_4B_5A_2^2}{B_8A_1B_1\left[2\left(1 + \frac{A_2}{2A_1B_1}\right)\left(1 + \frac{A_2}{A_1B_1}\right) - \left(\frac{A_2}{A_3B_3} + \frac{A_2}{A_1B_1}\right)\right]} < 1 \text{ for stability}$$

The denominator is written in this form since Criterion I requires that the term in the bracket be positive.

The frequency of oscillation for the naturally stable system is $\omega = \sqrt{8\left(1 + \frac{A_2}{A_1B_1}\right)}$

in units of coolant transit time, or $\omega' = \frac{U}{z_1}\sqrt{8(1+\frac{A_2}{A_1B_1})}$ rad/sec.

This is the frequency at which the curve on the Nyquist plot crosses the negative real axis. The neutrally stable system is that for which the amplitude is exactly 1 when the curve crosses the negative real axis.

D.1.8 Application of the Stability Criteria

The two stability criteria are:

Criterion I

$$\frac{\frac{1}{2}\left(\frac{A_2}{A_3B_3}+\frac{A_2}{A_1B_1}\right)}{\left(1+\frac{A_2}{2A_1B_1}\right)\left(1+\frac{A_2}{A_1B_1}\right)} < 1$$

Criterion II

$$\frac{A_4B_5A_2^{\,2}}{B_8A_1B_1\left[2\left(1+\frac{1}{2}\frac{A_2}{A_1B_1}\right)\left(1+\frac{A_2}{A_1B_1}\right)-\left(\frac{A_2}{A_3B_3}+\frac{A_2}{A_1B_1}\right)\right]} < 1$$

When the operating conditions are determined, there remain the four parameters A_1, A_2, A_3, A_4, that can be varied. For the representative reactor operating at 600 psi $A_1 = \frac{V_{fuel}}{V_{coolant}}$ and $A_3 = \frac{V_{S.D.}}{V_{coolant}}$ were assumed fixed and critical values of $A_4 \approx -\frac{\partial K}{\partial fv}$ determined for different values of $A_2 = \bar{f}v_o$. Figure D-4 shows these results. The strong dependence on the average fractional void is clearly indicated. Figure 7.1 shows the same results for 1200 psi operating pressure but at a higher power.

The effect of any physical quantity on stability can be determined. It must be remembered however that all the physical quantities cannot be varied independently. The following relationship must always be satisfied:

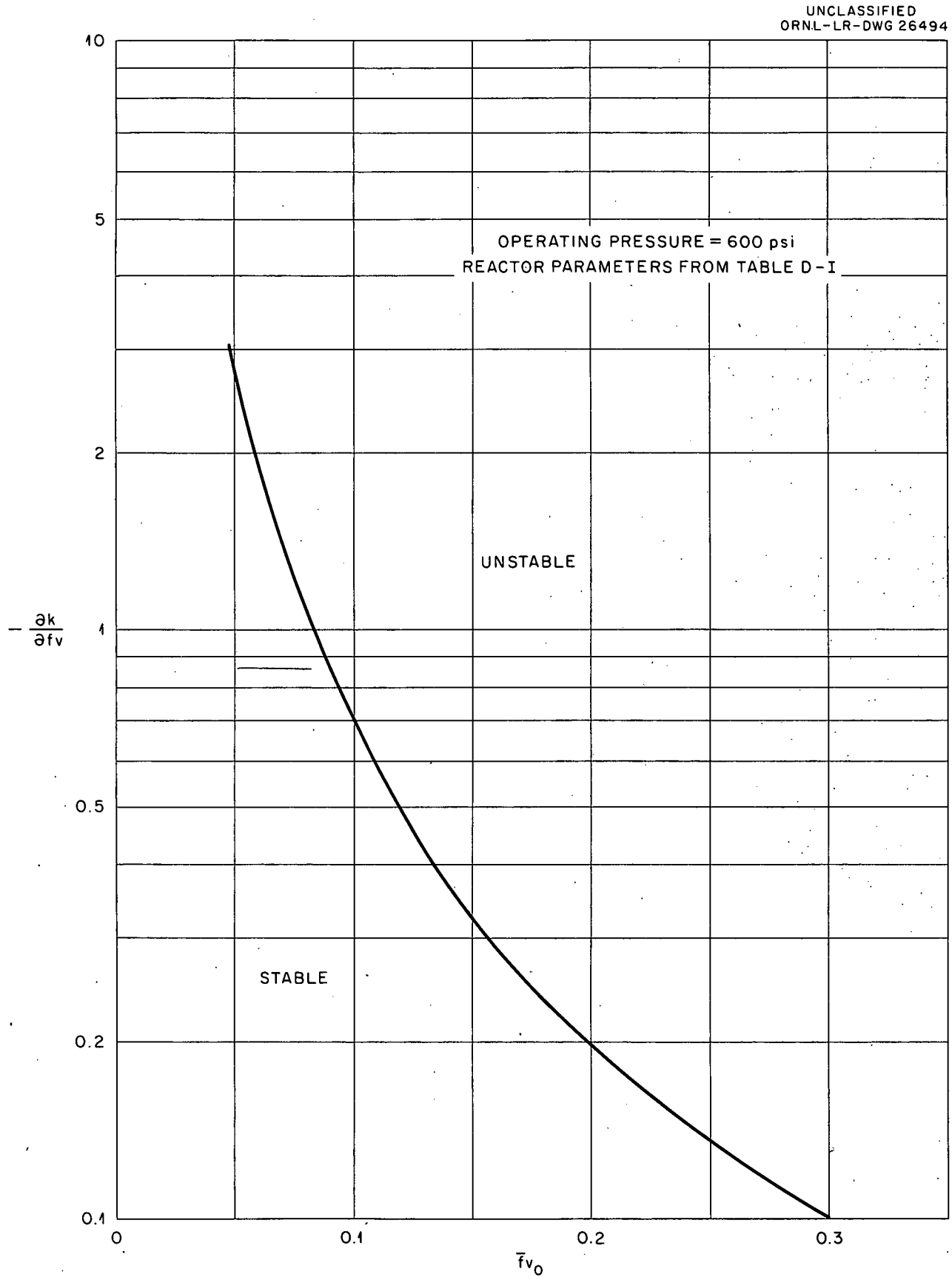

Fig. D–4 Curve Showing Region of Stability for $\frac{\partial k}{\partial \bar{f}v}$ and $\bar{f}v_0$.

$$P_o = A_F h (T_{Fo} - T_{So})$$
$$= 2UA \bar{f}v_o \rho_{go} h_{fgo}$$

As an example, if operating power is to be varied, at a fixed pressure both $(T_{Fo} \cong T_{so})$ and $\bar{f}v_o$ must be varied.

The qualitative effect of varying a number of physical quantities on stability is shown in Table 2.

The results presented in this section appear to be consistent with the empirical results wherever direct comparisons can be made. The frequency of oscillation for $U/Z_1 = 2$ equals $\approx$1 cps; for $U/Z_1 = 1$, .5 cps. This is the range of frequencies which have been experienced. The instabilities have been experienced with $\frac{\partial K}{\partial fv} \approx .3$ and with $\bar{f}v_o > .1$. Figure 4 shows that for $\frac{\partial K}{\partial fv} = .3$; $\bar{f}v_o = .15$ will result in an instability. It must be remembered, however, that the curve must be drawn using the actual physical constants of the system considered before quantitative comparisons can be made.

Conclusions

The effect of various physical quantities on the resonance instability in a boiling water reactor have been determined. This was accomplished by an analysis which proceeded by successive simplifications. If the results of this analysis can be verified as to qualitative and/or quantitative accuracy, the following benefits might result:

1. The reactor design can be pointed towards more inherent stability wherever possible.

2. The synthesis of an external feedback loop to stabilize an inherently unstable design is simplified. The Nyquist method used in the analysis is particularly suited for such a synthesis.

D2 Design of the Control System for the Proposed Reactor

D.2.1 Introduction

The control system for the proposed reactor is shown in block diagram form in Figure 7-3. Two control loops exist which require the design of control equations. This design study was carried out in a manner similar to the analysis in Section D.1, i.e., use of servo techniques. Simplified and linearized equations were used also. This means that the systems designed are applicable to situations which do not involve large changes in the variables from their steady state values. This restriction was not considered too discriminating since the function of the particular loops considered is to hold the variables as close to the steady state values as possible.

The design studies for the two loops were carried independently and then a possible but perhaps questionable method for determining the coupling between the two was worked out.

D.2.2 Design of the Pressure Control Loop

The equations used for this study are the same as in Appendix D.1 except for the dropping of some terms and the addition of a control equation. The terms dropped were those which were found to be unimportant in the resonance instability analysis and those which are important only at the higher frequencies. This is possible because the critical frequencies for the pressure control loop is expected to be much lower than the frequencies for resonance instabilities.

The Laplace transforms of the equations used in this study are:

1. Core

$$B_8 A_5 sf = (A_5 s + B_9)(\delta k_m + \delta k_c)$$

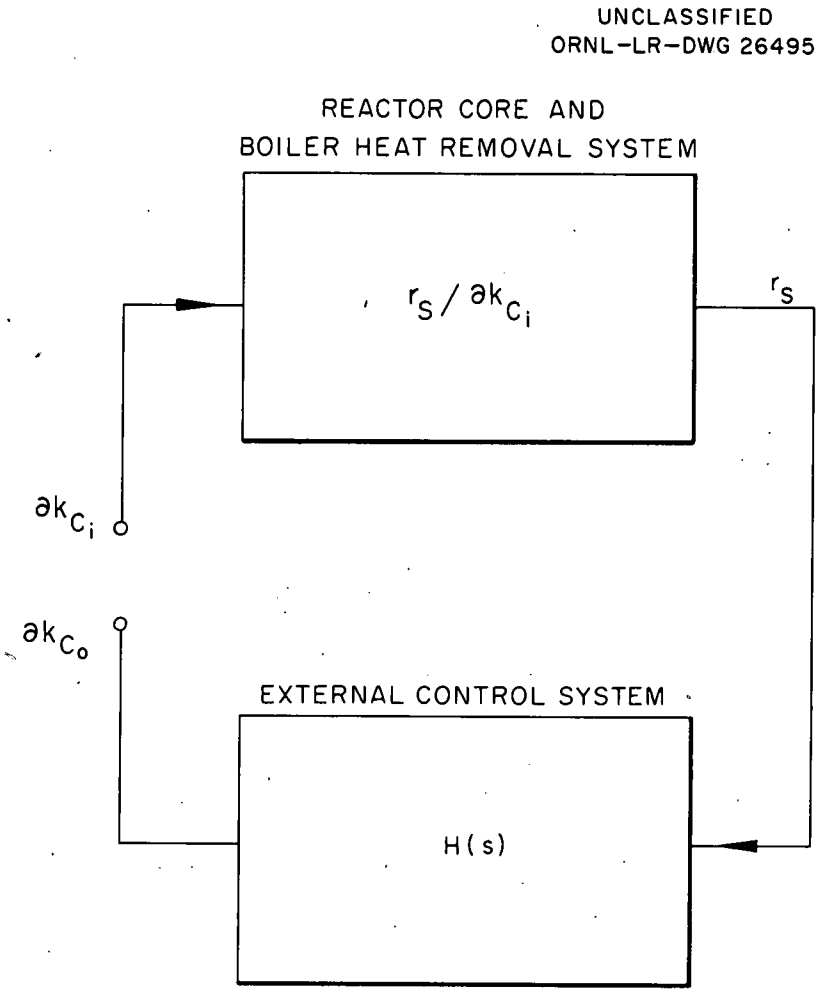

Fig. D-5. Block Diagram of Pressure Control Loop

2. Reactivity change due to moderator density change

$$\delta k_m = -A_4\left[B_5 A_2 z + B_6(1-A_2)\, r_s\right]$$

3. Fuel element heat balance

$$\frac{A_1 B_1}{2A_2}\, sr_F = f - g$$

4. Heat transfer to coolant

$$g = r_F - r_s$$

5. Heat removal rate from core

$$g = z(1 + 1/2\, s)$$

6. Heat balance in steam dome

$$\frac{A_3 B_3}{2A_2}\, sr_s = z$$

7. Control equation

$$\delta k_c = -H(s) r_s$$

The reactivity change has been split up into that contributed by the moderator density change and that contributed by control rod motion. The control rod motion is called for when a fractional change in saturation temperature (corresponsing to pressure change) exists. H(s) is the transfer function relating these quantities, i.e. the control system transfer function. Figure D-5 shows a block diagram of the loop considered and where the loop is opened for the analysis.

The design problem is to determine what H(s) must be to get the desired stability in the loop. This is accomplished by first determining the transfer function $r_s/\delta k_{ci}$. Then H(s) is synthesized such that the open loop transfer function $H(s)\left[r_s/\delta k_{ci}\right]$ satisfies the criterion for stability.

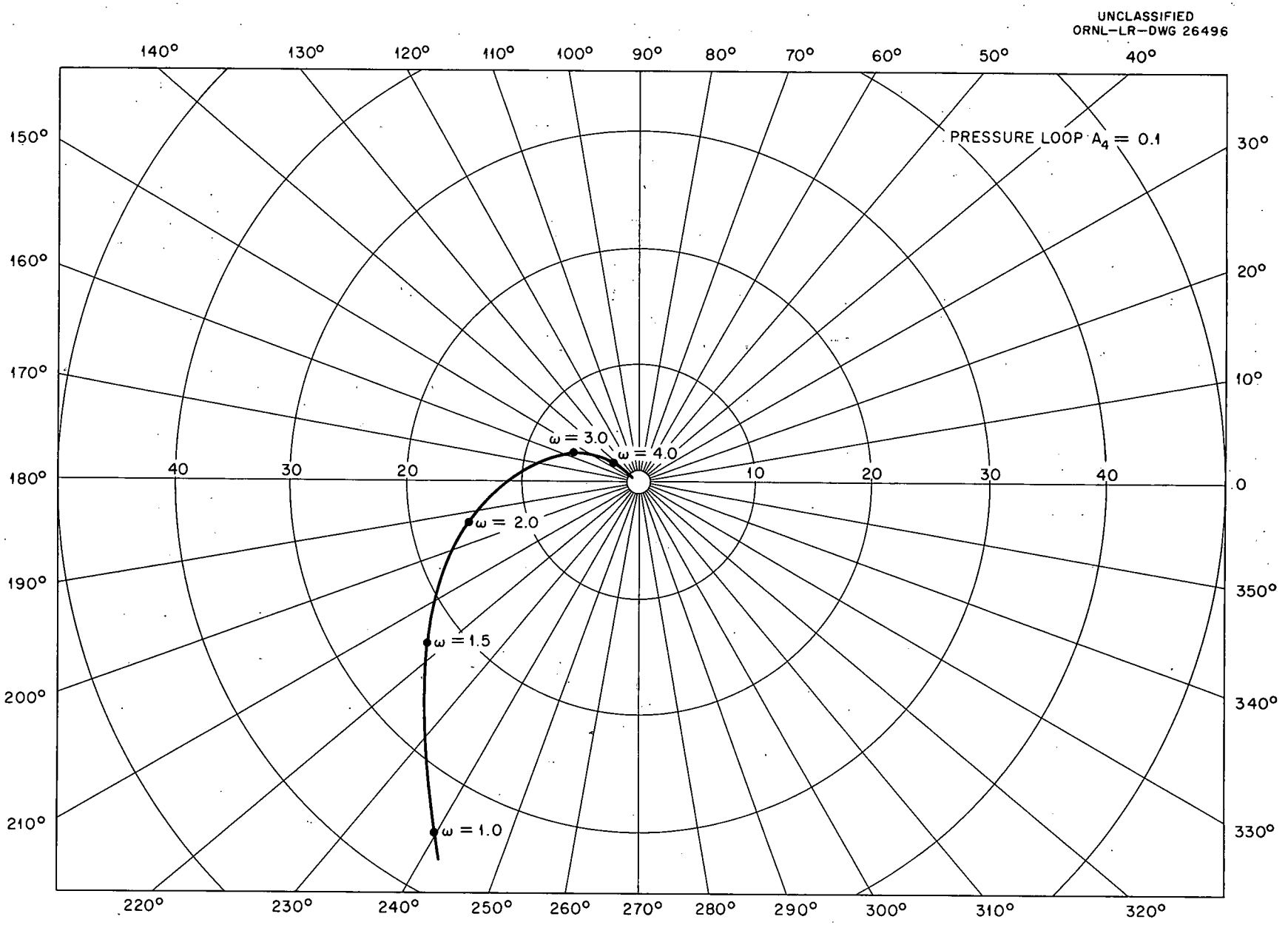

Fig. D–6. Nyguist Plot of $\frac{r_s}{\partial k_{c_i}}$

$r_s/\delta k_{ci}$ was determined by first writing equations 1 to 6 in the following manner:

$$\begin{bmatrix} B_8A_5s & 0 & -(A_5s+B_9) & 0 & 0 \\ 0 & A_4B_5A_2 & 1 & 0 & A_4B_6(1-A_2) \\ -1 & 0 & 0 & \frac{A_1B_1}{2A_2}s+1 & -1 \\ 0 & 1+1/2\ s & 0 & -1 & +1 \\ 0 & -1 & 0 & 0 & \frac{A_3B_3}{2A_2}\ s \end{bmatrix} \begin{bmatrix} f \\ z \\ Sk_{in} \\ rF \\ r_s \end{bmatrix} \begin{bmatrix} (A_5s+B_9)Sk_{ci} \\ 0 \\ = 0 \\ 0 \\ 0 \end{bmatrix}$$

Solving for $r_s/\delta k_{ci}$,

$$r_s/\delta k_{ci} = \frac{A_5s + B_9}{A_4B_6(1-A_2)B_9 + \left[A_4B_6(1-A_2)A_5 + \frac{A_3B_3A_4B_5B_9}{2}\right] s + \left[\frac{B_8A_5A_1B_1}{2A_2} + \frac{A_3B_3A_4B_5A_5}{2} + \frac{A_3B_3B_8A_5}{2A_2}\right] s^2 + \left[\frac{A_3B_3B_8A_5}{4A_2} + \frac{A_3B_3B_8A_5A_1B_1}{4A_2^2}\right] s^3 + \frac{A_3B_3B_8A_5A_1B_1}{8A_2^2} s^4}$$

Putting in the numbers from Table D-1 for the 1200 psi operating condition, the transfer function becomes

$$r_s/\delta k_{ci} = \frac{5.2\ (25\ s + 1)}{.009 + .3s + 3.99\ s^2 + 2.15\ s^3 + .765\ s^4}$$

$A_4 \approx -\frac{\partial K}{\partial fv}$ was assumed to be = .1. Figure D-6 shows the Nyquist plot of this transfer function.

The Nyquist plot shows that the simplest form that H(s) can take will be that of a constant gain term. This would be unacceptable, however, because a steady state error in pressure (corresponding to saturation pressure) would be required to hold δk_c at any value, i. e. it would have the form of a type 0

servo. H(s) must therefore have the form of an integrator at low frequencies. At higher frequencies $\omega \gtrsim 2$, the Nyquist plot shows that the 90° phase lag introduced by an integrator cannot be tolerated. This means that a lead-network to compensate for this is required at these higher frequencies.

From these considerations, it can be seen that the simplest form that H(s) can have is

$$H(s) = \frac{K(1 + Ts)}{s}$$

The values for K and T are determined by demanding that the open loop transfer function H(s) $r_s/\delta k_{ci}$ have an amplitude $\approx .3$ when the phase angle = 180°; and a phase angle $\approx 140^{\circ}$ when the amplitude = 1.0; i.e. a gain margin of 3 and a phase margin of 40°. K = .008 and T = 2.5 gives approximately these results.

Figure D-7 shows the Nyquist plot for H(s) $r_s/\delta k_{ci}$ with

$$H(s) = \frac{.008\ (1+2.5s)}{s}$$

In terms of pressure, the control equation is

$$\delta k_c = - \frac{.0685(1+2.5s)}{s} \frac{\Delta p}{p_o}$$

or at p_o = 1200 psi.

$$\delta k_c = - \frac{.000057(1+2.5s)}{s} \Delta p$$

Taking the inverse Laplace transform, remembering that $Y = \frac{U}{Z_1} t$ and $U/Z_1 = 2$.

$$\frac{dk}{dt} = -.000114\left[\Delta p + 1.25 \frac{dp}{dt}\right]$$

At low frequencies a change in pressure of 10 psi will call for .00114 δk/sec. At higher frequencies $\omega \gtrsim 1$. The 10 psi error will call for .00143 δk.

In any practical rod drive mechanism, additional phase lags will be

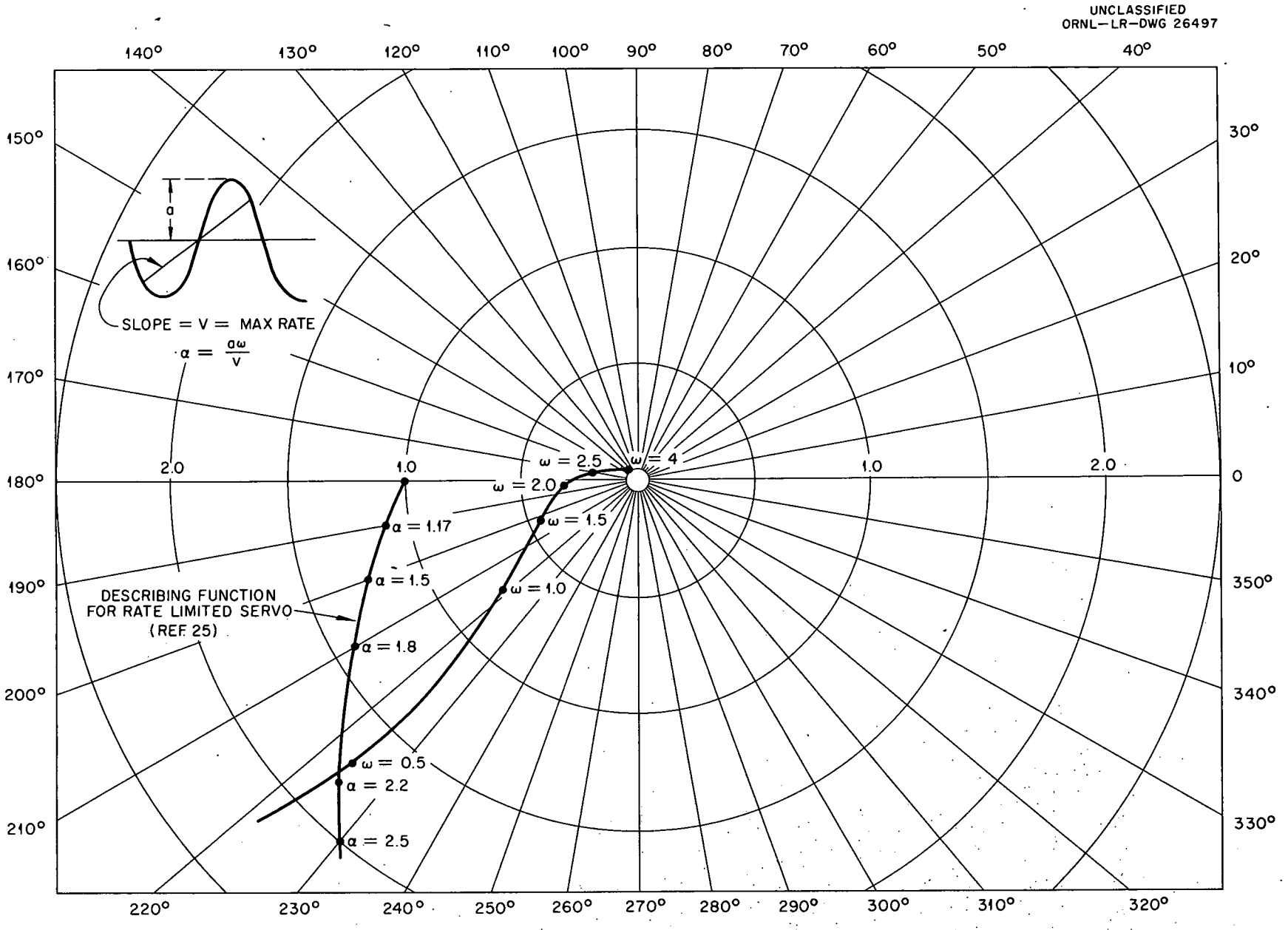

Fig. D-7. Nyquist Plot of $H(s) \frac{r_s}{\partial k_{c_i}}$ (Pressure Control Loop).

introduced and there will be a maximum rate of rod motion. The effect of the additional lag can be compensated with additional lead terms. The effect of the finite rod motion was determined by using the describing function method. The describing function (Ref. 25) for a rate limited servo is plotted on Figure D-7. This function is, in effect, the reciprocal of the amplitude dependent part of the open loop transfer function. The point of crossing of the two curves denoted the conditions for neutral stability.

The following inequality must be satisfied for stability, i.e. to prevent non-linear oscillation.

$$(\delta k_{\mathcal{C}}/\text{sec})_{max} > \frac{a\omega}{\alpha}$$

If it is desired to use a maximum reactivity insertion or removal rate of .001 δk/sec., the pressure error signal must be limited to $\leq$ 30 psi. Larger errors may exist physically, but the electrical error signal must be limited to this value.

D.2.3 Design of the Temperature Control Loop

The following simplified equations were assumed to describe the dynamics of the superheater heat removal system. The superscript $(\ )^s$ denotes superheater quantities.

1. Heat balance in fuel element

$$C_F^s \rho_F^s W_F^s \frac{dT_F^s}{dt} = P^s - Q^s$$

2. Heat transfer to steam

$$Q^s = A_F^s h^s (T_F^s - T_m^s)$$

where $T_m^s = 1/2\ (T_g^s + T_s^s)$,

T_g is the output steam temperature, and T_s the input steam temperature

3. Heat balance in steam channel

$$C_s V_s \rho_s \frac{dT_m^s}{dt} = Q^s + h_{fgo}\rho_g X - P_o$$

$h_{fgo}\rho_g X$ is the heat output from the boiler section and P is the total heat removal rate at the exit of the superheater. It will be assumed that P_o = constant for the remainder of the analysis.

Non-dimensional variables which represent incremental fractional changes were defined. The fractional changes for variables representing power are with respect to superheater steady state power.

The superheater steady state power is

$$P_o^s = P_o - h_{fgo}\rho_{go} X$$

$$= A_F^s h^s (T_{Fo}^s - T_{mo}^s)$$

Fractional temperature changes are with respect to $T_{Fo}^s - T_{mo}^s$. A relationship exists between R_s^s and R_s for the boiler.

$$R_s^s = R_s \left(\frac{T_{Fo} - T_{so}}{T_{Fo}^s - T_m^s} \right) = C_4 R_s$$

The physical constants are grouped together into non-dimensional parameters. The same independent variable used in the boiler analysis is used, i.e. $Y = \frac{U}{Z_1} t$

The transformed equations using the non-dimensional variables are:

1. Heat Balance in fuel element

$$C_1 s r_F^s = f^s - g^s$$

2. Heat transfer to steam

$$g^s = r_F^s - \frac{r_g^s}{2} + \frac{r_s^s}{2}$$

3. Heat balance in steam channel

$$C_2 (s r_g^s - C_4 s r_s) = g^s + C_3 r_s$$

The core euqation is the same as for the boiler region except for the superheater parameters.

4. Core

$$A_5^s B_8^s s f^s = (A_5^s s + B_9^s)\delta k_c^s$$

The only thing known about the control equation is that it relates δk_c^s to r_g^s.

5. Control equation

$$\delta k_c^s = -H^s(s) r_g^s$$

The design problem is to determine the form of $H^s(s)$. The system transfer function $r_g^s/\delta k_{ci}^s$ can be derived simply from equations 1 to 4.

$$r_g^s/\delta k_{ci}^s = \frac{A_5^s s + B_g}{A_5^s B_8^s s^2 (C_1 C_2 s + 1/2\, C_1 + C_2)}$$

The input steam temperature was assumed constant, i.e. $r_s = 0$. Substituting the numbers from Table D-3, the transfer function becomes

$$r_g^s/\delta k_{c2}^s = \frac{.8 \times 10^{-6} (1+25\, s)}{1.25 \times 10^{-9} (1+4.72 \times 10^{-5} s) s^2}$$

For frequencies $\omega \approx 1$ to 10

$$r_g^s/\delta k_{c2}^s \simeq \frac{1.6 \times 10^4}{s}$$

The form of $H^s(s)$ will be the same as for the pressure control loop

$$H^s(s) = \frac{K^s(1+T^s s)}{s}$$

The integration is required to drive the temperature error to zero for steady state and the lead term is required to remove the lag from the integrator at higher frequencies.

The open loop transfer function becomes

$$H^s(s)(r_g^s/\delta k_{ci}^s) = \frac{1.6 \times 10^4\, K^s(1+T^s s)}{s^2}$$

The values for K^s and T^s can be determined by considering the characteristic equation for the system which is the numerator of

$$1 + H^s(s)(r_g{}^s/\delta k_{ci}{}^s)$$

or

$$S^2 + 1.6 \times 10^4 K^s T^s s + 1.6 \times 10^4 K^s = 0$$

The usual notation for the second order characteristic equation is

$$S^2 + 2\xi\omega_o s + \omega_o{}^2 = 0$$

where ω_o is the natural frequency and ξ is the fraction of critical damping. The choice of ω_o for the system is governed by the following considerations:

1. The larger it is, the faster the temperature errors will be removed.

2. The larger it is, the more difficult it would be to compensate for the lags in the drive mechanisms and the effect of the limited rate will be greater.

3. If its value is separated from the critical frequency of the pressure control loop as much as possible, the coupling between the two loops will be minimized.

Choosing a value of 5 for ω_o and .7 for ξ, $H^s(s)$ becomes

$$H^s(s) = \frac{.00156\ (1+.28s)}{s}$$

Figure D-8 shows the Nyquist plot for $H^s(s)(r_g{}^s/\delta k_{ci}{}^s)$. A phase margin of 65^o exists, but the crossover frequency is ≈ 8 or 16 rad/sec which means that the lags introduced by the drive mechanisms might reduce this margin considerably.

The control equation is

$$\delta k_c{}^s = - \frac{.00156(1+.28s)}{s} \frac{\Delta T_g}{T_{Fo} - T_{mo}}$$

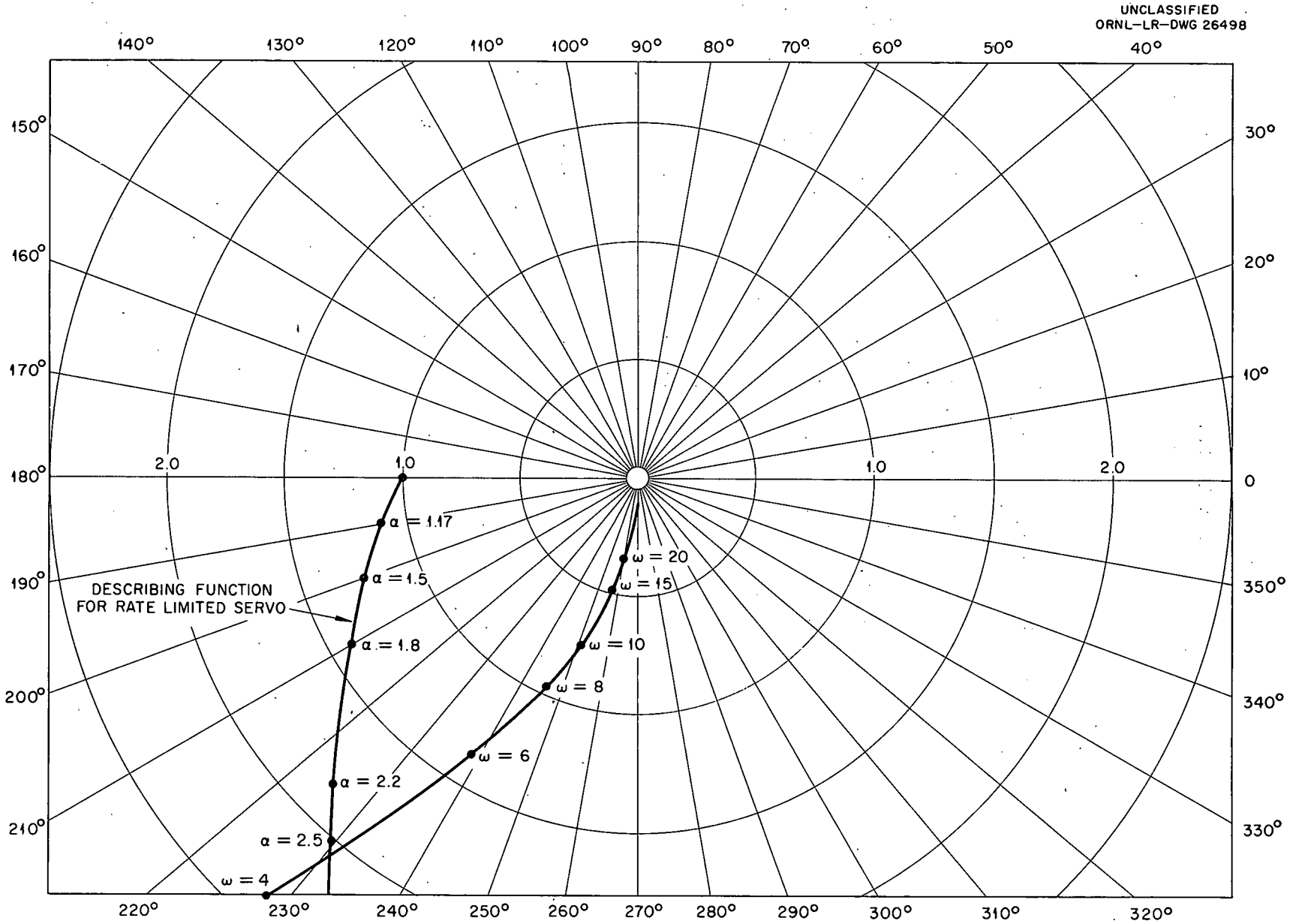

Fig. D-8. Nyguist Plot of $H^s(s)\left(\frac{r_g^s}{\partial k_{c_i}^s}\right)$ (Temperature Control Loop).

and for $T_{Fo} - T_{mo} = 150^{o}F$

$$\delta k_c^{\ s} = - \frac{.0000104(1+.28s)}{s} \Delta T_g$$

Taking the inverse transform and remembering the independent variable, Y $= \frac{U}{Z_1} t$, and $U/Z_1 = 2$.

$$\frac{dK}{dt} = -.0000208\left[\Delta T_g + .14 \frac{dT_g}{dt}\right]$$

At low frequencies $\omega \lesssim 1$ a $100^{o}F$ temperature error calls for .00208 δk/sec. At higher frequencies $\omega \gtrsim 5$ a $100^{o}F$ temperature error calls for .00029 δk.

To prevent non-linear oscillations, the electrical temperature error signal must be limited to $\leq 75^{o}F$. This was again determined by use of the describing function method. The describing function plotted on Figure D-8 is the same as on Figure D-7. A maximum insertion and removal rate of .0005 δk/sec was assumed for the superheater since the worth of the superheater rod alone would be less than that for the whole system.

D.2.4 Analysis of Coupling Between Pressure and Temperature Control Loops

Only a possible method for analyzing the coupling between the two loops is presented. The validity of the method might well be questioned.

It was assumed that the following transformed core equations can be written:

1. Boiler core

$$A_5^{b} B_8^{b} sf^{b} = (A_5^{b} s + B_9^{b})(\delta k_c^{\ b} + b\delta k_c^{\ s} + \delta k_m)$$

2. Superheater core

$$A_5^{s} B_8^{s} sf^{s} = (A_5^{s} s + B_9^{s})(\delta k_c^{\ s} + a\delta k_c^{\ b} + m\delta k_m)$$

f^{b} represents the fractional power change in the boiler.

f^{s} represents the fractional power change in the superheater.

δk_c^s represents the change in reactivity in the superheater region due to superheater control rod motion.

δk_c^b represents the change in reactivity in the boiler region due to boiler control rod motion.

δk_m represents the change in reactivity in the boiler region due to boiler coolant density change.

$b\delta k_c^s$ represents the effective reactivity change in the boiler region due to superheater control rod motion.

$a\delta k_c^b$ represents the effective reactivity change in the superheater region due to boiler control rod motion.

$m\delta k_m$ represents the effective reactivity change in the superheater region due to boiler coolant density change.

The control equations are:

3. Boiler region control rod

$$\delta k_c^b = -H^b(s)r_s + dH^s(s)r_g^s$$

4. Superheater region control rod

$$\delta k_c^s = -H^b(s)r_s - H^s(s)r_g^s$$

These equations state that a pressure error signal corresponding to r_s will call for ganged motion of both control rods. A steam temperature error signal, r_g^s, will call for differential motion. d represents the fractional amount the boiler rod will move with respect to the amount the superheater rod moves when there is a temperature error. $H^b(s)$ and $H^s(s)$ are the feedback transfer functions determined in the sections on pressure control and temperature control designs respectively.

The remaining equations for the boiler region and superheater regions are also from these sections.

Boiler region equations are :

5. Reactivity change due to coolant density

$$\delta k_m = -A_4 \left[B_5 A_2 z + B_6 (1-A_2) r_s^b \right]$$

6. Fuel element heat balance

$$\frac{A_1 B_1}{2A_2} s r_F^b = f^b - r_F^b + r_s^b$$

7. Heat removal rate from core

$$r_F^b - r_s^b = z(1 + 1/2\ s)$$

8. Heat balance in steam dome

$$\frac{A_3 B_3}{2A_2} s r_s^b = z$$

Superheater equations are:

9. Fuel element heat balance

$$(C_1 s + 1) r_F^s = f^s + \frac{r_g^s}{2} - \frac{C_4}{2} r_s^b$$

10. Steam channel heat balance

$$(C_2 s + 1/2) r_g^s = (C_2 C_4 s + \frac{C_4}{2} + C_3)\ r_s^b + r_F^s$$

The equations as written assume a constant power removal rate from the complete system. The temperature coefficient of reactivity in the superheater region is ignored.

The boiler equations and the superheater equations can be grouped together in the following manner:

Boiler equations

$$\begin{bmatrix} -A_5B_8s & 0 & 0 & -(A_5s+B_9)H^b(s)(1+b) & A_5s+B_9 \\ 0 & A_4B_5A_2 & 0 & A_4B_6(1-A_2) & 1 \\ -1 & 0 & \frac{A_1B_1}{2A_2}s+1 & -1 & 0 \\ 0 & 1+1/2s & -1 & +1 & 0 \\ 0 & -1 & 0 & \frac{A_3B_3}{2A_2}s & 0 \end{bmatrix} \begin{bmatrix} f_b \\ z \\ r_F{}^b \\ r_s{}^b \\ \delta k_m \end{bmatrix} = \begin{bmatrix} H^s(s)(A_5{}^s s+B_9{}^s)(b-d)r_g{}^s \\ 0 \\ 0 \\ 0 \\ 0 \end{bmatrix}$$

Superheater equations

$$\begin{bmatrix} -A_5{}^sB_8{}^ss & 0 & H^s(s)(A_5{}^ss+B_9{}^s)(a-1) \\ -1 & C_1s+1 & -1/2 \\ 0 & 1 & -(C_2s+1/2) \end{bmatrix} \begin{bmatrix} f^s \\ r_F{}^s \\ r_g{}^s \end{bmatrix} = \begin{bmatrix} (A_5s+B_9)H^b(s)(1+a)r_s{}^b-(A_5s+B_9)m\delta k_m \\ -\frac{C_4}{2}r_s{}^b \\ -(C_2C_4s+\frac{C_4}{2}+C_3)r_s{}^b \end{bmatrix}$$

If b = d there will be no coupling from the superheater to the boiler and there will be no possibility of instability due to coupling between the two systems. In general this will not be true since the boiler rod cannot always move exactly the right amount to cancel the effect of the superheater rod motion when there is a temperature error. Figure D-9 shows a block diagram of the coupled system and indicates where the loop will be opened for the analysis.

The analysis requires the derivation of the open loop transfer function. This is done by first deriving the transfer functions $r_s{}^b/r_{gi}{}^s$ and $\delta k_m/r_{gi}s$ from the boiler equations. The superheater equations can be seen to be of the form

$$r_{go} = f_1(s)r_s{}^b + f_2(s)\delta k_m$$

where f_1 and f_2 are ratios of polynomials in "s".

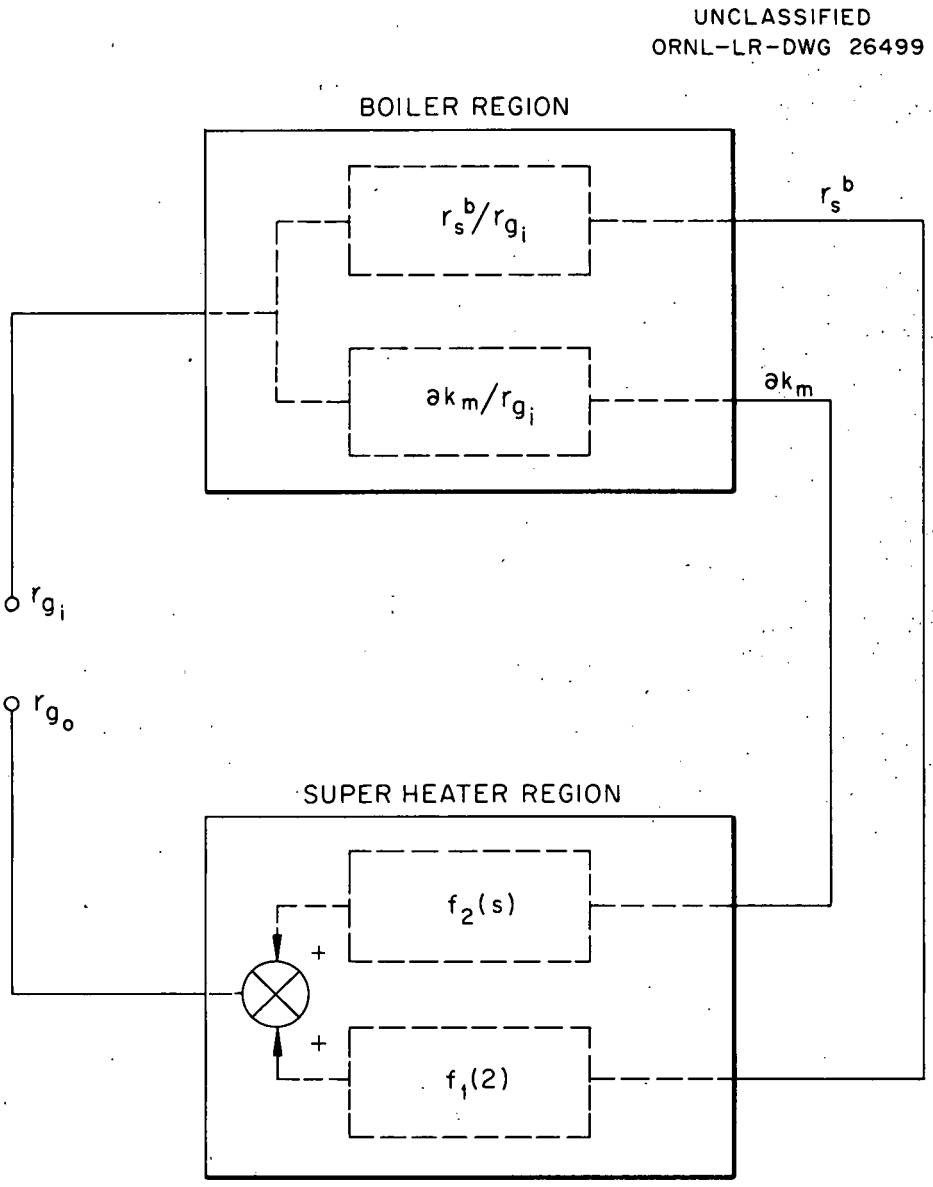

Fig. D-9. Block Diagram of Coupled System

The open loop transfer function then becomes

$$-r_{go}/r_{gi} = -f_1(s)(r_s{}^b/r_{gi}{}^s) - f_2(s)(Sk_m/r_{gi}{}^s)$$

The usual stability criterion can now be applied to this open loop transfer function.

Table D-1

Numerical values for a Representative Reactor

Operating Pressure	600 psi	1200 psi
$c_F\rho_F$	56 BTU/ft^3 70% stainless steel 30% uranium	56 BTU/ft^3
$T_{Fo}-T_{so}$	14°	14°
n	10 BTU/ft^3°F	7.5 BTU/ft^3°F
μ	.024 lb/ft^3°F	.013 lb/ft^3°F
$\|\nu\|$	.0824 lb/ft^3°F	.074 lb/ft^3°F
B_1	.825	.495
B_2	.11	.087
B_3	.14	.127
B_5	.975	.94
B_6	.0208	.0204
B_7	.0261	.062
B_8	.0075	.0075
B_9	β = .0075 λ = .08sec^{-1} l = 6.5x10^{-5}sec 5.2x10^{-6} "	5.2 x 10^{-6}
$A_1 = \frac{V_F}{V_{cool}}$	.5	.5

Table D-1
contd.

Operating Pressure	600 psi	1200 psi
$A_2 = \bar{f}v_o$	.1	.1
$A_3 = \frac{V_{sd}}{V_{cool}}$	2	2
$A_4 = \rho_{fo} \frac{\partial K}{\partial \rho_{cool}}$	—	—
$A_5 = \frac{U}{Z}1$	1.3×10^{-4} $U/Z_1 = 2$	1.3×10^{-4}

Table D-2

Effect on Stability of Increasing the Values of Physical Quantities

Physical Quantity	Effect on Stability	Order
$\bar{f}v_o$	hurts	$\approx$2nd power
$\frac{\partial K}{\partial \rho}_{mod} \approx \frac{1}{\rho_{fo}} \frac{\partial K}{\partial \bar{f}v}$	hurts	$\approx$ linear
Power level	hurts	$\approx$ linear
Operating pressure (Power held constant)	helps	$\approx \frac{1}{\rho_{go} h_{fgo}}$
$A_F h$	hurts	$\approx$ linear
Volumetric coolant flow rate (Power held constant)	helps	$\approx$ 2nd power
$\frac{\text{Volume fuel}}{\text{Volume coolant channel}}$	helps	$\approx$ linear
$c_F \rho_F$	helps	$\approx$ linear
$\frac{\text{Volume steam dome}}{\text{Volume coolant channel}}$	Must be large enough to satisfy Criterion I	

Table D-3

Physical Constants for Superheater Region

Quantity	Value
V_F^s	.000422 ft^3
V_s	.00128 ft^3
$c_s^s \rho_F^s$	56 BTU/ft^3
$c_s^s \rho_s^s$	1.31 BTU/ft^3
$T_{Fo}-T_{so}$	150°F
C_1	1.62×10^{-3}
C_2	2.42×10^{-5}
A_5^s	2×10^{-4}
B_8^s	.0075
B_9^s	8×10^{-6}

List of Symbols for Section D2a

A = coolant flow area (ft^3)

A_F = fuel element conduction area (ft^2)

C_F = specific heat of fuel elements (BTU/lb^oF)

D = conversion factor $\frac{\text{Reactor Power}}{\text{Neutron Population}}$

$\bar{f}v$ = average fractional void

$\bar{f}v_o$ = average fractional void at t = 0

δf_v = $\bar{f}v - \bar{f}v_o$

F = fractional reactor power change = $\frac{P-P_o}{P_o}$

f = Laplace transform of F

G = fractional change in heat transferral rate to coolant = $\frac{Q-P_o}{P_o}$

q = Laplace transform of G

h = heat transfer coefficient ($\frac{BTU}{sec\ ft^2\ ^oF}$)

$h_{gs.o.}$ = specific enthalpy of steam in steam dome (BTU/lb)

h_{gc} = " " " " leaving core

h_{go} = " " " " " steam dome

h_{fg} = latent heat of vaporization (BTU/lb)

h_{fgo} = " " " " at t = 0

I = fractional change in volumetric flow rate out of steam dome

K = reactor multiplication constant

δK = incremental change in K

= K-1

δk = Laplace transform of δK

l = average neutron lifetime (sec)

P = reactor power (BTU/sec)

P_o = reactor power at t = 0

Q = heat transferral rate from fuel element to coolant (BTU/sec)

R_s = ratio of saturation temperature change to initial film drop

$$= \frac{\Delta T_s}{T_{fo}-T_{so}}$$

r_s = Laplace transform of R_s

R_F = ratio of fuel element temperature change to initial film drop

$$= \frac{\Delta T_F}{T_{Fo}-T_{so}}$$

r_F = Laplace transform of R_F

s = Laplace transform variable

T_F = fuel element temperature (^oF)

T_{Fo} = " " " at t = 0

ΔT_F = incremental fuel temperature change = T_F-T_{Fo}

T_s = saturation temperature of coolant (^oF)

T_{so} = " " " " at t = 0

ΔT_s = incremental saturation temperature change = T_s-T_{so}

U = coolant flow velocity (Ft/sec)

V_F = fuel element volume (ft^3)

V_{cool} = coolant channel volume (Ft^3) = AZ_1

V_{sd} = steam dome volume (Ft^3)

$\bar{X}$ = volumetric flow rate out of steam dome (ft^3/sec)

$\bar{X}_o$ = " " " " " " " at t = 0

$\Delta\bar{X}$ = incremental change in $\bar{X}$ = $\bar{X}-\bar{X}_o$

Y = independent variable = $\frac{U}{Z_1}t$

Z = fractional change in average void fraction = $\frac{\delta fv}{\bar{f}v_o}$

z = Laplace transform of Z

Z_1 = height of core

β = delayed neutron fraction

λ = reciprocal delayed neutron lifetime (sec^{-1})

∂ = $\frac{\partial K}{\partial \rho_{mod}} = \frac{\partial K}{\partial \rho_{cool}}$ = coolant density coefficient of reactivity

ρ_{cool} = average density of coolant including voids (lb/ft^3)

ρ_F = density of fuel element (lb/ft^3)

ρ_g = density of steam (lb/ft^3)

ρ_{go} = " " " at t = 0

ρ_f = density of water (lb/ft^3)

ρ_{fo} = density of water at t = 0

η = $\left.\frac{\partial \rho_g h_{fg}}{\partial T}\right|_{T=T_{so}}$

μ = $\left.\frac{\partial \rho_g}{\partial T}\right|_{T=T_{so}}$

$|V|$ = $\left|\left.\frac{\partial \rho_f}{\partial T}\right|_{T=T_{so}}\right|$

ω = non dimensional frequency

ω' = $\frac{U}{Z}\omega$ = frequency (rad/sec)

List of Non-dimensional Parameters

$A_1 = \frac{V_F}{V_{cool}}$

$A_2 = \bar{f} v_o$

$A_3 = \frac{V_{SD}}{V_{cool}}$

$A_4 = \partial \rho_{fo}$

$A_5 = \frac{U}{Z} 1$

$B_1 = \frac{C_F \rho_F (T_{Fo} - T_{so})}{\rho_{go} h_{fgo}}$

$B_2 = \frac{\eta (T_{Fo} - T_{so})}{\rho_{go} h_{fgo}}$

$B_3 = \frac{\mu (T_{Fo} - T_{so})}{\rho_{go}}$

$B_5 = \frac{\rho_{fo} - \rho_{go}}{\rho_{fo}}$

$B_6 = \frac{|V| (T_{Fo} - T_{so})}{\rho_{fo}}$

$B_7 = \frac{\rho_{go}}{\rho_{fo}}$

$B_8 = 1(\lambda + \beta/1)$

$B_9 = 1\lambda$

Additional Symbols for Section D2b

a	=	amplitude of sinusoidal error signal (see Figure D-5)
α	=	parameter for describing function (see Figure D-5)
$H(s)$	=	feedback transfer function
K	=	gain term
δk_c	=	Laplace transform of reactivity change due to control rod motion
p	=	steam dome pressure (psi)
T	=	non-dimensional time constant
V	=	maximum insertion or removal rate of δk

Additional Symbols for Section D2c

A_F^s	=	heat transfer area in superheater region (ft^2)
c_s	=	specific heat of steam (BTU/lb)
c_F^s	=	specific heat of fuel element in superheater region (BTU/lb)
F^s	=	$\frac{Ps-P_o^s}{P_o^s}$
f^s	=	Laplace transform of F^s
G^s	=	$\frac{Q^s-P_o^s}{P_o^s}$
g^s	=	Laplace transform of G^s
$H^s(s)$	=	Feedback transfer function
K^s	=	gain term
δk_c^s	=	Laplace transform of reactivity change in the superheater region due to control rod motion
P^s	=	superheater region power (BTU/sec)
P_o^s	=	steady state superheater region power (BTU/sec)
Q^s	=	heat transfer rate to steam (BTU/sec)

R_F^s = $\frac{T_F^s - T_{Fo}^s}{T_{Fo}^s - T_{mo}^s}$

r_F^s = Laplace transform of R_F^s

R_g^s = $\frac{T_g^s - T_{go}^s}{T_{Fo}^s - T_{mo}^s}$

r_g^s = Laplace transform of R_g^s

R_s^s = $\frac{T_s^s - T_{so}^s}{T_{Fo}^s - T_{mo}^s}$

r_s^s = Laplace transform of R_s^s

T_F^s = Average temperature of fuel element in superheater region (^oF)

T_{Fo}^s = Steady-state average temperature of fuel element in superheater region (^oF)

T_m^s = Mean temperature of steam in superheater region (^oF)

T_{mo}^s = Steady state mean temperature of steam in superheater region (^oF)

T_g^s = Temperature of steam at outlet of superheater region (^oF)

T_{go}^s = Steady state temperature of steam at outlet of superheater region (^oF)

T_s^s = Temperature of steam at input to superheater region (^oF)

T_{so}^s = Steady state temperature of steam at input to superheater region (^oF)

V_F^s = Volume of fuel element in superheater region (ft^3)

V_s = Volume of steam channel in superheater region (ft^3)

ρ_F^s = density of superheater fuel element (lb/ft^3)

ρ_s = density of steam (lb/ft^3)

ω_o = natural frequency for a second order system

ζ = damping coefficient for a second order system

Non Dimensional Coefficients

C_1 = $\frac{U c_F^s \rho_F^s V_F^s (T_{Fo}^s - T_{mo}^s)}{Z_1 P_o^s}$

$$C_2 = \frac{U c_s \rho_s V_s (T_{Fo}^s - T_{mo}^s)}{2 Z_1 P_o^s}$$

$$C_3 = \frac{\eta X_o (T_{Fo} - T_{so})}{P_o^s}$$

$$C_4 = \frac{T_{Fo} - T_{so}}{T_{Fo}^s - T_{mo}^s}$$

Bibliography

(1) Ginsburgh, et al, "Consideration of a 30,000KW Heterogeneous Boiling Reactor Power Plant," ORNL 53-8-226(61), August, 1953.

(2) Cunningham, S. E., ORNL, personal communication

(3) "Investigation of Materials for a Water Cooled and Moderated Reactor", (Cl) ORNL 1915.

(4) "Corrosion of Stainless Steel in Supercritical Water," BMI-901.

(5) "Irradiation Data for Fuel Elements," (Cl) CF-55-6-33.

(6) Glasstone, S., "Principles of Nuclear Reactor Engineering".

(7) "A Small Ship Gas Cooled Reactor," (Cl) ORSORT ORNL CF-56-8-212.

(8) "The Reactor Handbook," USAEC Vol. 2, May, 1955.

(9) McAdams, "Heat Transmission," 3rd Edition.

(10) Bailey and Zmola, "Power Removal from Boiling Nuclear Reactors," CF-55-7-43.

(11) Edlund and Glasstone, "The Elements of Nuclear Reactor Theory".

(12) Davidson, Hardie, Humphreys, and Murleson, "Studies of Heat Transfer Through Boiler Tubing at Pressures from 500-3300 Pounds," Transactions of the ASME, 1943.

(13) Marks, "Mechanical Engineers Handbook," 4th Edition.

(14) Boch, Gall, Leichsenving, and Livingston, "A Conceptual Design of a Pressurized-Water Package Power Reactor," (Cl) ORNL-1613, December 3, 1956.

(15) Bate, Einstein, and Kinney, "Description and Operating Manual for the Three-Group, Three-Region Reactor Code for ORACLE," CF-55-1-76, January 15, 1955.

(16) Young, "Critical Mass Needed to Override Xe," Mon P-457, December 29, 1947.

(17) Pomerance and Macklin, "Resonance Capture Integrals," Geneva Paper, pg. 833, 1955.

(18) Gallagher, "Two-Group Calculations for a Steel-Water Critical Experiment and the APPR," (Cl) CF-55-9-167, September 28, 1955.

(19) Hughes and Bragdon, "The Diffusion Length of Thermal Neutrons in Uranium," CP-1732, May 27, 1944.

(20) Chestnut and Mayer, "Servo Mechanisms and Regulating System Design," Vol. 1.

(21) Shultz, "Control of Nuclear Reactors and Power Plants".

(22) "How to Control a Boiling Reactor," Nucleonics, December, 1955.

(23) Argonne Staff, "Significance of EBWR," Nucleonics, July, 1957.

(24) "Transient and Steady State Characteristics of a Boiling Reactor," ANL 5211.

(25) "Sinusoidal Analysis of Feedback Control Systems Containing Non-linear Elements," AIEE, July, 1952.

(26) Hughes, "The Diffusion Length in the Beryllium Oxide Pile," CF-3562, July 10, 1946.

(27) Murray, "Nuclear Reactor Physics".

(28) "The Reactor Handbook," Vol. 1, USAEC, 1955.

(29) Holmes and Meghreblian, "Notes on Reactor Analysis," Part II, CF-54-7-88, August, 1955.

(30) Mesger, "Outline of Lectures on Neutron Physics and Reactor Analysis".

(31) "Unfired Pressure Vessel Code", 1956.

(32) Robertson, "Kanigen Process for Nickle Plating," ORNL, June 21, 1957.

(33) "Steam and Its Uses," B and W Co.

(34) "The EBWR," ANL 5607.

(35) Kroeger, H. R., Neou, I. M., and Meem, J. L., "The Effect of Gamma Heating on the APPR-1 Pressure Shell," APAE-Memo-85.

(36) ORNL Dwg. No. 21839.

(37) "Reactor Shielding Design Manual," TID-7004.

(38) Blizard, E. P., "Nuclear Radiation Shielding".

(39) Keenan and Keys, "Thermodynamic Properties of Steam".

(40) Stevenson, "Introduction to Nuclear Engineering".

(41) Mittleman, P. S., and Liedtke, R. A., "Gamma Rays from Thermal Neutron Capture," Nucleonics, May, 1955.

(42) "Code for Pressure Piping," ASA B31.1-1955, ASME.

(43) ORNL 1915.

(44) "Specs. for APPR-1 Fuel and Control Rod Components," ORNL 2225.

(45) "Beryllium Oxide - Properties of," BMI-T-18.